Dynamic phasor modelling of VSC-FACTS devices for small signal stability studies

Thesis presented for the degree of

Doctor of Philosophy

at the University of Strathclyde

by

Khaled Issa Abojlala

BSc., MSc.

Department of Electronic and Electrical Engineering

University of Strathclyde

2019

DECLARATION

This thesis is the result of the author's original research. It has been composed by the author and has not been previously submitted for examination which has led to the award of a degree.

ACKNOWLEDGEMENTS

First and foremost, all praise is to Allah the Almighty, the only one God, for lighting my way and directing me through each and every success and achievement I have ever reached or may reach. I humbly and sincerely thank Allah, the most gracious and merciful, who gave me the ability and means to accomplish this work.

Firstly I thank my supervisor Dr Derrick Holliday for his supervision and valuable guidance throughout my PhD. His encouragement and help contributed greatly to my current achievements.

A special thanks to Dr Grain Phillip Ased for his great support and for long technical discussions that helped me focus in on my research objectives.

I extend my thanks to Dr Khaled Ahmed for his valuable assistance on reviewing my thesis and his tremendous inputs and comments.

Also, I would like to thank the staff and my colleagues at the Department of Electronic and Electrical Engineering at the University of Strathclyde for their valuable discussions during the years of my research.

I would like to acknowledge the Ministry of Higher Education and Scientific Research in Libya, for offering me a scholarship to complete my PhD studies.

Last but not least, heartfelt gratitude goes to my mum and my father ‘who passed away during my study, may Allah grant him a high place in Jannah’ for their prayers, support and encouragement. I deeply appreciate all the sacrifices and endless support of my wife and my children have given throughout my PhD period. I also wish to extend my thanks to my brothers and sisters for their support and encouragement during this research work.

LIST OF ABBREVIATIONS

CIGRE	International Council on Large Electric Systems
CPL	Constant-power load
d	Direct axis component
DDSRF	Decoupled double synchronous reference frame
DFIG	Doubly-fed induction generator
DFT	Discrete Fourier transform
DP	Dynamic phasor
dq	Park's transformation
DVR	Dynamic voltage restorer
EMP	Exponentially modulated periodic
EMTDC	Electromagnetic Transient Design and Control
EMTP	Electromagnetic transient program
FACTS	Flexible ac transmission system
FFT	Fast Fourier transform
GNC	Generalised Nyquist criterion
HP	High pressure of turbine
HSS	Harmonic state-space
HTF	Harmonic transfer function
HVDC	High voltage direct current
IDVR	Interline dynamic voltage restorer
IEEE	Institute of Electrical and Electronics Engineers
IMU	Impedance measurement unit
IP	Intermediate pressure of turbine
KCL	Kirchhoff's current law
KVL	Kirchhoff's voltage law
LP_A	Section A of Low pressure of turbine
LP_B	Section B of Low pressure of turbine

LTI	Linear time-periodic
LTP	Linear time-periodic
md	Measurement delay
MMC	Modular multilevel converter
NPC	Neutral Point Clamped inverter
PI	Proportional integral
PIR	Proportional integral resonant
PLL	Phase locked loop
PNDQ	Positive and negative sequence based synchronous dq method
PSCAD	Power System Computer Aided Design
PWM	Pulse width modulation
q	Quadrature axis component
RSC	Rotor-side-converter
SCR	Short circuit ratio
SVI	Series virtual impedance
SHVI	Shunt virtual impedance
SNR	Signal to noise ratio
SRCI	Series-capacitive virtual impedance
SRF	Synchronous reference frame
SRII	Series resistive-inductive
SSCI	Sub-synchronous control interaction
SSR	Sub-synchronous oscillation
SSSC	Static synchronous series compensator
STATCOM	Static synchronous compensator
TCSC	Thyristor controlled series compensation
UPFC	Unified power flow controller
USSC	Unified series-shunt compensator
VSC	Voltage source converter
VSC-FACTS	Voltage source converter based flexible ac transmission system

LIST OF SYMBOLS

A	Linearized state matrix of size $(n \times n)$
AA	State matrix of synchronous machine
AC_f, AC_h	Mutual effect between the fundamental frequency and harmonics
A_{DP}	Generalised state matrix of arbitrary system
A_I	Synchronous dq state matrix of SSSC controlled with impedance control mode
AI_{DP}	Generalised dq-dynamic phasor state matrix of SSSC controlled with impedance control mode
A_P	Synchronous dq state matrix of SSSC controlled with power control mode
AP_{DP}	Synchronous dq state matrix of SSSC controlled with power control mode
Asq	Synchronous dq state matrix of STATCOM controlled with reactive power control mode
Asv	Synchronous dq state matrix of STATCOM controlled with direct voltage control mode
As_{DP}	Generalised state matrix of a STATCOM
A_V	Synchronous dq state matrix of SSSC controlled with voltage control mode
AV_{DP}	Generalised dq-dynamic phasor state matrix of SSSC controlled with voltage control mode
B	Linearized input matrix of size $(n \times r)$
BB	Input matrix of synchronous machine
B_{DP}	Generalised input matrix of arbitrary system
B_I	Synchronous dq input matrix of SSSC controlled with impedance control mode
BI_{DP}	Generalised dq-dynamic phasor input matrix of SSSC controlled with impedance control mode
B_P	Synchronous dq input matrix of SSSC controlled with power control mode
BP_{DP}	Generalised dq-dynamic phasor input matrix of SSSC controlled with power control mode
Bs_{DP}	Generalised input matrix of a STATCOM
Bsq	Synchronous dq input matrix of STATCOM controlled with reactive power control mode
Bsv	Synchronous dq input matrix of STATCOM controlled with direct voltage control mode

B_V	Synchronous dq input matrix of SSSC controlled with voltage control mode
BV_{DP}	Generalised dq-dynamic phasor input matrix of SSSC controlled with voltage control mode
C	Linearized output matrix of size ($j \times n$)
C_{dc}	dc side capacitor
C_f	Harmonic filter capacitor
D_i	Damping coefficient
D	Linearized feedforward matrix of size ($j \times r$)
C_{DP}	Generalised output matrix of arbitrary system
D_{DP}	Generalised feedforward matrix of arbitrary system
h	Number of harmonics to be included in the study
H_i	Inertia constant of mass i
i	Phases (a, b or c)
i_{ca}	Converter current
i_{dc}	dc link current
i_{dq}	Voltages of ac side in synchronous dq frame
$\mathbf{i_{inj\_abc}}$	Harmonic output current or the injected current vector
$\mathbf{i'^{r}_{kdqx}}$	Current flow in damper (x), where x= 1,2
$\mathbf{i^{r}_{mdq}}$	Magnetizing current viewed from rotor
i_{sd}	Direct axis components of STATCOM current
i_{sed}	Direct component of SSSC current
i_{sq}	Quadrature axis components of STATCOM current
i_{seq}	Quadrature component of SSSC current
k	An integer number represents harmonic order and define the accuracy of the approximation of the original waveform
$\bar{k}$	Conjugate of the harmonic (k)
k_{ij}	Shaft stiffness of section $i\ j$
K_{iid}	Integral control gain of direct axis current
K_{iiq}	Integral control gain of quadrature axis current
K_{ivd}	Integral control gain of direct axis voltage
K_{ivq}	Integral control gain of quadrature axis voltage
K_{pid}	Proportional control gain of direct axis current
K_{piq}	Proportional control gain of quadrature axis current
K_{pvd}	Proportional control gain of direct axis voltage

K_{pvq}	Proportional control gain of quadrature axis voltage
$\mathcal{L}_a$	Number of states of the studied system
$\mathcal{L}_b$	Number of inputs of the studied system
L_{dq}	Return ratio matrix of grid-load
l_f	Harmonic filter inductance
L_f	STATCOM inductance
L'_{fd}	Field inductance
L_g	Grid inductance
L'_{kd1}	Inductance of d-axis damper 1
L'_{kqx}	Inductance of q-axis dampers
L_{md}	Magnetizing inductance of direct axis viewed from rotor
L_{mq}	Magnetizing inductance of quadrature axis viewed from rotor
L_{ls}	Stator leakage inductance
L_{se}	SSSC inductance
LL_{mdq}	Magnetizing inductance matrix
M	A diagonal matrix which represents the transformation of differential variables of the system to dynamic phasor
m_c	Modulation index
m_{sd}	Direct component of the modulation index of STATCOM converter
m_{sq}	Quadrature component of the modulation index of STATCOM converter
m_{sed}	Direct component of the modulation index of SSSC converter
m_{seq}	Quadrature component of the modulation index of SSSC converter
n	A vector of all positive and negative harmonic orders except (k)
P	The number of pole pairs of synchronous machine
P_{line}	Active power flow in the transmission line
P^*_{line}	Line active power reference
P_1	Active power at the sending end
P_2	Active power at the receiving end
Q_{line}	Reactive power flow in the transmission line
Q^*_{line}	Line reactive power reference
Q_1	Reactive power at the sending end
Q_2	Reactive power at the receiving end
R	Sum of the converter, filter and transformer resistances
r_c	Converter resistance

R_f	STATCOM resistance
r_f	Filter resistance
r'^r_{fd}	Field resistance
R_g	Grid resistance
r'^r_{kd1}	Resistance of d-axis damper 1
r'^r_{kqx}	Resistance of q-axis dampers
r_s	Stator resistance
R_{se}	SSSC resistance
r_t	Series transformer resistance
S'_a , S_a	Switching function of bridge arm of phase (a)
S_{base}	System base power
T_{IP}	Intermediate pressure of turbine torque
T_{HP}	High pressure of turbine torque
T_{LP_A}	Section A of Low pressure of turbine torque
T_{LP_B}	Section B of Low pressure of turbine torque
$\mathbf{u}$	System input vector
v_{base}	System base voltage
v_{ca}	Converter output voltage for phase a
v_{dc}	dc link voltage
v^*_{dc}	Reference dc link voltage
v_{dk}	Direct voltage at harmonic order (k)
v_{dq}	voltages of ac side in synchronous dq frame
$\mathbf{v_{inj\_abc}}$	Harmonic output voltage or the injected voltage vector
V_k	Voltage magnitude
$\mathbf{v'^r_{kdqx}}$	Voltage across damper (x), where x= 1,2
v_{NE}	Voltage between dc reference point (N) and earth (E)
v_{qk}	Quadrature voltage at harmonic order (k)
v_{sed}	Direct component SSSC voltage
v_{seq}	Quadrature component of SSSC voltage
v^*_{seq}	Quadrature voltage reference of SSSC
ω	Fundamental angular frequency
ω_i	Sliding frequency of injected frequencies
ω_r	Speed of the rotor reference frame

$\mathbf{x}$	System state vector
$\mathbf{x_{inj}}$	Instantaneous value of injected signal
$X_k(t)$	A function of time representing the complex Fourier coefficient ‘‘dynamic phasor parameter’’ of the periodic signal
$\mathbf{x_m}$	Magnitude of injected signal
x_{seq}	SSSC quadrature impedance
$\mathbf{y}$	System output vector
Y_{device}	Device admittance in synchronous dq frame
$\langle Y_{device} \rangle_k$	Device admittance in dq-dynamic phasor
$\left\| Y_{NT}^{dq} \right\|_1$	Unity norm of admittance
YZ_{dq}	system admittance/impedance
Z_{DP}	Generalised impedance of arbitrary system
Z_{Ddd}	Diagonal impedances of d axis channel
Z_{Ddq}	Off-diagonal impedances of d axis channel
Z_{Dqd}	Off-diagonal impedances of q axis channel
Z_{Dqq}	Diagonal impedances of q axis channel
$Z_{DPSTATCOM}$	Generalised STATCOM impedance model controlled with reactive power mode
Z_g	Grid impedance in synchronous dq frame
$\langle Z_g \rangle_k$	Grid impedance in dq-dynamic phasor
$\left\| Z_g^{dq} \right\|_\infty$	Infinity norm of impedance
Zi_{SSSC}	Synchronous dq impedance of SSSC controlled with impedance control mode
Z_{ISSSC}	Generalised dq-dynamic phasor impedance of SSSC controlled with impedance control mode
Z_{pSSSC}	Synchronous dq impedance of SSSC controlled with power control mode
Z_{PSSSC}	Generalised dq-dynamic phasor impedance of SSSC controlled with power control mode
$Z_{STATCOMQ}$	STATCOM impedance with reactive power control mode
$Z_{STATCOMV}$	STATCOM impedance with voltage control mode
Z_{synch}	Synchronous machine impedances
Z_{synch_M}	Impedance of synchronous machine including turbine and generator mechanics
Z_{vSSSC}	Synchronous dq impedance of SSSC controlled with voltage control mode

Z_{VSSSC}	Generalised dq-dynamic phasor impedance of SSSC controlled with voltage control mode
ZZ	Electrical part of synchronous machine impedance
Δi_{xd}	Measured current at 1st (x=1) and 2nd (x=2) measurement
$\mathbf{\Delta u}$	Linearized input vector of dimension (r)
Δvv_{xd}	Measured voltage at 1st (x=1) and 2nd (x=2) measurement
Δv_{1dq}	Direct and quadrature axis components of sending end voltage
Δv_{2dq}	Direct and quadrature axis components of receiving end voltage
$\mathbf{\Delta x}$	Linearized state vector of dimension (n)
$\mathbf{\Delta y}$	Linearized output vector of dimension (j)
$\boldsymbol{\lambda'^{\mathbf{r}}_{\mathbf{kdqx}}}$	Damper (x) flux linkage, where x= 1,2
ε_k	Coupling matrices between fundamental frequency and harmonics
$\mu_{k,0}$	Coupling between the harmonics and the fundamental frequency
δ	Firing angle
$\Delta\delta_1$	Internal angle of generator
$\Delta\delta_2$	Internal angle of Section Low pressure A of turbine
$\Delta\delta_3$	Internal angle of Section Low pressure B of turbine
$\Delta\delta_4$	Internal angle of Intermediate pressure of turbine
$\Delta\delta_5$	Internal angle of High pressure of turbine
α	Phase angle between system phase (0 , $-\frac{2\pi}{3}$, $\frac{2\pi}{3}$)
λ_{dq}	Eigenvalues of return ratio matrix
μ	Input control parameter of the d-axis control
ρ	Frequency coupling at the fundamental frequency caused by the existence of positive and negative harmonics at a specific harmonic
σ	Input control parameter of the q-axis control

ABSTRACT

The existence of harmonics and oscillations represent major problems for reliable operation of power system components. Therefore, investigating their response requires finding an appropriate model which reflects their response including these variations. The mathematical derivation of the state space models and impedance models of some of voltage source converters in flexible ac transmission systems (VSC-FACTS) systems is presented using synchronous dq and dq-dynamic phasor approach. Two types of the VSC-FACTS devices are studied in this thesis; the static synchronous compensator (STATCOM) due to its popularity in the power system network and static synchronous series compensator (SSSC) due to its effective on damping system oscillations. The effect of mechanical section of the synchronous machine and turbine sections on the machine impedance is analysed. A generalised state space and impedance modelling is proposed by converting the synchronous dq models to dq-dynamic phasor models. A development of harmonic stability criteria for the proposed modelling is presented. The proposed modelling is employed to present the harmonics effect on the STATCOM and SSSC response and to identify their unbalanced operation in frequency domain. The main features of the proposed modelling technique are compared comprehensively with the conventional modelling techniques for stability studies assessment. It shows the advantages of proposed method and the importance of including the harmonics in the stability studies. A comparison between different control modes of the SSSC is discussed in the frequency domain. The effectiveness of these control modes on damping system oscillations is investigated using the impedance concept. It presented the effectiveness of impedance control mode on damping system oscillations over the other control modes. A fast impedance measurement unit (IMU) is proposed to monitor the small signal stability. The proposed IMU can measure accurately the system impedance within a very short time without any filtering requirements. The effect of changing the STATCOM control gains on the impedance norm is investigated. Also, the effect of shunt and series virtual impedances on the infinite norm of the STATCOM impedance which can be used by network operators to retain the stability is discussed.

TABLE OF CONTENTS

LIST OF TABLES

LIST OF FIGURES

CHAPTER 1

INTRODUCTION

1.1 Background

The existence of voltage source converter based flexible ac transmission systems (VSC-FACTS) has widely increased in recent years. They were proposed to control the operation of transmission systems and damp systems' oscillations. Since the first introduction of the VSC-FACTS devices, several connections to the grid and topologies have been proposed such as shunt, series and shunt-series connections. Analysing their performance requires finding an appropriate model which reflects the device's response in different operating conditions. Modelling the steady-state operation of VSC-FACTS is usually carried out using simple modelling techniques such as voltage or current supply where the devices' dynamics are ignored. However, the transient response of these devices needs more attention due to the huge parameters that affect it. In addition, modelling of these devices becomes harder to develop in the presence of harmonics and predicts their response. Therefore, the proper modelling of VSC-FACTS devices is essential in order to assess their stability in presence of harmonics or unbalanced conditions [1]. Modelling of VSC and its application in power system for transient conditions has been presented in the literature using different techniques. The efficiency and suitability of these techniques vary depending on the application and the accuracy required. For instance, detailed modelling can reflect most of the VSC-FACTS response, however, it increases the computational time thereby imposing a practical limitation on the number of components that can be simulated simultaneously [2]. Similarly, the implementation of Park's transformation (synchronous dq) to the time domain variables is commonly used transformation coordinates to model systems and analyse their stability. However, it is unable to represent all harmonic frequencies that might co-exist at power frequency and affect steady-state and dynamic operation

of the system [3][4]. Alternatively, the dynamic phasor approach, which is extracted from time-domain differential equations, offers numerous benefits compared to traditional modelling approaches [5]. The dynamic phasor covers a broad bandwidth of frequencies where it uses a small integration step at high frequencies and increases the integration steps at lower frequencies. It is more appropriate for small signal studies where the dynamic phasor parameters are time-invariant parameters which reduce errors due to system linearization. Two forms of dynamic phasor modelling have been introduced, the abc-dynamic phasor and dq-dynamic phasor. The first type suffers from a large number of equations required for modelling as well as it does not suit the modelling control systems. The dq-dynamic phasor technique uses fewer equations and is more suitable for stability analysis and it could model different types of control systems.

The existence of harmonics and oscillations are found over a wide range of frequencies which represent major problems for the reliable operation of power systems. These harmonics and oscillations could be initiated by different events in the power system; for example, low-frequency oscillations can be initiated due to the sub-synchronous resonance (SSR), while the high-frequency variations are largely initiated by switching of power electronics converters [6][7]. In the literature, including the harmonics in the modelling was carried out by mapping the input frequencies to the output. Frequency mapping produces infinite outputs with possibly infinite harmonics due to the interaction between different frequencies within the system. Neglecting higher order harmonics to enforce frequency mapping could lead to a significant error on the modelling due to the influence of some of truncated harmonics. Thus it is important to select all frequencies which are relevant to the study under consideration and ignore those are irrelevant [8].

1.2 Research motivation

Two methods were found in the literature based on the frequency mapping concept; the harmonic linearization method and harmonic state space (HSS) method. The inclusion of harmonics in modelling using harmonic linearization method has a disadvantage as it does not include the frequency coupling between the studied

harmonics without the transformation via the symmetrical components. Alternatively, with the high order matrices utilised by HSS, it is difficult to study the unbalanced systems and the time-variant parameters which enforce the linearization to be around this time-periodic operating trajectory, not around the steady-state operating point, are the main disadvantages [9][10]. It the literature, the implementation of the generalised form of dq-dynamic phasor has not been widely presented to study systems' stability and unbalanced conditions identification. The use of dq-dynamic phasor modelling in stability analysis offers significant advantages over the HSS counterpart; for example, it has reduced the order of matrices, is more suitable for studying control systems, retains mutual coupling of harmonics, and simplifies stability study under unbalanced conditions. Also, dq-dynamic phasor parameters are linearized around steady-state point like synchronous dq which reduces the error of linearization compared to HSS. In addition, it is valid for studying the stability of complex power electronics devices such as VSC-FACTS devices with the presence of harmonics and unbalanced networks without the need for any transformation. The dq-dynamic phasor modelling manages to reproduce the typical response of VSC-FACTS device at the fundamental frequency as well as at significant harmonics.

1.3 Research objectives

- Develop state space models and impedance models for small signal stability analysis using dq-dynamic phasor approach.
- Design an impedance measurement unit for fast monitoring and assessment of system stability.
- Investigate the effect of harmonics and oscillations on the response of VSC-FACTS devices and their damping capabilities.

1.4 Thesis methodology

In this thesis, to successfully include the harmonics in modelling of VSC-FACTS devices and present their effect and their control method, the following research activities will be conducted:

- Derive the synchronous dq models of VSC-FACTS devices and their transformation to dynamic phasor.
- Investigate the characteristics of dynamic phasor modelling on presenting the performance of VSC-FACTS devices.
- Propose generalised state space and impedance model of STATCOM using dq-dynamic phasor modelling
- Propose generalised state space and impedance model of SSSC for three different control types using dq-dynamic phasor modelling.
- Present the efficiency of proposed modelling methods when including harmonics and identifying the unbalanced conditions.
- Propose an impedance monitoring unit (IMU) for the application of stability control and fast monitoring.
- Assess the contribution of VSC-FACTS devices' control parameters and other active techniques on stability.
- Compare the effectiveness of SSSC on damping system oscillation and the effect of harmonics on their operation.

1.5 Thesis layout

The thesis comprises seven chapters as follows:

- Chapter 1 gives an introduction to the thesis and presents its background and thesis outlines.
- Chapter 2 presents a literature review of modelling techniques and presents a comprehensive survey in harmonic stability assessment and identification.
- Chapter 3 presents the modelling of the static synchronous series compensator (SSSC), static synchronous compensator (STATCOM) devices and synchronous machine using synchronous dq coordinates and the dq-dynamic phasor approach.
- Chapter 4 discusses stability problems and the stability criteria used to assess system's performance in the synchronous dq frame. Secondly, the mathematical derivation of the state space equations and impedances of the SSSC, STATCOM is presented. Lastly modelling the synchronous machine is introduced as it will be required for the stability analyses in the following chapters.

- Chapter 5 presents firstly a development of harmonic stability criteria for dq-dynamic phasor modelling. Secondly, a generalised state space and impedance models of STATCOM and SSSC with different control modes using dq-dynamic phasor are proposed. Lastly, the chapter presents a comparison between the proposed modelling and the conventional modelling techniques.
- Chapter 6 introduces an impedance measurement unit (IMU) for the application of control system-based impedance concept and fast monitoring application. Also, the chapter presents the effect of changing the STATCOM parameters on the impedance norms. It presents the effect of implementing control parameters (virtual impedance) on the infinite norm of STATCOM impedance. Lastly, the effectiveness of the SSSC is investigated on re-shaping the network impedance to stabilise the system or damping the system oscillations.
- Chapter 7 presents the conclusions and author's contributions, including remarks and recommendations for further research on the field of VSC modelling.

CHAPTER 2

MODELLING AND STABILITY ANALYSIS TECHNIQUES

In this chapter, a review of voltage source converters modelling in flexible ac transmission systems (VSC-FACTS) for stability assessment is presented. The review shows also the capability of modelling techniques of including and identifying the harmonics and oscillations in stability studies.

2.1 Modelling techniques of VSC- FACTS devices

The application of VSC-FACTS has been introduced widely in the literature. These applications require more attention in modelling to reflect their actual response under steady-state and transient-state conditions. They vary in complexity, accuracy as well as the suitability to different operating conditions. The modelling approach, the integration method and different target of modelling are the main reasons that challenge the interfacing and the selection between the modelling techniques [11]. The main classification of the modelling techniques for stability assessment is shown in Figure 2.1 and they are classified as:

2.1.1 Time domain detailed modelling

Time domain detailed modelling or called abc modelling is one of the first modelling techniques implemented to represent the power system response in balanced and unbalanced conditions. Each phase of the modelled system is represented by its magnitude multiplied by a sinusoidal function of its frequency, time and phase shift. It provides the basis for deriving other modelling techniques [12][13]. A system's stability can be assessed by the mathematical modelling or using simulations in the time domain [14][15]. Usually, time domain modelling is carried using a single phase to reduce the complexity of the analysis.

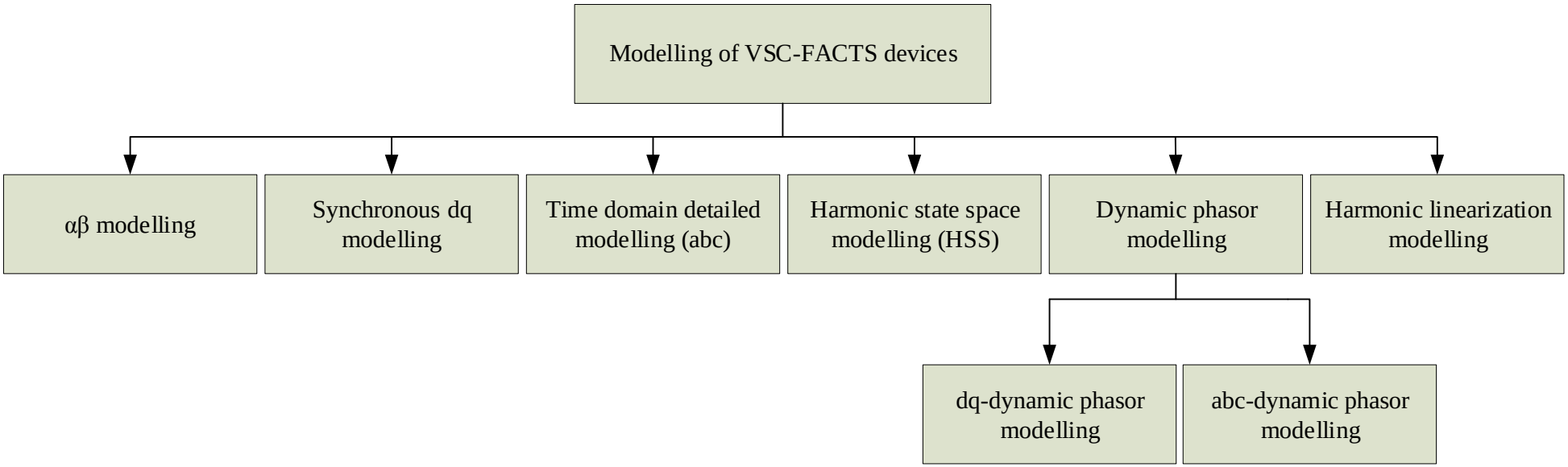

Figure 2.1. Classification of VSC-FACTS modelling

In the meantime, the use of time domain simulations is much simpler where no mathematical model is required. It was employed to assess the effect of time delays in communication signals on system stability [14] and to present the effectiveness of HVDC control system as in [15]. Even though abc modelling is a powerful technique that can represent the response of any system such as VSC-FACTS systems accurately and effectively, it is inefficient due to the presence of variable quantities even at steady state conditions. The existence of variable quantities increases the error due to the linearization in small signal stability studies. Also, the time domain simulation introduces little insight into the system and is less sensitive to small changes in the system parameters [16].

2.1.2 Synchronous dq modelling

Synchronous dq or Park's transformation provides a unique form of describing the three phase quantities in two rotating dc component located at quadrature coordinates by shifting system's frequencies by $(\pm\omega)$ [17]. It has advantages of modelling balanced and unbalanced systems by applying a single coordinate and two coordinates respectively. The synchronous dq quantities are linear time invariant (LTI) quantities which suit small signal stability studies where the operating point can be linearized around a steady state point. The implementation of synchronous dq modelling is commonly used coordinate to analyse the systems and their stabilities such as the work in [3], [4], [9], [10]. Also, it was employed in well-known state space models and impedance models for small signal stability studies [18][19]. The former models were used to show the instability of the system and oscillations for the whole studied network while the latter were used to predict the system's oscillations and stability at the point of connection with limited observability compared with state space analysis [20]. The synchronous dq impedance models were successfully implemented in the application of detecting system's oscillations in [21][22], and on studying the effect of control gains on the system stability in [23][24]. In addition, the synchronous dq models were employed to study the interaction between different power system components such as in [25]–[27], and to study the stability of the dc-

link of a VSC connected to a weak grid [28]. The main disadvantage of synchronous dq modelling is its limited capability to include harmonics in the modelling using single coordinate.

2.1.3 $\alpha\beta$ modelling

$\alpha\beta$ modelling transforms a three-phase system into a two-phase stationary orthogonal system [29].This refer to the fact that each component of the three-phase system can always be expressed by two components. $\alpha\beta$ modelling is superior in modelling large system over the use of other modelling techniques such as synchronous dq modelling where it uses a single stationary frame rather than using multiple frames [30]. In one application, the $\alpha\beta$ model was used to simplify the stability assessment of a VSC based system by converting the system into a single input single output system as positive and negative sequence system. This concept was employed in [31] to study a VSC connected to a grid. However, ignoring the frequency coupling between the sequence quantities can affect the results of analysing large systems where couplings usually present. Alternatively, in [32][33], the coupling between the positive sequence and negative sequence quantities was considered. The relationship between $\alpha\beta$ modelling and different modelling techniques was revealed in [30]. The work was employed to study the effect of phase locked loop (PLL) behaviour on VSC response using an impedance model. The main disadvantage of this analysis was its limited capability for frequencies more than twice the fundamental frequency. Furthermore it cannot include system harmonics using single coordinates [34]. In addition, the time-varying nature of the $\alpha\beta$ modelling components is not suitable for system linearization over small signal disturbances.

2.1.4 Harmonic linearization modelling

In harmonic linearization modelling, the system inputs are expanded by an infinite number of harmonics which are convoluted to produce an infinite number of output harmonics [35]. It has an advantage of including selected harmonics in the stability analysis and presents their effect on the output of the modelled system. Harmonic linearization modelling was employed in different applications in literature. It was

employed to study the interactions between VSC-FACTS devices and other system components in [36][37]. Also, it was used to derive the impedance model of VSC including PLL response and digital control delay such as in [38]. Representing balanced and unbalanced systems was another application of harmonic linearization modelling. It was utilised to study unbalanced systems by the help of symmetrical component theory in [38] and by including the unbalance as a new variable in the analysis as in [39]. Harmonic linearization modelling was also used to design the components of VSC-FACTS devices in the existence of harmonics such as in [40]. It was employed to design the optimal static synchronous compensator (STATCOM) based pulse width modulation (OPWM) to ensure the effective operation of STATCOMs when harmonics were present. Even though harmonic linearization modelling can reveal the frequency coupling between the positive and negative sequence quantities, the modelling cannot present the frequency coupling that might occur between other existing harmonics in case of linear time invariant (LTI) parameters has been employed.

2.1.5 Harmonic state space (HSS) modelling

Harmonic state space modelling is based on Fourier series analysis of system quantities. It decomposes the dynamic system quantities according to their frequencies to be presented by complex exponential quantities. HSS maps these exponentially modulated periodic (EMP) of the input signal and the EMP of the output signal in linear time-periodic (LTP) systems [41][42]. The linear operator that maps the frequencies is called the harmonic transfer function (HTF) [43]. HSS modelling can be used to identify the causes of the oscillations in the systems as well as to present the effect of these oscillations on system response. In system modelling including harmonics, harmonic state space modelling presents an advantage in comparison with other conventional techniques such as synchronous dq and $\alpha\beta$ modelling [44]. This refers to their capability of including the harmonics and presenting the frequency coupling between harmonics. The effectiveness of this modelling was presented also using the experimental work where the eigenvalues of HSS modelling were compared with the eigenvalues of a model based measurement [45]. The use of HSS modelling in stability assessment was presented in [46][1]. It

was employed to study the balanced and unbalanced operation of VSC-FACTS and their interface with the system in the presence of harmonics. Also, HSS modelling was utilised to present a comprehensive understanding of the HVDC system [47]. It was used to present the transformation of system harmonics between the ac and dc sides of a HVDC system as well as the frequency coupling in each stage of the studied system. The high order matrices utilised by HSS modelling, the difficulty of studying the unbalanced systems without the use of reduced forms of HSS and the time-variant parameters which enforce the linearization to be around this time-periodic operating trajectory are the main disadvantages of this method.

2.1.6 Dynamic phasor modelling

Dynamic phasor modelling was developed based on the generalised average modelling using the time varying Fourier coefficient in complex form [9]. It converts the ac periodic parameters to dc parameters which reduce the simulation time and suits the small signal stability studies. Dynamic phasor modelling can include harmonics and investigate the unbalanced conditions of the systems.

The utilisation of dynamic phasor approach for modelling and developing interfacing algorithms was widely presented in the literature. Alternatively, the use of these modelling in stability assessment has been rarely mentioned. For modelling of balanced VSC-FACTS systems, the main targets of dynamic phasor modelling were reduce the simulation time and present an average response of the modelled systems such as in [53]–[57], therefore, the fundamental frequency was used in the derivation. In the meantime, the modelling of unbalanced VSC-FACTS systems was usually carried out by the help of symmetrical component theory which converts the abc form of the dynamic phasor into dynamic symmetrical components [58]–[61].

The implementation of dynamic phasor modelling for stability assessment was usually carried out using the abc-dynamic phasor components. Such a use increases the number of equations required for the analysis. Therefore, single-phase models were used to simplify the analysis. Even though, the use of these models has a disadvantage of the limited capability to study the unbalanced systems. It has several advantages in comparison with the other modelling technique such as synchronous

dq modelling [62]. These advantages have been employed to design a solid state transformer controller in the presence of disturbances using state space analysis [63]. Also, dynamic phasor modelling was utilised to identify the low frequency oscillations present in series compensated systems. It was employed in a state space model to study the effect of phase unbalance on system oscillations [64]. Similarly, the small signal impedance of a single-phase dynamic phasor model was utilised to identify the causes of sub-synchronous resonance (SSR) [65]. The formulation of the diagonal impedances as pure real and pure imaginary impedances are entirely ambiguous, where in fact, all impedances are in a complex form. Also, the implementation of single-phase models and disregarding the co-existence of SSR frequencies in the analysis can affect the results where the model is unable to capture system characteristics during dynamic conditions [7], [66], [67]. Using more comprehensive model, the harmonics were included in a stability assessment in [68]. The analysis employed the fundamental and second harmonics for the converter's dc side and the fundamental frequency for the ac side. The main limitation of this work was the derivation has been made for specific harmonics and was not made to include more harmonics. In general, the main limitations of previous work on dynamic phasor modelling were the use of abc-dynamic phasor and the consideration of the fundamental frequency only in the analysis. This reduces the benefit of dynamic phasor modelling and its application on system analysis. Also, the use of abc-dynamic phasor modelling is not suitable to include the control systems and studying the unbalanced operations without transforming system parameters. Therefore, the use of the dq-dynamic phasor modelling for stability analysis can get rid of these limitations as well as the limitations of the other modelling techniques that have been presented in the previous sections.

2.2 Small signal Impedance measurement

The measurement of the dq small-signal stability is proposed in [69] using several practical methods such as power converters for low power applications, chopper circuit for high power application and wound-rotor induction machines using phase injection. Also, the paper developed the stability criteria based on dq synchronous frame. Alternatively, the researchers in [70] and [71] proposed an algorithm based on

the line-to-line injection using chopper circuit to measure the dq impedance. In [72], the paper presented a design of a measurement unit for medium grid voltage applications. Due to the dependent of the power demand on the system frequency on droop controlled microgrids, the paper in [73] proposed an injection circuit using three-phase buck converter for passive loads. In the meantime, the injected signal was proposed on different forms such as sinusoidal waveform [69],[70] and [72] or as chirp signal such as in [74]. The second method reduced the measurement time of the impedance considerably because it generates different frequencies over a short period. The advantage of such method is reducing the possibility of changing the system states during the measurement. Implementing the online impedance measurement as an ancillary function within the grid side converter was proposed in [75] which has importance on monitoring systems' stability. The estimation of the grid positive and negative sequence impedances was done by injecting pulses of currents from the converter and analysed the measured signal using online discrete Fourier transform (DFT). The comparison of the measurement circuit results with the offline measurement showed a proper alignment. The necessity to inject a continuous harmonics is the main limitation of such measurement unit in the practical use. As stated, the use of impedance measurement in fast monitoring of system stability has not been mentioned in the literature. So, this thesis proposes an impedance measurement unit (IMU) which can be employed by network operators or a supplementary control system to retain the stability.

2.3 Summary

Different modelling techniques of VSC-FACTS system for stability studies were reviewed. The main finding and the outcomes can be summarised as:

- The selection between modelling techniques depends on the application and the accuracy required in the output results.
- Synchronous dq modelling and $\alpha\beta$ modelling can be used to identify the causes of harmonics. Both modelling techniques are unable to assess the contribution of harmonics to the system response using single coordinate. The implementation of

the fundamental frequency in these models and neglecting of the co-existence harmonics can affect the stability assessment.

- Harmonic linearization modelling cannot present the frequency coupling between the harmonics once the LTI modelling has been used. The modelling can present the coupling between the positive and negative sequence quantities of the studies system.
- Even though harmonic state space (HSS) is a generalised modelling technique that can include harmonics, it has high matrix orders and it is difficult to use when studying unbalanced systems.
- The HSS enforces the linearization to be carried out around time-periodic operating trajectory not around the steady-state operating point as linear time invariant system which could lead to an error in the results of the derived model.
- In the literature, dynamic phasor modelling was carried out at the fundamental frequency and ignored the effect of harmonics. In addition, it used the abc-dynamic phasor to analyse the balanced and unbalanced systems, where, studying unbalanced systems was carried out using symmetrical components which enforces additional transformation of the system quantities.
- The use of impedance analysis is more visible for the new electrical installation and offline studies rather than the online stability studies. This is referred to the injected harmonics required for impedance measurement which could enforce a limitation on the use of impedance based assessment.

CHAPTER 3

DQ-DYNAMIC PHASOR MODELLING OF VSC-BASED FACTS DEVICES

In this chapter dq-dynamic phasor modelling of the VSC-FACTS devices and other power system components is presented. These models will be used to analyse the operation of VSC-FACTS devices and their controllers for small signal stability analysis.

3.1 Dynamic phasor based modelling (DP modelling)

Power system operation experiences two types of transients; high frequency transients and low frequency transients. The dynamic phasor approach provides adequate modelling of a wide range of frequencies rather than using specific modelling for each specific range such as electromagnetic transient (EMT) or transient stability models [76]. The integration of the system parameters is carried out using small steps at high frequencies and increases to larger steps at lower frequency events. In addition, the dynamic phasor offers numerous benefits compared to traditional modelling approaches, such as it covers a broad bandwidth of frequencies. Also, it is more appropriate for fast numerical simulation, accurate, fast for power components and VSC-FACTS simulation [57], [77]–[79]. Alternatively, the main difference between dynamic phasor modelling and the synchronous dq modelling is that the dynamic phasor modelling shifts all system's frequencies to $(\omega = 0)$ "constant (dc)". However, the synchronous dq transformation shifts all system's frequencies by (ω) as shown in Figure 3.1.

.

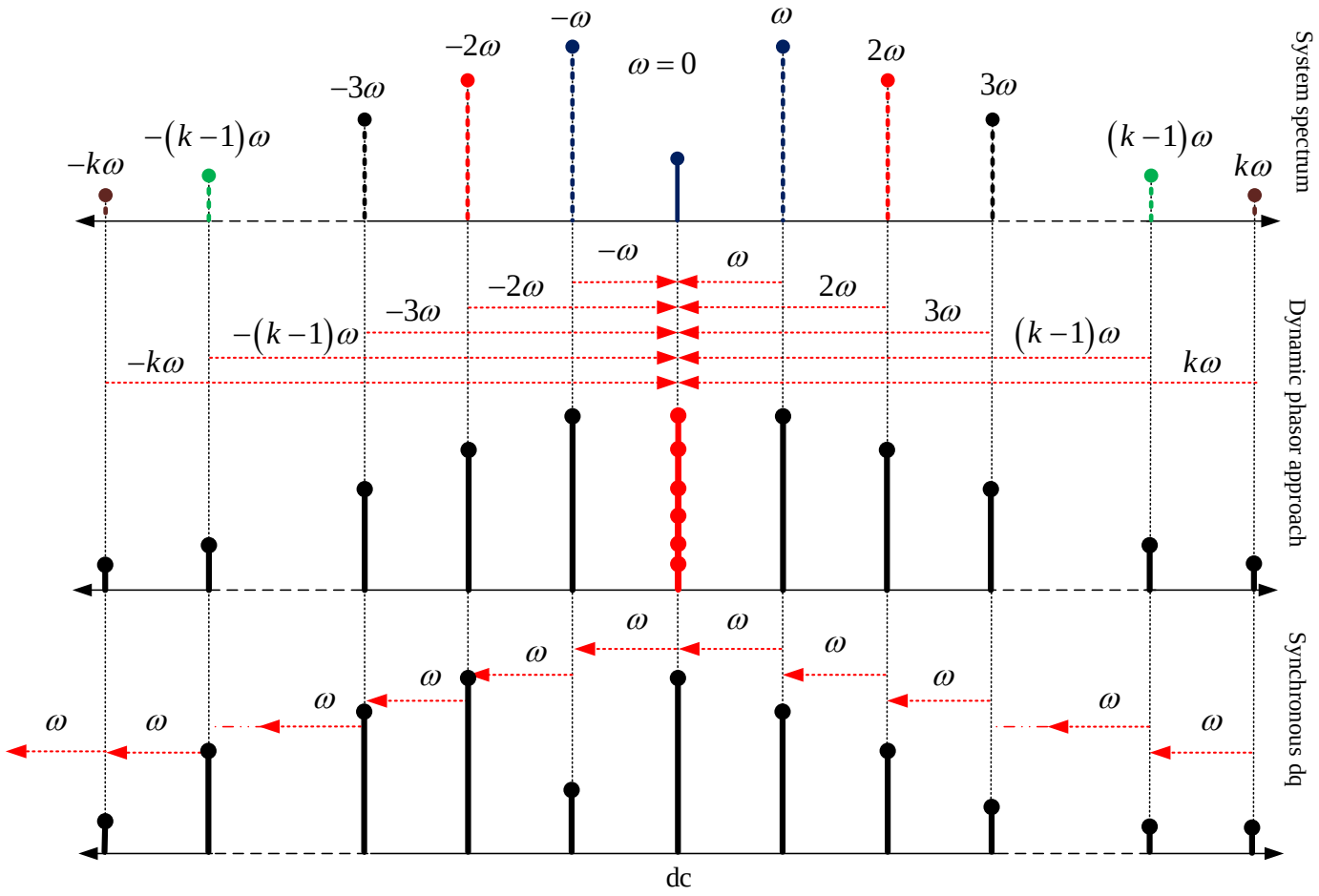

Figure 3.1. Frequency shifting for synchronous dq and dynamic phasor modelling.

Two types of dynamic phasor modelling are proposed and investigated in the literature:

- abc-dynamic phasor modelling: it shifts the three-phase quantities of the studied system to dynamic phasor.
- dq-dynamic phasor modelling: it transforms the synchronous dq quantities to a dynamic phasor. This type of modelling will be employed in this thesis for device modelling and stability analysis in Chapter 5 due to its simplicity and suitability for the VSC-FACTS devices control systems and unbalanced conditions.

Dynamic phasor modelling is extracted from the system time domain equations (differential equations) by the application of the generalised average procedure using time varying Fourier coefficient in complex form. Any complex periodic waveform $x(\tau)$ found on interval $\tau \in (t-T, t)$, can be presented using Fourier series as [80][81]:

$$x(\tau) = \sum_{k=-\infty}^{\infty} X_k(t) e^{jk\omega\tau} \tag{3.1}$$

where,

ω is the fundamental angular frequency.

k is an integer number the represents harmonic order and defines the accuracy of the approximation of the original waveform.

$X_k(t)$ is a function of time representing the complex Fourier coefficient ‘‘dynamic phasor parameter’’ of the periodic signal.

The k^{th} dynamic phasor is determined at time (t) from (3.2) as:

$$X_k(t) = \frac{1}{T}\int_{t-T}^{t} X(\tau) e^{-jk\omega\tau} = x_k \tag{3.2}$$

Two properties of dynamic phasors are used to solve the systems which are:

- The dynamic phasor modelling of the time variable derivative is:

$$\langle \frac{dx}{dt} \rangle_k = \frac{d\langle x \rangle_k}{dt} + jk\omega \langle x \rangle_k \tag{3.3}$$

The property in equation (3.3) can be used exclusively to represent the dynamic phasor quantities of the studied system using the dynamic phasor approach, however, the modelling ignores the coupling between different frequencies [82].

- The second property is that the product of two time domain variables is equal to:

$$\langle xy \rangle_k = \sum_{i=-\infty}^{\infty} \langle x \rangle_{k-i} \langle y \rangle_i \tag{3.4}$$

Equation (3.4) can be expanded to more than two variables using the same technique as depicted in Appendix-A. It is a valuable feature of the dynamic phasor which represents the interaction between different frequencies in the system. The modelling using dq-dynamic phasor approach requires extracting its Fourier coefficients which can be extracted by generalising the Euler form of the measured quantities. The voltage vector (v_i) including harmonics is given [80]:

$$v_i = \sum_{k=\pm\infty} V_k \cos(k\omega t + \alpha) \tag{3.5}$$

where,

i is phases (a, b or c).

V_k is the voltage magnitude.

α is the phase angle between system phases (0 , $-\frac{2\pi}{3}$, $\frac{2\pi}{3}$).

Substituting equation (3.5) by its Euler form will result in:

$$v_i = \sum_{k=\pm\infty} \frac{\vec{v}e^{jk\omega t} + \vec{v}e^{-jk\omega t}}{2} \tag{3.6}$$

The transformation of equation (3.6) to dq by shifting it by $\left(e^{-j\omega t}\right)$ with some rearrangement and multiplying it by (2/3) to have a generalised form gives:

$$\vec{\boldsymbol{V}}e^{-j\omega t} = v_d + jv_q = \frac{2}{3}(v_a + a^2 v_b + a v_c)e^{jn\omega t} \tag{3.7}$$

Multiplying equation (3.7) by $\left(e^{j\omega t}\right)$ gives:

$$\vec{\mathbf{V}} = v_d + jv_q = \left(v_{dk} + jv_{qk}\right) + \sum_{\substack{n=-\infty \\ k\neq n}}^{\infty}\left(v_{dn} + jv_{qn}\right)e^{j(n-k)\omega t} \tag{3.8}$$

where,

The bold symbols in previous equations represent the voltage vector,

n is a vector of all positive and negative harmonic orders except (k).

v_{dk} is the direct voltage at harmonic order (k).

v_{dk} is the quadrature voltage at harmonic order (k).

The existence of any harmonic on the abc domain is transformed into two harmonics in the dq-dynamic phasor which means that two main oscillatory frequencies will be generated as shown in equation (3.8). This doubles the number of equations in dynamic phasor compared with the number of equations in synchronous dq modelling. The dq-dynamic phasor can represent balanced and unbalanced operating conditions using the same modelling. Positive and negative sequence quantities are generated from each frequency present in the time domain quantities. The coefficient $(-k = \bar{k})$ represents the negative sequence components of the system and the coefficient $\left(\bar{k} = -2\right)$ represents the unbalanced conditions. The measured quantities are transformed into dq-dynamic phasor quantities at each harmonic (k) of interest. Then the output signal is filtered using a low pass filter to get rid of the other harmonics as shown in Figure 3.2.

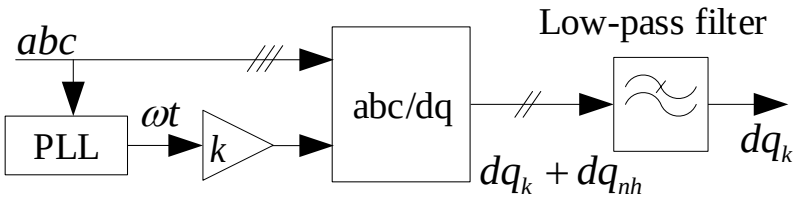

Figure 3.2. Dynamic phasor parameter extraction.

The chosen harmonics order (k) is different between the ac quantities, dq quantities and dc quantities. For example, harmonics order (k) at the fundamental frequency for the ac quantities is equal to 1, while at the fundamental frequency for the dq and dc systems will be equal to zero. From the fundamental frequency prospective, the 2nd harmonic in the dq appears in dq-dynamic phasor based on the initiation of this harmonic in the abc coordinate. The 3rd harmonic appears as 2nd harmonic rotates clock wise and the unbalance rotates in the opposite direction as shown in Figure 3.3. This can be explained using equation (3.8). Shifting the voltage vector by $e^{-j\omega t}$ at the fundamental frequency generates a 2nd order component at ($k = -2$) while, shifting the voltage vector by $e^{-j2\omega t}$ for the 3rd harmonic generates a 2nd harmonic at ($k = 2$). It is noted that pre-knowledge of the system harmonics and behaviour helps to reduce the number of equations required to represent the system and consequently reduces the modelling complexity.

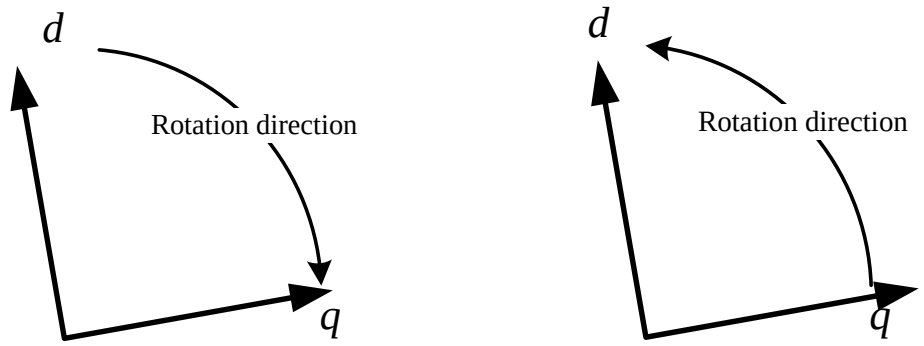

(a) (b)

Figure 3.3. The existence harmonic and unbalance in dq-dynamic phasor:

(a) 2nd harmonic due to 3rd abc harmonic, and (b) 2nd harmonic due to unbalance.

3.2 Modelling some of power system components

The modelling of the basic components of FACTS devices is presented in this section as well as the synchronous machine.

3.2.1 Voltage source converter

The voltage source converter (VSC) is considered to be a key component of VSC-FACTS devices. It can be found in these devices as a single VSC such as SSSC or STATCOM, or back-to-back VSC such as the UPFC. Figure 3.4 shows the basic structure of a three-phase VSC. The mathematical derivation is carried out with assumption that the VSC operates in three phase balanced conditions. The converter voltage and current relations can be derived as follows:

$$v_{ca} = (v_{dc} - r_c . i_{ca}) . S_a - (i_{ca} . r_c) . S'_a + v_{NE} \tag{3.9}$$

where,

v_{ca} is the converter output voltage for phase a.

v_{NE} is the voltage between dc reference point (N) and earth (E).

i_{ca} is the converter current.

r_c is the converter resistance.

S'_a and S_a are the switching function of bridge arm of phase (a) ($S_a + S'_a = 1$).

For power system studies, eliminating the high order frequencies and considering the fundamental and dc component is an acceptable approximation to get the equivalent dynamic phasor model of switching functions [13]. By substituting the switching functions relations in (3.9), and by considering the system is balanced and adding the three phase voltages to get the output voltages ($\mathbf{v_{c\_abc}}$) as:

$$\mathbf{v_{c\_abc}} = \frac{m_c}{2} v_{dc} . cos\left(\omega t - \boldsymbol{\delta}_{\mathbf{c\_abc}} + \boldsymbol{\alpha}_{\mathbf{abc}}\right) - r_c . \mathbf{i_{c\_abc}} \tag{3.10}$$

where,

m_c is the modulation index.

δ is the firing angle.

v_{dc} is the dc link voltage.

The bold symbols represent the vectors of parameters which equal for equation (3.10) as:

$$\mathbf{v_{c\_abc}} = [v_{c\_a} \quad v_{c\_b} \quad v_{c\_c}]^T \qquad \mathbf{i_{c\_abc}} = [i_{c\_a} \quad i_{c\_b} \quad i_{c\_c}]^T$$

$$\boldsymbol{\delta}_{\mathbf{c_{abc}}} = [\delta_{c_a} \quad \delta_{c_b} \quad \delta_{c_c}]^T \qquad \boldsymbol{\alpha}_{\mathbf{abc}} = \left[0 \quad -\frac{2\pi}{3} \quad \frac{2\pi}{3}\right]$$

Moreover, the current equation could be as:

$$\mathbf{i_{c\_abc}} = m_c C_{dc} . \frac{dv_{dc}}{dt} . cos\left(\omega t - \boldsymbol{\delta}_{\mathbf{c_{abc}}} + \boldsymbol{\alpha}_{\mathbf{abc}}\right) - C_{dc} \frac{dv_{dc}}{dt} \tag{3.11}$$

The dq format of equations (3.10) and (3.11) is given by:

$$\mathbf{v_{cdq}} = \mathbf{m_{cdq}} v_{dc} - r_c \mathbf{i_{cdq}} \tag{3.12}$$

$$\mathbf{i_{cdq}} = C_{dc} \frac{dv_{dc}}{dt} \mathbf{m_{cdq}} - C_{dc} \beta \frac{dv_{dc}}{dt} \tag{3.13}$$

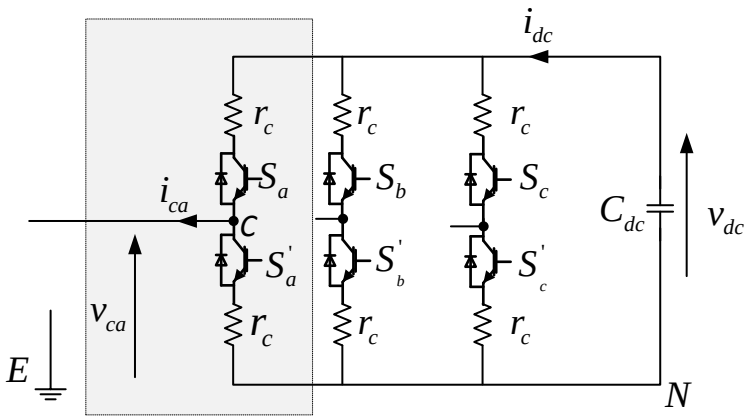

Figure 3.4. Voltage source converter (VSC).

where,

$\mathbf{v_{cdq}} = [v_{cd} \quad v_{cq}]^T$ $\mathbf{i_{cdq}} = [i_{cd} \quad i_{cq}]^T$

$\beta = [1 \quad 0]^T$ $\mathbf{m_{cdq}} = [m_{cd} \quad m_{cq}]^T$

C_{dc} is the dc link capacitance.

The dq-dynamic phasor is given by transforming equations (3.12) and (3.13):

$$\langle \mathbf{v_{cdq}} \rangle_\mathbf{k} = \langle \mathbf{v_{dc}} \mathbf{m_{dq}} \rangle_\mathbf{k} - r_c \langle \mathbf{i_{cdq}} \rangle_\mathbf{k} \tag{3.14}$$

$$\langle \mathbf{i_{cdq}} \rangle_\mathbf{k} = C_{dc} \langle \frac{\mathbf{dv_{dc}}}{\mathbf{dt}} \mathbf{m_{dq}} \rangle_\mathbf{k} - C_{dc} \beta \langle \frac{dV_{dc}}{dt} \rangle_k \tag{3.15}$$

where the vectors in equations (3.14) and (3.15) are defined as:

$$\langle \frac{\mathbf{dv_{dc}}}{\mathbf{dt}} \mathbf{m_{dq}} \rangle_\mathbf{k} = \left[\langle \frac{dv_{dc}}{dt} m_d \rangle_k \quad \langle \frac{dv_{dc}}{dt} m_q \rangle_k \right]^T$$

$$\langle \mathbf{v_{dc}} \mathbf{m_{dq}} \rangle_\mathbf{k} = [\langle v_{dc} m_d \rangle_k \quad \langle v_{dc} m_q \rangle_k]^T$$

It is noted from equations (3.14), (3.15) that the current at fundamental frequency as well as at the harmonics are coupled due to the existence of the harmonics and fundamental frequency terms respectively in these equations.

3.2.2 The dc link of VSC-FACTS devices

The dc branch is one of the main components of the VSC-FACTS devices, where the energy stored in the dc capacitor is used to compensate the dc link voltage change. The power balance at the dc side of the VSC-FACTS devices including the losses is given by:

$$P_{ac} - P_{dc} - P_{loss} = 0$$

$$\frac{3}{2} v_d . i_d + \frac{3}{2} v_q . i_q - C_{dc} v_{dc} \frac{dv_{dc}}{dt} - i_d^2 . R = 0 \tag{3.16}$$

where,

R is the sum of the converter (r_c), filter (r_f) and transformer resistances (r_t).

v_{dq}, i_{dq} are the voltages and currents of ac side in the synchronous dq frame.

The dc link plays a crucial role in the coupling between harmonics in VSC-FACTS devices operations as shown in equations (3.14) and (3.15). This coupling is caused due to the variation in the ac power as presented in equation (3.16).

3.2.3 Harmonics filter

The operation of VSC is normally accompanied with certain harmonics due to several causes such as the switching of its converter which requires filitering those harmonics. From Figure 3.5, the voltage injected (phase a) to the transformer if required can be derived using Kirchhoff's voltage law (KVL) to get the three phase form (abc) as:

$$\mathbf{v_{inj\_abc}} = \mathbf{v_{c\_abc}} - l_f \frac{d}{dt} \mathbf{i_{c_{abc}}} - r_f . \mathbf{i_{c\_abc}} \tag{3.17}$$

$$\mathbf{i_{inj\_abc}} = \mathbf{i_{c\_abc}} - C_f \frac{d}{dt} \mathbf{v_{inj\_abc}} \tag{3.18}$$

where,

l_f is harmonic filter inductance.

C_f is harmonic filter capacitor.

$\mathbf{v_{inj\_abc}}$ is harmonic output voltage or the injected voltage:

$\mathbf{v_{inj\_abc}} = [v_{inj_a} \quad v_{inj_b} \quad v_{inj_c}]^T$

$\mathbf{i_{inj\_abc}}$ is harmonic output current or the injected current:

$\mathbf{i_{inj\_abc}} = [i_{inj_a} \quad i_{inj_b} \quad i_{inj_c}]^T$

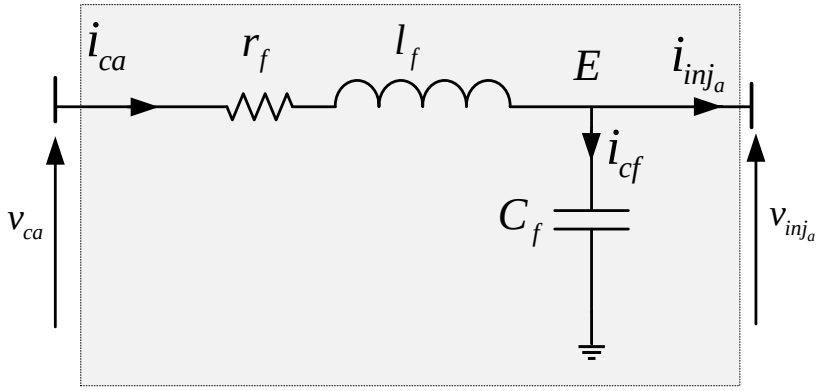

Figure 3.5. Harmonic filter circuit.

Equations (3.17) and (3.18) can be transformed into dq format as:

$$\mathbf{v_{inj_{dq}}} = \mathbf{v_{cdq}} - L_f \frac{d}{dt}\mathbf{i_{cdq}} + \left(\gamma\omega_0 l_f - r_f\right)\mathbf{i_{cdq}} \tag{3.19}$$

$$\mathbf{i_{inj_{dq}}} = \mathbf{i_{cdq}} - C_f \frac{d}{dt}\mathbf{v_{cdq}} + \gamma\omega_0 C_f . \mathbf{v_{cdq}} \tag{3.20}$$

where,

$\mathbf{v_{cdq}} = [v_{cd} \quad v_{cq}]^{\boldsymbol{T}}$ $\qquad$ $\mathbf{i_{inj_{dq}}} = [i_{inj_d} \quad i_{inj_q}]^{\boldsymbol{T}}$

$\mathbf{v_{inj_{dq}}} = [i_{inj_d} \quad i_{inj_q}]^{\boldsymbol{T}}$ $\qquad$ $\mathbf{i_{cdq}} = [i_{cd} \quad i_{cq}]^{\boldsymbol{T}}$

$\gamma = \begin{bmatrix} 0 & 1 \\ -1 & 0 \end{bmatrix}$

The transformation of equations (3.19) and (3.20) to dynamic phasor form yields:

$$\langle \mathbf{v_{inj_{dq}}} \rangle_{\mathbf{k}} = \langle \mathbf{v_{cdq}} \rangle_{\mathbf{k}} - L_f \frac{d}{dt}\langle \mathbf{i_{cdq}} \rangle_{\mathbf{k}} + \left(\gamma\omega L_f - r_f - jk\omega L_f\right)\langle \mathbf{i_{cdq}} \rangle_{\boldsymbol{k}} \tag{3.21}$$

$$\langle \mathbf{i_{inj_{dq}}} \rangle_{\mathbf{k}} = \langle \mathbf{i_{cdq}} \rangle_{\boldsymbol{k}} - C_f \frac{d}{dt}\langle \mathbf{v_{inj_{dq}}} \rangle_{\mathbf{k}} + (\gamma - jk)\omega C_f \ \langle \mathbf{v_{inj_{dq}}} \rangle_{\mathbf{k}} \tag{3.22}$$

3.2.4 Series injection transformer

To integrate the VSC model with power network, the equivalent circuit of series transformer should be taken into consideration. For simplicity, the transformer inductances and resistances are lumped on the secondary side of the transformer, and the magnetisation branch is neglected (approximate equivalent circuit) for a transformer with a turns ratio of 1:1, as in Figure 3.6:

$$\mathbf{v}_{\boldsymbol{L}_{\mathbf{abc}}} = \mathbf{v}_{\mathbf{pcc\_abc}} + \mathbf{v}_{\mathbf{inj\_abc}} - L_t \frac{d}{dt} \mathbf{i}_{\mathbf{pcc\_abc}} - r_t \mathbf{i}_{\mathbf{pcc\_abc}} \tag{3.23}$$

where,

r_t is the resistance of series transformer L_t is the inductance of series transformer

$\mathbf{v}_{\boldsymbol{L}_{\mathbf{abc}}} = [v_{L_a} \quad v_{L_b} \quad v_{L_c}]^T$ $\mathbf{i}_{\mathbf{pcc\_abc}} = [i_{pcc_a} \quad i_{pcc_b} \quad i_{pcc_c}]^T$

$\mathbf{v}_{\mathbf{pcc\_abc}} = [v_{pcc_a} \quad v_{pcc_b} \quad v_{pcc_c}]^T$

Transforming equation (3.23) to synchronous dq to find:

$$\mathbf{v}_{\mathbf{L\_dq}} = \mathbf{v}_{\mathbf{pcc\_dq}} + \mathbf{v}_{\mathbf{inj_{dq}}} - L_t \frac{d}{dt} \mathbf{i}_{\mathbf{pcc\_dq}} - r_t \mathbf{i}_{\mathbf{pcc\_dq}} + \gamma \omega L_t \mathbf{i}_{\mathbf{pcc\_dq}} \tag{3.24}$$

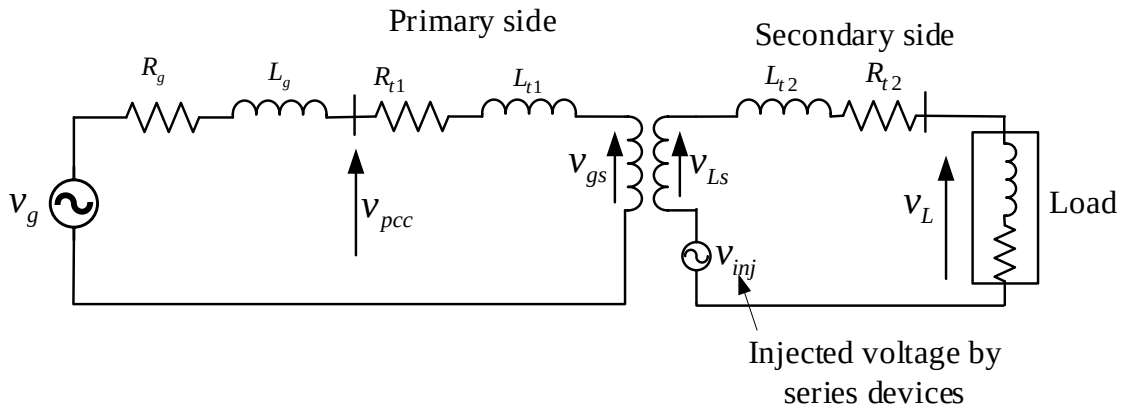

Figure 3.6. Approximate equivalent circuit of two winding transformer.

where,

$\mathbf{v_{L\_dq}} = [v_{L_d} \quad v_{L_q}]^T$ $\mathbf{i_{pcc\_dq}} = [i_{pcc_d} \quad i_{pcc_q}]^T$

$\mathbf{v_{pcc\_dq}} = [v_{pcc_d} \quad v_{pcc_q}]^T$

The transformation of the transformer voltages presented in equation (3.24) to dynamic phasor is given as:

$$\langle \mathbf{v_{L\_dq}} \rangle_\mathbf{k} = \langle \mathbf{v_{pcc\_dq}} \rangle_\mathbf{k} + \left(\gamma\omega L_t - \frac{d}{dt} - r_t - jkL_t\omega\right) \langle \mathbf{i_{pcc\_dq}} \rangle_\mathbf{k} + \langle \mathbf{v_{inj_{dq}}} \rangle_\mathbf{k} \qquad (3.25)$$

The dynamic phasor transformation presented in equation (3.25) shows no frequency coupling between system frequencies. Therefore, the dq-dynamic phasor quantities at the fundamental frequency are equal to the synchronous dq quantities. The equalisation means that the behaviour of these components at different frequencies will be seen as separate networks working at these frequencies without affecting each other.

3.2.5 Synchronous machine modelling

The synchronous machine is one of the most common components in the power system networks. So, having its mathematical model is very crucial especially in studying the effectiveness of VSC-FACTS on damping the SSR oscillation using small signal impedance. The synchronous machine voltage equations are expressed referred to rotor reference frame as shown in Figure 3.7. Detailed derivations of the following equations are found in [83] and [84]:

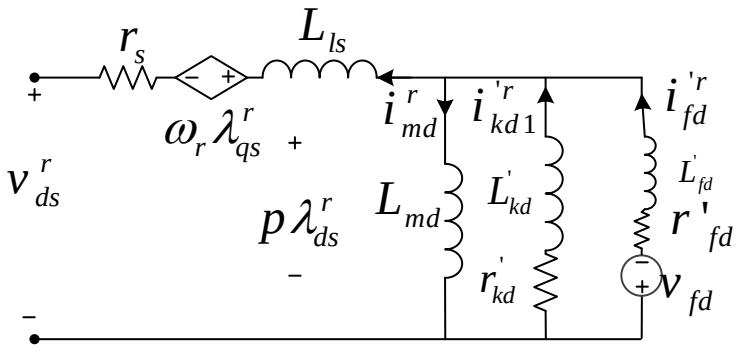

(a)

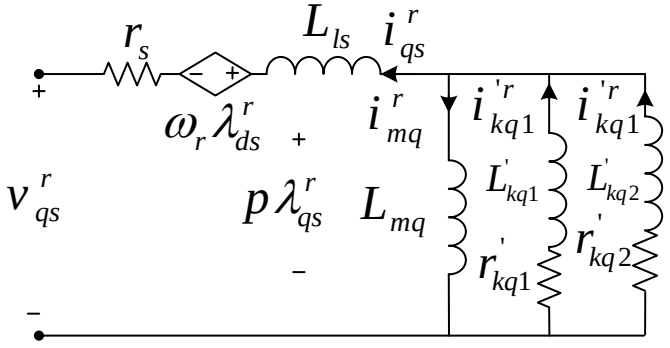

(b)

Figure 3.7. Synchronous generator equivalent circuit:

(a) d-axis equivalent circuit and (b) q-axis equivalent circuit.

From the equivalent circuit in Figure 3.7, the voltages in the synchronous dq form are given as:

$$\begin{bmatrix} \mathbf{v^r_{dqs}} \\ \mathbf{v'^r_{kdq1}} \\ \mathbf{v'^r_{kdq2}} \end{bmatrix} = -diag[r_s \quad r_s \quad r'^r_{kd1} \quad r'^r_{kq1} \quad r'^r_{fd} \quad r'^r_{kq2}] \begin{bmatrix} \mathbf{i^r_{dqs}} \\ \mathbf{i'^r_{kdq1}} \\ \mathbf{i'^r_{kdq2}} \end{bmatrix} +$$

$$\frac{d}{dt} \begin{bmatrix} \boldsymbol{\lambda}^{\mathbf{r}}_{\mathbf{dqs}} \\ \boldsymbol{\lambda}'^{\mathbf{r}}_{\mathbf{kdq1}} \\ \boldsymbol{\lambda}'^{\mathbf{r}}_{\mathbf{kdq2}} \end{bmatrix} + \begin{bmatrix} 0 & -\omega_r & \\ \omega_r & 0 & zeros(6\times 2) \\ zeros(4\times 2) & & \end{bmatrix} \begin{bmatrix} \boldsymbol{\lambda}^{\mathbf{r}}_{\mathbf{dqs}} \\ \boldsymbol{\lambda}'^{\mathbf{r}}_{\mathbf{kdq1}} \\ \boldsymbol{\lambda}'^{\mathbf{r}}_{\mathbf{kdq2}} \end{bmatrix} \tag{3.26}$$

where,

r_s is the stator resistance.

r'^r_{kd1} is the resistance of d-axis damper.

r'^{r}_{kqx} is the resistance of q-axis damper.

r'^{r}_{fd} is the field resistance.

$\mathbf{v'^{r}_{kdqx}}$ is the voltage across damper (x), where x= 1,2.

$\mathbf{i'^{r}_{kdqx}}$ is the current flow in damper (x), where x= 1,2.

$\boldsymbol{\lambda'^{\mathbf{r}}_{\mathbf{kdqx}}}$ is the damper (x) flux linkage, where x= 1,2.

$$\mathbf{v^{r}_{dqs}} = [v^{r}_{ds} \quad v^{r}_{ds}]^T \qquad \mathbf{v'^{r}_{kdq1}} = [v'^{r}_{kd1} \quad v'^{r}_{kq1}]^T \qquad \mathbf{v'^{r}_{kdq2}} = [v'_{fd} \quad v'^{r}_{kq2}]^T$$

$$\boldsymbol{\lambda}^{\mathbf{r}}_{\mathbf{dqs}} = [\lambda^{r}_{ds} \quad \lambda^{r}_{ds}]^T \qquad \boldsymbol{\lambda'^{\mathbf{r}}_{\mathbf{kdq1}}} = [\lambda'^{r}_{kd1} \quad \lambda'^{r}_{kq1}]^T \qquad \boldsymbol{\lambda'^{\mathbf{r}}_{\mathbf{kdq2}}} = [v'_{fd} \quad v'^{r}_{kq2}]^T$$

$$\mathbf{i^{r}_{dqs}} = [i^{r}_{ds} \quad i^{r}_{ds}]^T \qquad \mathbf{i'^{r}_{kdq1}} = [i'^{r}_{kd1} \quad i'^{r}_{kq1}]^T \qquad \mathbf{i'^{r}_{kdq2}} = [i'_{fd} \quad i'^{r}_{kq2}]^T$$

The flux linkages can be written as:

$$\begin{bmatrix} \boldsymbol{\lambda}^{\mathbf{r}}_{\mathbf{dqs}} \\ \boldsymbol{\lambda'^{\mathbf{r}}_{\mathbf{kdq1}}} \\ \boldsymbol{\lambda'^{\mathbf{r}}_{\mathbf{kdq2}}} \end{bmatrix} = diag[-L_{ls} \;\; -L_{ls} \;\; L'_{kd1} \;\; L'_{kq1} \;\; L'_{fd} \;\; L'_{kq2}] \begin{bmatrix} \mathbf{i^{r}_{dqs}} \\ \mathbf{i'^{r}_{kdq1}} \\ \mathbf{i'^{r}_{kdq2}} \end{bmatrix} + \begin{bmatrix} LL_{mdq} \\ LL_{mdq} \\ LL_{mdq} \end{bmatrix} \mathbf{i^{r}_{mdq}} \qquad (3.27)$$

where,

L_{ls} is the leakage inductance .

L'_{kd1} is the inductance of d-axis damper.

L'_{kqx} is inductance of q-axis damper.

L'_{fd} is the field inductance.

L_{md}, L_{mq} are the magnetizing inductance viewed from rotor.

$\mathbf{i^{r}_{mdq}}$ is the magnetizing current viewed from rotor as: $\mathbf{i^{r}_{mdq}} = [i^{r}_{md} \quad i^{r}_{mq}]^T$

LL_{mdq} is the magnetizing inductance matrix: $LL_{mdq} = [L_{md} \quad L_{mq}] \begin{bmatrix} 1 & 0 \\ 0 & 1 \end{bmatrix}$

ω_r is the speed of the rotor reference frame.

The rotor variables are referred to the stator windings for convenience, and the electric torque is calculated as:

$$T_e = \frac{3}{2}\left(\frac{P}{2}\right)\left(\lambda^r_{ds}.\, i^r_{qs} - \lambda^r_{qs}.\, i^r_{ds}\right) \tag{3.28}$$

where,

P is the number of pole pairs of synchronous machine.

The transformation of equation (3.26) and (3.27) to dynamic phasor form is:

$$\begin{bmatrix} \langle \mathbf{v^r_{dqs}} \rangle_k \\ \langle \mathbf{v'^r_{kdq1}} \rangle_k \\ \langle \mathbf{v'^r_{kdq2}} \rangle_k \end{bmatrix} = -diag[r_s \quad r_s \quad r'^r_{kd1} \quad r'^r_{kq1} \quad r'^r_{fd} \quad r'^r_{kq2}] \begin{bmatrix} \langle \mathbf{i^r_{dqs}} \rangle_k \\ \langle \mathbf{i'^r_{kdq1}} \rangle_k \\ \langle \mathbf{i'^r_{kdq2}} \rangle_k \end{bmatrix} +$$
$$\frac{d}{dt}\begin{bmatrix} \langle \boldsymbol{\lambda}^{\mathbf{r}}_{\mathbf{dqs}} \rangle_k \\ \langle \boldsymbol{\lambda}'^{\mathbf{r}}_{\mathbf{kdq1}} \rangle_k \\ \langle \boldsymbol{\lambda}'^{\mathbf{r}}_{\mathbf{kdq2}} \rangle_k \end{bmatrix} + jk\omega \begin{bmatrix} \langle \boldsymbol{\lambda}^{\mathbf{r}}_{\mathbf{dqs}} \rangle_k \\ \langle \boldsymbol{\lambda}'^{\mathbf{r}}_{\mathbf{kdq1}} \rangle_k \\ \langle \boldsymbol{\lambda}'^{\mathbf{r}}_{\mathbf{kdq2}} \rangle_k \end{bmatrix} +$$
$$\left\langle \begin{bmatrix} 0 & -\omega_r & \\ \omega_r & 0 & zeros(6\times 2) \\ zeros(4\times 2) & & \end{bmatrix} \begin{bmatrix} \boldsymbol{\lambda}^{\mathbf{r}}_{\mathbf{dqs}} \\ \boldsymbol{\lambda}'^{\mathbf{r}}_{\mathbf{kdq1}} \\ \boldsymbol{\lambda}'^{\mathbf{r}}_{\mathbf{kdq2}} \end{bmatrix} \right\rangle_k \tag{3.29}$$

$$\begin{bmatrix} \langle \boldsymbol{\lambda}^{\mathbf{r}}_{\mathbf{dqs}} \rangle_k \\ \langle \boldsymbol{\lambda}'^{\mathbf{r}}_{\mathbf{kdq1}} \rangle_k \\ \langle \boldsymbol{\lambda}'^{\mathbf{r}}_{\mathbf{kdq2}} \rangle_k \end{bmatrix} = diag[-L_{ls} \quad -L_{ls} \quad L'_{kd1} \quad L'_{kq1} \quad L'_{fd} \quad L'_{kq2}] \begin{bmatrix} \langle \mathbf{i^r_{dqs}} \rangle_k \\ \langle \mathbf{i'^r_{kdq1}} \rangle_k \\ \langle \mathbf{i'^r_{kdq2}} \rangle_k \end{bmatrix} +$$
$$\left\langle \begin{bmatrix} LL_{mdq} \\ LL_{mdq} \\ LL_{mdq} \end{bmatrix} \mathbf{i^r_{mdq}} \right\rangle_k \tag{3.30}$$

While, the electrical torque transformation to dynamic phasor form is given by:

$$\langle T_e \rangle_k = \frac{3}{2}\left(\frac{P}{2}\right)\left(\left\{\sum_{i=-\infty}^{\infty} \langle \lambda^r_{ds} \rangle_{k-i} \langle i^r_{qs} \rangle_i\right\} - \left\{\sum_{i=-\infty}^{\infty} \langle \lambda^r_{qs} \rangle_{k-i} \langle i^r_{ds} \rangle_i\right\}\right) \tag{3.31}$$

It is obvious from equation (3.31) that the harmonics are affecting the operation of the synchronous machine at the fundamental frequency as well at the harmonics,

which will be coupled with the fundamental frequency as shown by the electrical torque equation (3.31).

3.3 VSC-FACTS devices control

This section presents an overview of the control system of the VSC-FACTS. These control systems are employed with the previous derivation of power system components based on the required application for the VSC-FACTS. The control of two types of VSC-FACTS is presented here, the SSSC due to its application in damping system oscillations and the STATCOM due to its popularity in power system networks.

3.3.1 Static synchronous series compensator (SSSC) control system

The purpose of the series compensator is to inject series voltage that controls the active and reactive power flow through the line. The structure of SSSC connected to a grid is shown in Figure 3.8. The resistance (R_{se}) and the inductance (L_{se}) represent the sum of the converter, harmonic filter and series transformer resistances and inductances respectively. Three control methods have been proposed in literature to control the injected voltage, using the power flow through the line, the voltage at the load side or the line impedance as presented in Figure 3.9. For most of the power system applications, the SSSC is used to inject the reactive power without injecting any active power. Thus, the SSSC injected voltage is kept in quadrature with the line current, where, the leading voltage injects a series inductive load with the line, while the lagging voltage injects a series capacitive load [85].

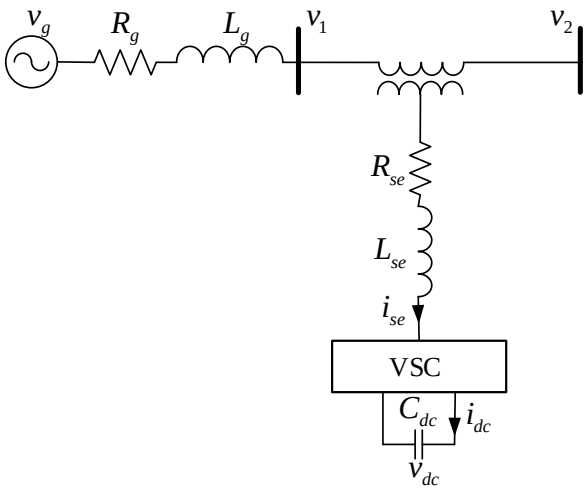

Figure 3.8. Structure of SSSC connected to a grid.

3.3.1.1 Power control mode

For SSSC operation, it is normal to use the sending/receiving end of the transmission line as the input to the controller as shown in Figure 3.9(a). So, the injected voltage depends on these inputs. The power flow through the compensated line can be given as:

$$P_{line} = P_1 - P_2 \tag{3.32}$$

$$Q_{line} = Q_1 - Q_2 \tag{3.33}$$

where,

P_{line} is the line active power.

Q_{line} is the line reactive power.

P_1, Q_1 are the powers at the sending end.

P_2, Q_2 are the powers at the receiving end.

The general expression of active and reactive powers in dq form is equal to:

$$P = \frac{3}{2}\left(v_d . i_d + v_q . i_q\right) \tag{3.34}$$

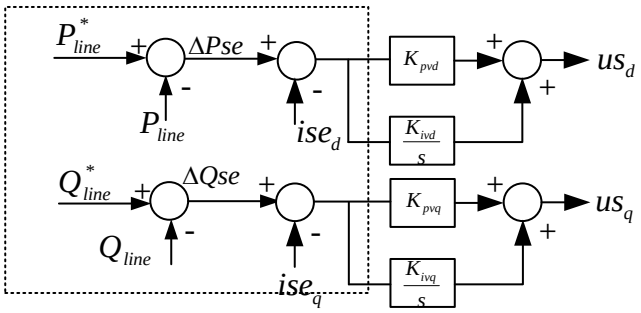

(a)

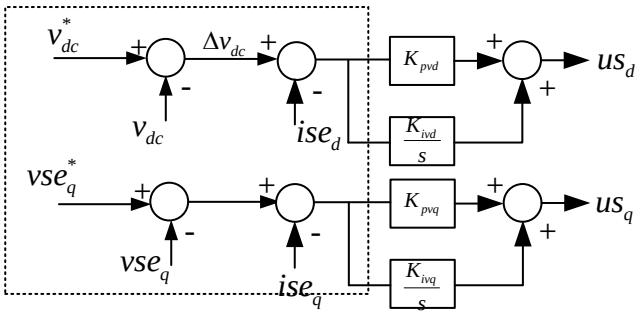

(b)

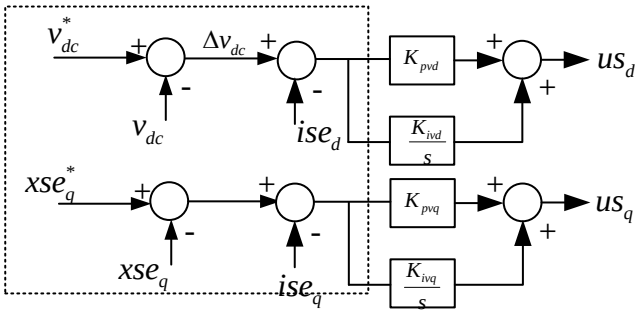

(c)

Figure 3.9. SSSC control systems: (a) Power control mode, (b) Voltage control mode and (c) Impedance control mode.

$$Q = \frac{3}{2}\left(-v_q . i_d + v_d . i_q\right) \tag{3.35}$$

where, the subscripts (d and q) refer to direct and quadrature quantities.

Based on Figure 3.9, the SSSC control signals can be written as:

$$u_{sed} = K_{pvd}(P^*_{line} - P_{line}) + x_1 \tag{3.36}$$

$$u_{seq} = K_{pvq}(Q^*_{line} - Q_{line}) + x_2 \tag{3.37}$$

where,

P^*_{line} is the line active power reference.

Q^*_{line} is the line reactive power reference.

$$x_1 = K_{ivd} \int (P^*_{line} - P_{line})dt \tag{3.38}$$

$$x_2 = K_{ivq} \int (Q^*_{line} - Q_{line})dt \tag{3.39}$$

K_{pvd} is the proportional control gain of direct axis voltage.

K_{pvq} is the proportional control gain of quadrature axis voltage.

K_{ivd} is the integral control gain of direct axis voltage.

K_{ivq} is the integral control gain of quadrature axis voltage.

3.3.1.2 Voltage control mode

The second type of SSSC control employs the quadrature voltage of SSSC (v_{seq}) and the dc link voltage as inputs. The SSSC voltage is utilised to control the reactive power of the SSSC using a previous knowledge of the operating conditions of the compensated system. Alternatively, the active power is controlled through the dc link voltage of the SSSC as shown in Figure 3.9. The control signal equations are:

$$u_{sed} = K_{pvd}(v^*_{dc} - v_{dc}) + x_1 \tag{3.40}$$

$$u_{seq} = K_{pvq}\left(v^*_{seq} - v_{seq}\right) + x_2 \tag{3.41}$$

$$x_1 = K_{ivd} \int (v_{dc}^* - v_{dc}) dt \tag{3.42}$$

$$x_2 = K_{ivq} \int \left(v_{seq}^* - v_{seq}\right) dt \tag{3.43}$$

v_{dc}^* is the reference dc link voltage.

v_{seq}^* is the reference quadrature voltage of SSSC.

3.3.1.3 Impedance control mode

In this operating mode, the line impedance is varied by a specific inserted impedance, to control the voltage magnitude as a proportional to the line current. The difficulty of this control mode is related to its practical use where it will be difficult to use the device impedance as an input. The SSSC impedance could have resistive, inductive or capacitive behaviour according to the quadrature line impedance required [86]. The SSSC impedance $\left(x_{seq}\right)$ is equal to:

$$x_{seq} = \frac{v_{seq}}{i_{seq}} \tag{3.44}$$

In the meantime, the d-axis input parameter is the dc link voltage of the SSSC (v_{dc}). This configuration is capable of controlling the reactive power generated and consumed active power losses of the device. The control signal equations are given as:

$$u_{sed} = K_{pvd}(v_{dc}^* - v_{dc}) + x_1 \tag{3.45}$$

$$u_{seq} = K_{pvq}\left(x_{seq}^* - x_{seq}\right) + x_2 \tag{3.46}$$

$$x_1 = \int K_{ivd}(v_{dc}^* - v_{dc}) dt \tag{3.47}$$

$$x_2 = \int K_{ivq}\left(x_{seq}^* - x_{seq}\right) dt \tag{3.48}$$

The three control modes transformation to dynamic phasor can be done by the use of equations (3.1) to (3.4) to have the following ones:

$$\langle u_{sed} \rangle_k = K_{pvd}(\langle \mu^* \rangle_k - \langle \mu \rangle_k) + \langle x_1 \rangle_k \tag{3.49}$$

$$\langle u_{seq} \rangle_k = K_{pvq}(\langle \sigma^* \rangle_k - \langle \sigma \rangle_k) + \langle x_2 \rangle_k \tag{3.50}$$

Also, the integral term can be transformed as:

$$\langle x_1 \rangle_k = \frac{K_{ivd}(\langle \mu^* \rangle_k - \langle \mu \rangle_k)}{s + jk\omega} \tag{3.51}$$

$$\langle x_2 \rangle_k = \frac{K_{ivq}(\langle \sigma^* \rangle_k - \langle \sigma \rangle_k)}{s + jk\omega} \tag{3.52}$$

where,

μ is the input control parameter of the d-axis control.

σ is the input control parameter of the q-axis control.

3.3.2 Static synchronous compensator (STATCOM) control system

The structure of a STATCOM connected to a power network is illustrated in Figure 3.10. The STATCOM is modelled as resistance and inductance behind a voltage source. The resistance (R_f) and the inductance (L_f) represent the sum of the converter, harmonic filter and series transformer resistances and inductances.

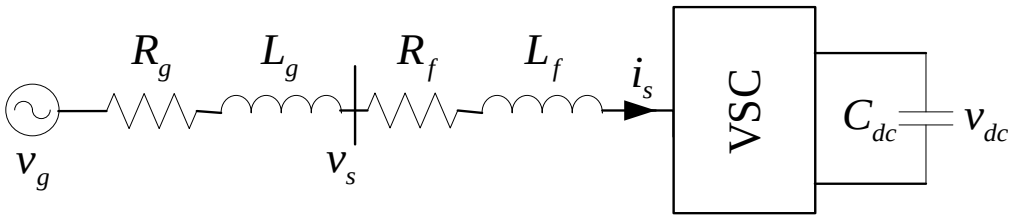

Figure 3.10. Structure of STATCOM connected to a grid.

The suitability of the outer controller's inputs depends on the stiffness and the topology of the network. The quadrature voltage is controlled using the two following methods:

3.3.2.1 Direct voltage control

The detailed equations describing the STATCOM controller can be found in several papers [87]–[89]. For weak ac grids, the dc link voltage of STATCOM and ac voltage of the controlled busbar are chosen as inputs to the voltage control loop to achieve better controlabilty of the bus voltage due to the change of powr flow [90]. The STATCOM control system contains four proportional integral (PI) controllers as shown in Figure 3.11. According to Figure 3.11, the converter control voltage of the STATCOM is given by:

$$u_{sd} = -K_{pid}(i_{sd}^{*} - i_{sd}) - x_1 \tag{3.53}$$

$$u_{sq} = -K_{piq}\left(i_{sq}^{*} - i_{sq}\right) - x_2 \tag{3.54}$$

$$x_1 = K_{iid}\int(i_{sd}^{*} - i_{sd})dt \tag{3.55}$$

$$x_2 = K_{iiq}\int\left(i_{sq}^{*} - i_{sq}\right)dt \tag{3.56}$$

where,

K_{pid} is the proportional control gain of direct axis current.

K_{piq} is the proportional control gain of quadrature axis current.

K_{iid} is the integral control gain of direct axis current.

K_{iiq} is the integral control gain of quadrature axis current.

i_{sd} is the direct axis components of STATCOM current.

i_{sq} is the quadrature axis components of STATCOM current.

In the meantime, the reference currents are:

$$i_{sd}^{*} = K_{pvd}(v_{dc}^{*} - v_{dc}) + x_3 \tag{3.57}$$

$$i_{sq}^{*} = K_{pvq}(v_{sd}^{*} - v_{sd}) + x_4 \tag{3.58}$$

$$x_3 = K_{ivd} \int (v_{dc}^* - v_{dc}) dt \tag{3.59}$$

$$x_4 = K_{ivq} \int (v_{sd}^* - v_{sd}) dt \tag{3.60}$$

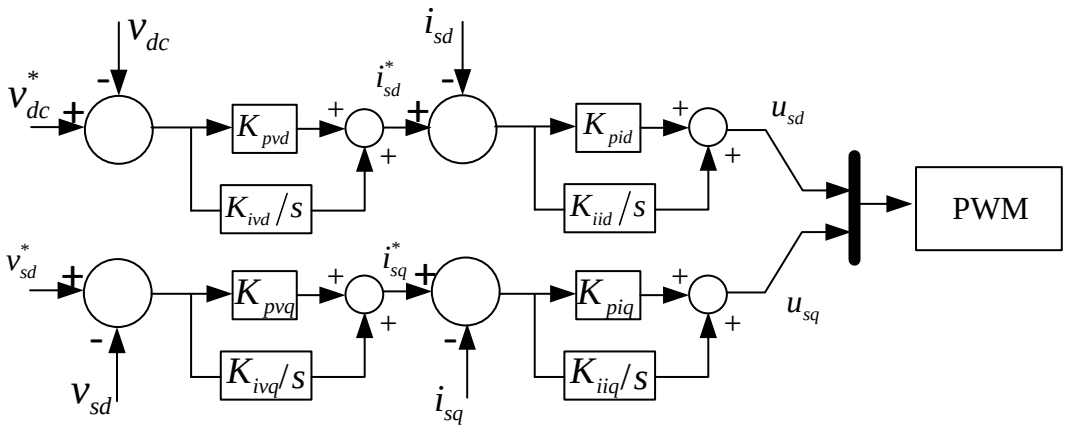

Figure 3.11. ac voltage controller of STATCOM.

where,

K_{pvd} is the proportional control gain of direct axis voltage.

K_{pvq} is the proportional control gain of quadrature axis voltage.

K_{ivd} is the integral control gain of direct axis voltage.

K_{ivq} is the integral control gain of quadrature axis voltage.

The transformation of equations (3.53) to (3.60) can be carried out using a similar procedure followed for the SSSC section as:

$$\langle u_{sd} \rangle_k = -K_{pid}(\langle i_{sd}^* \rangle_k - \langle i_{sd} \rangle_k) - \langle x_1 \rangle_k \tag{3.61}$$

$$\langle u_{sq} \rangle_k = -K_{piq}\left(\langle i_{sq}^* \rangle_k - \langle i_{sq} \rangle_k\right) - \langle x_2 \rangle_k \tag{3.62}$$

$$\langle x_1 \rangle_k = \frac{K_{iid}(\langle i_{sd}^* \rangle_k - \langle i_{sd} \rangle_k)}{s + jk\omega} \tag{3.63}$$

$$\langle x_2 \rangle_k = \frac{K_{iiq}\left(\langle i_{sq}^* \rangle_k - \langle i_{sq} \rangle_k\right)}{s + jk\omega} \tag{3.64}$$

$$\langle i_{sd}^* \rangle_k = K_{pvd}(\langle v_{dc}^* \rangle_k - \langle v_{dc} \rangle_k) + \langle x_3 \rangle_k \tag{3.65}$$

$$\langle i_{sq}^* \rangle = K_{pvq}(\langle v_{sd}^* \rangle_k - \langle v_{sd} \rangle_k) + \langle x_4 \rangle_k \tag{3.66}$$

$$\langle x_3 \rangle_k = \frac{K_{ivd}(\langle v_{dc}^* \rangle - \langle v_{dc} \rangle)}{s + jk\omega} \tag{3.67}$$

$$\langle x_4 \rangle_k = \frac{K_{ivq}(\langle v_{sd}^* \rangle - \langle v_{sd} \rangle)}{s + jk\omega} \tag{3.68}$$

3.3.2.2 Reactive power control

Figure 3.12 shows the STATCOM controller using reactive power control. The quadrature reference current equation is given as:

$$i_{sq}^* = K_{pvq}(Q^* - Q) + x_4 \tag{3.69}$$

$$x_4 = K_{ivq} \int (Q^* - Q) dt \tag{3.70}$$

where, the reactive power is calculated as:

$$Q = \frac{3}{2}\left(v_{sq} i_{sd} - v_{sd} i_{sq}\right) \tag{3.71}$$

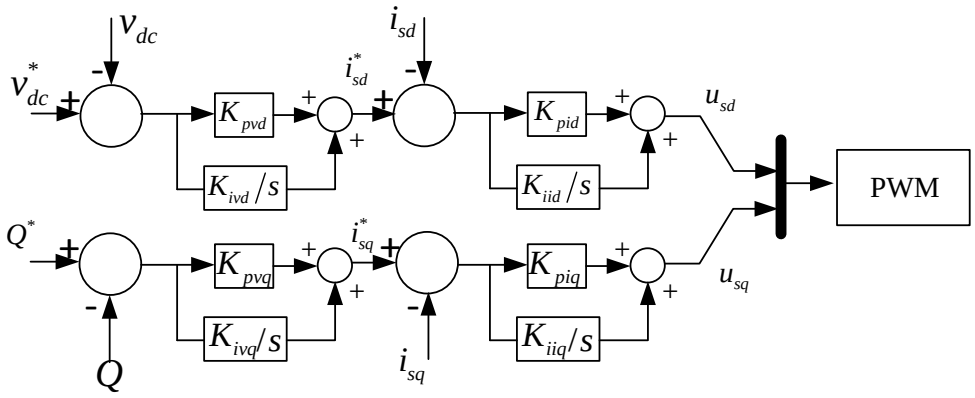

Figure 3.12. Reactive power control of STATCOM.

The dynamic phasor transformation of equations (3.69) to (3.71) is given as:

$$\langle i_{sq}^{*}\rangle_k = K_{pvq}(\langle Q^{*}\rangle_k - \langle Q\rangle_k) + \langle x_4\rangle_k \tag{3.72}$$

$$\langle x_4\rangle_k = K_{ivq}(\langle Q^{*}\rangle_k - \langle Q\rangle_k) \tag{3.73}$$

$$\langle Q\rangle_k = \frac{3}{2}\left(\langle v_{sq}\rangle_0\langle i_{sd}\rangle_k + \langle v_{sq}\rangle_k\langle i_{sd}\rangle_0 - \langle v_{sd}\rangle_0\langle i_{sq}\rangle_k - \langle v_{sd}\rangle_k\langle i_{sq}\rangle_0\right) \tag{3.74}$$

Equation (3.74) presents the frequency coupling between the input parameters of the STATCOM due to the use of the reactive power as an input to its quadrature voltage control. Also, this control mode presented a higher frequency coupling than the use of direct voltage control of the STATCOM.

3.4 STATCOM simulation including harmonics and unbalance

In this case study, the STATCOM behaviour is simulated in the presence of the harmonics firstly under unbalanced conditions. Two harmonics are injected by the source which has been considered in the STATCOM simulating (5^{th} and 7^{th} harmonics). The grid and STATCOM parameters are listed in Table 3.1. Using the abc-dq transformation matrix presented to extract the positive and negative sequence quantities of the STATCOM, the fundamental frequency and considered harmonics (5^{th} and 7^{th}) are transformed to dq-dynamic phasor form as shown in Table 3.2. the section of the 5^{th} and the 7^{th} harmonics in this thesis is based on the existence of these harmonics in nowadays power networks. The resultant quantities are filtered using a low pass filter to get rid of the harmonics associated with these quantities. It is noted from Table 3.2 that each frequency in the abc frame is transformed to two frequencies in dq-dynamic phasor using equation (3.8), one is rotating in the positive direction and the other is rotating in the negative direction. It is assumed in this simulation that PLL effects are ignored. The time domain detailed model and the dq-dynamic phasor model are shown in Figure 3.13. Both modelling plots are well matched to each other which prove the validity of dq-dynamic phasor modelling to represent the VSC-FACTS devices under these distorted conditions. The complex part of dq-dynamic phasor modelling results from the multiplication of voltages and currents by the capacitor and inductances. The ignorance of this part has insignificant

error as shown in Figure 3.14 parts (a) and (b). So, this part can be neglected in the STATCOM modelling.

Table 3.1. Grid and STATCOM parameters.

Parameter	value	Parameter	value
S_{base}	1.1 kVA	K_{pvd}	10 V/A
v_{base}	415 kV	K_{ivd}	0.001 V/A.s
R_g, L_g	0.25 Ω, 1 mH	K_{pvq}	0.01 V/A
R_f, L_f	0.1 Ω, 5 mH	K_{ivq}	2 V/A.s
f	50 Hz	v_{dc}	1000 V
K_{pidq}	50 A/V	C_{dc}	400 µF
K_{iidq}	1000 A/V.s		

Table 3.2. Extraction of dynamic phasor quantities of studied system.

Reference in abc	Harmonic order (k)	dq-dynamic phasor parameters
ω	0	$v_{d0} + jv_{q0}$
5ω	4	$v_{d_4} + jv_{q_4}$
7ω	6	$v_{d_6} + jv_{q_6}$
$-\omega$	-2	$v_{d_{-2}} + jv_{q_{-2}}$
-5ω	-6	$v_{d_{-6}} + jv_{q_{-6}}$
-7ω	-8	$v_{d_{-8}} + jv_{q_{-8}}$

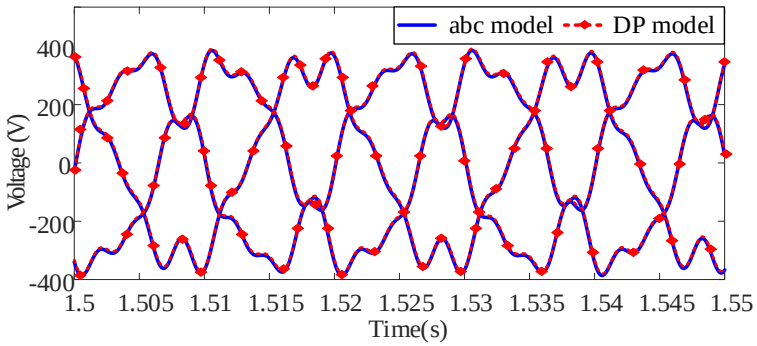

Figure 3.13. Comparison between time domain and dq-dynamic phasor in time domain.

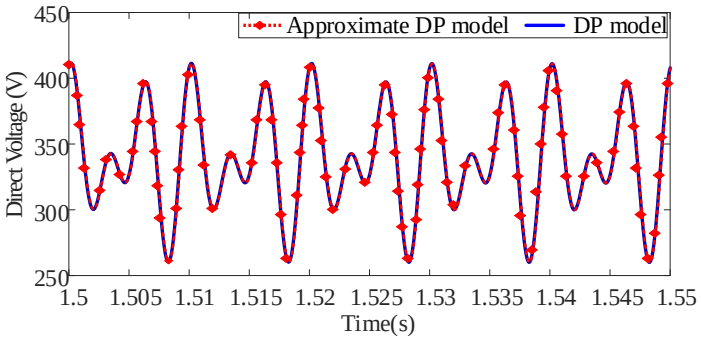

(a)

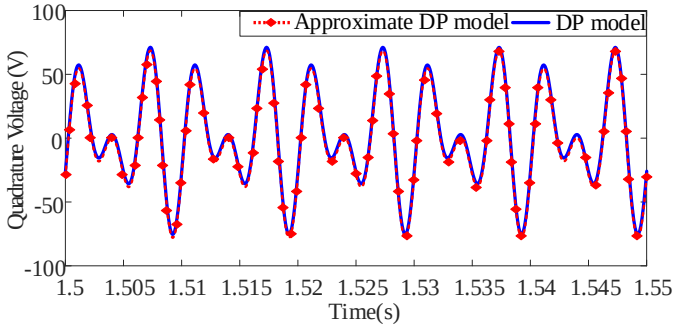

(b)

Figure 3.14. Comparison between the real and complex representation of d and q quantities: (a) v_d output of the STATCOM and (b) v_q output of the STATCOM.

The operation of the STATCOM under the unbalanced conditions can be represented as shown in Figure 3.15. In this case, the fundamental frequency ($k = 0$) and the negative sequence quantity ($k = -2$) are used to simulate the unbalanced operation. The dq-dynamic phasor model of STATCOM shows a well agreed performance compared with the STATCOM detailed model.

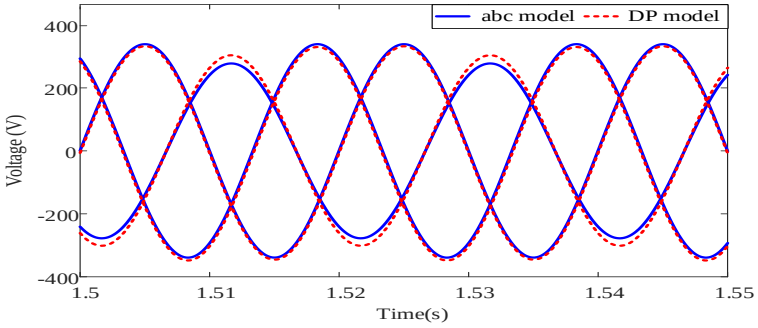

Figure 3.15. Comparison between dq-dynamic phasor model and time-domain model of STATCOM under unbalanced operating conditions.

3.5 Summary

This chapter presented the dq-dynamic phasor modelling of basic components of FACTS devices and the synchronous machine. These models will be used as the base models for the analysis of VSC-FACTS devices in the following chapters on studying the small signal stability. Some findings are:

- Dynamic phasor modelling shifts all system frequencies to become at zero which improves the speed of the simulation, especially for large systems. Also, the dynamic phasor approach slows down the variation of system parameters which improves the observation of changing those parameters.
- Modelling using dq-dynamic phasor at the fundamental frequency is equal to the synchronous dq where the harmonics order $(k = 0)$ in the dynamic phasor equations.
- The expansion of dq-dynamic phasor can simplify the analysis when studying the balanced and unbalanced systems.
- The third harmonic and the unbalanced frequency are seen as 2nd order harmonics in dq-dynamic phasor. However, the two components rotate in different directions, where the 2nd order harmonic rotates clockwise, and the unbalanced component rotates anti clockwise.
- The extraction of the dq-dynamic phasor showed the suitability of this approach in simulating balanced and unbalanced conditions.
- Also, the results revealed that the complex part caused by the transformation of the differentiation can be neglected. This conclusion is beneficial for stability studies once the system needs to be linearized using MATLAB/Simulink which has limitation when on linearizing complex quantities.

CHAPTER 4

SMALL SIGNAL STABILITY OF VSC BASED FACTS IN SYNCHRONOUS DQ FRAME

Small signal stability assessment in the dq frame is presented in this chapter. It gives an introduction to the stability problem and the stability criteria when using synchronous dq modelling to assess a system's performance. Secondly, the chapter presents the measurement techniques of the small signal impedance based on a black-box concept where the measurements of the device terminal are used to calculate the impedance. Lastly, the mathematical derivation of the state space equations and impedances of the SSSC, STATCOM and the synchronous machine are presented. The eigenvalue analysis is a conventional and fast technique used to implement and assess the system's behaviour. The benefit of using eigenvalue analysis is that the analysis can show the system instability and the oscillations for the whole studied network. Alternatively, the small signal impedance is both powerful and practical, especially in real-world applications where creating a fully detailed model of the power network becomes a challenging task compared to the eigenvalue analysis. In addition, it predicts system oscillations and stability at the point of connection using the generalised Nyquist plot or called eigenloci of the impedance. It employs the phase-margin as an indication of harmonic oscillation, where that low phase-margin means that the system exhibit harmonics. The main disadvantage of eigenloci is that the validity of the prediction of system's stability is limited for the simultaneous parameter change in the control loop only.

4.1 The basic principle of small signal stability

The capability of a system to remain stable after being exposed to a small disturbance is defined as small signal stability. Solving the stability problem under these disturbances can be simplified by linearizing the system equations over the period of the event [91]. If a system described in the state space form:

$$\mathbf{x}' = A\mathbf{x} + B\mathbf{u} \tag{4.1}$$

$$\mathbf{y} = C\mathbf{x} + D\mathbf{u} \tag{4.2}$$

where, the bold symbols represent vectors and,

x is the system state vector.

u is the system input vector.

y is the system output vector.

The linearized form of these state space equations is given by:

$$\mathbf{\Delta x}' = A\mathbf{\Delta x} + B\mathbf{\Delta u} \tag{4.3}$$

$$\mathbf{\Delta y} = C\mathbf{\Delta x} + D\mathbf{\Delta u} \tag{4.4}$$

where,

Δx is the linearized state vector of dimension (n).

Δu is the linearized input vector of dimension (r).

Δy is the linearized output vector of dimension (j).

A is the linearized state matrix of size ($n \times n$).

B is the linearized input matrix of size ($n \times r$).

C is the linearized output matrix of size ($j \times n$).

D is the linearized feedforward matrix of size ($j \times r$).

4.2 Small signal stability criteria

Based on equations (4.3) and (4.4), two stability measures have been developed to assess the stability of the system. The first is the eigenvalue analysis of the state matrix (A) and the second is the small signal impedance which defines the

relationship between the system inputs and outputs. These methods are less demanding computationally compared with the nonlinear equivalents [3]. Also, the system admittance/impedance can be derived from the system state space equations as [92]:

$$YZ_{dq} = C[sI - A]^{-1}B + D \tag{4.5}$$

Deriving the system impedance using (4.5) is limited for certain systems where the system states can be derived as a function of terminal quantities. The output of (4.5) can be the impedance or admittance based on the inputs and the outputs of the system.

4.2.1 Stability criteria-based eigenvalue analysis

The eigenvalue analysis is a conventional and fast technique used to implement and assess the system's response. The benefit of eigenvalue analysis is that the analysis can show the system instability and the oscillations for the whole studied network. It ensures the system stability if the system eigenvalues (λ_n) satisfy the following criterion where:

$$\lambda_n \leq 0 \tag{4.6}$$

4.2.2 Stability criteria-based small signal impedance

Small signal impedance modelling is a powerful and practical alternative to eigenvalues analysis, especially in situations where creating a fully detailed model of the power network is tedious [23][67]. In addition, it predicts system oscillations and stability at the point of connection using the generalised Nyquist plot or called eigenloci of the impedance [18]. The criteria developed for this technique will be investigated in more depth in the following section. The generalised Nyquist criterion (GNC) is one of the most important stability criteria used to assess the stability of the systems using small signal impedance. The GNC employs the phase-margin as an indication of harmonic oscillation, where that low phase-margin means that the system exhibits harmonics [3][18]. It was developed firstly to assess dc system stability and modified later for ac systems. The criterion examines whether or

not the eigenvalues of the product of generator (device) impedance (Z_D) and system admittance (Z_{sys}) encircles the point (-1, 0) in the complex plane [93]. In the synchronous dq frame, the impedance of a device connected to a system is given by:

$$Z_D = \begin{bmatrix} Z_{Ddd} & Z_{Ddq} \\ Z_{Dqd} & Z_{Dqq} \end{bmatrix} \tag{4.7}$$

where,

Z_{Ddd}, Z_{Dqq} are the diagonal impedances of d and q axis channels.

Z_{Ddq} , Z_{Dqd} are the off-diagonal impedances of d and q axis channels.

The small signal impedance of the system as seen by the device/generator is of the form:

$$Z_{sys} = \begin{bmatrix} Z_{sysdd} & Z_{sysdq} \\ Z_{sysqd} & Z_{sysqq} \end{bmatrix} \tag{4.8}$$

The ac network impedance represents the equivalent of all system components as being seen by the device (Figure 4.1). The return ratio matrix (L_{dq}) of system and generator is given as:

$$L_{dq} = Z_{Ddq}.Y_{sysdq} \tag{4.9}$$

$$L_{dq} = \begin{bmatrix} Z_{Ddd} & Z_{Ddq} \\ Z_{Dqd} & Z_{Dqq} \end{bmatrix} \begin{bmatrix} Z_{sysdd} & Z_{sysdq} \\ Z_{sysqd} & Z_{sysqq} \end{bmatrix} \tag{4.10}$$

The result of equation (4.10) is a (2×2) matrix which has eigenvalues [33] obtained as:

$$\det(L_{dq} + \lambda_{dq}.I) = 0 \tag{4.11}$$

where,

λ_{dq} is the eigenvalues of return ratio matrix.

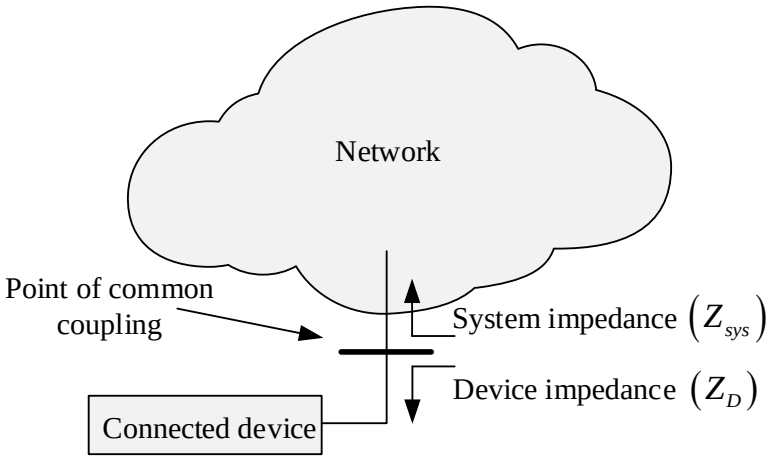

Figure 4.1. Device/generator and system impedance.

The system stability is ensured if and only if the set of the characteristic plot of L_{dq} in the complex plane does not encircle the critical point (-1, 0) or the total sum of anticlockwise encirclement is equal to the total number of right hand side of (Z_D) and (Y_{sys}) lies on complex plan [94]. Applying this definition requires the use of the relationship between the characteristic plot of L_{dq} and its eigenvalues, where the absolute of (λ_{dq}) should satisfy the following criterion for all the frequencies to guarantee system stability:

$$\lambda_{dq} \leq 0 \qquad -\infty \leq f \leq \infty \tag{4.12}$$

Some other criteria were derived based on the Generalised Nyquist which transformed the GNC to become more mathematical rather than a plot. It employs the norm of relation matrix (L_{dq}) to assess the stability based on the impedances/admittances magnitude. In addition, the stability norms suit the use of impedance measurement to control the stability. These stability criteria such as infinite one norm, the G-norm and maximum singular value which can be defined as [95]:

- The infinite-one norm is:

$$ZY_{\infty 1} = \left\|Z_g^{dq}\right\|_{\infty} \left\|Y_{NT}^{dq}\right\|_1 < 0.5 \tag{4.13}$$

where,

$\left\|Z_g^{dq}\right\|_\infty$ is the infinity norm of impedance.

$\left\|Y_{NT}^{dq}\right\|_1$ is the unity norm of admittance.

- Alternatively, the G-norm is:

$$ZY_{GG} = \left\|Z_g^{dq}\right\|_G \left\|Y_{NT}^{dq}\right\|_G < 0.25 \tag{4.14}$$

where,

$$\left\|Z_g^{dq}\right\|_G = \max\left(|Z_{gdd}|, |Z_{gdq}|, |Z_{gqd}|, |Z_{gqq}|\right)$$

$$\left\|Y_{NT}^{dq}\right\|_G = \max\left(|Y_{NTdd}|, |Y_{NTdq}|, |Y_{NTqd}|, |Y_{NTqq}|\right)$$

- A third criterion which examines the stability of the system based on the maximum singular value of both sides of the interfacing point of the system:

$$ZY_{\sigma\sigma} = \bar{\sigma}\left(Z_g^{dq}\right)\bar{\sigma}\left(Y_{NT}^{dq}\right) < 1 \tag{4.15}$$

Even though the use of such criteria simplifies the stability assessment, they are sufficient criteria but not necessary to predict stability. Also, they cannot assess instability caused due to the change of system phase angle.

4.3 Small signal impedance measurement

The dynamic nature of power systems due to the installation of new equipment, connecting and disconnecting system components tends to affect the stability. From the impedance technique point of view, these changes in the power system are referred to the change in the system impedance. According to the stability criteria listed in Section 4.2.2, maintaining the system impedance at certain levels can ensure a system's stability and avoid any oscillations with the power system. This section presents the impedance measurement method and presents the methods to disturb a system for such measurement.

4.3.1 Impedance measurement definition

Measuring the small signal impedance requires injecting small disturbance (voltage/current) to the measured device. The measured quantities are used to find the impedances at different dq coordinates as described by:

$$\begin{bmatrix} Z_{dd} & Z_{dq} \\ Z_{qd} & Z_{qq} \end{bmatrix} = \begin{bmatrix} \Delta vv_{1d} & \Delta vv_{1q} \\ \Delta vv_{2d} & \Delta vv_{2q} \end{bmatrix} \begin{bmatrix} \Delta i_{1d} & \Delta i_{1q} \\ \Delta i_{2d} & \Delta i_{2q} \end{bmatrix}^{-1} \tag{4.16}$$

where,

Δvv_{xd} is the measured voltage at 1st (x=1) and 2nd (x=2) measurement.

Δi_{xd} is the measured current at 1st (x=1) and 2nd (x=2) measurement.

Two measurements are needed to solve equation (4.16) which can be done by disturbing the system twice at the same frequency. The injection of the perturbation signal is carried out in series with the device (voltage injection) or in parallel (current injection). The selection between the two types is based on factors such as the suitability to system configuration and the existence of the harmonics in the measured system [74][96].

4.3.2 Impedance measurement using multi-tone perturbation signal

Different types of perturbation signals have been introduced in the literature to measure the impedance, such as sinusoidal signal injection [96], chirp perturbation signal [74] and multi-tone perturbation signal [97]. The multi-tone signal employs a superposition theory to inject multiple of frequencies (multi-tone) within the range of interest to perturb the measured network/device. It is proposed here to be of the form shown in equation (4.17) where the injected signal can be a voltage or current:

$$\mathbf{x_{inj}} = \mathbf{x_m} \cos\left(\omega t + \alpha + \phi_{inj}\right) \sum_{i=1}^{n} \cos(\omega_i t) \tag{4.17}$$

where,

$\mathbf{x_{inj}}$ is the instantaneous value of injected signal.

$\mathbf{x_m}$ is the magnitude of injected signal.

ω is the system natural frequency.

ω_i is the sliding frequency of injected frequencies.

A minimum number of frequencies should be used in the multi-tone signal to ensure the effectiveness of this signal in comparison with the chirp signal [97]. Two injections are enough to measure the impedance using multi-tone signal with minimum filtering effort which is considered as an advantage of this technique. This method is proposed in this thesis to develop an impedance measurement unit (IMU), which can be used for fast stability assessment via network operators or a supplementary control system. The construction of the IMU and the control system will be presented in Chapter 6.

4.4 Small signal derivation of power system components

As stated, the system impedance can be extracted by direct measurement at system terminals or using the mathematical derivation. The derivation is more convenient to add system's delays such as the delay caused by pulse width modulation. The state space and impedance models of some VSC-FACTS devices, as well as the synchronous machine, are presented in this section.

4.4.1 Small signal derivation of SSSC

The linearization of the three control methods (power control mode, voltage control mode and impedance control mode) presented in Chapter 3 is introduced. The state space equations of the SSSC presented in Chapter 3 can be linearized as:

$$\mathbf{\Delta i'_{sedq}} = \frac{1}{L_{se}}\mathbf{\Delta v_{sedq}} - \frac{R_{se}}{L_{se}}\mathbf{\Delta i_{sedq}} - \frac{1}{L_{se}}\mathbf{\Delta m_{sedq}} + \gamma\omega\mathbf{\Delta i_{sedq}} \tag{4.18}$$

where,

R_{se} , L_{se} are the SSSC resistance and inductance respectively.

i_{sed} is the direct component of SSSC current.

i_{seq} is the quadrature component of SSSC current.

v_{sed} is the direct component of SSSC voltage.

v_{seq} is the quadrature component of SSSC voltage.

m_{sed} is the direct component of the SSSC converter modulation index.

m_{seq} is the quadrature component of the SSSC converter modulation index.

The current, voltage and modulation vectors are defined as:

$$\mathbf{i_{sedq}} = [i_{sed} \quad i_{seq}]^T$$

$$\mathbf{v_{sedq}} = [v_{sed} \quad v_{seq}]^T$$

$$\mathbf{m_{sedq}} = [m_{sed} \quad m_{seq}]^T$$

4.4.1.1 State space analysis of SSSC with power control mode

This linearized form of the power control mode equations is given by:

$$\mathbf{\Delta x'_{12}} = K_{ivdq}\mathbf{PQ^*_{line}} - K_{ivdq}\mathbf{\Delta PQ_{line}} \tag{4.19}$$

$$\mathbf{\Delta m_{sedq}} = K_{pvdq}\mathbf{PQ^*_{line}} - K_{pvdq}\mathbf{\Delta PQ_{line}} + I.\mathbf{\Delta x_{12}} \tag{4.20}$$

where,

P_{line} is the active power flow in the transmission line.

Q_{line} is the reactive power flow in the transmission line.

$$\mathbf{\Delta x_{12}} = [\Delta x_1 \quad \Delta x_2]^T, \quad I = \begin{bmatrix} 1 & 0 \\ 0 & 1 \end{bmatrix}, \quad \mathbf{PQ_{line}} = [P_{line} \quad Q_{line}]^T$$

The active and reactive power flow through the controlled transmission line can be calculated as:

$$\mathbf{\Delta PQ_{line}} = \mathbf{\Delta PQ_1} - \mathbf{\Delta PQ_2} \tag{4.21}$$

$$\mathbf{\Delta PQ_{line}} = \frac{3}{2}\begin{bmatrix} -i_{sed} & i_{sed} & -i_{seq} & i_{seq} \\ -i_{seq} & i_{seq} & i_{sed} & -i_{sed} \end{bmatrix}\begin{bmatrix} \mathbf{\Delta v_{12d}} \\ \mathbf{\Delta v_{12q}} \end{bmatrix} + \frac{3}{2}\begin{bmatrix} v_{2d} - v_{1d} & v_{2q} - v_{1q} \\ v_{1q} - v_{2q} & v_{2d} - v_{1d} \end{bmatrix}\mathbf{\Delta i_{sedq}} \quad (4.22)$$

where,

v_{1d} is the direct axis component of sending end bus.

v_{2d} is the direct axis component of receiving end bus.

v_{1q} is the quadrature axis component of sending end bus.

v_{2q} is the quadrature axis component of receiving end bus.

The bus voltage vector is equal to:

$$\mathbf{\Delta v_{12}} = [\Delta v_1 \quad \Delta v_2]$$

The arrangement of equations from (4.19) to (4.22) can be written in the following form:

$$\begin{bmatrix} \mathbf{\Delta x'_{12}} \\ \mathbf{\Delta i'_{sedq}} \end{bmatrix} = AP\begin{bmatrix} \mathbf{\Delta x_{12}} \\ \mathbf{\Delta i_{sedq}} \end{bmatrix} + B_P\begin{bmatrix} \mathbf{\Delta v_{sedq}} \\ \mathbf{\Delta v_{12d}} \\ \mathbf{\Delta v_{12q}} \\ \mathbf{\Delta PQ^*_{line}} \end{bmatrix} \quad (4.23)$$

where, the state matrix (A_P) is given as:

$$A_P = \begin{bmatrix} 0 & 0 & -\frac{3}{2}K_{ivd}(v_{1d} - v_{2d}) & -\frac{3}{2}K_{ivd}(v_{2q} - v_{1q}) \\ 0 & 0 & \frac{3}{2}K_{ivq}(v_{2q} - v_{1q}) & -\frac{3}{2}K_{ivq}(v_{1d} - v_{2d}) \\ -\frac{1}{L_{se}} & 0 & -\frac{R_{se}}{L_{se}} + \frac{3}{2}\frac{K_{pvd}}{L_{se}}(v_{1d} - v_{2d}) & \frac{3}{2}\frac{K_{pvd}}{L_{se}}(v_{2q} - v_{1q}) + \omega \\ 0 & -\frac{1}{L_{se}} & \frac{3}{2}\frac{K_{pvq}}{L_{se}}(v_{2q} - v_{1q}) - \omega & -\frac{R_{se}}{L_{se}} + \frac{3}{2}\frac{K_{vpq}}{L_{se}}(v_{1d} - v_{2d}) \end{bmatrix}$$

While, the input matrix (B_P) is given in the form:

$$B_P =$$

$$\begin{bmatrix} 0 & 0 & -\frac{3}{2}K_{ivd}i_{sed} & \frac{3}{2}K_{ivd}i_{seq} & -\frac{3}{2}K_{ivd}i_{seq} & \frac{3}{2}K_{ivd}i_{sed} & K_{ivd} & 0 \\ 0 & 0 & -\frac{3}{2}K_{ivq}i_{seq} & -\frac{3}{2}K_{ivq}i_{sed} & \frac{3}{2}K_{ivq}i_{sed} & \frac{3}{2}K_{ivq}i_{seq} & 0 & K_{ivq} \\ \frac{1}{L_{se}} & 0 & \frac{3}{2}\frac{K_{pvd}}{L_{se}}i_{sed} & -\frac{3}{2}\frac{K_{pvd}}{L_{se}}i_{seq} & \frac{3}{2}\frac{K_{pvd}}{L_{se}}i_{seq} & -\frac{3}{2}\frac{K_{pvd}}{L_{se}}i_{sed} & -\frac{K_{pvd}}{L_{se}} & 0 \\ 0 & \frac{1}{L_{se}} & \frac{3}{2}\frac{K_{pvq}}{L_{se}}i_{seq} & \frac{3}{2}i_{sed} & -\frac{3}{2}\frac{K_{pvq}}{L_{se}}i_{sed} & -\frac{3}{2}\frac{K_{pvq}}{L_{se}}i_{seq} & 0 & -\frac{K_{pvq}}{L_{se}} \end{bmatrix}$$

4.4.1.2 State space analysis of SSSC with voltage control mode

The controlling the power flow by controlling the voltage drop between the buses is the second control method found in the literature. The quadrature component of bus voltage (v_{seq}) is used as an input to the voltage control loop. It is employed to control the reactive power of the SSSC. Alternatively, the active power is controlled through the dc link voltage of the SSSC.

$$\begin{bmatrix} \mathbf{\Delta x'_{12}} \\ \mathbf{\Delta i'_{sedq}} \\ \Delta v'_{dc} \end{bmatrix} = A_V \begin{bmatrix} \mathbf{\Delta x_{12}} \\ \mathbf{\Delta i_{sedq}} \\ \Delta v_{dc} \end{bmatrix} + B_V \begin{bmatrix} v^*_{dc} \\ v^*_{seq} \\ \mathbf{\Delta v_{sedq}} \end{bmatrix} \tag{4.24}$$

where,

v^*_{dc} is the dc link reference voltage.

v^*_{seq} is the quadrature voltage reference.

The definition of the state matrix (A_V) and the input matrix (B_V) are given as:

$$A_V = \begin{bmatrix} 0 & 0 & 0 & 0 & -K_{ivd} \\ 0 & 0 & 0 & 0 & 0 \\ -\frac{1}{L_{se}} & 0 & -\frac{R_{se}}{L_{se}} & \omega & \frac{K_{pvd}}{L_{se}} \\ 0 & -\frac{1}{L_{se}} & -\omega & -\frac{R_{se}}{L_{se}} & 0 \\ 0 & 0 & \frac{\frac{3}{2}v_{sed}-2i_{sed}.R_{se}}{C_{dc}v_{dc}} & \frac{3}{2}\frac{v_{seq}}{Cv_{dc}} & \frac{i^2_{sed}.R_{se}-\frac{3}{2}(v_{sed}.i_{sed}+v_{seq}.i_{seq})}{C_{dc}v^2_{dc}} \end{bmatrix}$$

$$B_V = \begin{bmatrix} K_{ivd} & 0 & 0 & 0 \\ 0 & K_{ivq} & 0 & -K_{ivq} \\ -\frac{1}{L_{se}}K_{pvd} & 0 & \frac{1}{L_{se}} & 0 \\ 0 & -\frac{K_{pvq}}{L_{se}} & 0 & \frac{1}{L_{se}}(1+K_{pvq}) \\ 0 & 0 & \frac{3}{2}\frac{i_{sed}}{C_{dc}v_{dc}} & \frac{3}{2}\frac{i_{seq}}{C_{dc}v_{dc}} \end{bmatrix}$$

4.4.1.3 State space analysis of SSSC with impedance control mode

The linearized form of the impedance control mode is given by the state space equation as:

$$\begin{bmatrix} \mathbf{\Delta x'_{12}} \\ \mathbf{\Delta i'_{sedq}} \\ \Delta v'_{dc} \end{bmatrix} = A_I \begin{bmatrix} \mathbf{\Delta x_{12}} \\ \mathbf{\Delta i_{sedq}} \\ \Delta v_{dc} \end{bmatrix} + B_I \begin{bmatrix} v^*_{dc} \\ x^*_{seq} \\ \mathbf{\Delta v_{sedq}} \end{bmatrix} \tag{4.25}$$

where,

x^*_{seq} is the quadrature impedance reference.

The state matrix (A_I) and the input matrix (B_I) are given as:

$$A_I = \begin{bmatrix} 0 & 0 & 0 & 0 & -K_{ivd} \\ 0 & 0 & 0 & \frac{K_{ivq}v_{seq}}{i^2_{seq}} & 0 \\ \frac{-1}{L_{se}} & 0 & -\frac{R_{se}}{L_{se}} & \omega & \frac{K_{pvd}}{L_{se}} \\ 0 & \frac{-1}{L_{se}} & -\omega & -\frac{v_{seq}}{i^2_{seq}}\frac{1}{L_{se}}K_{pvq} & -\frac{R_{se}}{L_{se}} \quad 0 \\ 0 & 0 & \frac{\frac{3}{2}v_{sed}-2i_{sed}.R_{se}}{C_{dc}v_{dc}} & \frac{3}{2}\frac{v_{seq}}{C_{dc}v_{dc}} & \frac{is^2_d.R_{se}-\frac{3}{2}(v_{sed}.i_{sed}+v_{seq}.i_{seq})}{C_{dc}v^2_{dc}} \end{bmatrix}$$

$$B_I = \begin{bmatrix} K_{ivd} & 0 & 0 & 0 \\ 0 & K_{ivq} & 0 & -\frac{K_{ivq}}{i_{seq}} \\ -\frac{K_{pvd}}{L_{se}} & 0 & \frac{1}{L_{se}} & 0 \\ 0 & -\frac{K_{pvq}}{L_{se}} & 0 & \frac{1}{L_{se}}\left(1+\frac{K_{pvq}}{i_{seq}}\right) \\ 0 & 0 & \frac{3}{2}\frac{i_{sed}}{C_{dc}v_{dc}} & \frac{3}{2}\frac{i_{seq}}{C_{dc}v_{dc}} \end{bmatrix}$$

4.4.1.4 dq impedance model of SSSC with power control mode

The generalised impedance model of SSSC controlled by the power control mode can be derived using the following generalised equations:

$$\mathbf{\Delta v_{sedq}} = ap_{se}\mathbf{\Delta i_{sedq}} + \mathbf{\Delta m_{sedq}} \tag{4.26}$$

$$\mathbf{\Delta m_{sedq}} = bp_{se}\mathbf{\Delta PQ^{*}_{line}} - bp_{se}\ \mathbf{\Delta PQ_{line}} \tag{4.27}$$

$$\mathbf{\Delta PQ_{line}} = -cp_{se}\mathbf{\Delta v_{sedq}} + cp_{se}\mathbf{\Delta v_{Ldq}} + dp_{se}\mathbf{\Delta i_{sedq}} - fp_{se}\mathbf{\Delta i_{sedq}} \tag{4.28}$$

Using back substitution of equations (4.26) to (4.28), the impedance of SSSC controlled by active and reactive is given as:

$$Z_{pSSSC} = (I - bp_{se}cp_{se})^{-1}(ap_{se} + bp_{se}fp_{se} - bp_{se}dp_{se}) \tag{4.29}$$

The definition of the matrices in equation (4.29) can be given as:

- The SSSC topology matrix:

$$ap_{se} = \begin{bmatrix} sL_{se} + R_{se} & -\omega L_{se} \\ \omega L_{se} & sL_{se} + R_{se} \end{bmatrix}$$

- The SSSC current controller:

$$bp_{se} = \begin{bmatrix} K_{pvd} + \frac{K_{ivd}}{s} & 0 \\ 0 & K_{pvq} + \frac{K_{ivq}}{s} \end{bmatrix}$$

- The active and reactive powers calculations matrix:

$$cp_{se} = \frac{3}{2}\begin{bmatrix} i_{sed} & i_{seq} \\ i_{seq} & -i_{sed} \end{bmatrix} \qquad dp_{se} = \frac{3}{2}\begin{bmatrix} v_{sed} & v_{seq} \\ -v_{seq} & v_{sed} \end{bmatrix} \qquad fp_{se} = \frac{3}{2}\begin{bmatrix} v_{Ld} & v_{Lq} \\ -v_{Lq} & v_{Ld} \end{bmatrix}$$

4.4.1.5 dq impedance model of SSSC with voltage control mode

The SSSC impedance controlled by voltage control mode is derived as:

$$\mathbf{\Delta v_{sedq}} = ap_{se}\mathbf{\Delta i_{sedq}} + \mathbf{\Delta m_{sedq}} \tag{4.30}$$

$$\mathbf{\Delta m_{sedq}} = bp_{se}\mathbf{\Delta VV}^{*} - bp_{se}\mathbf{\Delta VV} \tag{4.31}$$

$$cv_{se}\mathbf{\Delta VV} = dv_{se}\mathbf{\Delta v_{sedq}} + ev_{se}\mathbf{\Delta i_{sedq}} \tag{4.32}$$

where,

$\mathbf{\Delta VV} = [v_{dc} \quad v_{seq}]$

The dc link voltage and quadrature voltage matrices are:

$$cv_{se} = \begin{bmatrix} C_{dc}sv_{dc} + \frac{\frac{3}{2}v_{sed}.i_{sed} + \frac{3}{2}v_{seq}.i_{seq} - i_{sed}^{2}.R_{se}}{v_{dc}} & 0 \\ 0 & 1 \end{bmatrix}$$

$$dv_{se} = \begin{bmatrix} \frac{3}{2}i_{sed} & \frac{3}{2}i_{seq} \\ 0 & 1 \end{bmatrix} \quad ev_{se} = \begin{bmatrix} \frac{3}{2}v_{sed} - 2i_{sed}.R_{f} & \frac{3}{2}v_{seq} \\ 0 & 0 \end{bmatrix}$$

So, the impedance, in this case, is:

$$Z_{vSSSC} = \{\mathbf{I} + bv_{se}(cv_{se})^{-1}dv_{se}\}^{-1}\{av_{se} - bv_{se}(cv_{se})^{-1}ev_{se}\} \tag{4.33}$$

4.4.1.6 dq impedance model of SSSC with impedance control mode

Similar to the voltage control mode, the generalised impedance model of SSSC controlled by impedance control mode is given as:

$$\mathbf{\Delta v_{sedq}} = av_{se}\mathbf{\Delta i_{sedq}} + \mathbf{\Delta m_{sedq}} \tag{4.34}$$

$$\mathbf{\Delta m_{sedq}} = bv_{se}\mathbf{\Delta VX}^{*} - bv_{se}\mathbf{\Delta VX} \tag{4.35}$$

$$cv_{se}\mathbf{\Delta VX} = di_{se}\mathbf{\Delta v_{sedq}} + ei_{se}\mathbf{\Delta i_{sedq}} \tag{4.36}$$

where,

$\mathbf{\Delta VX} = [v_{dc} \quad x_{seq}]^{T}$

The dc link voltage and impedance calculation matrix as:

$$di_{se} = \begin{bmatrix} \frac{3}{2}i_{sed} & \frac{3}{2}i_{seq} \\ 0 & \frac{1}{i_{seq}} \end{bmatrix} \qquad ei_{se} = \begin{bmatrix} \frac{3}{2}v_{sed} - 2i_{sed}.R_f & \frac{3}{2}v_{seq} \\ 0 & \frac{v_{seq}}{i_{seq}^2} \end{bmatrix}$$

In the same way, the impedance of a SSSC controlled by impedance is:

$$Z_{iSSSC} = \{\mathbf{I} + bi_{se}(ci_{se})^{-1}di_{se}\}^{-1}\{ai_{se} - bi_{se}(ci_{se})^{-1}ei_{se}\} \tag{4.37}$$

4.4.1.7 Stability norms of SSSC control modes

The effect of different control modes on the small signal impedance has not been investigated in the literature. So, to identify the similarity and the differences between control modes over the frequency, the impedances of the three control modes are compared under the same operating conditions as seen in Figure 4.2. Both impedance control mode and voltage control mode has the same impedances over all frequencies.

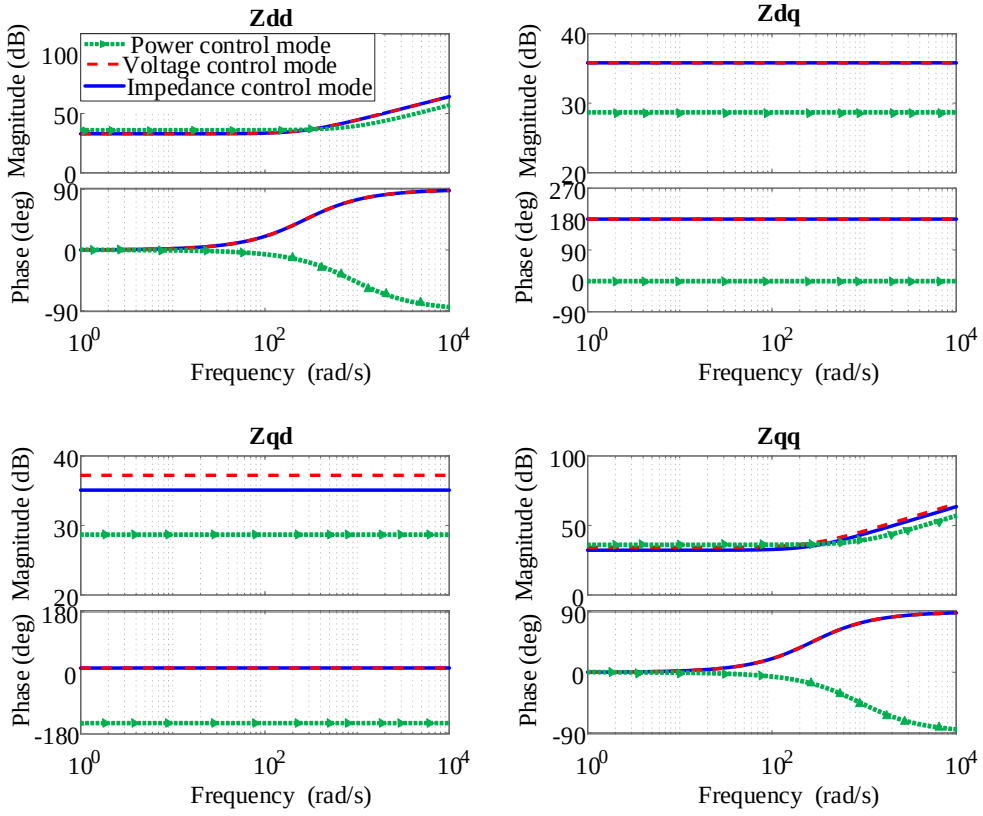

Figure 4.2. SSSC impedance comparison for different control modes.

This is referred to the use of the SSSC impedance is similar to the use of the SSSC voltage. Alternatively, the power control mode is slightly different in magnitude for the diagonal impedances; in the meantime, this difference is increased for the off-diagonal impedances. Similarly, the phase shifts of the power control mode have 180^{o} phase difference over the whole range of frequency in the off-diagonal impedances and only at higher frequencies for the diagonal impedances. This appears the operation of the power control mode as a decreased capacitive while the voltage and impedance control modes as an increased inductive.

4.4.1.8 The validation of SSSC control modes

Three control methods of the SSSC are validated using the small signal impedance measurement of the SSSC detailed model. Such validation ensures the validity of the average and linearized model of the SSSC. The series voltage injection is implemented in these measurements to perturb the SSSC. The SSSC is operating at the same operating conditions for the three control modes, which has the parameters listed in Table 4.1. Due to the series connection of the SSSC; the impedance of the SSSC can be measured as a two-port circuit, which will have different values in each measurement direction, or it can be measured as a converter and harmonic filter. The second measurement provides the easiest way where the total impedance of the SSSC will be equal to the filter, converter and the series injection transformer impedance as shown in Figure 4.3. In the case of the delay elements embedded in the model, the typical derivation of the impedance is more convenient to add such delays.

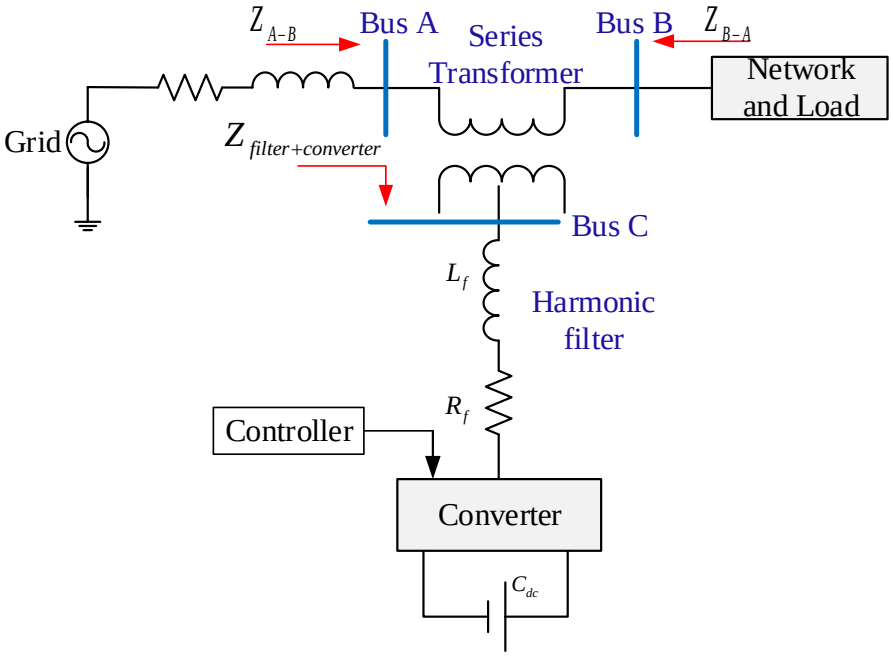

Figure 4.3. Impedance measurement of SSSC.

Table 4.1. SSSC control modes parameters.

Parameter	value
R_f, L_f	0.5 Ω, 5 mH
R_{se}, L_{se}	15.60 Ω, 70 mH
C_{dc}	800 µF
v_{dc}	1000 V
K_{pvd}, K_{ivd}	-0.15 V/A, 0.001 V/A.s
K_{pvq}, K_{ivq}	-0.15 V/A, 0.001 V/A.s
v_{se}	100 V
f_s	50 Hz

The measured impedance calculated using the measured voltages and currents at the bus (A) in Figure 4.3. In the measurement, series injection method is employed to extract the impedances of the three control mode of SSSC time domain Simulink model. The four impedances (Z_{dd}, Z_{dq}, Z_{qd} and Z_{qq}) are agreed with the calculated impedance as shown in Figure 4.4, and Figure 4.6 which validate the mathematical models of the SSSC.

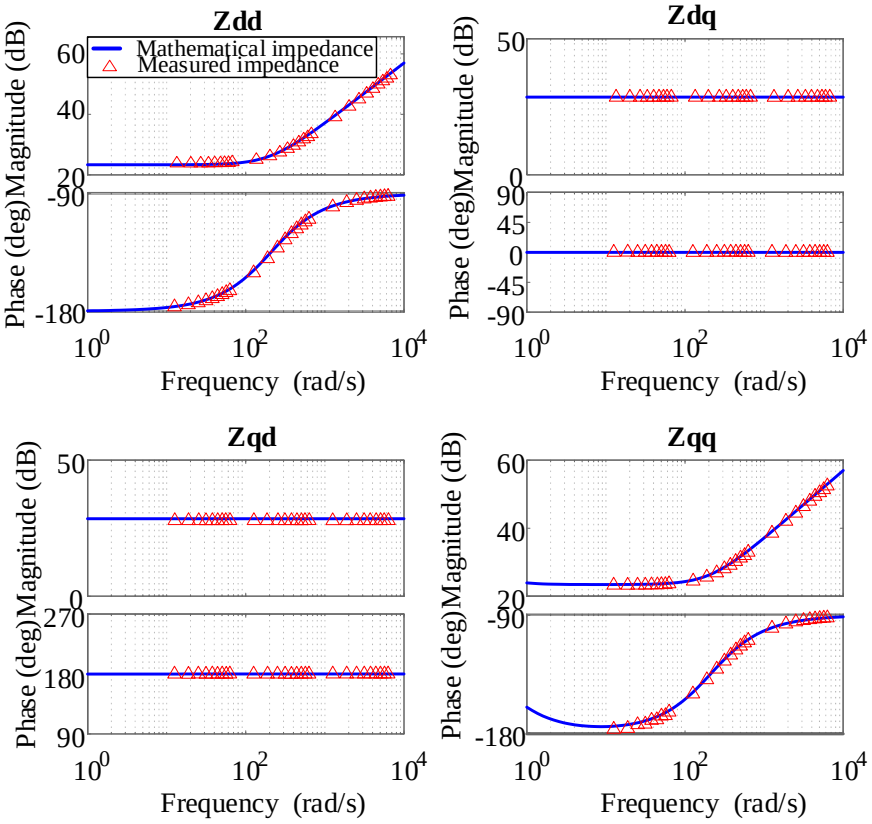

Figure 4.4. SSSC impedance for power control mode.

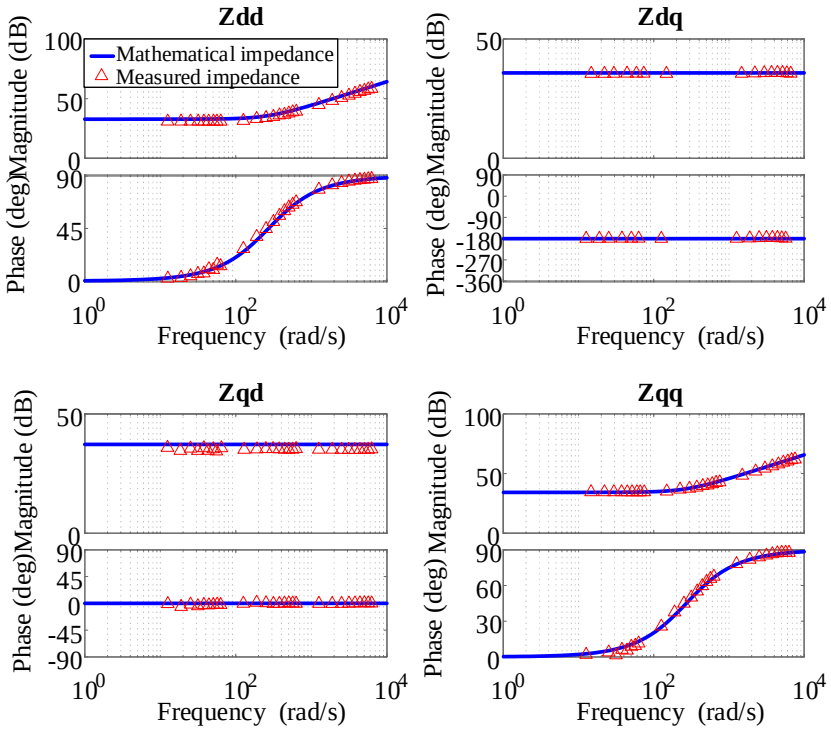

Figure 4.5. SSSC impedance for voltage control mode.

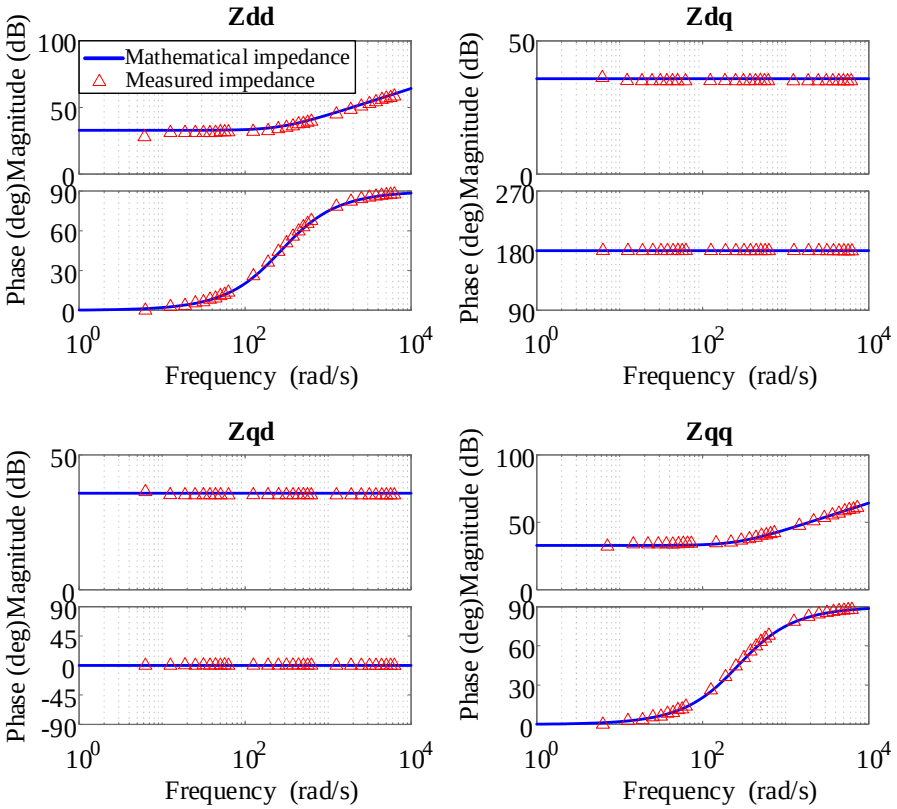

Figure 4.6. SSSC impedance for impedance control mode.

The previous plots the accuracy of the mathematical model of the three control modes of the SSSC on representing its response in the analysis.

4.4.2 Small signal derivation of STATCOM

The STATCOM is the second type of the VSC-FACTS devices which is modelled here. The phase-locked loop (PLL) effect is ignored in the analysis. Two control modes for the STATCOM are considered in this section. These are the voltage control mode and reactive power control mode.

4.4.2.1 State space analysis of STATCOM with direct voltage control

The linearized state space equations of the STATCOM presented in chapter 3 are given as:

$$\frac{d}{dt}\begin{bmatrix}\mathbf{\Delta x_{12}}\\ \mathbf{\Delta x_{34}}\\ \mathbf{\Delta i_{sdq}}\\ \Delta v_{dc}\end{bmatrix} = Asv\begin{bmatrix}\mathbf{\Delta x_{12}}\\ \mathbf{\Delta x_{34}}\\ \mathbf{\Delta i_{sdq}}\\ \Delta v_{dc}\end{bmatrix} + Bsv\begin{bmatrix}\mathbf{\Delta v_{sdq}}\\ \mathbf{v}^*\end{bmatrix} \tag{4.38}$$

$$\mathbf{\Delta i_{sdq}} = C_{STAT}[\mathbf{\Delta x_{12}} \quad \mathbf{\Delta x_{34}} \quad \mathbf{\Delta i_{sdq}} \quad \Delta v_{dc}]^T \tag{4.39}$$

where,

$\mathbf{\Delta x_{12}} = [\Delta x_1 \quad \Delta x_2]^{\boldsymbol{T}}$ $\qquad$ $\mathbf{\Delta x_{34}} = [\Delta x_3 \quad \Delta x_4]^{\boldsymbol{T}}$

$\mathbf{\Delta is_{dq}} = [\Delta i_{sd} \quad \Delta i_{sq}]^T$ is the linearized current vector of STATCOM currents.

$\mathbf{\Delta vs_{dq}} = [\Delta v_{sd} \quad \Delta v_{sq}]^T$ is the linearized voltage vector of STATCOM voltages.

$\mathbf{v}^* = [v_{dc} \quad v_{sd}]$ is the dc link voltage and direct voltage vector.

The state matrix (Asv) and the input matrix (Bsv) are:

$$Asv = \begin{bmatrix} 0 & 0 & K_{iid} & 0 & -K_{iid} & 0 & -K_{iid}K_{pvd} \\ 0 & 0 & 0 & K_{iiq} & 0 & -K_{iiq} & 0 \\ 0 & 0 & 0 & 0 & 0 & 0 & -K_{ivd} \\ 0 & 0 & 0 & 0 & 0 & 0 & 0 \\ \frac{1}{L_f} & 0 & \frac{K_{pid}}{L_f} & 0 & \frac{K_{pid}-R_f}{L_f} & \omega & \frac{K_{pid}K_{pvd}}{L_f} \\ 0 & \frac{1}{L_f} & 0 & \frac{K_{piq}}{L_f} & -\omega & \frac{K_{piq}-R_f}{L_f} & 0 \\ 0 & 0 & 0 & 0 & \frac{\frac{3}{2}v_{sd}-2i_{sd}.R_f}{C_{dc}v_{dc}} & \frac{3}{2}\frac{v_{sq}}{C_{dc}v_{dc}} & \frac{i_{sd}^2.R_f-\frac{3}{2}v_{sd}i_{sd}-\frac{3}{2}v_{sq}.i_{sq}}{C_{dc}v_{dc}^2} \end{bmatrix}$$

$$Bsv = \begin{bmatrix} 0 & 0 & 0 & K_{iid}K_{pvd} \\ -K_{iiq}K_{pvq} & 0 & K_{iiq}K_{pvq} & 0 \\ 0 & 0 & 0 & K_{ivd} \\ -K_{ivq} & 0 & K_{ivq} & 0 \\ \frac{1}{L_f} & 0 & 0 & \frac{K_{pid}K_{pvd}}{L_f} \\ -\frac{K_{piq}K_{pvq}}{L_f} & \frac{1}{L_f} & \frac{K_{piq}K_{pvq}}{L_f} & 0 \\ \frac{3}{2}\frac{i_{sd}}{C_{dc}v_{dc}} & \frac{3}{2}\frac{i_{sq}}{C_{dc}v_{dc}} & 0 & 0 \end{bmatrix}$$

K_{pidq} K_{iidq}: represent the proportional and integral gains of current controller of direct and quadrature components

K_{pvdq} K_{ivdq}: represent the proportional and integral gains of voltage controller of direct and quadrature components

4.4.2.2 State space analysis of STATCOM with reactive power control

Using the reactive power required at a busbar is the second type of control modes of the STATCOM as shown in Chapter 3. The state space matrix (Asq) and the input matrix (Bsq) of the STATCOM which their quadrature voltage magnitude is controlled with the reactive power is given as follows:

$$Asq = \begin{bmatrix} 0 & 0 & K_{iid} & 0 & -K_{iid} & 0 & -K_{iid}K_{pvd} \\ 0 & 0 & 0 & K_{iiq} & -\frac{3}{2}K_{iiq}K_{pvq}v_{sq} & \frac{3}{2}K_{iiq}K_{pvq}v_{sd} - K_{iiq} & 0 \\ 0 & 0 & 0 & 0 & 0 & 0 & -K_{ivd} \\ 0 & 0 & 0 & 0 & -\frac{3}{2}K_{ivq}v_{sq} & \frac{3}{2}K_{ivq}v_{sd} & 0 \\ \frac{1}{L_f} & 0 & \frac{K_{pid}}{L_f} & 0 & \frac{-R_f - K_{pid}}{L_f} & \omega & \frac{-K_{pid}K_{pvd}}{L_f} \\ 0 & \frac{1}{L_f} & 0 & \frac{K_{piq}}{L_f} & -\frac{3}{2}\frac{K_{piq}K_{pvq}v_{sq}}{L_f} - \omega & \frac{-R_f - K_{piq} + \frac{3}{2}K_{piq}K_{pvq}v_{sd}}{L_f} & 0 \\ 0 & 0 & 0 & 0 & \frac{\frac{3}{2}v_{sd} - 2i_{sd}.R_f}{C_{dc}v_{dc}} & \frac{3}{2}\frac{v_{sq}}{C_{dc}v_{dc}} & \frac{\alpha_{dc}}{C_{dc}v_{dc}^2} \end{bmatrix}$$

$$Bsq = \begin{bmatrix} 0 & 0 & K_{iid}K_{pvd} & 0 \\ \frac{3}{2}K_{iiq}K_{pvq}i_{sq} & \frac{-3}{2}K_{iiq}K_{pvq}i_{sd} & 0 & K_{iiq}K_{pvq} \\ 0 & 0 & K_{ivd} & 0 \\ \frac{3}{2}K_{ivq}i_{sq} & \frac{-3}{2}K_{ivq}i_{sd} & 0 & Ki_{vq} \\ \frac{1}{L_f} & 0 & \frac{K_{pid}K_{pvd}}{L_f} & 0 \\ \frac{3}{2}\frac{K_{piq}K_{pvq}i_{sq}}{L_f} & \frac{1-\frac{3}{2}K_{piq}K_{pvq}i_{sd}}{L_f} & 0 & \frac{K_{piq}}{L_f} \\ \frac{3}{2}\frac{i_{sd}}{C_{dc}v_{dc}} & \frac{3}{2}\frac{i_{sq}}{C_{dc}v_{dc}} & 0 & 0 \end{bmatrix}$$

where, the linearization of the reactive power is given as:

$$\Delta Q = \frac{3}{2} v_{sq} \Delta i_{sd} - \frac{3}{2} v_{sd} \Delta i_{sq} - \frac{3}{2} i_{sq} \Delta v_{sd} + \frac{3}{2} i_{sd} \Delta v_{sq} \quad (4.40)$$

4.4.2.3 dq impedance of STATCOM based direct voltage control

The impedance model of the STATCOM can be derived by the arrangement of the STATCOM linearized equations (4.38) and (4.39) to have:

$$\mathbf{\Delta v_{sdq}} = a_Z \mathbf{\Delta i_{sdq}} - b_Z \mathbf{\Delta i^*_{sdq}} \quad (4.41)$$

$$\mathbf{\Delta i^*_{sdq}} = c_Z \mathbf{v}^* - c_Z \mathbf{v} \quad (4.42)$$

The definition of symbols in equations (4.41) and (4.42) is found in the previous sections. The voltage controller is responsible for controlling the dc link and bus voltages using:

$$d_z \mathbf{v} = f v_z \mathbf{\Delta v_{sdq}} + e v_z \mathbf{\Delta i_{sdq}} \quad (4.43)$$

where, the submatrices are defined as:

- The topology matrix:

$$a_Z = \begin{bmatrix} L_f s + R_f + \left(K_{pid} + \frac{K_{iid}}{s}\right) & -\omega L_f \\ \omega L_f & R_f + L_f s + \left(K_{piq} + \frac{K_{iiq}}{s}\right) \end{bmatrix}$$

- The current and voltage controller matrices are defined as:

$$b_Z = -\begin{bmatrix} \left(K_{pid} + \frac{K_{iid}}{s}\right) & 0 \\ 0 & \left(K_{piq} + \frac{K_{iiq}}{s}\right) \end{bmatrix} \quad c_Z = \begin{bmatrix} \left(K_{pvd} + \frac{K_{ivd}}{s}\right) & 0 \\ 0 & \left(K_{pvq} + \frac{K_{ivq}}{s}\right) \end{bmatrix}$$

- The dc link voltage calculation matrices

$$d_z = \begin{bmatrix} \frac{sC_{dc}v_{dc}^2 - \alpha_{dc}}{v_{dc}} & 0 \\ 0 & 1 \end{bmatrix} \qquad ev_z = \begin{bmatrix} \left(\frac{3}{2} v_{sd} - 2 i_{sd}.R_f\right) & \frac{3}{2} v_{sq} \\ 0 & 0 \end{bmatrix}$$

$$fv_z = \begin{bmatrix} \frac{3}{2}i_{sd} & \frac{3}{2}i_{sq} \\ 1 & 0 \end{bmatrix} \qquad \alpha_{dc} = i_{sd}^2.R_f - \frac{3}{2}\left(v_{sd}i_{sd} + v_{sq}.i_{sq}\right)$$

Equations (4.42) and (4.43) show the STATCOM impedance in synchronous dq coordinates. The full derivation of STATCOM impedance is found in Appendix-B. Using Mason's gain formula or any block reduction method, the total transfer function of the small signal STATCOM impedance is as follows:

$$\mathbf{\Delta v_{sdq}} = Z_{STATCOMV}\mathbf{\Delta i_{sdq}} + D_{dq}\mathbf{v}^* \tag{4.44}$$

where, the STATCOM impedance ($Z_{STATCOMV}$) is given as:

$$Z_{STATCOMV} = \frac{a_Z + b_Z c_Z d_Z^{-1} e v_z}{I - b_Z c_Z d_Z^{-1} f v_z} \tag{4.45}$$

The STATCOM operation is considered in this thesis to be ideal, meaning that the pulse width modulation delay (PWM) and the measurement delay (md) are ignored. The main effect of ignoring the PWM delay is that the off-diagonal impedance will be very small, whilst the measurement delay is significant only in large systems. These delays can be added to the model as shown in Figure 4.7 or by making the stability assessment more conservative.

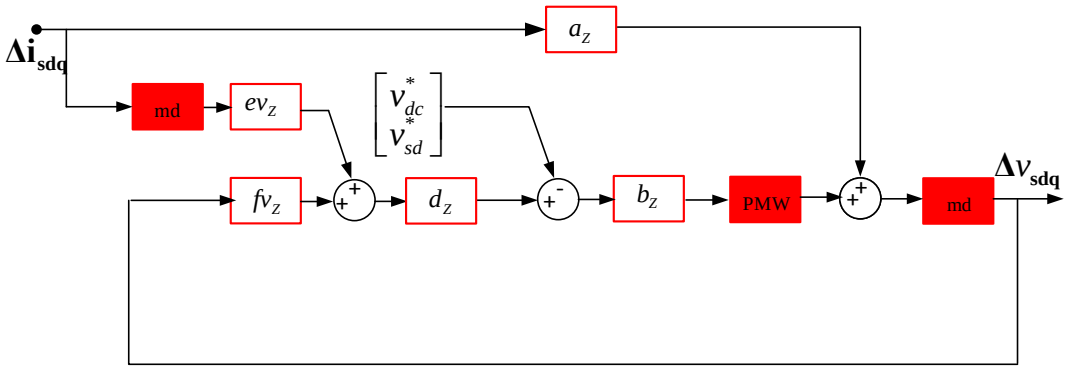

Figure 4.7. Block diagram of STATCOM impedance model of direct voltage control.

4.4.2.4 dq impedance of STATCOM with reactive power control

The second type of STATCOM control is the control with reactive power control. It is derived in similar way as the previous analysis as (details in Appendix-D):

$$Z_{STATCOMQ} = (\mathrm{I} - b_z c_z d_z^{-1} f_z)^{-1}(a_z + b_z c_z d_z^{-1} e_z) \tag{4.46}$$

The definitions of the matrices in equation (4.46) are:

$$f_z = \frac{3}{2}\begin{bmatrix} i_{sd} & i_{sq} \\ -i_{sq} & i_{sd} \end{bmatrix} \qquad e_z = \begin{bmatrix} \left(\frac{3}{2}v_{sd} - 2R_f i_{sd}\right) & \frac{3}{2}v_{sq} \\ \frac{3}{2}v_{sq} & -\frac{3}{2}v_{sd} \end{bmatrix}$$

4.4.2.5 The validation of STATCOM model

The impedance injection method is used to validate the linearized model of the STATCOM. This model is compared with the linearized equations derived here by finding the small signal admittance of the two models as shown in Figure 4.8. The resulted impedances of the two models are equal over the range of the frequency of study which validates the linearized equations. The effect of the operating point on the measured impedance has been reported in [87], therefore, both average and mathematical models of the STATCOM are measured at the same operating conditions.

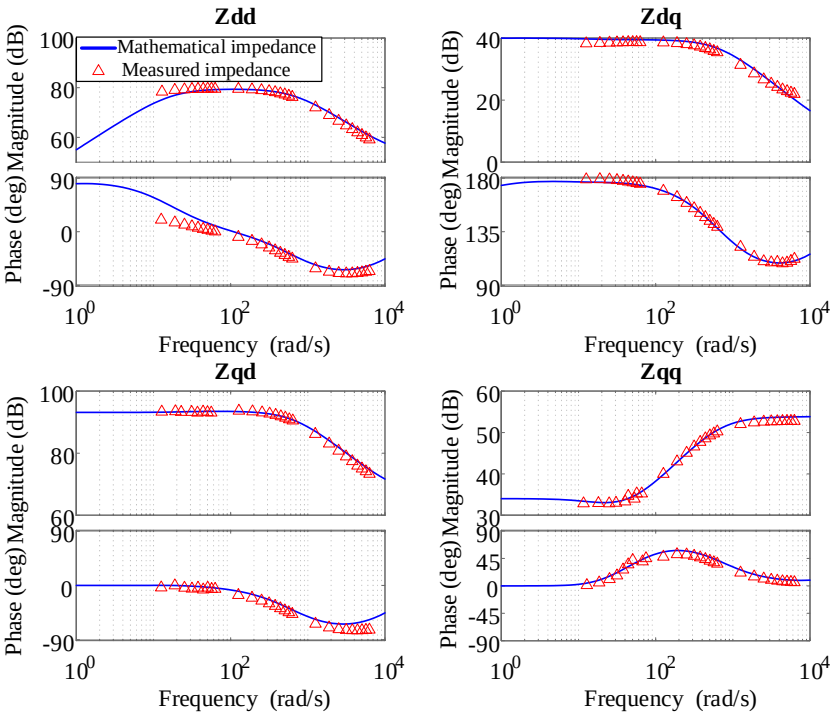

Figure 4.8. Validation of STATCOM impedance model based direct voltage control.

The accuracy of the measured impedance can be improved by repeating the measurement several times with different magnitudes and phase of the injected signal. The impedance representation of the STATCOM shows off-diagonal impedances is fixed impedance at low frequencies while it decreases at high frequencies. In the meantime for the diagonal impedance, the Z_{dd} changes its magnitude and phase by the change of the frequency while the Z_{qq} has affixed magnitude and phase at low frequencies and tend to increase at higher frequencies.

4.4.3 Small signal derivation of synchronous machines

The synchronous machine is one of the main factors, which ensures the stability issues and might responsible for the system oscillations. The performance of VSC-FACTS devices will be examined on damping those oscillations and compared between their effectiveness.

4.4.3.1 State space analysis of the synchronous generator

The arrangement of the linearized equations of the synchronous generator presented as [98].

$$\frac{d}{dt}\begin{bmatrix} \mathbf{\Delta i^{r}_{dqs}} \\ \mathbf{\Delta i`^{r}_{kq12}} \\ \mathbf{\Delta i`^{r}_{fkd}} \\ \mathbf{\Delta i^{r}_{mdq}} \\ \mathbf{\Delta\omega\delta} \end{bmatrix} = -D_{syn}^{-1}A_{Syn}\begin{bmatrix} \mathbf{\Delta i^{r}_{dqs}} \\ \mathbf{\Delta i`^{r}_{kq12}} \\ \mathbf{\Delta i`^{r}_{fkd}} \\ \mathbf{\Delta i^{r}_{mdq}} \\ \mathbf{\Delta\omega\delta} \end{bmatrix} + D_{syn}^{-1}\begin{bmatrix} \mathbf{\Delta v^{r}_{dqs}} \\ \mathbf{\Delta v`^{r}_{fkd}} \\ \mathbf{\Delta v`^{r}_{kq12}} \\ \Delta T_m \\ 0 \end{bmatrix} \tag{4.47}$$

The inclusion of the mechanical part can be included as shown the state space equation (4.48) as:

$$D_{syn}\frac{d}{dt}\begin{bmatrix} \mathbf{\Delta i^{r}_{dqs}} \\ \mathbf{\Delta i`^{r}_{kq12}} \\ \mathbf{\Delta i`^{r}_{fkd}} \\ \mathbf{\Delta\delta} \\ \mathbf{\Delta\omega} \end{bmatrix} = AA\begin{bmatrix} \mathbf{\Delta i^{r}_{dqs}} \\ \mathbf{\Delta i`^{r}_{kq12}} \\ \mathbf{\Delta i`^{r}_{fkd}} \\ \mathbf{\Delta\delta} \\ \mathbf{\Delta\omega} \end{bmatrix} + BB\begin{bmatrix} \mathbf{\Delta v^{r}_{dqs}} \\ \mathbf{\Delta v`^{r}_{kq12}} \\ \mathbf{\Delta v`^{r}_{fkd}} \\ \mathbf{T_{tu}} \end{bmatrix} \tag{4.48}$$

where,

- The stator current vector and voltage vector referred to the rotor is given as:

$\mathbf{\Delta i^{r}_{dqs}} = [\Delta i^{r}_{ds} \quad \Delta i^{r}_{qs}]^T$ $\mathbf{\Delta v^{r}_{dqs}} = [\Delta v^{r}_{ds} \quad \Delta v^{r}_{qs}]^T$

- The quadrature dampers currents and voltage vector are:

$\mathbf{\Delta i`^{r}_{kq12}} = [\Delta v`^{r}_{kq1} \quad \Delta v`^{r}_{kq2}]^T$

$\mathbf{\Delta v`^{r}_{kq12}} = [\Delta v`^{r}_{kq1} \quad \Delta v`^{r}_{kq2}]^T$

- The excitation field and direct damper voltage and current vectors are:

$\mathbf{\Delta i`^{r}_{fkd}} = \left[\mathbf{\Delta i`^{r}_{fd}} \quad \mathbf{\Delta i`^{r}_{kd}}\right]^{T}$ $\mathbf{\Delta v`^{r}_{fkd}} = \left[\mathbf{\Delta v`^{r}_{fd}} \quad \mathbf{\Delta v`^{r}_{kd}}\right]^{T}$

- The speed of the turbine masses vector:

$\mathbf{\Delta\omega} = [\Delta\omega_1 \quad \Delta\omega_2 \quad \Delta\omega_3 \quad \Delta\omega_4 \quad \Delta\omega_5]^T$

- The angular position of turbine masses vector

$\mathbf{\Delta\delta} = [\Delta\delta_1 \quad \Delta\delta_2 \quad \Delta\delta_3 \quad \Delta\delta_4 \quad \Delta\delta_5]^T$

- The mechanical torques developed by the respective turbine sections:

$$\mathbf{T_{tu}} = [T_{LP_A} \quad T_{LP_B} \quad T_{IP} \quad T_{HP}]^T$$

$$\mathbf{\Delta\omega\delta} = [\Delta\delta \quad \Delta\omega]$$

While, the definition of the matrices (D_{syn}), (AA) and $(BB)$are:

$$AA = \begin{bmatrix} AA_{11} & AA_{12} & AA_{13} \\ AA_{21} & AA_{22} & AA_{23} \\ AA_{31} & AA_{32} & AA_{33} \end{bmatrix}$$

The definitions of the submatrices of the matrix (AA) are:

$$A_{11} = \begin{bmatrix} r_s & 0 & 0 & -\omega_r L_{ls} - \omega_r L_{mq} & \omega_r L_{mq} & \omega_r L_{mq} \\ 0 & r_{kd1}^{`r} & 0 & 0 & 0 & 0 \\ 0 & 0 & r_{fd}^{`r} & 0 & 0 & 0 \\ \omega_r L_{ls} + \omega_r L_{md} & -\omega_r L_{md} & -\omega_r L_{md} & r_s & 0 & 0 \\ 0 & 0 & 0 & 0 & r_{kq1}^{`r} & 0 \\ 0 & 0 & 0 & 0 & 0 & r_{kq2}^{`r} \end{bmatrix}$$

$$AA_{32} = \begin{bmatrix} -\frac{k_{12}}{2H_1} & \frac{k_{12}}{2H_1} & 0 & 0 & 0 \\ \frac{k_{12}}{2H_2} & -\frac{k_{23}}{2H_2} - \frac{k_{12}}{2H_2} & \frac{k_{23}}{2H_2} & 0 & 0 \\ 0 & \frac{k_{23}}{2H_3} & -\frac{k_{34}}{2H_3} - \frac{k_{23}}{2H_3} & \frac{k_{34}}{2H_3} & 0 \\ 0 & 0 & \frac{k_{34}}{2H_4} & -\frac{k_{45}}{2H_4} - \frac{k_{34}}{2H_4} & \frac{k_{45}}{2H_4} \\ 0 & 0 & 0 & \frac{k_{45}}{2H_5} & -\frac{k_{45}}{2H_5} \end{bmatrix}$$

$$AA_{12} = Zeros[6 \times 5]$$

$$AA_{21} = zeros\ [5 \times 6]$$

$$AA_{13} = \begin{bmatrix} -L_{ls} i_{ds}^r + L_{mq}\left(-i_{kq2}^{`r} - i_{kq1}^{`r} + i_{qs}^r\right) & 0 & 0 & 0 & 0 \\ L_{ls} i_{ds}^r - L_{md}\left(i_{fd}^{`} + i_{kd1}^{`r} - i_{ds}^r\right) & 0 & 0 & 0 & 0 \\ 0 & 0 & 0 & 0 & 0 \\ 0 & 0 & 0 & 0 & 0 \\ 0 & 0 & 0 & 0 & 0 \\ 0 & 0 & 0 & 0 & 0 \end{bmatrix}$$

$$AA_{22} = Zeros[5 \times 5]$$

$$AA_{23} = \begin{bmatrix} \omega & 0 & 0 & 0 & 0 \\ 0 & \omega & 0 & 0 & 0 \\ 0 & 0 & \omega & 0 & 0 \\ 0 & 0 & 0 & \omega & 0 \\ 0 & 0 & 0 & 0 & \omega \end{bmatrix} \quad AA_{33} = \begin{bmatrix} -\frac{D_1}{2H_1} & 0 & 0 & 0 & 0 \\ 0 & -\frac{D_2}{2H_2} & 0 & 0 & 0 \\ 0 & 0 & -\frac{D_3}{2H_3} & 0 & 0 \\ 0 & 0 & 0 & -\frac{D_4}{2H_4} & 0 \\ 0 & 0 & 0 & 0 & -\frac{D_5}{2H_5} \end{bmatrix}$$

$$AA_{31} = \frac{\omega_1}{2H_1}[aa_{1_{31}} \quad aa_{2_{31}}]$$

$$aa_{1_{31}} = \begin{bmatrix} \left(L_{mq} i^r_{ds0}\right) & -\left(L_{md} i^r_{qs0}\right) & -\left(L_{md} i^r_{qs0}\right) \\ & & \end{bmatrix}$$

$$aa_{2_{31}} = \begin{bmatrix} \left(-L_{md} i^r_{qs0} + L_{mq} i^r_{qs0}\right) & \left(L_{mq} i^r_{ds0} - L_{md}(i^r_{ds0} - i^{`r}_{fd0})\right) & \left(L_{mq} i^r_{ds0}\right) \\ & & zeros\ (4 \times 6) \end{bmatrix}$$

Also, the definition of the matrices (D_{syn}) and (BB) is:

$$D_{syn}$$

$$= \begin{bmatrix} -L_{ls} - L_{md} & L_{md} & L_{md} & 0 & 0 & 0 & \\ -L_{md} & L_{lkd1}^{`} + L_{md} & L_{md} & 0 & 0 & 0 & \\ -L_{md} & L_{md} & L_{lfd}^{`} + L_{md} & 0 & 0 & 0 & zeros(6 \times 10) \\ 0 & 0 & 0 & -L_{ls} - L_{mq} & L_{mq} & L_{mq} & \\ 0 & 0 & 0 & -L_{mq} & L_{lkq1}^{`} + L_{mq} & L_{mq} & \\ 0 & 0 & 0 & -L_{mq} & L_{mq} & L_{lkq2}^{`} + L_{mq} & \\ & & & zeros(10 \times 6) & & & I(10 \times 6) \end{bmatrix}$$

$$BB = \begin{bmatrix} I(6\times 6) & & & zeros(6\times 3) \\ & zeros(6\times 9) & & \\ & \frac{1}{2H_2} & 0 & 0 & 0 \\ & 0 & \frac{1}{2H_3} & 0 & 0 \\ zeros(4\times 5) & 0 & 0 & \frac{1}{2H_4} & 0 \\ & 0 & 0 & 0 & \frac{1}{2H_5} \end{bmatrix}$$

4.4.3.2 dq impedance of the synchronous generator

The synchronous machine equation can be linearizing and by substituting the mutual inductance equation in voltage equations to have:

$$\begin{bmatrix} \mathbf{\Delta v^r_{dqs}} \\ \mathbf{\Delta v^{`r}_{fkd}} \\ \mathbf{\Delta v^{`r}_{kq12}} \end{bmatrix} = \begin{bmatrix} -r_s - sL_{ls} & \omega_r L_{ls} & 0 & 0 & 0 & 0 \\ -\omega_r L_{ls} & -r_s - sL_{ls} & 0 & 0 & 0 & 0 \\ 0 & 0 & -r^{`r}_{kd1} + sL^{`}_{lkd1} & 0 & 0 & 0 \\ 0 & 0 & 0 & -r^{`r}_{fd} + sL^{`}_{lfd} & 0 & 0 \\ 0 & 0 & 0 & 0 & -r^{`r}_{kq1} + sL^{`}_{lkq1} & 0 \\ 0 & 0 & 0 & 0 & 0 & -r^{`r}_{kq2} + sL^{`}_{lkq2} \end{bmatrix} \begin{bmatrix} \mathbf{\Delta i^r_{dqs}} \\ \mathbf{\Delta i^{`r}_{fkd}} \\ \mathbf{\Delta i^{`r}_{kq12}} \end{bmatrix} + \begin{bmatrix} sL_{md} & -\omega_r L_{mq} \\ sL_{md} & 0 \\ sL_{md} & 0 \\ \omega_r L_{md} & sL_{mq} \\ 0 & sL_{mq} \\ 0 & sL_{mq} \end{bmatrix} \mathbf{\Delta i^r_{mdq}} + \begin{bmatrix} L_{ls} i^r_{qs} - L_{mq} i^r_{mq} & 0 \\ 0 & 0 \\ 0 & 0 \\ L_{md} i^r_{md} - L_{ls} i^r_{ds} & 0 \\ 0 & 0 \\ 0 & 0 \end{bmatrix} \mathbf{\Delta\omega\delta} \quad (4.49)$$

$$\mathbf{\Delta i^r_{mdq}} = [\Delta i^r_{md} \quad \Delta i^r_{mq}]^T$$

According to current directions assumed in synchronous machine equivalent circuit presented in chapter 3, and using KCL and with the assumption that the field voltage is constant during the operation ($\Delta v^{`}_{fd} = 0$), the stator voltage is given as:

$$\mathbf{\Delta v^{r}_{dqs}} = \begin{bmatrix} (-r_s - sL_{ls}) + sL_{md}A_{msd} & \omega_r L_{ls} - \omega_r L_{mq}A_{msq} \\ -\omega_r L_{ls} + \omega_r L_{md}A_{msd} & (-r_s - SL_{ls}) + sL_{mq}A_{msq} \end{bmatrix} \mathbf{\Delta i^{r}_{dqs}} + \begin{bmatrix} (L_{ls}i^r_{qs} - L_{mq}i^r_{mq}) & 0 \\ (L_{md}i^r_{md} - L_{ls}i^r_{ds}) & 0 \end{bmatrix} \mathbf{\Delta \omega \delta} \quad (4.50)$$

$$\mathbf{\Delta v^{r}_{dqs}} = \begin{bmatrix} Z_{dd} & Z_{dq} \\ Z_{qd} & Z_{qq} \end{bmatrix} \mathbf{\Delta i^{r}_{dqs}} + \begin{bmatrix} (L_{ls}i^r_{qs} - L_{mq}i^r_{mq}) & 0 \\ (L_{md}i^r_{md} - L_{ls}i^r_{ds}) & 0 \end{bmatrix} \mathbf{\Delta \omega \delta} \quad (4.51)$$

$$\mathbf{\Delta v^{r}_{dqs}} = ZZ\mathbf{\Delta i^{r}_{dqs}} + A\lambda\, \mathbf{\Delta \omega \delta} \quad (4.52)$$

By linearizing the electrical torque equation and substituting the mutual inductance and the currents in torque equation for getting the form:

$$\mathbf{\Delta Tem} = \left(\frac{3}{2}\right)\left(\frac{P}{2}\right) \begin{bmatrix} T_d & T_q \\ 0 & 0 \end{bmatrix} \mathbf{\Delta i^{r}_{dqs}} \quad (4.53)$$

where, $\mathbf{\Delta Tem} = [\Delta T_e \quad \Delta T_m]^T$

$$\mathbf{\Delta Tem} = GT_{dq}\mathbf{\Delta i^{r}_{dqs}} \quad (4.54)$$

The rotor speed deviation ($\Delta\omega_r$) can be found as:

$$\frac{d}{dt}\Delta\omega_r = \frac{1}{2H}(\Delta T_m - \Delta T_e - D_1.\Delta\omega_r) \quad (4.55)$$

$$\mathbf{\Delta \omega \delta} = AH.GT_{dq}\mathbf{\Delta i^{r}_{dqs}} \quad (4.56)$$

$$AH = \begin{bmatrix} \frac{-1}{2HS+D_1} & 0 \\ 0 & 0 \end{bmatrix}, \qquad GT_{dq} = \begin{bmatrix} T_d & T_q \\ 0 & 0 \end{bmatrix}$$

Substituting (4.56) in (4.52) to have:

$$\mathbf{\Delta v^{r}_{dqs}} = \left(ZZ + A\lambda\,.AH.GT_{dq}\right)\mathbf{\Delta i^{r}_{dqs}} \quad (4.57)$$

$$\mathbf{\Delta v^{r}_{dqs}} = Z_{synch}\mathbf{\Delta i^{r}_{dqs}} \quad (4.58)$$

A detailed full derivation is included in Appendix-C. The validation of the synchronous machine impedance (4.58) is carried out using the direct measurement of the synchronous impedance using the impedance measurement method presented previously in this chapter. A voltage injection method is employed to perturb the synchronous machine. The injected frequencies are between (1 to 10000) rad/s. The parameters of the synchronous machine are listed in Table 4.2. The mathematical model in equation (4.58) is validated by comparing it with the impedance measurement of the detiled model as shown in Figure 4.9. The two measurements are generally well matched except for (Z_{dd}) at very low frequencies. This is attributed to the nonlinearity response of the synchronous machine to low frequency measurements which affected the results.

Table 4.2. Synchronous machine parameters.

Parameter	Value	Parameter	Value
r_s, L_{ls}	2.85 mΩ, 21 mH	L_{md}, L_{mq}	1.785 mΩ, 0.54 H
R_{fd}, L_{lfd}	86.85 mΩ, 0.171H	R_{kd1}, L_{lkd1}	97.8 mΩ, 0.7701 H
R_{kq1}, L_{lkq1}	43 mΩ, 0.383	R_{kq2}, L_{lkq2}	11.6 mΩ, 1.375 H
i_{fd0}	0.6586 A	i_{kq1}	23.3μA
i_{kd1}	-9.5467 μA	i_{kq2}	.273mA
H_1	2.82 s	H_2	0.88421 s
H_3	0.85867 s	H_4	0.1556 s
H_5	0.092897 s	K_{12}	70.858 pu/rad
K_{23}	52.038 pu/rad	K_{34}	34.929 pu/rad
K_{45}	19.303 pu/rad	[D_2 D_3 D_4 D_5]	[0 0 0 0]

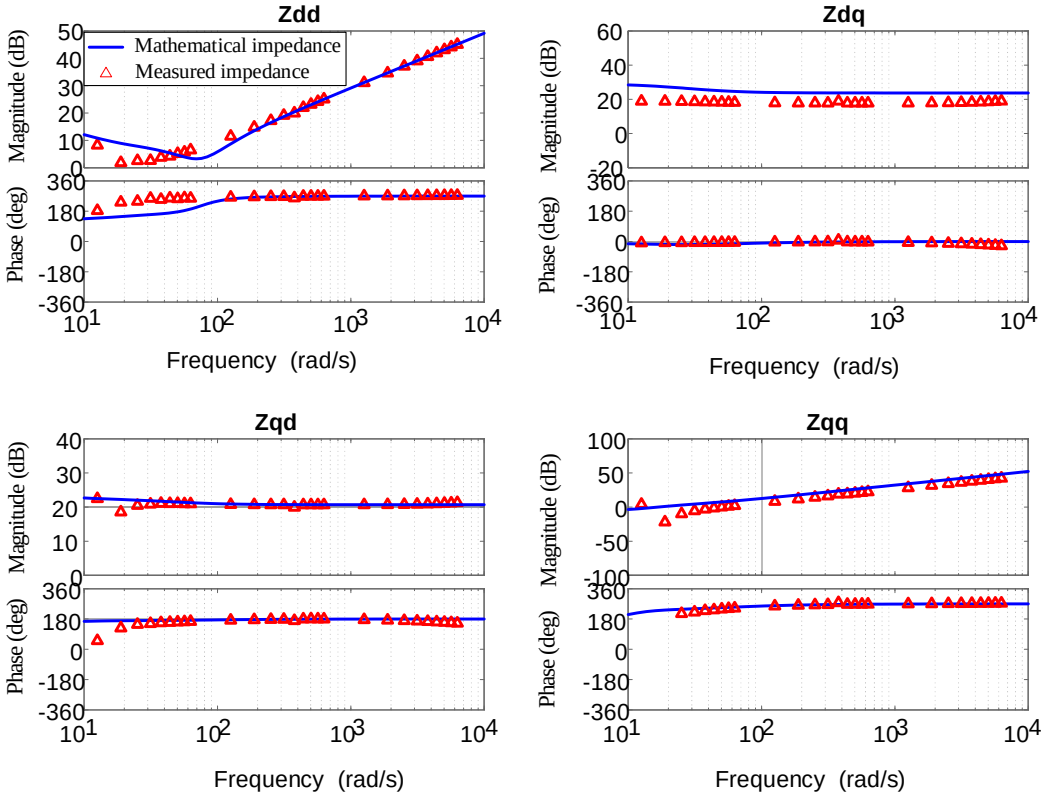

Figure 4.9. Validation of the impedance of electrical part of synchronous machine.

The general trend of the diagonal impedance shows an increase of the synchronous impedance magnitude while the phase is almost constant at 270^{o}. Alternatively, the off-diagonal impedances are constant at about 20 dB with a constant phase at 0^{o} and 180^{o} for the $Z_{dq}$and Z_{qd} respectively.

4.4.3.3 Effect of turbine dynamics on synchronous machine impedance

Including the mechanical part of the synchronous machine is introduced in this section. The mechanical part has four mass sections and the generator as shown in Figure 4.10 which is be beneficial for studying the system oscillations and the efficiency of VSC-FACTS on damping those oscillations. The turbine converts the stored energy of steam into rotating energy. Based on the pressure of the each turbine section, these sections are named as two low-pressure turbine section ($LP_{A,}$ LP_{B}), intermediate pressure (IP) and high pressure section (HP).

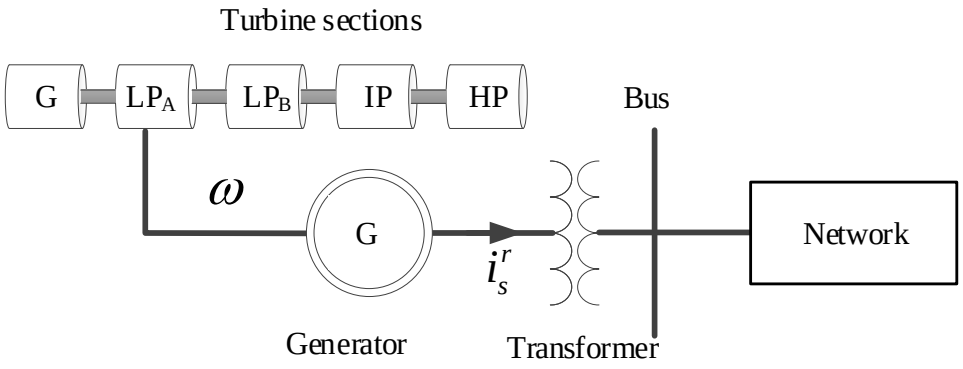

Figure 4.10. Turbine-generator system connected to grid.

The speed relations at the generator and the other for sections of turbine system shown in Figure 4.10 can be given as [91]:

- For the generator:

$$2H_1 \frac{d\Delta\omega_1}{dt} = k_{12}(\delta_2 - \delta_1) - T_e - D_1\Delta\omega_1$$

$$\Delta\omega_1 = \frac{S\Delta\delta_1}{\omega} \tag{4.59}$$

- Low pressure (LP$_A$):

$$2H_2 \frac{d\Delta\omega_2}{dt} = T_{LP_A} + k_{23}(\delta_3 - \delta_2) - k_{12}(\delta_2 - \delta_1) - D_2\Delta\omega_2 \tag{4.60}$$

$$\Delta\omega_2 = \frac{S\Delta\delta_2}{\omega}$$

- Low pressure (LP$_B$):

$$2H_3 \frac{d\Delta\omega_3}{dt} = T_{LP_B} + k_{34}(\delta_4 - \delta_3) - k_{23}(\delta_3 - \delta_2) - D_3\Delta\omega_3 \tag{4.61}$$

$$\Delta\omega_3 = \frac{S\Delta\delta_3}{\omega}$$

- Intermediate pressure (IP):

$$2H_4\frac{d\Delta\omega_4}{dt} = T_{IP} + k_{45}(\delta_5 - \delta_4) - k_{34}(\delta_4 - \delta_3) - D_4\Delta\omega_4 \tag{4.62}$$

$$\Delta\omega_4 = \frac{S\Delta\delta_4}{\omega}$$

- High pressure (HP):

$$2H_5\frac{d\Delta\omega_5}{dt} = T_{IP} + k_{45}(\delta_5 - \delta_4) - k_{34}(\delta_4 - \delta_3) - D_4\Delta\omega_4 \tag{4.63}$$

$$\Delta\omega_5 = \frac{S\Delta\delta_5}{\omega}$$

The back substitution of equations (4.59) to (4.63) to find $(\Delta\omega_1)$ as a function of the turbine/generator sections yields:

$$\Delta\omega_1 = \frac{sk_{12}\omega}{A_1A_2}T_{LP_A} + \frac{sk_{12}k_{23}\omega^2}{A_1A_2A_3}T_{LP_B} + \frac{sk_{12}k_{23}k_{34}\omega^3}{A_1A_2A_3A_4}T_{IP} + \frac{sk_{12}k_{23}k_{34}k_{45}\omega^4}{A_1A_2A_3A_4\mathrm{A}_5}T_{HP} - \frac{s}{A_1}\Delta T_e \tag{4.64}$$

where,

H_i is the inertia constant of mass i.

ω is the rated speed.

k_{ij} is the shaft stiffness of section $i\ j$

D_i is the damping coefficient.

$$A_1 = 2H_1\mathrm{s}^2 + k_{12}\omega + sD_1 - \frac{(k_{12}\omega)^2}{A_2}$$

$$A_2 = 2H_2 s^2 + k_{23}\omega + k_{12}\omega + sD_2 - \frac{(k_{23}\omega)^2}{A_3}$$

$$A_3 = 2H_3 s^2 + k_{34}\omega + k_{23}\omega + sD_3 - \frac{(k_{34}\omega)^2}{A_4}$$

$$A_4 = 2H_4 s^2 + k_{45}\omega + k_{34}\omega + sD_4 - \frac{(k_{45}\omega)^2}{\mathrm{A}_5}$$

$$\mathrm{A}_5 = 2H_5 s^2 - sD_5 + k_{45}\omega$$

The relation between the electrical torque including the mechanical part can be found by modifying equation (4.56) by substituting equation (4.64) to yields the form:

$$\mathbf{\Delta\omega\delta} = AH_M \mathbf{\Delta Tem} + AH_{M2}\mathbf{T_{tu}} \tag{4.65}$$

where,

$$AH_M = \begin{bmatrix} -\frac{s}{A_1} & 0 \\ 0 & 0 \end{bmatrix}$$

$$AH_{M2} = \begin{bmatrix} \frac{K_{12}\omega}{sA_4A_5} & \frac{K_{12}k_{23}\omega^2}{s^2A_3A_4A_5} & \frac{K_{12}k_{23}k_{34}\omega^3}{s^3A_2A_3\mathrm{A}_4A_5} & \frac{K_{12}k_{23}k_{45}\omega^4}{s^4A_1A_2A_3\mathrm{A}_4A_5} \\ 0 & 0 & 0 & 0 \end{bmatrix}$$

Substituting equation (4.65) and equation (4.54) into equation (4.57) yields:

$$\mathbf{\Delta v^r_{dqs}} = \left(ZZ + A\lambda\,.\,AH_M.\,GT_{dq}\right)\mathbf{\Delta i^r_{dqs}} + A\lambda\,.\,AH_{M2}\mathbf{\Delta T_{tu}} \tag{4.66}$$

$$\mathbf{\Delta v^r_{dqs}} = Z_{synch\_M}\mathbf{\Delta i^r_{dqs}} \tag{4.67}$$

where,

ZZ is the impedance of electrical part of synchronous machine

Z_{synch_M} is the impedance of synchronous machine including turbine and generator mechanics which equal to:

$$Z_{synch\_M} = ZZ + A\lambda \,.\, AH_M . GT_{dq}$$

The full derivation of these equations is included in Appendix-C. The synchronous machine impedance can be represented using equation (4.66), as shown in Figure 4.11.

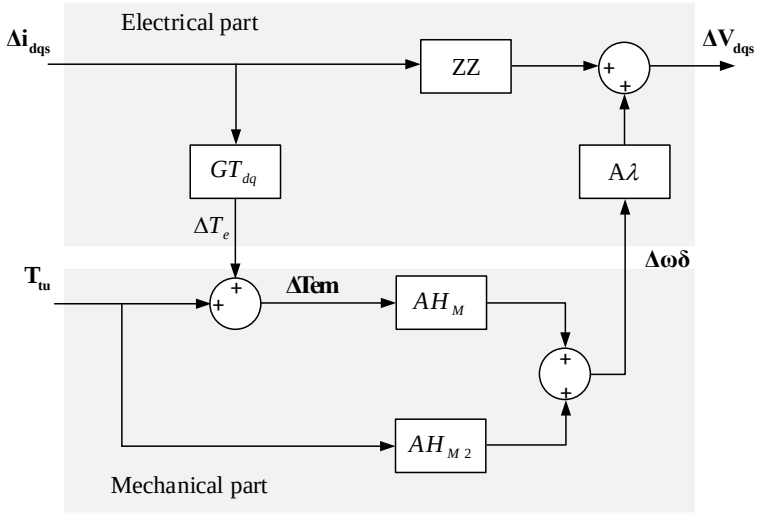

Figure 4.11. Impedance model of the synchronous machine.

The effect of including the mechanical parts to the machine impedance is shown in Figure 4.12. The three impedances (electrical impedance (ZZ) electrical impedance and generator dynamics (Z_{synch}) and generator and turbine impedance (Z_{synch_M}) are equal for direct impedance (Z_{dd}). The off-diagonal impedances (Z_{dq}, Z_{qd}) are equal for the three impedances except some spikes around the 100 rad/s shown by the impedance of turbine-generator impedance (Z_{synch_M}). The main difference between these impedances is found in the quadrature impedance (Z_{qq}). At low frequency the three impedances have different magnitudes; however, the impedances of generator (Z_{synch}) and turbine-generator have almost the same phase. In the meantime, at higher frequencies (over 200 rad/s) the impedance of the electrical part (ZZ) and the turbine-generator impedance have equal values in phase and magnitude. This is referred to the effect of synchronous machine inductances which will be much larger than effect of other system parameters on the total impedance. So, the electrical

impedance of the synchronous machine is sufficient to represent the machine in power frequency studies.

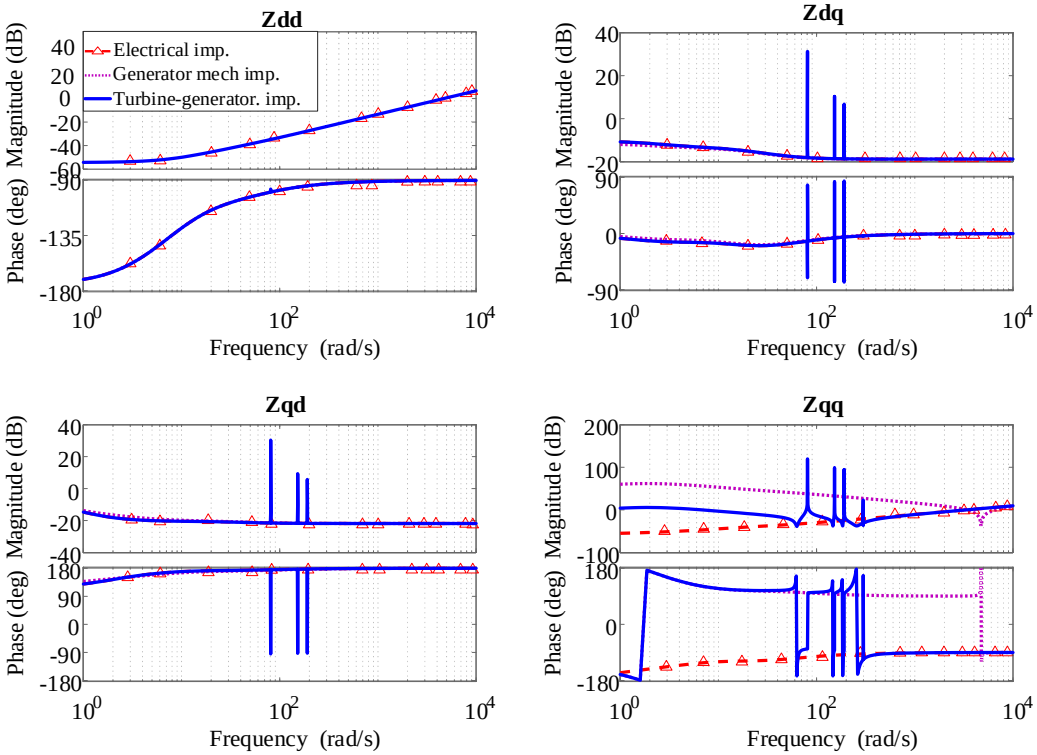

Figure 4.12. Effect of turbine dynamics on synchronous machine impedance.

The combined turbine-generator impedance and the electrical impedance of the synchronous machine can be understood from equation (4.66), where the second part of equation becomes almost zero at high frequencies to have the synchronous machine impedance equal to:

$$Z_{synch\_M} = ZZ + A\lambda \,.\, AH_M . GT_{dq} \approx ZZ \text{ (at high frequencies)} \qquad (4.68)$$

Alternatively, the impedance including only the generator mechanics (Z_{synch}) requires much higher frequencies to align to the electrical impedance (ZZ) as shown in Figure 4.12 due to the mechanical effect of the generator. Also, at high frequencies, the synchronous machine inductances will be dominant where all the other effects can be ignored.

The difference between the mechanical effect of the generator and turbine-generator on the synchronous machine response is presented in Figure 4.13. As expected, the inverse of the mechanical constant of the turbine-generator (s/A_1) is much bigger than the mechanical constant of the generator ($1/2Hs + D_1$) alone. Also, the magnitude of turbine-generator mechanical constant is peaked sharply close to the fundamental frequency due to the oscillatory modes of individual turbine masses which change the phase by 180^o at each mass [99].

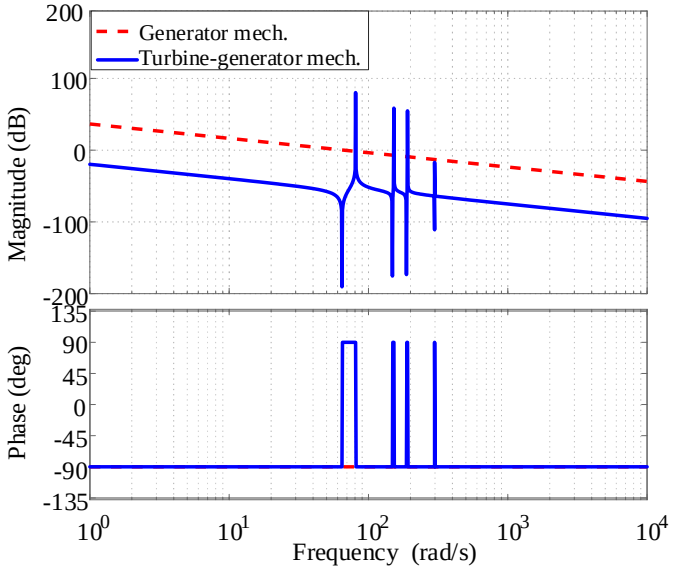

Figure 4.13. Mechanical effect of generator and turbine-generator mechanics.

4.5 Summary

The small signal stability in dq coordinates was discussed in this chapter. Some stability criteria have been reviewed and presented which will be used in Chapter 6 to assess the stability of VSC-FACTS based systems. The chapter also presented the methods used to extract the small signal stability models for the state space and impedance analysis techniques. These models found by direct measurements for the impedance analysis or by finding the mathematical model of the system which is essential for the state space analysis. In addition, the small signal model for the SSSC controlled using three control modes, and the STATCOM were presented. The chapter included the mechanical part effect of the synchronous machine in the state space and impedance models. The derived models in this chapter will be utilised to

examine the response of the VSC-FACTS devices in power systems and include the harmonics in stability problem in Chapter 6. The following points summarise the main outcomes of the chapter:

- The small signal stability-based state space equations require a mathematical derivation which might be difficult to find. However, it eases the modification and design of the control system and presents the contribution of each parameter on the stability problem.
- The small signal impedance provides the concept of black-box control, where the impedance is extracted by the system/device measurements. This feature is very helpful in practical applications, where having full details about the system components become difficult.
- The impedance measurement can be found by perturbing the device/system using series or shunt injection. The perturbation signal could be sinusoidal, chirp or multi-tune signal. The selection between these signals can be carried out based on the application and the time allowed for measurements where the accuracy increases as the measurement time increases.
- The SSSC controlled with power control mode presented some differences in the impedance magnitude and phase in comparison with the voltage and impedance control modes. The other two control mode appeared having the same impedance magnitude and phase where the SSSC impedance is derived from SSSC voltage and current quantities.
- The effect of including the turbine dynamics to the synchronous machine is the effect of the quadrature impedance (Z_{qq}) present mainly at low-frequency range (below the fundamental frequency) where it might affect the stability and cause low-frequency oscillations.
- The difference between the electrical-part impedance, generator mechanical impedance and the turbine-generator impedance were presented. The impedances are equal at high frequencies, where the machine equation denominator of the mechanical effect goes to infinity at high frequencies.

CHAPTER 5

DQ-DYNAMIC PHASOR BASED SMALL SIGNAL STABILITY ANALYSIS FOR VSC-FACTS DEVICES

This chapter proposes a generic dq-dynamic phasor model for studying stability of VSC-FACTS devices in the presence of harmonics and unbalanced conditions. Equations in this chapter are presented for each stage separately to reduce the complexity of dynamic phasor transformation and present the sources of frequency coupling at each stage of the studied system. A development of harmonic stability criteria is presented at the beginning of this chapter. Secondly, generalised state space and impedance models of STATCOM and SSSC with different control modes are presented and simulated. Lastly, high level qualitative comparisons between the proposed model and other conventional modelling techniques are discussed.

5.1 Introduction

In synchronous dq coordinates, the small signal stability using the eigenvalue analysis and equivalent impedance are two methods widely employed to assess system stability. In most cases, the effect of the harmonics is ignored, and this may lead to significant system stability problems, particularly, when the system operates in harmonic polluted environment. Typically, harmonic state space (HSS) facilitates stability studies of linear time-periodic (LTP) systems, which consider the impact of harmonics on system stability. LTP systems produce infinite outputs, with possibly infinite harmonics, due to the interaction between different frequencies within the system. The use of dq-dynamic phasor offers significant advantages over the HSS counterpart; for example, it has reduced order of matrices, more suitable for studying control systems, retains mutual coupling of harmonics, and simplifies stability study under unbalanced conditions.

5.2 Proposed dq-dynamic phasor for small signal stability analysis

In this section, the development of the new dq-dynamic phasor model for small signal stability studies is discussed. The dynamic phasor transformations of the state space equations of an arbitrary system in the synchronous dq frame are given as:

$$\langle \frac{\mathbf{d}}{\mathbf{dt}} \mathbf{\Delta X} \rangle_k = \sum_{k=-\infty}^{\infty} \langle A_{dq} \mathbf{\Delta X} \rangle_k + \sum_{k=-\infty}^{\infty} \langle B_{dq} \mathbf{\Delta U} \rangle_k \tag{5.1}$$

$$\langle \mathbf{\Delta Y} \rangle_k = \sum_{k=-\infty}^{\infty} \langle C_{dq} \mathbf{\Delta X} \rangle_k + \langle D_{dq} \mathbf{\Delta U} \rangle_k \tag{5.2}$$

Equations (5.1) and (5.2) can be written as:

$$\frac{\mathbf{d}}{\mathbf{dt}} \langle \mathbf{\Delta X} \rangle_\mathbf{k} = A_{DP} \langle \mathbf{\Delta X} \rangle_\mathbf{k} + B_{DP} \langle \mathbf{\Delta U} \rangle_\mathbf{k} \tag{5.3}$$

$$\langle \mathbf{\Delta Y} \rangle_\mathbf{k} = C_{DP} \langle \mathbf{\Delta X} \rangle_\mathbf{k} + D_{DP} \langle \mathbf{\Delta U} \rangle_\mathbf{k} \tag{5.4}$$

where,

A_{DP} is the generalised state matrix.

B_{DP} is the generalised input matrix.

C_{DP} is the generalised output matrix of size.

D_{DP} is the generalised feedforward matrix of size.

$\langle \mathbf{\Delta X} \rangle_\mathbf{k}$ is the state vector and equal to:

$$\langle \mathbf{\Delta X} \rangle_\mathbf{k} = [\langle \mathbf{\Delta X} \rangle_{k=0} \quad \langle \mathbf{\Delta X} \rangle_{k=k_1} \quad \langle \mathbf{\Delta X} \rangle_{k=\overline{k_1}} \quad \dots \quad \langle \mathbf{\Delta X} \rangle_{k=k_n}]^{\mathrm{T}}$$

$\langle \mathbf{\Delta U} \rangle_\mathbf{k}$ is the output vector and equal to:

$$\langle \mathbf{\Delta U} \rangle_\mathbf{k} = [\langle \mathbf{\Delta U} \rangle_{k=0} \ \langle \mathbf{\Delta U} \rangle_{k=k_1} \ \langle \mathbf{\Delta U} \rangle_{k=\overline{k_1}} \ \dots \ \langle \mathbf{\Delta U} \rangle_{k=k_n}]^{\mathrm{T}}$$

The bold symbols represent vectors which have an infinite length and include all the interested harmonics of interest in the study ($k = \pm\infty$). Equations (5.3) and (5.4) represent the generalised state space equations including the harmonics with infinite dimensions. The roll-off nature of the inductances and capacitances in the system

provides a reasonable size of the analysed systems matrices due to the low-pass characteristics of these components [100]. The optimum size of arbitrary system matrices can be found by scanning the frequency spectrum until the impedance does not change and the additional eigenvalues at the origin of complex plane [101]. The system matrix sizes are calculated using the following equations as follows:

$$size(A_{DP}) = (2(1+h)\mathcal{L}_a, 2(1+h)\mathcal{L}_a) \tag{5.5}$$

$$size(B_{DP}) = (2(1+h)\mathcal{L}_a, 2(1+h)\mathcal{L}_b) \tag{5.6}$$

$$size(C_{DP}) = (2(1+h), 2(1+h)\mathcal{L}_a) \tag{5.7}$$

$$size(D_{DP}) = (2(1+h), 2(1+h)\mathcal{L}_b) \tag{5.8}$$

where,

h is the number of harmonics to be included in the study.

$\mathcal{L}_a$ is the number of states of the studied system.

$\mathcal{L}_b$ is the number inputs of the studied system.

For an example, when two harmonics ($h = 2$) plus fundamental are considered when analysing the stability of the STATCOM. The synchronous dq model of the STATCOM has ($\mathcal{L}_a = 7$) states and ($\mathcal{L}_b$= 4) inputs as:

$$\mathbf{\Delta X} = [\Delta x_1 \quad \Delta x_2 \quad \Delta x_3 \quad \Delta x_4 \quad \Delta i_{sdq} \quad \Delta v_{dc}]^T$$

$$\mathbf{\Delta U} = [\Delta v_{sd} \quad \Delta v_{sq} \quad \Delta v_{dc}^* \quad \mathrm{Q}^*]^T$$

So, the size of the state matrix (A_{DP}) becomes (42×42) and input matrix (B_{DP}) becomes (42×24). The state space equations (5.3) and (5.4) permit asymptote stability assessment of complex systems using eigenvalues. Equally, small signal impedance offers a powerful and practical alternative method for stability assessment, where synthesis of detailed system model is challenging [67][23]. It can be derived with some minor algebraic manipulations, which yields:

$$\langle \mathbf{\Delta Y} \rangle_{\mathbf{k}} = Z_{DP} \langle \mathbf{\Delta X} \rangle_{\mathbf{k}} \tag{5.9}$$

$$Z_{DP} = \{C_{DP} + D_{DP} B_{DP}^{-1} (S + jk\omega - A_{DP})\} \tag{5.10}$$

Similarly, the impedance (Z_{DP}) represents the generalised impedance of the system with infinite dimensions including all the harmonics of interest and can be written as:

$$Z_{DP} = \left[\begin{array}{ccc|ccc} \frac{\langle v_d \rangle_{k=0}}{\langle i_d \rangle_{k=0}} & \frac{\langle v_d \rangle_{k=0}}{\langle i_d \rangle_{k=k_1}} & \frac{\langle v_d \rangle_{k=0}}{\langle i_d \rangle_{k=\overline{k_n}}} & \frac{\langle v_d \rangle_{k=0}}{\langle i_q \rangle_{k=0}} & \frac{\langle v_d \rangle_{k=0}}{\langle i_q \rangle_{k=k_1}} & \frac{\langle v_d \rangle_{k=0}}{\langle i_q \rangle_{k=\overline{k_n}}} \\ \frac{\langle v_d \rangle_{k=k_1}}{\langle i_d \rangle_{k=0}} & \frac{\langle v_d \rangle_{k=k_1}}{\langle i_d \rangle_{k=k_1}} & \frac{\langle v_d \rangle_{k=k_1}}{\langle i_d \rangle_{k=\overline{k_n}}} & \frac{\langle v_d \rangle_{k=k_1}}{\langle i_q \rangle_{k=0}} & \frac{\langle v_d \rangle_{k=k_1}}{\langle i_q \rangle_{k=k_1}} & \frac{\langle v_d \rangle_{k=k_1}}{\langle i_q \rangle_{k=\overline{k_n}}} \\ \vdots & \ddots & \vdots & \vdots & \ddots & \vdots \\ \frac{\langle v_d \rangle_{k=\overline{k_n}}}{\langle i_d \rangle_{k=0}} & \frac{\langle v_d \rangle_{k=\overline{k_n}}}{\langle i_d \rangle_{k=k_1}} & \frac{\langle v_d \rangle_{k=\overline{k_n}}}{\langle i_d \rangle_{k=\overline{k_n}}} & \frac{\langle v_d \rangle_{k=\overline{k_n}}}{\langle i_q \rangle_{k=0}} & \frac{\langle v_d \rangle_{k=\overline{k_n}}}{\langle i_q \rangle_{k=k_1}} & \frac{\langle v_d \rangle_{k=\overline{k_n}}}{\langle i_q \rangle_{k=\overline{k_n}}} \\ \hline \frac{\langle v_q \rangle_{k=0}}{\langle i_d \rangle_{k=0}} & \frac{\langle v_q \rangle_{k=0}}{\langle i_d \rangle_{k=k_1}} & \frac{\langle v_q \rangle_{k=0}}{\langle i_d \rangle_{k=\overline{k_n}}} & \frac{\langle v_q \rangle_{k=0}}{\langle i_q \rangle_{k=0}} & \frac{\langle v_q \rangle_{k=0}}{\langle i_q \rangle_{k=k_1}} & \frac{\langle v_q \rangle_{k=0}}{\langle i_q \rangle_{k=\overline{k_n}}} \\ \frac{\langle v_q \rangle_{k=k_1}}{\langle i_d \rangle_{k=0}} & \frac{\langle v_q \rangle_{k=k_1}}{\langle i_d \rangle_{k=k_1}} & \frac{\langle v_q \rangle_{k=k_1}}{\langle i_d \rangle_{k=\overline{k_n}}} & \frac{\langle v_q \rangle_{k=k_1}}{\langle i_q \rangle_{k=0}} & \frac{\langle v_q \rangle_{k=k_1}}{\langle i_q \rangle_{k=k_1}} & \frac{\langle v_q \rangle_{k=k_1}}{\langle i_q \rangle_{k=\overline{k_n}}} \\ \vdots & \ddots & \vdots & \vdots & \ddots & \vdots \\ \frac{\langle v_q \rangle_{k=\overline{k_n}}}{\langle i_d \rangle_{k=0}} & \frac{\langle v_q \rangle_{k=\overline{k_n}}}{\langle i_d \rangle_{k=k_1}} & \frac{\langle v_q \rangle_{k=\overline{k_n}}}{\langle i_d \rangle_{k=\overline{k_n}}} & \frac{\langle v_q \rangle_{k=\overline{k_n}}}{\langle i_q \rangle_{k=0}} & \frac{\langle v_q \rangle_{k=\overline{k_n}}}{\langle i_q \rangle_{k=k_1}} & \frac{\langle v_q \rangle_{k=\overline{k_n}}}{\langle i_q \rangle_{k=\overline{k_n}}} \end{array}\right] \tag{5.11}$$

where,

$\overline{k}$ is the conjugate of harmonic order (k).

$\langle v_{dq} \rangle_k$ is the direct and quadrature voltage at harmonic order (k).

$\langle i_{dq} \rangle_k$ is the direct and quadrature current at harmonic order (k).

5.3 Stability criteria for the new generalised dq-dynamic phasor modelling

In this section, the development of the stability criteria for the proposed generalised dq-dynamic phasor modelling is introduced. The generalised state space equation in (5.3) with infinite dimensions can be written in a frequency coupling form as:

$$\frac{\mathbf{d}}{\mathbf{dt}} \mathbf{\Delta X}_{\boldsymbol{k}} = \begin{bmatrix} A - \mathrm{M} + \rho & AC_f \\ AC_h & A - \mathrm{M} + \rho \end{bmatrix} \mathbf{\Delta X}_{\boldsymbol{k}} + \begin{bmatrix} B & BC \\ BC & B \end{bmatrix} \mathbf{\Delta U}_k \tag{5.12}$$

where,

AC_f, AC_h are the mutual effect between the fundamental frequency and harmonics.

ρ is the frequency coupling at the fundamental frequency caused by the existence of positive and negative harmonics at a specific harmonic.

M is a diagonal matrix which represents the transformation of differential variables of the system to dynamic phasor, and it is defined as:

$$\mathrm{M} = \mathrm{diag}[0 \quad j\omega I \quad -j\omega I \quad jk_1\omega I \quad -jk_1\omega I \quad \cdots \quad -jk_n\omega I]$$

So, the eigenvalues of the generalised state matrix in (5.12) can be written as [102]:

$$\boldsymbol{\lambda_k}(A_{DP}) = \det(A_{DP} - \lambda) = (A - \mathrm{M}) + \rho \pm \left(AC_f . AC_h\right)^{1/2} \tag{5.13}$$

According to equation (5.13), the inclusion of harmonics in a stable system generates repeated eigenvalues and does not affect the stability of the system if and only if the frequency coupling terms $\left\{\rho \pm \left(AC_f . AC_h\right)^{1/2}\right\}$ are equal to zero. The stability of the system is ensured when the system eigenvalues ($\boldsymbol{\lambda_k}$) satisfy the condition in equation (5.14) which guarantees that all system eigenvalues will be located at the left hand side of the plane:

$$\boldsymbol{\lambda_k}(A_{DP}) \leq 0 \qquad (-\infty \leq \omega \leq +\infty) \tag{5.14}$$

Using the small signal impedance (Z_{DP}) from equation (5.10), the stability at the connection of the device to the grid can be evaluated by the generalised Nyquist stability criterion [103][104]. It is carried out by creating a Nyquist plot of the eigenvalues of the return ratio matrix (L_R) which can predict the stability of the system as:

$$\boldsymbol{\Delta\lambda_k} = \det(\boldsymbol{\lambda_k} I - \langle L_R \rangle_k) = 0 \tag{5.15}$$

$$\langle L_R \rangle_k = \langle Z_g \rangle_k . \langle Y_{device} \rangle_k \tag{5.16}$$

where,

Y_{device} is the device admittance in the synchronous dq frame.

Z_g is the grid impedance in synchronous dq frame.

$\langle Z_g \rangle_k$ is the grid impedance in dq-dynamic phasor.

$\langle Y_{device} \rangle_k$ is the device admittance in dq-dynamic phasor.

In the case where the frequency coupling is ignored, the impedance is equal for all frequencies. Consequently, it is a repeated plot for all impedances. The frequency range of the Nyquist plot in equation (5.15) is $(-\infty \leq \omega \leq +\infty)$ where the parameters of the proposed model are linear time invariant which is similar to the frequency range presented in Chapter 4 for synchronous dq criteria.

5.4 Proposed generalised dq-dynamic phasor modelling for STATCOM device

This section proposes a generalised state space and impedance model for the STATCOM based on the proposed dq-dynamic phasor modelling that can facilitate stability studies considering the effects of harmonics and network unbalance. As stated, simplified forms of the synchronous dq equations are transformed to dq-dynamic phasor to avoid the complexity of dynamic phasor transformation and identify the causes of the system frequency coupling.

5.4.1 Generalised state space model of STATCOM

The proposed generalised state space model is developed by transforming the STATCOM synchronous dq model presented in Chapter 4 to dq-dynamic phasor. This transformation includes the system harmonics that could affect the system stability. For STATCOM, the state model is depicted in Figure 5.1, while the state representation in generalised form as:

$$\langle \frac{\mathbf{d}}{\mathbf{dt}} \mathbf{\Delta X} \rangle_{\mathbf{k}} = As_{DP} \langle \mathbf{\Delta X} \rangle_{\mathbf{k}} + Bs_{DP} \langle \mathbf{\Delta U} \rangle_{\mathbf{k}} \tag{5.17}$$

$$\langle \mathbf{\Delta is_{dq}} \rangle_{\mathbf{k}} = Cs_{DP} \langle \mathbf{\Delta X} \rangle_{\mathbf{k}} + Ds_{DP} \langle \mathbf{\Delta U} \rangle_{\mathbf{k}} \tag{5.18}$$

where,

ΔX is the STATCOM state variables which equal to:

$$\mathbf{\Delta X} = [\Delta x_1 \quad \Delta x_2 \quad \Delta x_3 \quad \Delta x_4 \quad \Delta i_{sdq} \quad \Delta v_{dc}]^T$$

$$\langle \mathbf{\Delta X} \rangle_{\mathbf{k}} = [\langle \mathbf{\Delta X} \rangle_{\mathrm{k=0}} \quad \langle \mathbf{\Delta X} \rangle_{\mathrm{k=k_1}} \quad \langle \mathbf{\Delta X} \rangle_{\mathrm{k=}\overline{\mathrm{k_1}}} \quad \ldots \quad \langle \mathbf{\Delta X} \rangle_{\mathrm{k=k_n}} \quad \langle \mathbf{\Delta X} \rangle_{\mathrm{k=}\overline{\mathrm{k_n}}}]^{\boldsymbol{T}}$$

$$\mathbf{\Delta U} = [\Delta v_{sd} \quad \Delta v_{sq} \quad \Delta v_{dc}^* \quad \mathrm{Q}^*]^T$$

$$\langle \mathbf{\Delta U} \rangle_{\mathbf{k}} = [\langle \mathbf{\Delta U} \rangle_{\mathrm{k=0}} \quad \langle \mathbf{\Delta U} \rangle_{\mathrm{k=k_1}} \quad \langle \mathbf{\Delta U} \rangle_{\mathrm{k=}\overline{\mathrm{k_1}}} \quad \ldots \quad \langle \mathbf{\Delta U} \rangle_{\mathrm{k=k_n}} \quad \langle \mathbf{\Delta U} \rangle_{\mathrm{k=}\overline{\mathrm{k_n}}}]^{\boldsymbol{T}}$$

The definitions of state vector and input vector can be found in Chapter 3, and the state matrix (As_{DP}) and input matrix (Bs_{DP}) are given as:

$$As_{DP} = \begin{bmatrix} a_{k=0} & ac_{k=\overline{k_1}} & ac_{k=k_1} & \cdots & ac_{k=\overline{k_n}} & ac_{k=k_n} \\ ac_{k=k_1} & a_{k=k_1} & & & 0 & 0 \\ ac_{k=\overline{k_1}} & & a_{k=\overline{k_1}} & & 0 & 0 \\ \vdots & & & \ddots & & \vdots \\ & 0 & 0 & & a_{k=kn} & \\ ac_{k=\overline{k_n}} & 0 & 0 & \cdots & & a_{k=\overline{k_n}} \end{bmatrix}$$

$$Bs_{DP} = \begin{bmatrix} b_{k=0} & bc_{k=\overline{k_1}} & bc_{k=k_1} & \cdots & bc_{k=\overline{k_n}} & bc_{k=k_n} \\ bc_{k=k_1} & b_{k=k_1} & & & 0 & 0 \\ bc_{k=\overline{k_1}} & & b_{k=\overline{k_1}} & & 0 & 0 \\ \vdots & & & \ddots & & \vdots \\ bc_{k=k_n} & 0 & 0 & & b_{k=kn} & \\ bc_{k=\overline{k_n}} & 0 & 0 & \cdots & & b_{k=\overline{k_n}} \end{bmatrix}$$

The bar notation ($\bar{k}$) represents the conjugate of the harmonic (k). The submatrices of the generalised state matrix (A_{DP}) can be defined as:

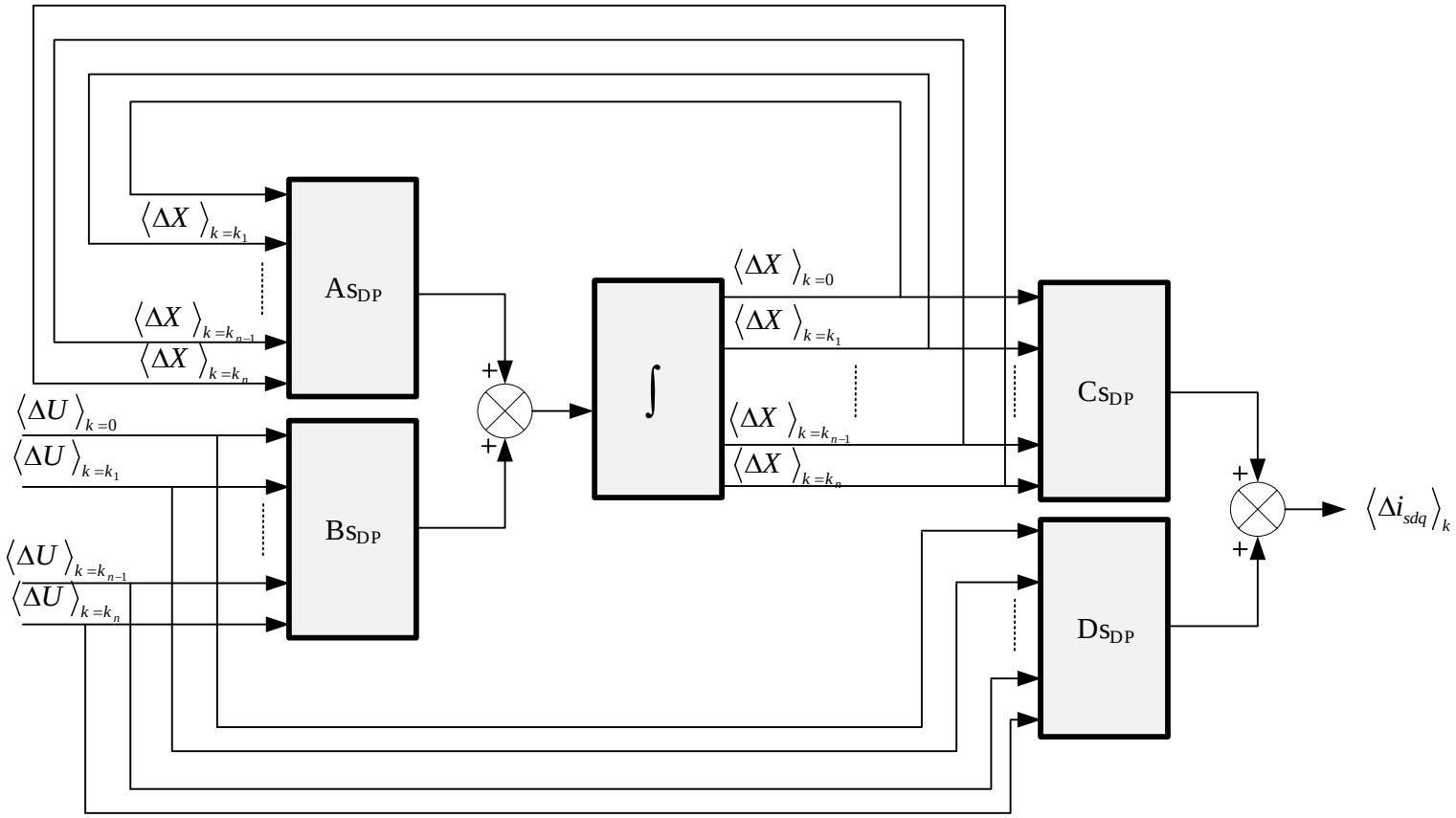

Figure 5.1. Generalised state space model of STATCOM.

- The diagonal submatrices ($a_{k=0}, a_{k=k_1} \dots\dots, a_{k=\overline{k_n}}$) represent the state matrices of the system at specific harmonic order (k) including the frequency coupling caused by the dc link voltage which equals to:

$$a_{k,k} = \begin{bmatrix} -jk\omega & 0 & K_{iid} & 0 & -K_{iid} & 0 & -K_{iid}K_{pvd} \\ 0 & -jk\omega & 0 & K_{iiq} & -\frac{3}{2}K_{iiq}K_{pvq}\langle v_{sq}\rangle_0 & \frac{3}{2}K_{iiq}K_{pvq}\langle v_{sd}\rangle_0 - K_{iiq} & 0 \\ 0 & 0 & -jk\omega & 0 & 0 & 0 & -K_{ivd} \\ 0 & 0 & 0 & -jk\omega & -\frac{3}{2}K_{ivq}\langle v_{sq}\rangle_0 & \frac{3}{2}K_{ivq}\langle v_{sd}\rangle_0 & 0 \\ \frac{1}{L_f} & 0 & \frac{K_{pid}}{L_f} & 0 & \frac{-R_f-K_{pid}}{L_f} - jk\omega & \omega & \frac{-K_{pid}K_{pvd}}{L_f} \\ 0 & \frac{1}{L_f} & 0 & \frac{K_{piq}}{L_f} & -\omega - \frac{\frac{3}{2}K_{piq}K_{pvq}\langle v_{sq}\rangle_0}{L_f} & \frac{\frac{3}{2}K_{piq}K_{pvq}\langle v_{sd}\rangle_0 - R_f - K_{piq}}{L_f} - jk\omega & 0 \\ 0 & 0 & 0 & 0 & \alpha 1 & \alpha 2 & \alpha 3 - jk\omega \end{bmatrix}$$

The parameters of the matrix ($a_{k,k}$) are defined as:

$$\alpha 1 = \frac{3}{2}\frac{1}{C_{dc}}\sum_i^{k=0}\langle v_{sd}\rangle_{k-i}\langle\frac{1}{v_{dc}}\rangle_i - \frac{2R_f}{C_{dc}}\sum_i^{k=0}\langle i_{sd}\rangle_{k-i}\langle\frac{1}{v_{dc}}\rangle_i$$

$$\alpha 2 = \frac{3}{2}\frac{1}{C_{dc}}\sum_i^{k=0}\langle v_{sq}\rangle_{k-i}\langle\frac{1}{v_{dc}}\rangle_i$$

$$\alpha 3 = \frac{R_f}{C_{dc}}\sum_i^{k=0}\langle i_{sd}^2\rangle_{k-i}\langle\frac{1}{v_{dc}^2}\rangle_i - \frac{3}{2}\frac{1}{C_{dc}}\sum_i^{k=0}\langle v_{sd}\rangle_{k-i}\langle i_{sd}\rangle_i\langle\frac{1}{v_{dc}^2}\rangle_0 -$$
$$\frac{3}{2}\frac{1}{C_{dc}}\sum_i^{k=\bar{k}}\langle v_{sd}\rangle_{k-i}\langle i_{sd}\rangle_i\langle\frac{1}{v_{dc}^2}\rangle_k - \frac{3}{2}\frac{1}{C_{dc}}\sum_i^{k=k}\langle v_{sd}\rangle_{k-i}\langle i_{sd}\rangle_i\langle\frac{1}{v_{dc}^2}\rangle_{\bar{k}} -$$
$$\frac{3}{2}\frac{1}{C_{dc}}\sum_i^{k=0}\langle v_{sq}\rangle_{k-i}\langle i_{sq}\rangle_i\langle\frac{1}{v_{dc}^2}\rangle_0 - \frac{3}{2}\frac{1}{C_{dc}}\sum_i^{k=\bar{k}}\langle v_{sq}\rangle_{k-i}\langle i_{sq}\rangle_i\langle\frac{1}{v_{dc}^2}\rangle_k -$$
$$\frac{3}{2}\frac{1}{C_{dc}}\sum_i^{k=k}\langle v_{sq}\rangle_{k-i}\langle i_{sq}\rangle_i\langle\frac{1}{v_{dc}^2}\rangle_{\bar{k}}$$

- The submatrices $\left(ac_{k=\overline{k_1}}, ac_{k=\overline{k_2}}, \dots, ac_{k=\overline{k_n}}\right)$ and the matrices $\left(ac_{k=k_1}, ac_{k=k_1}, \dots, ac_{k=k_n}\right)$ represent the effect of positive and negative sequence components on the fundamental frequency, and the coupling of the fundamental frequency on the negative and positive components is:

$$ac_{k=k} = \begin{bmatrix} zeros(7\times 4) & \begin{matrix} 0 & 0 & 0 \\ -\frac{3}{2}K_{iiq}K_{pvq}\langle v_{sq}\rangle_{\bar{k}} & \frac{3}{2}K_{iiq}K_{pvq}\langle v_{sd}\rangle_{\bar{k}} & 0 \\ 0 & 0 & 0 \\ -\frac{3}{2}K_{ivq}\langle v_{sq}\rangle_{\bar{k}} & \frac{3}{2}K_{ivq}\langle v_{sd}\rangle_{\bar{k}} & 0 \\ 0 & 0 & 0 \\ -\frac{\frac{3}{2}K_{piq}K_{pvq}\langle v_{sq}\rangle_{\bar{k}}}{L_f} & \frac{3}{2}\frac{K_{piq}K_{pvq}\langle v_{sd}\rangle_{\bar{k}}}{L_f} & 0 \\ \alpha 4 & \alpha 5 & \alpha 6 \end{matrix} \end{bmatrix}$$

The parameters in the matrix ($ac_{k=k}$) are defined as:

$$\alpha 4 = \frac{3}{2}\frac{1}{C_{dc}}\sum_i^{k=\bar{k}}\langle v_{sd}\rangle_{k-i}\langle\frac{1}{v_{dc}}\rangle_i - \frac{2R_f}{C_{dc}}\sum_i^{k=\bar{k}}\langle i_{sd}\rangle_{k-i}\langle\frac{1}{v_{dc}}\rangle_i$$

$$\alpha 5 = \frac{3}{2}\sum_i^{k=\bar{k}}\langle v_{sq}\rangle_{k-i}\langle\frac{1}{v_{dc}}\rangle_i$$

$$\alpha 6 = \frac{R_f}{C_{dc}}\sum_i^{k=\bar{k}}\langle i_{sd}^2\rangle_{k-i}\langle\frac{1}{v_{dc}^2}\rangle_i - \frac{3}{2}\frac{1}{C_{dc}}\sum_i^{k=0}\langle v_{sd}\rangle_{k-i}\langle i_{sd}\rangle_i\langle\frac{1}{v_{dc}^2}\rangle_{\bar{k}} -$$
$$\frac{3}{2}\frac{1}{C_{dc}}\sum_i^{k=\bar{k}}\langle v_{sd}\rangle_{k-i}\langle i_{sd}\rangle_i\langle\frac{1}{v_{dc}^2}\rangle_0 - \frac{3}{2}\frac{1}{C_{dc}}\sum_i^{k=0}\langle v_{sq}\rangle_{k-i}\langle i_{sq}\rangle_i\langle\frac{1}{v_{dc}^2}\rangle_{\bar{k}} -$$
$$\frac{3}{2}\frac{1}{C_{dc}}\sum_i^{k=\bar{k}}\langle v_{sq}\rangle_{k-i}\langle i_{sq}\rangle_i\langle\frac{1}{v_{dc}^2}\rangle_0$$

Similarly, the submatrices of input matrix (B_{DP}) are defined as:

- The diagonal submatrices ($b_{k=0}, b_{k=k_1}, \dots\dots, b_{k=\overline{k_n}}$) represent the intput matrices at specific harmonic order (k) including the frequency coupling of the dc link voltage and equal to:

$$B_{k,k} = \begin{bmatrix} 0 & 0 & K_{iid}K_{pvd} & 0 \\ \frac{3}{2}K_{iiq}K_{pvq}\langle i_{sq}\rangle_0 & -\frac{3}{2}K_{iiq}K_{pvq}\langle i_{sd}\rangle_0 & 0 & K_{iiq}K_{pvq} \\ 0 & 0 & K_{ivd} & 0 \\ \frac{3}{2}K_{ivq}\langle i_{sq}\rangle_0 & -\frac{3}{2}K_{ivq}\langle i_{sd}\rangle_0 & 0 & Ki_{vq} \\ \frac{1}{L_f} & 0 & \frac{K_{pid}K_{pvd}}{L_f} & 0 \\ \frac{3}{2}\frac{K_{piq}K_{pvq}\langle i_{sq}\rangle_0}{L_f} & \frac{1}{L_f} - \frac{3}{2}\frac{K_{piq}K_{pvq}\langle i_{sd}\rangle_0}{L_f} & 0 & \frac{K_{piq}K_{pvq}}{L_f} \\ \frac{3}{2}\sum_{i=\pm\infty}^{k=0}\langle\frac{1}{C_{dc}v_{dc}}\rangle_{\bar{k}}\langle i_{sd}\rangle_{\bar{k}} & \frac{3}{2}\sum_{i=\pm\infty}^{k=0}\langle\frac{1}{C_{dc}v_{dc}}\rangle_{k-i}\langle i_{sq}\rangle_i & 0 & 0 \end{bmatrix}$$

- The other submatrices that include the frequency coupling ($bc_{k=\overline{k_1}}, bc_{k=\overline{k_2}}, \ldots, bc_{k=\overline{k_n}}$) and ($bc_{k=k_1}, bc_{k=k_2}, \ldots., bc_{k=k_n}$) are:

$$bc_{k=k} = \begin{bmatrix} 0 & 0 \\ \frac{3}{2}K_{iiq}K_{pvq}\langle i_{sq}\rangle_{\bar{k}} & -\frac{3}{2}K_{iiq}K_{pvq}\langle i_{sd}\rangle_{\bar{k}} \\ 0 & 0 \\ \frac{3}{2}K_{ivq}\langle i_{sq}\rangle_{\bar{k}} & -\frac{3}{2}K_{ivq}\langle i_{sd}\rangle_{\bar{k}} \\ 0 & 0 \\ \frac{3}{2}\frac{K_{piq}K_{pvq}\langle i_{sq}\rangle_{\bar{k}}}{L_f} & \frac{1}{L_f} - \frac{3}{2}\frac{K_{piq}K_{pvq}\langle i_{sd}\rangle_{\bar{k}}}{L_f} \\ \frac{3}{2}\sum_{i=\pm\infty}^{k=\bar{k}}\langle\frac{1}{C_{dc}v_{dc}}\rangle_{\bar{k}}\langle i_{sd}\rangle_{\bar{k}} & \frac{3}{2}\sum_{i=\pm\infty}^{k=\bar{k}}\langle\frac{1}{C_{dc}v_{dc}}\rangle_{k-i}\langle i_{sq}\rangle_{i} \end{bmatrix} \quad zeros(7\times 2)$$

The derivation of the generalised state and input matrices presented in (5.17) and (5.18) are found in Appendix-D. The matrices (A_{DP}, and B_{DP}) are linear time invariant (LTI) matrices which could include harmonics similar to the harmonic state space (HSS) modelling. However, the LTI systems have an advantage of being more suitable for small signal stability than the time variant systems. The generalised state matrix and input matrix presented in equation (5.17) and (5.18) are capable to include the fundamental frequency ($k = 0$) as well as an infinite number of harmonics ($k = \mp\infty$). Each harmonic frequency except the fundamental frequency generates two components; the positive and negative sequence components of the kth harmonic (depicted as k and $\bar{k}$ respectively). In the meantime, for the fundamental frequency, the dq-transformation generates one component at the fundamental frequency and another at the 2nd harmonic order ($k = -2$), which is characteristic of the system response at unbalanced conditions. The existence of the positive and negative sequence components in equation (5.3) and (5.4) facilitates stability studies of balanced and unbalanced systems.

5.4.2 Generalised impedance model for STATCOM device

The frequency domain analysis of power system presents some valuable information about system oscillations and can be utilised to assess the stability at the point of common coupling. Similar to the previous section, the generalised impedance model of STATCOM is derived from synchronous dq model equations presented in Chapter 4:

$$\sum_{k=-\infty}^{\infty}\langle \mathbf{\Delta v_{sdq}} \rangle_k = \sum_{-\infty}^{\infty}\langle a_z \mathbf{\Delta i_{sdq}} \rangle_k + \sum_{-\infty}^{\infty}\langle b_z \mathbf{\Delta i_{sdq}^*} \rangle_k \tag{5.19}$$

$$\sum_{k=-\infty}^{\infty}\langle \mathbf{\Delta i_{sdq}^*} \rangle_k = \sum_{k=-\infty}^{\infty}\langle c_z \mathbf{v}^* \rangle_k - \sum_{k=-\infty}^{\infty}\langle c_z \mathbf{\Delta v} \rangle_k \tag{5.20}$$

$$\sum_{k=-\infty}^{\infty}\langle d_z \mathbf{\Delta v} \rangle_k = \sum_{-\infty}^{\infty}\langle e_z \mathbf{\Delta v_{sdq}} \rangle_k + \sum_{-\infty}^{\infty}\langle f_z \mathbf{\Delta i_{sdq}} \rangle_k \tag{5.21}$$

After expanding equations (5.19) to (5.21) and re-arrangements, yield:

$$\langle \mathbf{\Delta v_{sdq}} \rangle_\mathbf{k} = A_z \langle \mathbf{\Delta i_{sdq}} \rangle_\mathbf{k} + B_z \langle \mathbf{\Delta i_{sdq}^*} \rangle_\mathbf{k} \tag{5.22}$$

$$\langle \mathbf{\Delta i_{sdq}^*} \rangle_\mathbf{k} = C_z \langle \mathbf{v}^* \rangle_\mathbf{k} - C_z \langle \mathbf{\Delta v} \rangle_\mathbf{k} \tag{5.23}$$

$$D_z \langle \mathbf{\Delta v} \rangle_\mathbf{k} = E_z \langle \mathbf{\Delta v_{sdq}} \rangle_\mathbf{k} + F_z \langle \mathbf{\Delta i_{sdq}} \rangle_\mathbf{k} \tag{5.24}$$

where,

- The input voltage vector at all harmonics is:

$$\langle \mathbf{\Delta v_{sdq}} \rangle_\mathbf{k} = [\langle \mathbf{\Delta v_{sdq}} \rangle_\mathbf{k=0} \ \langle \mathbf{\Delta v_{sdq}} \rangle_\mathbf{k=k_1} \ \langle \mathbf{\Delta v_{sdq}} \rangle_\mathbf{k=\overline{k_1}} \ \cdots \ \langle \mathbf{\Delta v_{sdq}} \rangle_\mathbf{k=\overline{k_n}}]^T$$

- The STATCOM current vector at all harmonics is:

$$\langle \mathbf{\Delta i_{sdq}} \rangle_\mathbf{k} = [\langle \mathbf{\Delta i_{sdq}} \rangle_\mathbf{k=0} \ \langle \mathbf{\Delta i_{sdq}} \rangle_\mathbf{k=k_1} \ \langle \mathbf{\Delta i_{sdq}} \rangle_\mathbf{k=\overline{k_1}} \ \cdots \ \langle \mathbf{\Delta i_{sdq}} \rangle_\mathbf{k=\overline{k_n}}]^T$$

- The inputs of voltage control loop of the STATCOM are:

$$\langle \mathbf{\Delta v} \rangle_\mathbf{k} = [\langle \mathbf{\Delta v} \rangle_\mathbf{k=0} \ \langle \mathbf{\Delta v} \rangle_\mathbf{k=k_1} \ \langle \mathbf{\Delta v} \rangle_\mathbf{k=\overline{k_1}} \ \cdots \ \langle \mathbf{\Delta v} \rangle_\mathbf{k=\overline{k_n}}]^\mathrm{T}$$

$$\mathbf{\Delta v} = [v_{dc} \quad Q]^\mathrm{T}$$

After further manipulations of (5.22) to (5.24), the generalised STATCOM impedance model is obtained as:

$$Z_{DPSTATCOM} = (\mathrm{I} - B_z C_z D_z^{-1} F_z)^{-1}(A_z + B_z C_z D_z^{-1} E_z) \tag{5.25}$$

The resultant impedance (5.25) is similar to impedance derived for the synchronous dq in chapter 4, however, this impedance includes all harmonics and can be utilised

for stability studies. The block diagram of the generalised STATCOM impedance is presented in Figure 5.2. The impedance matrices in equation (5.25) follow the same pattern found in the derivation of the state space equations in (5.17) and (5.18), which are defined as follows:

- The matrices that represent the STATCOM are:

$$A_z = \begin{bmatrix} hd_{k=0} & hl_{k=\overline{k_1}} & hl_{k=k_1} & \cdots & hl_{k=k_n} \\ hl_{k=k_1} & hd_{k=k_1} & 0 & & 0 \\ hl_{k=\overline{k_1}} & 0 & hd_{k=\overline{k_1}} & & 0 \\ \vdots & 0 & 0 & \ddots & 0 \\ hl_{k=\overline{k_n}} & 0 & 0 & & hd_{k=\overline{k_n}} \end{bmatrix}$$

$$B_z = \begin{bmatrix} Bd_{k=0} & Bl_{k=\overline{k_1}} & Bl_{k=k_1} & \cdots & Bl_{k=k_n} \\ Bl_{k=k_1} & Bd_{k=k_1} & 0 & & 0 \\ Bl_{k=\overline{k_1}} & 0 & Bd_{k=\overline{k_1}} & & 0 \\ \vdots & 0 & 0 & \ddots & 0 \\ Bl_{k=\overline{k_n}} & 0 & 0 & & Bd_{k=\overline{k_n}} \end{bmatrix}$$

- The matrix that represents current control loop is:

$$C_z = \begin{bmatrix} Cd_{k=0} & Cl_{k=\overline{k_1}} & Cl_{k=k_1} & \cdots & Cl_{k=k_n} \\ Cl_{k=k_1} & Cd_{k=k_1} & 0 & & 0 \\ Cl_{k=\overline{k_1}} & 0 & Cd_{k=\overline{k_1}} & & 0 \\ \vdots & 0 & 0 & \ddots & 0 \\ Cl_{k=\overline{k_n}} & 0 & 0 & & Cd_{k=\overline{k_n}} \end{bmatrix}$$

where, their submatrices are:

$$Cd_k = \begin{bmatrix} K_{pvd} + \langle \frac{K_{ivd}}{s} \rangle_0 & 0 \\ 0 & K_{pvq} + \langle \frac{K_{ivq}}{s} \rangle_0 \end{bmatrix} \qquad Cl_{k=k_1} = \begin{bmatrix} \langle \frac{K_{ivd}}{s+jk\omega} \rangle_k & 0 \\ 0 & \langle \frac{K_{ivq}}{s+jk\omega} \rangle_k \end{bmatrix}$$

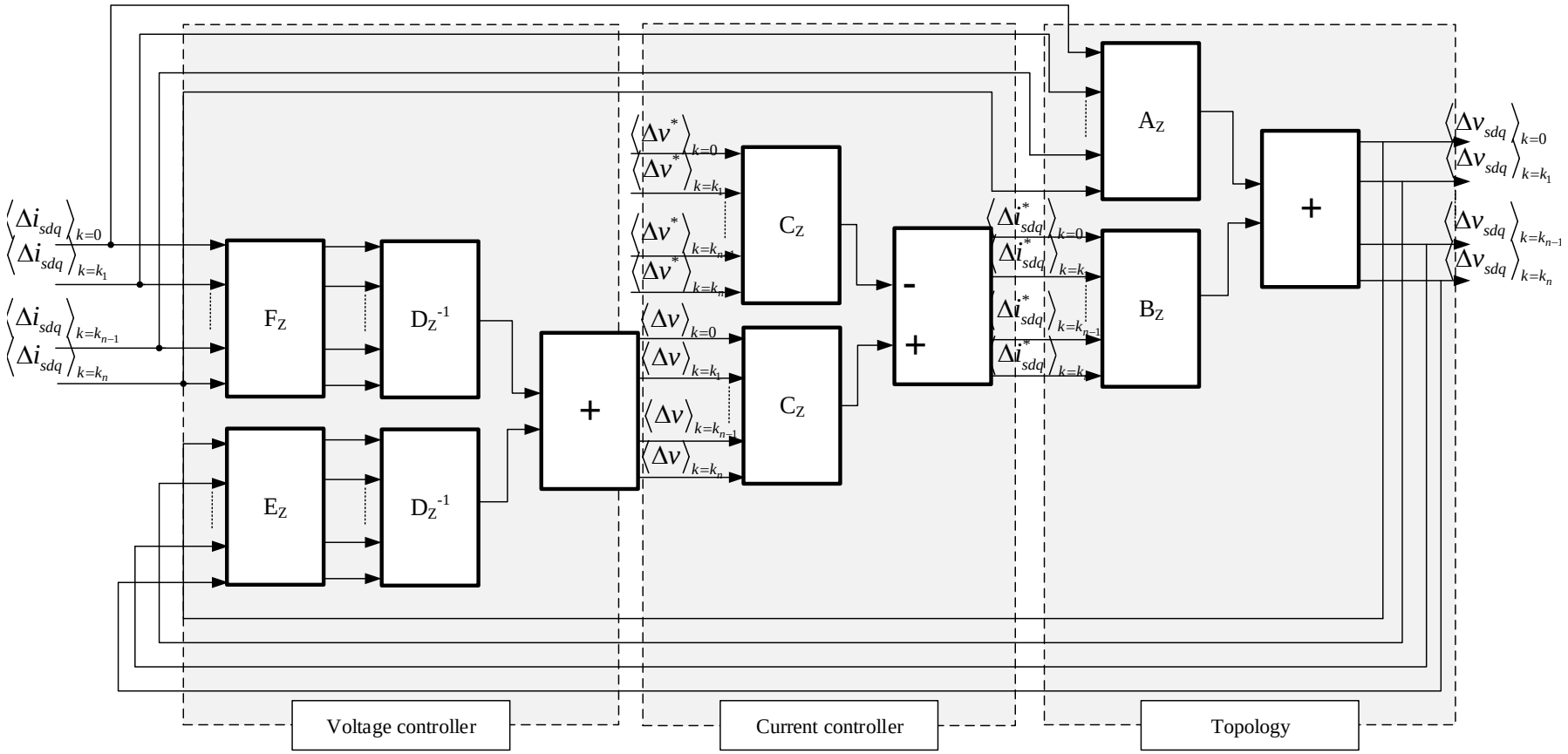

Figure 5.2. Block diagram of the generalised Impedance of STATCOM.

- The matrices that represent voltage control loop and their inputs are:

$$D_z = \begin{bmatrix} Dd_{k=0} & Dl_{k=\overline{k_1}} & Dl_{k=k_1} & \cdots & Dl_{k=k_n} \\ Dl_{k=k_1} & Dd_{k=k_1} & 0 & & 0 \\ Dl_{k=\overline{k_1}} & 0 & Dd_{k=\overline{k_1}} & & 0 \\ \vdots & 0 & 0 & \ddots & 0 \\ Dl_{k=\overline{k_n}} & 0 & 0 & & Dd_{k=\overline{k_n}} \end{bmatrix}$$

$$E_z = \begin{bmatrix} Ed_{k=0} & El_{k=\overline{k_1}} & El_{k=k_1} & \cdots & El_{k=k_n} \\ El_{k=k_1} & Ed_{k=k_1} & 0 & & 0 \\ El_{k=\overline{k_1}} & 0 & Ed_{k=\overline{k_1}} & & 0 \\ \vdots & 0 & 0 & \ddots & 0 \\ El_{k=\overline{k_n}} & 0 & 0 & & Ed_{k=\overline{k_n}} \end{bmatrix}$$

$$F_z = \begin{bmatrix} Fd_{k=0} & Fl_{k=\overline{k_1}} & Fl_{k=k_1} & \cdots & Fl_{k=k_n} \\ Fl_{k=k_1} & Fd_{k=k_1} & 0 & & 0 \\ Fl_{k=\overline{k_1}} & 0 & Fd_{k=\overline{k_1}} & & 0 \\ \vdots & 0 & 0 & \ddots & 0 \\ Fl_{k=\overline{k_n}} & 0 & 0 & & Fd_{k=\overline{k_n}} \end{bmatrix}$$

where, the sub-matrices of (D_z, E_z, F_z) are defined:

$$d_k = \begin{bmatrix} \langle K_{pid} + \frac{K_{iid}}{s} \rangle_0 & 0 \\ 0 & \langle K_{piq} + \frac{K_{iiq}}{s} \rangle_0 \end{bmatrix}, \qquad Dd_k = \begin{bmatrix} \alpha l_k & 0 \\ 0 & 1 \end{bmatrix},\ Dl_{k=k} = \begin{bmatrix} \alpha m_{k=k} & 0 \\ 0 & 0 \end{bmatrix}$$

$$Fd_k = \begin{bmatrix} \langle \frac{3}{2} v_{sd} \rangle_0 - \langle 2R_f i_{sd} \rangle_0 & \langle \frac{3}{2} v_{sq} \rangle_0 \\ \frac{3}{2} \langle v_{sq} \rangle_0 & -\frac{3}{2} \langle v_{sd} \rangle_0 \end{bmatrix}, \qquad Ed_k = \frac{3}{2} \begin{bmatrix} \langle i_{sd} \rangle_0 & \langle i_{sq} \rangle_0 \\ -\langle i_{sq} \rangle_0 & \langle i_{sd} \rangle_0 \end{bmatrix},$$

$$Fl_{k=k_1} = \begin{bmatrix} \langle \frac{3}{2} v_{sd} \rangle_k - \langle 2R_f i_{sd} \rangle_k & \langle \frac{3}{2} v_{sq} \rangle_k \\ \frac{3}{2} \langle v_{sq} \rangle_k & -\frac{3}{2} \langle v_{sd} \rangle_k \end{bmatrix}, \qquad El_{k=k_1} = \frac{3}{2} \begin{bmatrix} \langle i_{sd} \rangle_k & \langle i_{sq} \rangle_k \\ -\langle i_{sq} \rangle_{\bar{k}} & \langle i_{sd} \rangle_{\bar{k}} \end{bmatrix}$$

The previous submatrices represent the frequency coupling due to the dc link voltage and reactive power calculation. The definitions of the parameters are:

$$\alpha l_k = C_{dc} s\langle v_{dc}\rangle_0 - \left(\sum_i^{k=0} \langle \frac{1}{v_{dc}} \rangle_{k-i} \langle i_{sd}^2 R_f \rangle_i\right) + \frac{3}{2}\sum_i^{k=0} \langle \frac{1}{v_{dc}} \rangle_{k-i} \langle v_{sd}\rangle_i \langle i_{sd}\rangle_0 +$$
$$\frac{3}{2}\sum_i^{k=\bar{k}} \langle \frac{1}{v_{dc}} \rangle_{k-i} \langle v_{sd}\rangle_i \langle i_{sd}\rangle_k + \frac{3}{2}\sum_i^{k=k} \langle \frac{1}{v_{dc}} \rangle_{k-i} \langle v_{sd}\rangle_i \langle i_{sd}\rangle_{\bar{k}} +$$
$$\frac{3}{2}\sum_i^{k=0} \langle \frac{1}{v_{dc}} \rangle_{k-i} \langle v_{sq}\rangle_i \langle i_{sq}\rangle_0 + \frac{3}{2}\sum_i^{k=\bar{k}} \langle \frac{1}{v_{dc}} \rangle_{k-i} \langle v_{sq}\rangle_i \langle i_{sq}\rangle_k +$$
$$\frac{3}{2}\sum_i^{k=k} \langle \frac{1}{v_{dc}} \rangle_{k-i} \langle v_{sq}\rangle_i \langle i_{sq}\rangle_{\bar{k}}$$

$$\alpha m_{k=k} =$$
$$C_{dc}(s + jk\omega)\langle v_{dc}\rangle_k - \sum_i^{k=k} \langle \frac{1}{v_{dc}} \rangle_{k-i} \langle i_{sd}^2 R_f \rangle_i + \frac{3}{2}\sum_i^{k=0} \langle \frac{1}{v_{dc}} \rangle_{k-i} \langle v_{sd}\rangle_i \langle i_{sd}\rangle_k +$$
$$\frac{3}{2}\sum_i^{k=k} \langle \frac{1}{v_{dc}} \rangle_{k-i} \langle v_{sd}\rangle_i \langle i_{sd}\rangle_0 +$$
$$\frac{3}{2}\sum_i^{k=0} \langle \frac{1}{v_{dc}} \rangle_{k-i} \langle v_{sq}\rangle_i \langle i_{sq}\rangle_k + \frac{3}{2}\sum_i^{k=k} \langle \frac{1}{v_{dc}} \rangle_{k-i} \langle v_{sq}\rangle_i \langle i_{sq}\rangle_0$$

It is noted that the system analysis for harmonic order ($k = 0$), the generalised state space and the generalised impedance are equal to the derived forms for the synchronous dq model. A similarity between the synchronous dq modelling and the proposed DP modelling is therefore expected in the response and the criteria.

5.5 Stability assessment of STATCOM connected to the grid using the new generalised modelling

In this section, three case studies are presented to show the effectiveness of the proposed STATCOM dq-dynamic phasor model for stability assessment. The system under steady-state conditions is presented in Figure 5.3. The grid and the STATCOM parameters are listed in Table 5.1. In the simulation, the dynamic phasor quantities are extracted using a low-pass filter for the ac quantities and using a Fourier analysis for the dc quantities.

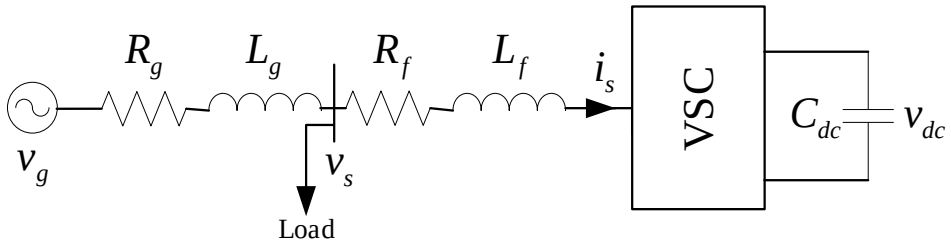

Figure 5.3. Simplified diagram of STATCOM connected to the grid.

Table 5.1. Test system parameters.

Parameter	value	Parameter	value
S_{base}	100 kVA	K_{pidq}, K_{iidq}	1000 V/A, 400 V/A.s
v_{base}	415 kV	K_{pvd} , K_{ivd}	20 A/V, 200 A/V.s
f	50 Hz	K_{pvq}, K_{ivq}	-0.002 A/VA, -0.1 A/VA.s
R_g, L_g	0.25 Ω, 1 mH	v_{dc}	1000 V
R_f, L_f	0.1 Ω, 5 mH	C_{dc}	400 µF
P_L, Q_L	65 kW, 12 kVAr		

5.5.1 Balanced operation of STATCOM with no harmonics

This case study is employed as a benchmark for the operation of the STATCOM. The STATCOM is assumed to operate in balanced conditions with no harmonics. In such an operating condition, the system can be modelled either by the synchronous dq model presented in Chapter 4 or using the generalised model with harmonic order ($k = 0$). In this case, the state space analysis of the test system generates seven stable states as seen in Table 5.2. Some of STATCOM eigenvalues are overdamped (λ_1 to λ_5) while the rest of the eigenvalues (λ_6 and λ_7) are repeated real eigenvalues (critically damped). The Bode plot of STATCOM impedance presented in equation (5.25) is shown in Figure 5.4 which is compared with other case studies later.

5.5.2 Unbalanced operation of the STATCOM

The unbalanced operation of the test system is assessed using the derived model of generalised state space and impedance analysis. The analysis of the unbalanced system displays two balanced systems operating at two different frequencies ($\omega_n, 2\omega_n$) as shown in Table 5.2. As the STATCOM has seven states as presented in Chapter 4, the studying of the unbalanced conditions will generate 14 states. The first seven states represent the system at the fundamental frequency while the rest represent the system at double frequency (-2ω). The eigenvalues related to the unbalanced operation (λ_8 to λ_{14}) are considered as underdamped eigenvalues. In the state space equation (5.12), the unbalanced operation of the test system is existed if the matrix (AC_h) exist, while the diagonal matrices show the frequencies of system

variation and the instability conditions of the system. The frequency coupling caused by the unbalanced conditions deviate the system eigenvalues to the right-hand side from their original position that means the unbalance will drag the system to become less stable as much as the unbalance increases. Alternatively, in the frequency domain, the effect of unbalanced conditions of the STATCOM can be seen by changing the level of unbalance such as changing the magnitude of phase (b) as:

$$|V_b| = [1.0 \quad 0.85 \quad 0.65]\text{pu}$$

Table 5.2. The eigenvalue analysis of the test system under balanced and unbalanced conditions.

Modes	Balanced condition	Unbalanced condition
λ_1	-1.54×10^5+j0.00	-1.49×10^5+j0.00
λ_2	-7.99×10^4+j0.00	-7.99×10^4+j0.00
λ_3	-221.58+j0.00	-204.51+j0.00
λ_4	-10.47+j0.00	-10.52+j0.00
λ_5	-24.04+j0.00	-23.09+j0.00
λ_6	-2.50+j0.00	-2.50+j0.00
λ_7	-2.50+j0.00	-2.50+j0.00
λ_8		-1.49×10^5+j628.32
λ_9		-7.99×10^4+j628.32
λ_{10}		-204.51+j628.32
λ_{11}		-10.52+j628.32
λ_{12}		-23.09+j628.32
λ_{13}		-2.50+j628.32
λ_{14}		-2.50+j628.32

As shown in Figure 5.4, the STATCOM has four impedances at each harmonic frequency, the diagonal impedances (Z_{dd}, Z_{qq}) and the off-diagonal impedances (Z_{qd}, Z_{qq}). For the balanced conditions, the fundamental impedances and the second order harmonic are equal for the balanced systems as the parameters coupling matrices are equal to zero. In addition, the sharp changes of second order impedance at the twice fundamental frequency are referred to the existence of the complex part

which represent the second order harmonic. Alternatively, the unbalanced condition do not affect the off-diagonal impedances due to the change of STATCOM operating conditions while the diagonal impedance decreases as the unbalance increases. This is referred to the coupling presented between the fundamental frequency and the negative sequence component. The two impedances at ($k = 0, -2$) match each other in case of balanced operation (with no harmonics) or in case of the coupling effect is ignored. This can be used as an indication for unbalance of the modelled systems which depends on the severity of the unbalance.

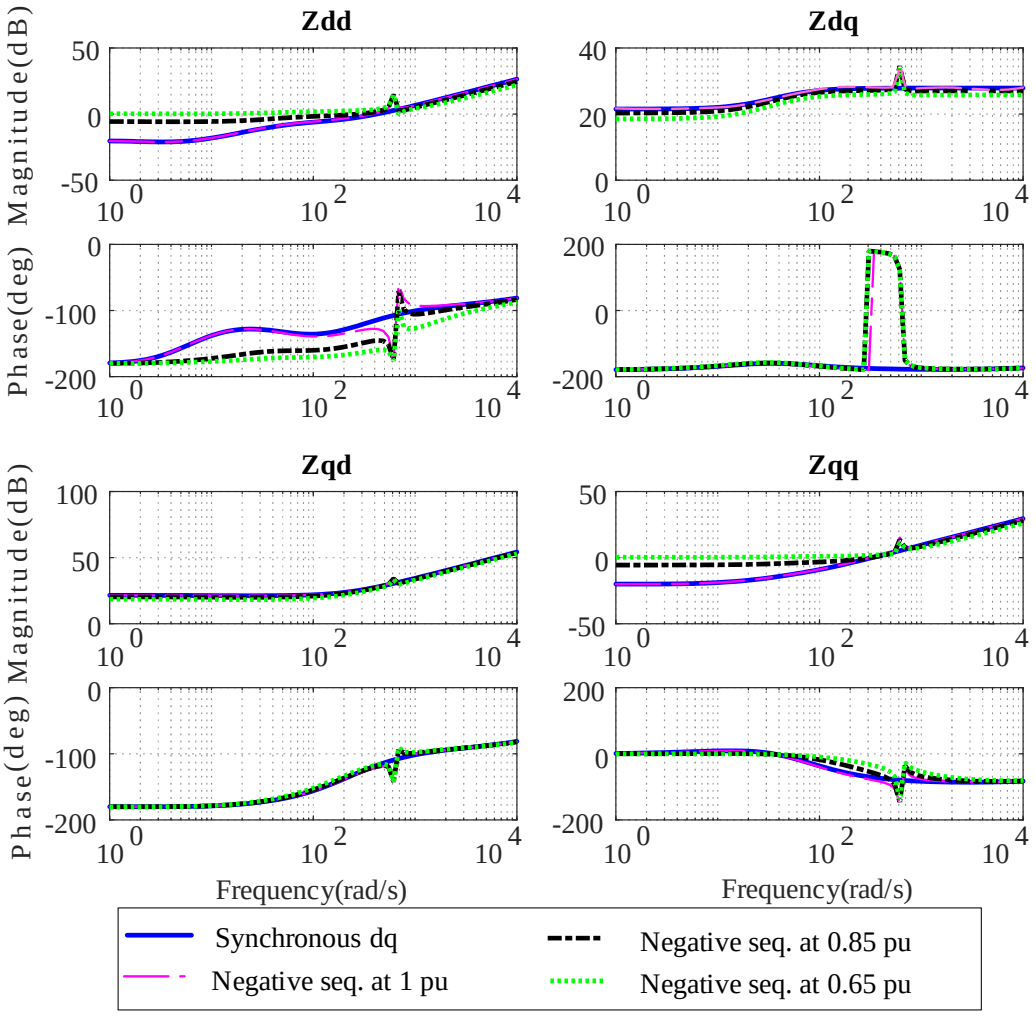

Figure 5.4. STATCOM impedance under different operating conditions (balanced and unbalanced).

The reason for the unbalanced effect presents at low frequencies is due to the presence of the coupling matrix where their effect will be insignificant at high frequencies due to the dominant of fundamental quantities.

The main difference between the proposed dq-dynamic phasor model and the positive and negative sequence based synchronous dq method (PNDQ) is the following:

- Unbalanced systems are derived for positive and negative quantities in PNDQ while in the proposed modelling is derived as fundamental frequency and 2nd order harmonic at double fundamental frequency rotating anti-clockwise ($k = -2$). The proposed modelling has an advantage of defining the frequency of the oscillations and their rotation direction which is helps in identifying the origin of the oscillation.
- The proposed model presents the effect of the fundamental frequency on the 2nd order harmonic while it does not present any effect of the 2nd harmonic on the fundamental frequency.
- In the proposed modelling, the coupling between the fundamental and harmonic frequency will disappear once the system is balanced while the PNDQ keeps presenting this coupling even at balanced conditions. This is an advantage of using the proposed modelling over the use of PNDQ.

5.5.3 STATCOM operation under harmonics

The operation assessment of the STATCOM under harmonics is discussed in this section by injecting two harmonics (5th and 7th). According to the transformation of these frequencies to the dq-dynamic phasor, six frequencies are generated in this domain. Each frequency component is transformed into a positive and negative component as k =(0, -2, 4, -6, 6, -8) respectively. The size of the state matrix (A_{DP}) and input matrix (B_{DP}) can be calculated as shown in equation (5.5) and (5.6):

Size (A_{DP}) = (2 (1+2) (7), 2 (1+2) (7)) = (42, 42) (5.26)

Size (B_{DP}) = (2 (1+2) (7), 2 (1+2) (4)) = (42, 24) (5.27)

So, 42 eigenvalues are generated in this case, seven at each frequency. The plot of the STATCOM eigenvalues is shown in Figure 5.5 to present the effect of coupling on its operation. In Figure 5.5a, the coupling between the harmonics is ignored. In this case, the harmonic inclusion is observed as multiple stable systems operate at different frequencies. Each of these systems is referred to its own coordinates. The newly added harmonics are repeated at these harmonics without any change of the system stability.

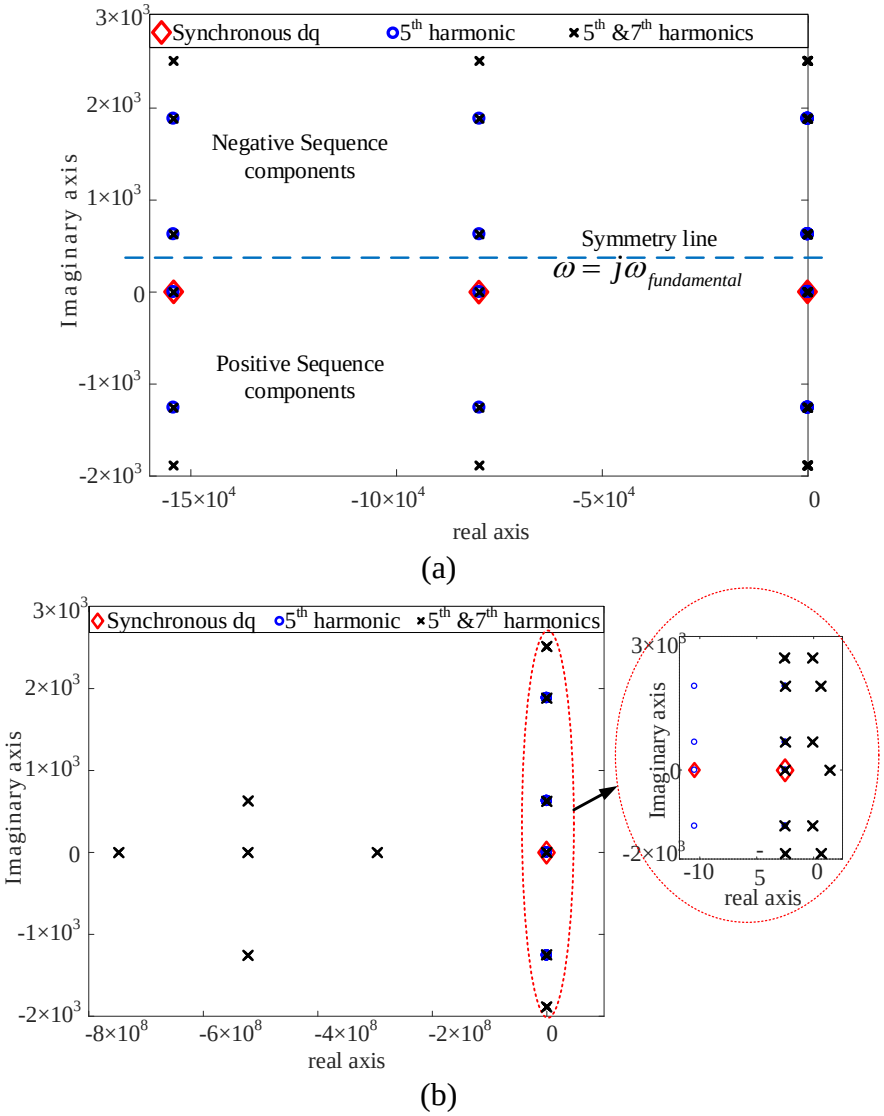

(a)

(b)

Figure 5.5. Eigenvalue analysis of STATCOM using dq-dynamic phasor modelling: (a) Coupling effect ignored and (b) Coupling effect considered.

The eigenvalues of the test system are shifted up by (ω) in the imaginary axis due to the dq-dynamic phasor transformation. Thus, the axis of symmetry is located at ($\omega = j\omega_{fundamental}$). The eigenvalues of the positive sequence components are in the upper part of the complex plane, while the negative sequence components are in the lower part of the complex plane. Alternatively, the frequency coupling causes a displacement of the system eigenvalues as more harmonics are included in the study which prevents the presence of the repeated frequencies (see Figure 5.5b). The system starts to become unstable as the harmonics are included. It can be concluded from Figure 5.5, that ignoring the frequency coupling between the fundamental frequency and the existed harmonics could lead to a major error in the analysis.

In Figure 5.6, the effect of including the harmonics is presented using the STATCOM impedance model. Ignoring the frequency coupling in the impedance model results the same impedance as synchronous dq impedance of the STATCOM. Alternatively, the frequency coupling increases the magnitude and the phase of STATCOM impedance, which reduces the stability margin of the STATCOM. Thus, the inclusion of the harmonics has a significant impact on the fundamental frequency due to the coupling.

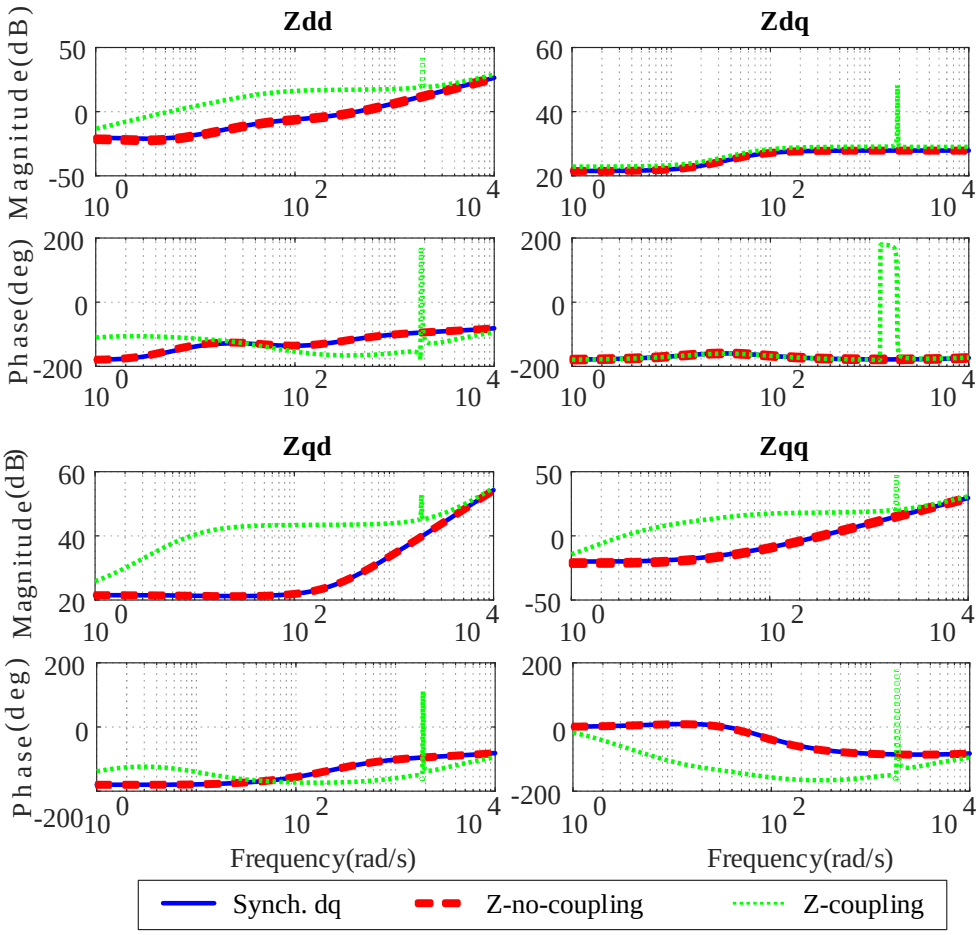

Figure 5.6. The effect of coupling on STATCOM impedance.

In the meantime, this effect can be insignificant in case of one harmonic is included or in case of two non-close harmonics (such as 5^{th} and 9^{th}) are considered. For the frequency analysis, the effect of including harmonics can be seen also using the generalised Nyquist plot, which is presented in Figure 5.7. The STATCOM impedance without any harmonics is presented by solid line in Figure 5.7 while the STATCOM impedance including the harmonics effect is presented by dotted line. Even though the Nyquist plot of the STATCOM impedance without harmonics presents a stable system the impedance plot including the harmonics shows an oscillatory system.

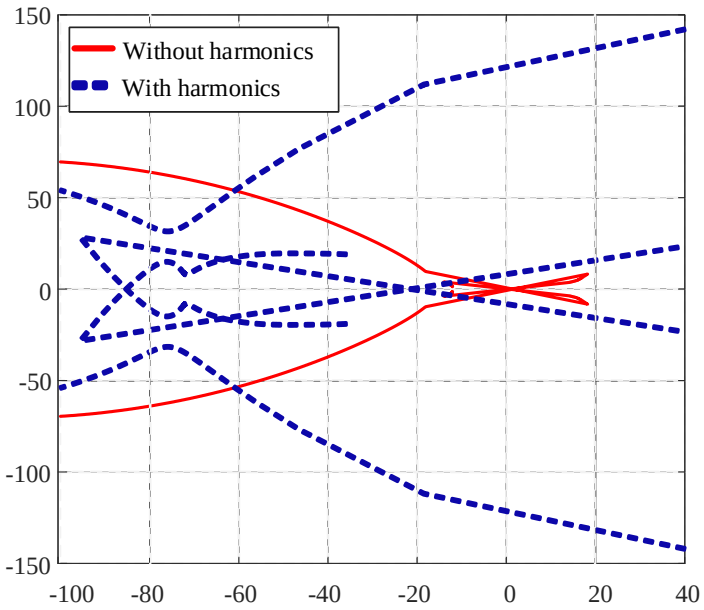

Figure 5.7. Generalised Nyquist plot of STATCOM with and without harmonics coupling.

5.6 Proposed generalised dq-dynamic phasor modelling for SSSC device

The generalised dq-dynamic phasor modelling development of SSSC with three control modes is presented in this section. It is essential to study the effect of harmonics such as SSR effect on the operation of SSSC and its control mode and how the harmonics can affect their performance due to their presence in this environment.

5.6.1 Generalised state space of SSSC

Likewise, the principle followed to derive the STATCOM, the SSSC state space and impedance models are presented for different control modes. Such derivation will help to compare between such control modes and consequently their suitability to use in different power system applications. The detailed derivation can be found in Appendix-E.

5.6.1.1 Generalised state space model of SSSC based power control mode

As stated in Chapter 3, the input parameters of SSSC in this control mode are the active and reactive powers. The transformation of these powers to dynamic phasor form is given as:

$$\begin{bmatrix}\langle\Delta P_m\rangle_0\\ \langle\Delta Q_m\rangle_0\\ \langle\Delta P_m\rangle_k\\ \langle\Delta Q_m\rangle_k\\ \langle\Delta P_m\rangle_{\bar{k}}\\ \langle\Delta Q_m\rangle_{\bar{k}}\end{bmatrix} = \frac{3}{2}\begin{bmatrix}\langle i_{sed}\rangle_0 & \langle i_{seq}\rangle_0 & \langle i_{sed}\rangle_{\bar{k}} & \langle i_{seq}\rangle_{\bar{k}} & \langle i_{sed}\rangle_k & \langle i_{seq}\rangle_k\\ \langle i_{seq}\rangle_0 & -\langle i_{sed}\rangle_0 & \langle i_{seq}\rangle_{\bar{k}} & -\langle i_{sed}\rangle_{\bar{k}} & \langle i_{seq}\rangle_k & -\langle i_{sed}\rangle_k\\ \langle i_{sed}\rangle_k & \langle i_{seq}\rangle_k & \langle i_{sed}\rangle_0 & \langle i_{seq}\rangle_0 & 0 & 0\\ \langle i_{seq}\rangle_k & -\langle i_{sed}\rangle_k & \langle i_{seq}\rangle_0 & -\langle i_{sed}\rangle_0 & 0 & 0\\ \langle i_{sed}\rangle_{\bar{k}} & \langle i_{seq}\rangle_{\bar{k}} & 0 & 0 & \langle i_{sed}\rangle_0 & \langle i_{seq}\rangle_0\\ \langle i_{seq}\rangle_{\bar{k}} & -\langle i_{sed}\rangle_{\bar{k}} & 0 & 0 & \langle i_{seq}\rangle_0 & -\langle i_{sed}\rangle_0\end{bmatrix}\begin{bmatrix}\langle\Delta v_{md}\rangle_0\\ \langle\Delta v_{mq}\rangle_0\\ \langle\Delta v_{md}\rangle_k\\ \langle\Delta v_{mq}\rangle_k\\ \langle\Delta v_{md}\rangle_{\bar{k}}\\ \langle\Delta v_{mq}\rangle_{\bar{k}}\end{bmatrix} +$$

$$\frac{3}{2}\begin{bmatrix}\langle v_{md}\rangle_0 & \langle v_{mq}\rangle_0 & \langle v_{md}\rangle_{\bar{k}} & \langle v_{mq}\rangle_{\bar{k}} & \langle v_{md}\rangle_k & \langle v_{mq}\rangle_k\\ -\langle v_{mq}\rangle_0 & \langle v_{md}\rangle_0 & -\langle v_{mq}\rangle_{\bar{k}} & \langle v_{md}\rangle_{\bar{k}} & -\langle v_{mq}\rangle_k & \langle v_{md}\rangle_k\\ \langle v_{md}\rangle_k & \langle v_{mq}\rangle_k & \langle v_{md}\rangle_0 & \langle v_{mq}\rangle_0 & 0 & 0\\ -\langle v_{mq}\rangle_k & \langle v_{md}\rangle_k & -\langle v_{mq}\rangle_0 & \langle v_{md}\rangle_0 & 0 & 0\\ \langle v_{md}\rangle_{\bar{k}} & \langle v_{mq}\rangle_{\bar{k}} & 0 & 0 & \langle v_{md}\rangle_0 & \langle v_{mq}\rangle_0\\ -\langle v_{mq}\rangle_{\bar{k}} & \langle v_{md}\rangle_{\bar{k}} & 0 & 0 & -\langle v_{mq}\rangle_0 & \langle v_{md}\rangle_0\end{bmatrix}\begin{bmatrix}\langle\Delta i_{sed}\rangle_0\\ \langle\Delta i_{seq}\rangle_0\\ \langle\Delta i_{sed}\rangle_k\\ \langle\Delta i_{seq}\rangle_k\\ \langle\Delta i_{sed}\rangle_{\bar{k}}\\ \langle\Delta i_{seq}\rangle_{\bar{k}}\end{bmatrix} \quad (5.28)$$

where, m is equal to 1 for the sending end powers and 2 for the receiving end powers. The transformation of the SSSC equations using power control mode to dynamic phasor is given by the expanding the synchronous dq model of SSSC to generalised state space model as:

$$\mathbf{\frac{d}{dt}}\langle\mathbf{\Delta X}\rangle_{\mathbf{k}} = AP_{DP}\langle\mathbf{\Delta X}\rangle_{\mathbf{k}} + BP_{DP}\langle\mathbf{\Delta U}\rangle_{\mathbf{k}} \quad (5.29)$$

where, it is given for the state matrix and input matrix as:

$$AP_{DP} = \begin{bmatrix} ap_{k=0} & acp_{k=\bar{k}} & acp_{k=k} & \dots & acp_{k=kn}\\ acp_{k=k} & ap_{k=k} & & & \\ acp_{k=\bar{k}} & & ap_{k=\bar{k}} & & \vdots\\ \vdots & & & \ddots & \\ acp_{k=\overline{kn}} & & & \dots & ap_{k=\overline{kn}}\end{bmatrix}$$

$$BP_{DP} = \begin{bmatrix} bp_{k=0} & bcp_{k=\bar{k}} & bcp_{k=k} & \dots & bcp_{k=kn}\\ bcp_{k=k} & bp_{k=k} & & & \\ bcp_{k=\bar{k}} & & bp_{k=\bar{k}} & & \vdots\\ \vdots & & & \ddots & \\ bcp_{k=\overline{kn}} & & & \dots & bp_{k=\overline{kn}}\end{bmatrix}$$

The submatrices of (AP_{DP}) and (BP_{DP}) are given as:

- The diagonal submatrices are:

$$ap_{k=k} =$$

$$\begin{bmatrix} -jk\omega & 0 & -\frac{3}{2}K_{ivd}(\langle v_{1d}\rangle_0 - \langle v_{2d}\rangle_0) & -\frac{3}{2}K_{ivd}\big(\langle v_{1q}\rangle_0 - \langle v_{2q}\rangle_0\big) \\ 0 & -jk\omega & -\frac{3}{2}K_{ivq}\big(-\langle v_{1q}\rangle_0 + \langle v_{2q}\rangle_0\big) & -\frac{3}{2}K_{ivq}(\langle v_{1d}\rangle_0 - \langle v_{2d}\rangle_0) \\ -\frac{1}{L_{se}} & 0 & \frac{3}{2}\frac{K_{pvd}}{L_{se}}(\langle v_{1d}\rangle_0 - \langle v_{2d}\rangle_0) - \frac{R_{se}}{L_{se}} - jk\omega & \frac{3}{2}\frac{K_{pvd}}{L_{se}}\big(\langle v_{1q}\rangle_0 - \langle v_{2q}\rangle_0\big) + \omega \\ 0 & -\frac{1}{L_{se}} & \frac{3}{2}\frac{K_{pvq}}{L_{se}}\big(-\langle v_{1q}\rangle_0 + \langle v_{2q}\rangle_0\big) - \omega & \frac{3}{2}\frac{K_{pvq}}{L_{se}}(\langle v_{1d}\rangle_0 - \langle v_{2d}\rangle_0) - \frac{R_{se}}{L_{se}} - jk\omega \end{bmatrix}$$

$$bp_{k=k} =$$

$$\begin{bmatrix} 0 & 0 & -\frac{3}{2}K_{ivd}\langle i_{sed}\rangle_0 & -\frac{3}{2}K_{ivd}\langle i_{seq}\rangle_0 & \frac{3}{2}K_{ivd}\langle i_{sed}\rangle_0 & \frac{3}{2}K_{ivd}\langle i_{seq}\rangle_0 & K_{ivd} & 0 \\ 0 & 0 & -\frac{3}{2}K_{ivq}\langle i_{seq}\rangle_0 & \frac{3}{2}K_{ivq}\langle i_{sed}\rangle_0 & \frac{3}{2}K_{ivq}\langle i_{seq}\rangle_0 & -\frac{3}{2}K_{ivq}\langle i_{sed}\rangle_0 & 0 & K_{ivq} \\ \frac{1}{L_{se}} & 0 & \frac{3}{2}\frac{K_{pvd}}{L_{se}}\langle i_{sed}\rangle_0 & \frac{3}{2}\frac{K_{pvd}}{L_{se}}\langle i_{seq}\rangle_0 & -\frac{3}{2}\frac{K_{pvd}}{L_{se}}\langle i_{sed}\rangle_0 & -\frac{3}{2}\frac{K_{pvd}}{L_{se}}\langle i_{seq}\rangle_0 & -\frac{K_{pvd}}{L_{se}} & 0 \\ 0 & \frac{1}{L_{se}} & \frac{3}{2}\frac{K_{pvq}}{L_{se}}\langle i_{seq}\rangle_0 & -\frac{3}{2}\frac{K_{pvq}}{L_{se}}\langle i_{sed}\rangle_0 & -\frac{3}{2}\frac{K_{pvq}}{L_{se}}\langle i_{seq}\rangle_0 & \frac{3}{2}\frac{K_{pvq}}{L_{se}}\langle i_{sed}\rangle_0 & 0 & -\frac{K_{pvq}}{L_{se}} \end{bmatrix}$$

- The non-diagonal matrices which cause the frequency coupling are:

$$acp_{k=k} = \frac{3}{2}\begin{bmatrix} 0 & 0 & -K_{ivd}(\langle v_{1d}\rangle_k - \langle v_{2d}\rangle_k) & -K_{ivd}\big(\langle v_{1q}\rangle_k - \langle v_{2q}\rangle_k\big) \\ 0 & 0 & -K_{ivq}\big(-\langle v_{1q}\rangle_k + \langle v_{2q}\rangle_k\big) & -K_{ivq}(\langle v_{1d}\rangle_k - \langle v_{2d}\rangle_k) \\ 0 & 0 & \frac{K_{pvd}}{L_{se}}(\langle v_{1d}\rangle_k - \langle v_{2d}\rangle_k) & \frac{K_{pvd}}{L_{se}}\big(\langle v_{1q}\rangle_k - \langle v_{2q}\rangle_k\big) \\ 0 & 0 & \frac{K_{pvq}}{L_{se}}\big(-\langle v_{1q}\rangle_k + \langle v_{2q}\rangle_k\big) & \frac{K_{pvq}}{L_{se}}(\langle v_{1d}\rangle_k - \langle v_{2d}\rangle_k) \end{bmatrix}$$

$$bcp_{k=k} = \frac{3}{2}\begin{bmatrix} 0 & 0 & -K_{ivd}\langle i_{sed}\rangle_k & -K_{ivd}\langle i_{seq}\rangle_k & K_{ivd}\langle i_{sed}\rangle_k & K_{ivd}\langle i_{seq}\rangle_k & 0 & 0 \\ 0 & 0 & -K_{ivq}\langle i_{seq}\rangle_k & K_{ivq}\langle i_{sed}\rangle_k & K_{ivq}\langle i_{seq}\rangle_k & -K_{ivq}\langle i_{sed}\rangle_k & 0 & 0 \\ 0 & 0 & \frac{K_{pvd}}{L_{se}}\langle i_{sed}\rangle_k & \frac{K_{pvd}}{L_{se}}\langle i_{seq}\rangle_k & -\frac{K_{pvd}}{L_{se}}\langle i_{sed}\rangle_k & -\frac{K_{pvd}}{L_{se}}\langle i_{seq}\rangle_k & 0 & 0 \\ 0 & 0 & \frac{K_{pvq}}{L_{se}}\langle i_{seq}\rangle_k & -\frac{K_{pvq}}{L_{se}}\langle i_{sed}\rangle_k & -\frac{K_{pvq}}{L_{se}}\langle i_{seq}\rangle_k & \frac{K_{pvq}}{L_{se}}\langle i_{sed}\rangle_k & 0 & 0 \end{bmatrix}$$

5.6.1.2 Generalised state space model of SSSC based voltage control mode

The transformation of SSSC controlled by voltage control mode to dq-dynamic phasor is as follows:

$$\mathbf{\frac{d}{dt}}\langle \mathbf{\Delta X}\rangle_{\mathbf{k}} = AV_{DP}\langle \mathbf{\Delta X}\rangle_{\mathbf{k}} + BV_{DP}\langle \mathbf{\Delta U}\rangle_{\mathbf{k}} \tag{5.30}$$

where,

- The state matrix is given as:

$$AV_{DP} = \begin{bmatrix} av_{k=0} & acv_{k=\bar{k}} & acv_{k=k} & \dots & acv_{k=kn} \\ acv_{k=k} & av_{k=k} & & & \\ acv_{k=\bar{k}} & & av_{k=\bar{k}} & & \vdots \\ \vdots & & & \ddots & \\ acv_{k=\overline{kn}} & & & \dots & av_{k=\overline{kn}} \end{bmatrix}$$

The sub-matrices are:

$$av_{k=k} = \begin{bmatrix} -jk\omega & 0 & 0 & 0 & -K_{ivd} \\ 0 & -jk\omega & 0 & 0 & 0 \\ -\frac{1}{L_{se}} & 0 & -\frac{R_{se}}{L_{se}} - jk\omega & \omega & \frac{K_{pvd}}{L_{se}} \\ 0 & -\frac{1}{L_{se}} & -\omega & -\frac{R_{se}}{L_{se}} - jk\omega & 0 \\ 0 & 0 & \left\langle \frac{\frac{3}{2}v_{sed} - 2i_{sed}.R_f}{C_{dc}v_{dc}} \right\rangle_0 & \left\langle \frac{3}{2}\frac{v_{seq}}{C_{dc}v_{dc}} \right\rangle_0 & \left\langle \frac{i_{sed}^2.R_f - \frac{3}{2}v_{sed}i_{sed} - \frac{3}{2}v_{seq}.i_{seq}}{C_{dc}v_{dc}^2} \right\rangle_0 - jk\omega \end{bmatrix}$$

$$acv_{k=k} = \begin{bmatrix} & & & Zero(4\times 5) & \\ & & & & \\ 0 & 0 & \left\langle \frac{\frac{3}{2}v_{sed} - 2i_{sed}.R_f}{C_{dc}v_{dc}} \right\rangle_k & \left\langle \frac{3}{2}\frac{v_{seq}}{C_{dc}v_{dc}} \right\rangle_k & \left\langle \frac{i_{sed}^2.R_f - \frac{3}{2}v_{sed}i_{sed} - \frac{3}{2}v_{seq}.i_{seq}}{C_{dc}v_{dc}^2} \right\rangle_k \end{bmatrix}$$

- And it is given for the input matrix as:

$$BV_{DP} = \begin{bmatrix} bv_{k=0} & bcv_{k=\bar{k}} & bcv_{k=k} & \dots & bcv_{k=kn} \\ bcv_{k=k} & bv_{k=k} & & & \\ bcv_{k=\bar{k}} & & bv_{k=\bar{k}} & & \vdots \\ \vdots & & & \ddots & \\ bcv_{k=\overline{kn}} & & & \dots & bv_{k=\overline{kn}} \end{bmatrix}$$

$$bv_{k=k} = \begin{bmatrix} 0 & 0 & K_{ivd} & 0 \\ 0 & -K_{ivq} & 0 & K_{ivq} \\ \frac{1}{L_{se}} & 0 & -\frac{K_{pvd}}{L_{se}} & 0 \\ 0 & \left(\frac{1}{L_{se}} + \frac{K_{pvq}}{L_{se}}\right) & 0 & -\frac{K_{pvq}}{L_{se}} \\ \left\langle \frac{3}{2}\frac{i_{sed}}{C_{dc}v_{dc}} \right\rangle_0 & \left\langle \frac{3}{2}\frac{i_{seq}}{C_{dc}v_{dc}} \right\rangle_0 & 0 & 0 \end{bmatrix}$$

$$bcv_{k=k} = \begin{bmatrix} & Zero\ (4\times 4) & \\ \langle\frac{3}{2}\frac{i_{sed}}{C_{dc}v_{dc}}\rangle_k & \langle\frac{3}{2}\frac{i_{seq}}{C_{dc}v_{dc}}\rangle_k & 0 \quad 0 \end{bmatrix}$$

From equation (5.30), the main cause of frequency coupling in SSSC controlled by voltage control mode is the dc link while the harmonics do not have any influence on the quadrature input because of the frequency coupling, which is caused by the multiplication of the system measured quantities or states.

5.6.1.3 Generalised state space of SSSC based impedance control mode

The generalised form of SSSC using impedance control mode is given as:

$$\frac{\mathbf{d}}{\mathbf{dt}}\langle\mathbf{\Delta X}\rangle_{\mathbf{k}} = AI_{DP}\langle\mathbf{\Delta X}\rangle_{\mathbf{k}} + BI_{DP}\langle\mathbf{\Delta U}\rangle_{\mathbf{k}} \tag{5.31}$$

- In this case, the state matrix of SSSC is given as:

$$AI_{DP} = \begin{bmatrix} ai_{k=0} & aci_{k=\bar{k}} & aci_{k=k} & \dots & aci_{k=kn} \\ aci_{k=k} & ai_{k=k} & & & \\ aci_{k=\bar{k}} & & ai_{k=\bar{k}} & & \vdots \\ \vdots & & & \ddots & \\ aci_{k=\overline{kn}} & & & \dots & ai_{k=\overline{kn}} \end{bmatrix}$$

where, the sub-matrices are defined as:

$$ai_{k=k} = \begin{bmatrix} -jk\omega & 0 & 0 & 0 & -K_{ivd} \\ 0 & -jk\omega & 0 & \langle\frac{K_{ivq}v_{seq}}{i_{seq}^2}\rangle_0 & 0 \\ -\frac{1}{L_{se}} & 0 & -\frac{R_{se}}{L_{se}} - jk\omega & \omega & \frac{K_{pvd}}{L_{se}} \\ 0 & -\frac{1}{L_{se}} & -\omega & \frac{-R_{se}}{L_{se}} - \langle\frac{K_{pvq}v_{seq}}{L_{se}i_{seq}^2}\rangle_0 - jk\omega & 0 \\ 0 & 0 & \langle\frac{\frac{3}{2}v_{sed} - 2i_{sed}.R_f}{C_{dc}v_{dc}}\rangle_0 & \langle\frac{3}{2}\frac{v_{seq}}{C_{dc}v_{dc}}\rangle_0 & \langle\frac{i_{sed}^2.R_f - \frac{3}{2}v_{sed}i_{sed} - \frac{3}{2}v_{seq}.i_{seq}}{C_{dc}v_{dc}^2}\rangle_0 - jk\omega \end{bmatrix}$$

$$aci_{k=k} = \begin{bmatrix} 0 & 0 & 0 & 0 & 0 \\ 0 & 0 & 0 & \langle \frac{K_{ivq} v_{seq}}{i_{seq}^2} \rangle_k & 0 \\ 0 & 0 & 0 & 0 & 0 \\ 0 & 0 & 0 & -\langle \frac{K_{pvq} v_{seq}}{L_{se} i_{seq}^2} \rangle_k & 0 \\ 0 & 0 & \langle \frac{\frac{3}{2} v_{sed} - 2 i_{sed} . R_f}{C_{dc} v_{dc}} \rangle_k & \langle \frac{3}{2} \frac{v_{seq}}{C_{dc} v_{dc}} \rangle_k & \langle \frac{i_{sed}^2 . R_f - \frac{3}{2} v_{sed} i_{sed} - \frac{3}{2} v_{seq} . i_{seq}}{C_{dc} v_{dc}^2} \rangle_k \end{bmatrix}$$

- The input matrix (BI_{DP}) is given as:

$$BI_{DP} = \begin{bmatrix} bi_{k=0} & bci_{k=\bar{k}} & bci_{k=k} & \dots & bci_{k=kn} \\ bci_{k=k} & bi_{k=k} & & & \\ bci_{k=\bar{k}} & & bi_{k=\bar{k}} & & \vdots \\ \vdots & & & \ddots & \\ bci_{k=\overline{kn}} & & & \dots & bi_{k=\overline{kn}} \end{bmatrix}$$

where, the coupling in these matrices is caused by the integral part of the SSSC controller, impedance calculation and the dc link power balance, which are:

$$bi_{k=k} = \begin{bmatrix} 0 & 0 & K_{ivd} & 0 \\ 0 & -\langle \frac{K_{ivq}}{i_{seq}} \rangle_0 & 0 & K_{ivq} \\ \frac{1}{L_{se}} & 0 & -\frac{K_{pvd}}{L_{se}} & 0 \\ 0 & \left\{ \frac{1}{L_{se}} + \langle \frac{K_{pvq}}{L_{se} i_{seq}} \rangle_0 \right\} & 0 & -\frac{Kp_{vq}}{L_{se}} \\ \langle \frac{3}{2} \frac{i_{sed}}{C_{dc} v_{dc}} \rangle_0 & \langle \frac{3}{2} \frac{i_{seq}}{C_{dc} v_{dc}} \rangle_0 & 0 & 0 \end{bmatrix}$$

$$bci_{k=k} = \begin{bmatrix} 0 & 0 & 0 & 0 \\ 0 & -\langle \frac{K_{ivq}}{i_{seq}} \rangle_k & 0 & 0 \\ 0 & 0 & 0 & 0 \\ 0 & \langle \frac{K_{pvq}}{L_{se} i_{seq}} \rangle_k & 0 & 0 \\ \langle \frac{3}{2} \frac{i_{sed}}{C_{dc} v_{dc}} \rangle_k & \langle \frac{3}{2} \frac{i_{seq}}{C_{dc} v_{dc}} \rangle_k & 0 & 0 \end{bmatrix}$$

It is evident that using the impedance (x_{seq}) as an input to the SSSC makes the SSSC become more coupled with the harmonics compared with the use of quadrature voltage of the SSSC. This is referred to the interaction between the quadrature current and quadrature voltage in this mode.

5.6.2 Generalised impedance model for SSSC device

In this section, the impedance model of SSSC when controlled with three different control modes is presented. The full derivation of these models can be found in Appendix-E. The impedance analysis of the system has many advantages in identifying system oscillations and providing the response of the system in the frequency domain.

5.6.2.1 Generalised impedance model of SSSC based power control mode

The generalised impedance model of the SSSC when controlled in the power control mode can be derived using the following generalised equations derived from the synchronous dq equations as:

$$\langle \mathbf{\Delta v_{sedq}} \rangle_{\mathbf{k}} = AP_{se} \langle \mathbf{\Delta i_{sedq}} \rangle_{\mathbf{k}} + \langle \mathbf{\Delta m_{sedq}} \rangle_{\mathbf{k}} \tag{5.32}$$

$$\langle \mathbf{\Delta m_{sedq}} \rangle_{\mathbf{k}} = BP_{se} \langle \mathbf{\Delta PQ^{*}_{line}} \rangle_{\mathbf{k}} - BP_{se} \langle \mathbf{\Delta PQ_{line}} \rangle_{\mathbf{k}} \tag{5.33}$$

The active and reactive power flow through the compensated line can be derived by the help of Figure 5.8. Using KVL, the relationship between the bus voltage and the SSSC voltage can be given as:

$$\Delta v_{Ld} - \Delta v_{sed} = \Delta v_{1d} - \Delta v_{2d} \tag{5.34}$$

$$\Delta v_{Lq} - \Delta v_{seq} = \Delta v_{1q} - \Delta v_{2q} \tag{5.35}$$

where,

Δv_{1dq} is the direct and quadrature axis components of sending end voltage.

Δv_{2dq} is the direct and quadrature axis components of receiving end voltage.

Using equation (5.28), the active and reactive power is equal to:

$$\langle \mathbf{\Delta PQ_{line}} \rangle_{\mathbf{k}} = -CP_{se} \langle \mathbf{\Delta v_{sedq}} \rangle_{\mathbf{k}} + CP_{se} \langle \mathbf{\Delta v_{Ldq}} \rangle_{\mathbf{k}} + DP_{se} \langle \mathbf{\Delta i_{sedq}} \rangle_{\mathbf{k}} - EP_{se} \langle \mathbf{\Delta i_{sedq}} \rangle_{\mathbf{k}} \tag{5.36}$$

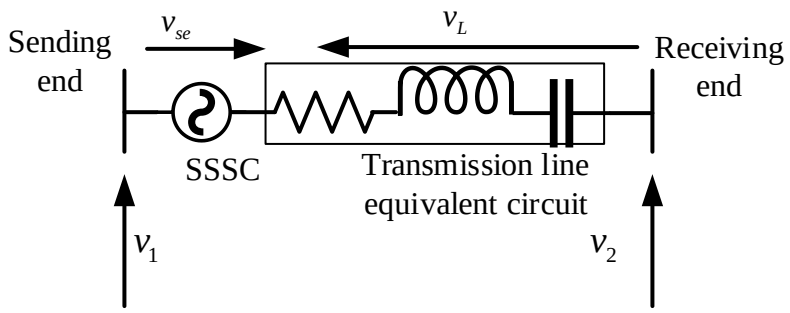

Figure 5.8. Phasor voltage of SSSC connected to a grid.

Using back substitution of equations (5.32) to (5.36), the impedance of SSSC controlled by active and reactive powers is given as:

$$Z_{PSSSC} = (I - BP_{se}CP_{se})^{-1}(AP_{seDP} + BP_{se}EP_{se} - BP_{se}DP_{se}) \quad (5.37)$$

For the sake of future comparison between the three control modes, the compensated line impedance is excluded from the SSSC impedance (Z_{PSSSC}) as shown in the analysis. The block diagram of generalised SSSC impedance controlled with power control mode is presented in Figure 5.9. The definitions of the matrices in equation (5.37) are as follows:

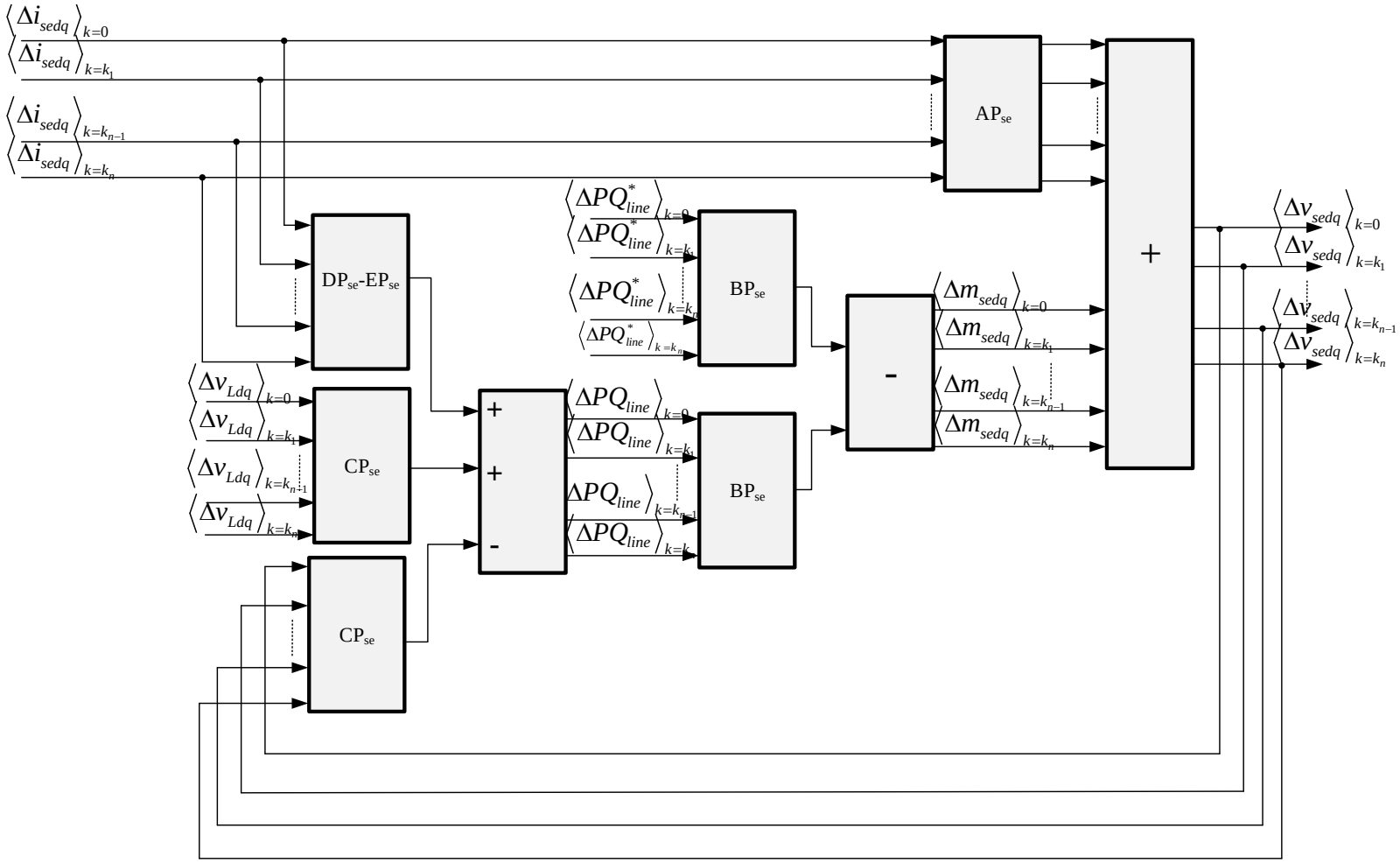

Figure 5.9. Block diagram of the generalised impedance of SSSC controlled with power control mode.

The topology matrix is:

$$AP_{se} = \begin{bmatrix} ap_{se_{k=0}} & 0 & 0 & 0 & 0 \\ 0 & ap_{se_{k=k}} & 0 & 0 & 0 \\ 0 & 0 & ap_{se_{k=\bar{k}}} & 0 & 0 \\ 0 & 0 & 0 & \ddots & 0 \\ 0 & 0 & 0 & 0 & ap_{se_{k=\overline{kn}}} \end{bmatrix}$$

$$ap_{se_{k=k}} = \begin{bmatrix} (s + jk\omega)L_{se} + R_{se} & -\omega L_{se} \\ \omega L_{se} & (s + jk\omega)L_{se} + R_{se} \end{bmatrix}$$

- The current control matrix is:

$$BP_{se} = \begin{bmatrix} Bp_{se_{k=0}} & bcp_{se_{k=\bar{k}}} & bcv_{se_{k=k}} & 0 & bcv_{se_{k=kn}} \\ bcp_{se_{k=k}} & Bp_{se_{k=k}} & 0 & 0 & 0 \\ bcp_{se_{k=\bar{k}}} & 0 & Bv_{se_{k=\bar{k}}} & 0 & 0 \\ \vdots & \vdots & \vdots & \ddots & \vdots \\ bcp_{se_{k=\overline{kn}}} & 0 & 0 & \dots & Bv_{se_{k=\overline{kn}}} \end{bmatrix}$$

$$Bp_{se_{k=k}} = \begin{bmatrix} \left(K_{pvd} + \langle \frac{K_{ivd}}{s} \rangle_0\right) & 0 \\ 0 & \left(K_{pvq} + \langle \frac{K_{ivq}}{s} \rangle_0\right) \end{bmatrix}$$

$$bcp_{se_{k=k}} = \begin{bmatrix} \langle \frac{K_{ivd}}{s + jk\omega} \rangle_k & 0 \\ 0 & \langle \frac{K_{ivq}}{s + jk\omega} \rangle_k \end{bmatrix}$$

- The calculation of active and reactive power matrices are:

$$CP_{se} = \begin{bmatrix} Cp_{se_{k=0}} & ccp_{se_{k=\bar{k}}} & ccp_{se_{k=k}} & 0 & ccp_{se_{k=kn}} \\ ccp_{se_{k=k}} & Cp_{se_{k=k}} & 0 & 0 & 0 \\ ccp_{se_{k=\bar{k}}} & 0 & Cp_{se_{k=\bar{k}}} & 0 & 0 \\ \vdots & \vdots & \vdots & \ddots & \vdots \\ ccp_{se_{k=\overline{kn}}} & 0 & 0 & \dots & Cp_{se_{k=\overline{kn}}} \end{bmatrix}$$

$$DP_{se} = \begin{bmatrix} Dp_{se_{k=0}} & dcp_{se_{k=\bar{k}}} & dcp_{se_{k=k}} & 0 & dcp_{se_{k=kn}} \\ dcp_{se_{k=k}} & Dp_{se_{k=k}} & 0 & 0 & 0 \\ dcp_{se_{k=\bar{k}}} & 0 & Dp_{se_{k=\bar{k}}} & 0 & 0 \\ \vdots & \vdots & \vdots & \ddots & \vdots \\ dcp_{se_{k=\overline{kn}}} & 0 & 0 & \dots & Dp_{se_{k=\overline{kn}}} \end{bmatrix}$$

$$EP_{se} = \begin{bmatrix} Ep_{se_{k=0}} & ecp_{se_{k=\bar{k}}} & ecp_{se_{k=k}} & 0 & ecp_{se_{k=kn}} \\ ecp_{se_{k=k}} & Ep_{se_{k=k}} & 0 & 0 & 0 \\ ecp_{se_{k=\bar{k}}} & 0 & Ep_{se_{k=\bar{k}}} & 0 & 0 \\ \vdots & \vdots & \vdots & \ddots & \vdots \\ ecp_{se_{k=\overline{kn}}} & 0 & 0 & \dots & Ep_{se_{k=\overline{kn}}} \end{bmatrix}$$

where, their submatrices are defines as

$$Cp_{se_{k=k}} = \frac{3}{2}\begin{bmatrix} \langle i_{sed}\rangle_0 & \langle i_{seq}\rangle_0 \\ \langle i_{seq}\rangle_0 & -\langle i_{sed}\rangle_0 \end{bmatrix} \qquad ccp_{se_{k=k}} = \frac{3}{2}\begin{bmatrix} \langle i_{sed}\rangle_k & \langle i_{seq}\rangle_k \\ \langle i_{seq}\rangle_k & -\langle i_{sed}\rangle_k \end{bmatrix}$$

$$Dp_{se_{k=k}} = \frac{3}{2}\begin{bmatrix} \langle v_{sed}\rangle_0 & \langle v_{seq}\rangle_0 \\ -\langle v_{seq}\rangle_0 & \langle v_{sed}\rangle_0 \end{bmatrix} \qquad dcp_{se_{k=k}} = \frac{3}{2}\begin{bmatrix} \langle v_{sed}\rangle_k & \langle v_{seq}\rangle_k \\ -\langle v_{seq}\rangle_k & \langle v_{sed}\rangle_k \end{bmatrix}$$

$$Ep_{se_{k=k}} = \frac{3}{2}\begin{bmatrix} \langle v_{Ld}\rangle_0 & \langle v_{Lq}\rangle_0 \\ -\langle v_{Lq}\rangle_0 & \langle v_{Ld}\rangle_0 \end{bmatrix} \qquad ecp_{k=k} = \frac{3}{2}\begin{bmatrix} \langle v_{Ld}\rangle_k & \langle v_{Lq}\rangle_k \\ -\langle v_{Lq}\rangle_k & \langle v_{Ld}\rangle_k \end{bmatrix}$$

5.6.2.2 Generalised impedance model of SSSC based voltage control mode

The SSSC impedance controlled by voltage control mode is derived in this section. In this case, the dc link voltage and the quadrature voltage are the controller references. The SSSC impedance can be derived in a generalised form as:

$$\langle \mathbf{\Delta v_{sedq}} \rangle_{\mathbf{k}} = AV_{se}\langle \mathbf{\Delta i_{sedq}} \rangle_{\mathbf{k}} + \langle \mathbf{\Delta m_{sedq}} \rangle_{\mathbf{k}} \tag{5.38}$$

$$\langle \mathbf{\Delta m_{sedq}} \rangle_{\mathbf{k}} = BV_{se}\langle \mathbf{\Delta V V^*} \rangle_{\mathbf{k}} - BV_{se}\langle \mathbf{\Delta V V} \rangle_{\mathbf{k}} \tag{5.39}$$

$$CV_{se}\langle \mathbf{\Delta V V} \rangle_{\mathbf{k}} = DV_{se}\langle \mathbf{\Delta v_{sedq}} \rangle_{\mathbf{k}} + EV_{se}\langle \mathbf{\Delta i_{sedq}} \rangle_{\mathbf{k}} \tag{5.40}$$

Using equations (5.38) to (5.40), the system block diagram can be plotted as presented in Figure 5.10, and the SSSC impedance can be derived as:

$$Z_{VSSSC} = \{\mathbf{I} + BV_{se}(CV_{se})^{-1}DV_{se}\}^{-1}\{AV_{se} - BV_{se}(CV_{se})^{-1}EV_{se}\} \tag{5.41}$$

Similarly, the definitions of the matrices presented in equation (5.41) are given as:

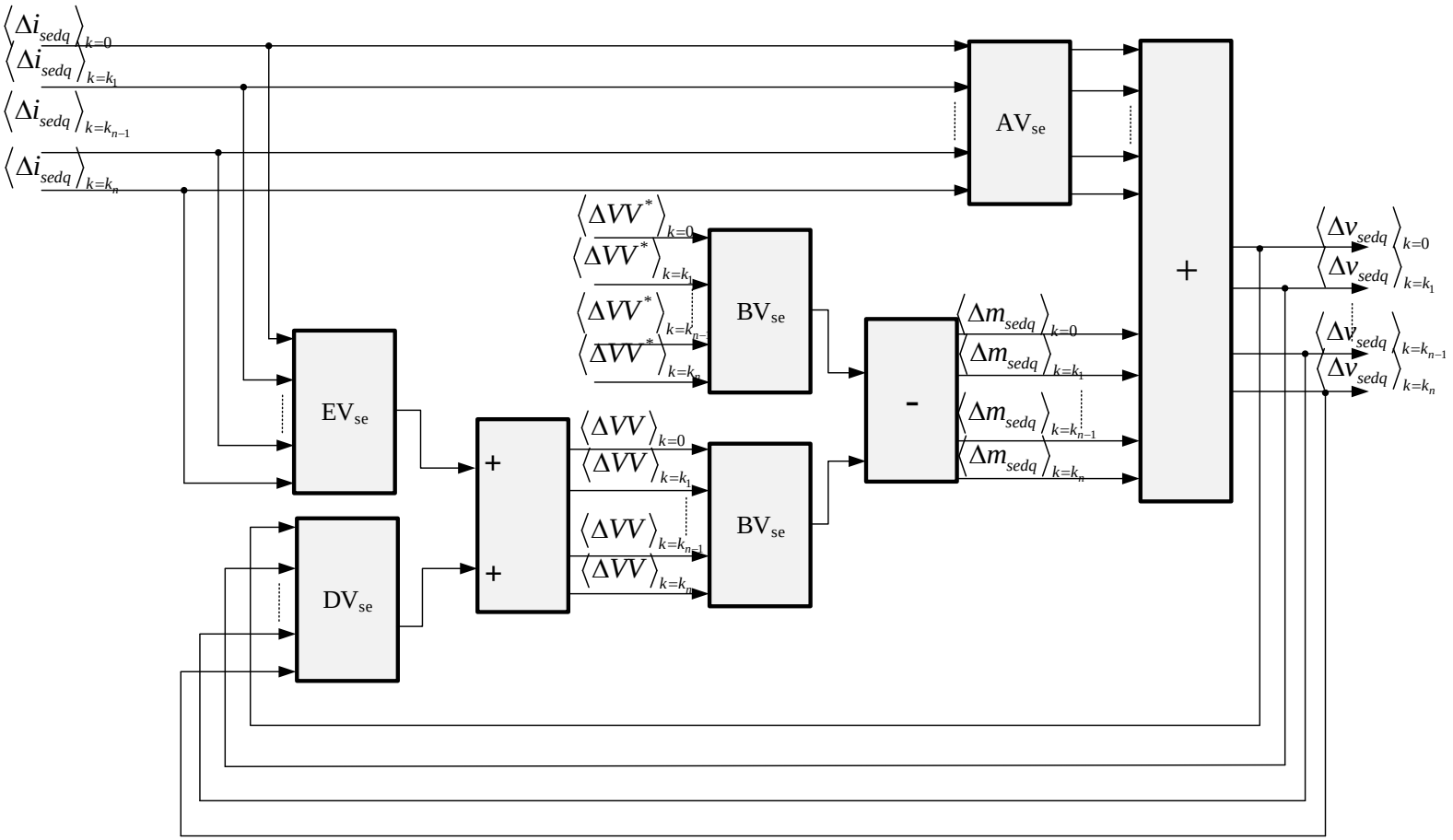

Figure 5.10. Block diagram of generalised SSSC impedance controlled with voltage control mode.

- The SSSC topology matrices are:

$$AV_{se} = \begin{bmatrix} Av_{se_{k=0}} & 0 & 0 & \cdots & 0 \\ 0 & Av_{se_{k=k}} & 0 & 0 & 0 \\ 0 & 0 & Av_{se_{k=\bar{k}}} & & 0 \\ \vdots & & 0 & \ddots & \vdots \\ 0 & 0 & \ldots & 0 & Av_{se_{k=\overline{kn}}} \end{bmatrix}$$

$$Av_{se_{k=k}} = \begin{bmatrix} L_{se}(s + jk\omega) + R_{se} & -\omega L_{se} \\ \omega L_{se} & L_{se}(s + jk\omega) + R_{se} \end{bmatrix}$$

- The current control matrix is:

$$BV_{se} = \begin{bmatrix} Bv_{se_{k=0}} & bcv_{se_{k=\bar{k}}} & bcv_{se_{k=k}} & \cdots & bcv_{se_{k=kn}} \\ bcv_{se_{k=k}} & Bv_{se_{k=k}} & 0 & 0 & 0 \\ bcv_{se_{k=\bar{k}}} & 0 & Bv_{se_{k=\bar{k}}} & & 0 \\ \vdots & & 0 & \ddots & \vdots \\ bcv_{se_{k=\overline{kn}}} & 0 & \ldots & 0 & Bv_{se_{k=\overline{kn}}} \end{bmatrix}$$

$$Bv_{se_{k=k}} = \begin{bmatrix} \left(K_{pvd} + \langle \frac{K_{ivd}}{s} \rangle_0\right) & 0 \\ 0 & \left(K_{pvq} + \langle \frac{K_{ivq}}{s} \rangle_0\right) \end{bmatrix}$$

$$bcv_{se_{k=k}} = \begin{bmatrix} \langle \frac{K_{ivd}}{s+jk\omega} \rangle_k & 0 \\ 0 & \langle \frac{K_{ivq}}{s+jk\omega} \rangle_k \end{bmatrix}$$

- The dc link voltage and quadrature voltage matrices are given as:

$$CV_{se} = \begin{bmatrix} Cv_{se_{k=0}} & ccv_{se_{k=\bar{k}}} & ccv_{se_{k=k}} & \cdots & ccv_{se_{k=kn}} \\ clv_{se_{k=k}} & Cv_{se_{k=k}} & 0 & 0 & 0 \\ clv_{se_{k=\bar{k}}} & 0 & Cv_{se_{k=\bar{k}}} & & 0 \\ \vdots & & 0 & \ddots & \vdots \\ clv_{se_{k=\overline{kn}}} & 0 & \ldots & 0 & Cv_{se_{k=\overline{kn}}} \end{bmatrix}$$

$$DV_{se} = \begin{bmatrix} Dv_{se_{k=0}} & dcv_{se_{k=\bar{k}}} & dcv_{se_{k=k}} & \cdots & dcv_{se_{k=kn}} \\ dcv_{se_{k=k}} & Dv_{se_{k=k}} & 0 & 0 & 0 \\ dcv_{se_{k=\bar{k}}} & 0 & Dv_{se_{k=\bar{k}}} & & 0 \\ \vdots & & 0 & \ddots & \vdots \\ dcv_{se_{k=\overline{kn}}} & 0 & \dots & 0 & Dv_{se_{k=\overline{kn}}} \end{bmatrix}$$

$$EV_{se} = \begin{bmatrix} Ev_{se_{k=0}} & ecv_{se_{k=\bar{k}}} & ecv_{se_{k=k}} & \cdots & ecv_{se_{k=kn}} \\ ecv_{se_{k=k}} & Ev_{se_{k=k}} & 0 & 0 & 0 \\ ecv_{se_{k=\bar{k}}} & 0 & Ev_{se_{k=\bar{k}}} & & 0 \\ \vdots & & 0 & \ddots & \vdots \\ ecv_{se_{k=\overline{kn}}} & 0 & \dots & 0 & Ev_{se_{k=\overline{kn}}} \end{bmatrix}$$

where, their submatrices are:

$$Cv_{se_{k=k}} = \begin{bmatrix} C_{dc}\langle v_{dc}\rangle_0(s+jk\omega) + \frac{3}{2}\langle\frac{\frac{3}{2}v_{sed}.i_{sed} + \frac{3}{2}v_{seq}.i_{seq} - i_{sed}^2.R_{se}}{v_{dc}}\rangle_0 & 0 \\ 0 & 1 \end{bmatrix}$$

$$ccv_{se_{k=k}} = \begin{bmatrix} C_{dc}\langle v_{dc}\rangle_k(s-jk\omega) + \langle\frac{\frac{3}{2}v_{sed}.i_{sed} + \frac{3}{2}v_{seq}.i_{seq} - i_{sed}^2.R_{se}}{v_{dc}}\rangle_k & 0 \\ 0 & 0 \end{bmatrix}$$

$$clv_{se_{k=k}} = \begin{bmatrix} C_{dc}\langle v_{dc}\rangle_k s + \langle\frac{\frac{3}{2}v_{sed}.i_{sed} + \frac{3}{2}v_{seq}.i_{seq} - i_{sed}^2.R_{se}}{v_{dc}}\rangle_k & 0 \\ 0 & 0 \end{bmatrix}$$

$$Dv_{se_{k=k}} = \begin{bmatrix} \langle\frac{3}{2}i_{sed}\rangle_0 & \langle\frac{3}{2}i_{seq}\rangle_0 \\ 0 & 1 \end{bmatrix}, ecv_{se_{k=k}} = \begin{bmatrix} \langle\frac{3}{2}v_{sed} - 2i_{sed}.R_f\rangle_k & \langle\frac{3}{2}v_{seq}\rangle_k \\ 0 & 0 \end{bmatrix}$$

$$Ev_{se_{k=k}} = \begin{bmatrix} \langle\frac{3}{2}v_{sed} - 2i_{sed}.R_f\rangle_0 & \langle\frac{3}{2}v_{seq}\rangle_0 \\ 0 & 0 \end{bmatrix}, dcv_{se_{k=k}} = \begin{bmatrix} \langle\frac{3}{2}i_{sed}\rangle_k & \langle\frac{3}{2}i_{seq}\rangle_k \\ 0 & 0 \end{bmatrix}$$

5.6.2.3 Generalised impedance model of SSSC based impedance control mode

In this section, the derivation of the generalised impedance model of SSSC controlled with impedance control mode is presented. It follows the same procedure followed for the previous sections. So, the generalised SSSC impedance is given as:

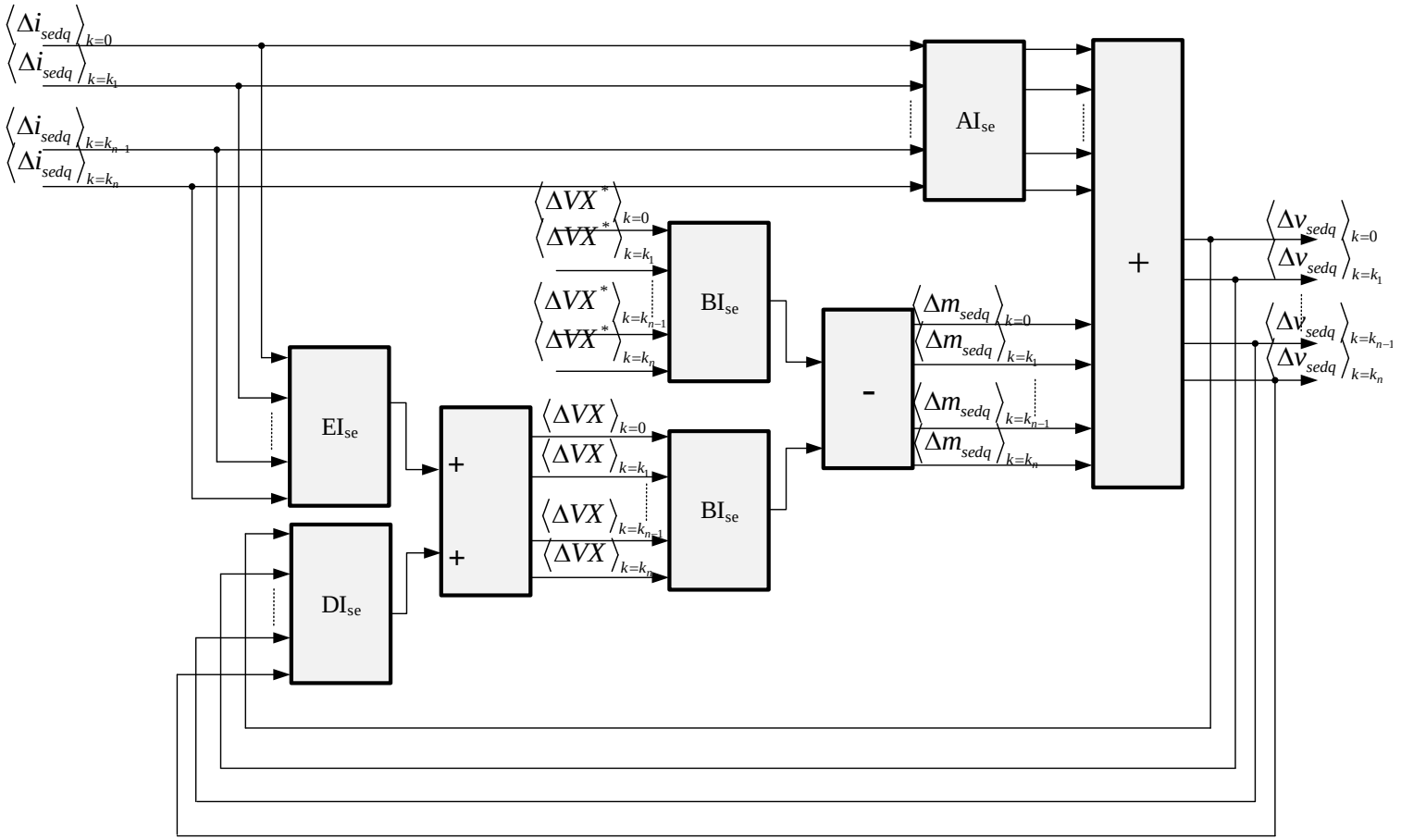

Figure 5.11. Block diagram of the generalised SSSC impedance controlled with impedance control mode.

$$\langle \mathbf{\Delta v_{sedq}} \rangle_{\mathbf{k}} = AI_{se} \langle \mathbf{\Delta i_{sedq}} \rangle_{\mathbf{k}} + \langle \mathbf{\Delta m_{sedq}} \rangle_{\mathbf{k}} \tag{5.42}$$

$$\langle \mathbf{\Delta m_{sedq}} \rangle_{\mathbf{k}} = BI_{se} \langle \mathbf{\Delta V X^{*}} \rangle_{\mathbf{k}} - BI_{se} \langle \mathbf{\Delta V X} \rangle_{\mathbf{k}} \tag{5.43}$$

$$CI_{se} \langle \mathbf{\Delta V X} \rangle_{\mathbf{k}} = DI_{se} \langle \mathbf{\Delta v_{sedq}} \rangle_{\mathbf{k}} + EI_{se} \langle \mathbf{\Delta i_{sedq}} \rangle_{\mathbf{k}} \tag{5.44}$$

The impedance of SSSC controlled by impedance is developed by the help of equations (5.42) to (5.44) and the block diagram of the SSSC impedance depicted in Figure 5.11. The SSSC impedance is:

$$Z_{ISSSC} = \{\mathbf{I} + BI_{se}(CI_{se})^{-1} DI_{se}\}^{-1} \{AI_{se} - BI_{se}(CI_{se})^{-1} EI_{se}\} \tag{5.45}$$

The definitions of the matrices in equation (5.45) are:

- The topology matrix is:

$$AI_{se} = \begin{bmatrix} Ai_{se_{k=0}} & 0 & 0 & \cdots & 0 \\ 0 & Ai_{se_{k=k}} & 0 & 0 & 0 \\ 0 & 0 & Ai_{se_{k=\bar{k}}} & & 0 \\ \vdots & & 0 & \ddots & \vdots \\ 0 & 0 & \ldots & 0 & Ai_{se_{k=\overline{kn}}} \end{bmatrix}$$

$$Ai_{se_{k=k}} = \begin{bmatrix} L_{se}(s + jk\omega) + R_{se} & -\omega L_{se} \\ \omega L_{se} & L_{se}(s + jk\omega) + R_{se} \end{bmatrix}$$

- The current control matrix is:

$$BI_{se} = \begin{bmatrix} Bi_{se_{k=0}} & bci_{se_{k=\bar{k}}} & bci_{se_{k=k}} & \cdots & bci_{se_{k=kn}} \\ bci_{se_{k=k}} & Bi_{se_{k=k}} & 0 & 0 & 0 \\ bci_{se_{k=\bar{k}}} & 0 & Bi_{se_{k=\bar{k}}} & & 0 \\ \vdots & & 0 & \ddots & \vdots \\ bci_{se_{k=\overline{kn}}} & 0 & \ldots & 0 & Bi_{se_{k=\overline{kn}}} \end{bmatrix}$$

$$Bi_{se_{k=k}} = \begin{bmatrix} \left(K_{pvd} + \langle \frac{K_{ivd}}{s} \rangle_0\right) & 0 \\ 0 & \left(K_{pvq} + \langle \frac{K_{ivq}}{s} \rangle_0\right) \end{bmatrix}, \; bci_{se_{k=k}} = \begin{bmatrix} \langle \frac{K_{ivd}}{s + jk\omega} \rangle_k & 0 \\ 0 & \langle \frac{K_{ivq}}{s + jk\omega} \rangle_k \end{bmatrix}$$

- The dc link voltage and SSSC impedance matrices are:

$$CI_{se} = \begin{bmatrix} Ci_{se_{k=0}} & cci_{se_{k=\bar{k}}} & cci_{se_{k=k}} & \cdots & cci_{se_{k=kn}} \\ cli_{se_{k=k}} & Ci_{se_{k=k}} & 0 & 0 & 0 \\ cli_{se_{k=\bar{k}}} & 0 & Ci_{se_{k=\bar{k}}} & & 0 \\ \vdots & & 0 & \ddots & \vdots \\ cli_{se_{k=\overline{kn}}} & 0 & \dots & 0 & Ci_{se_{k=\overline{kn}}} \end{bmatrix}$$

$$DI_{se} = \begin{bmatrix} Di_{se_{k=0}} & dci_{se_{k=\bar{k}}} & dci_{se_{k=k}} & \cdots & dci_{se_{k=kn}} \\ dci_{se_{k=k}} & Di_{se_{k=k}} & 0 & 0 & 0 \\ dci_{se_{k=\bar{k}}} & 0 & Di_{se_{k=\bar{k}}} & & 0 \\ \vdots & & 0 & \ddots & \vdots \\ dci_{se_{k=\overline{kn}}} & 0 & \dots & 0 & Di_{se_{k=\overline{kn}}} \end{bmatrix}$$

$$EI_{se} = \begin{bmatrix} Ei_{se_{k=0}} & eci_{se_{k=\bar{k}}} & eci_{se_{k=k}} & \cdots & eci_{se_{k=kn}} \\ eci_{se_{k=k}} & Ei_{se_{k=k}} & 0 & 0 & 0 \\ eci_{se_{k=\bar{k}}} & 0 & Ei_{se_{k=\bar{k}}} & & 0 \\ \vdots & & 0 & \ddots & \vdots \\ eci_{se_{k=\overline{kn}}} & 0 & \dots & 0 & Ei_{se_{k=\overline{kn}}} \end{bmatrix}$$

where, their submatrices are given for the diagonal submatrices which expand at the fundamental frequency of the system while the other matrices are expanded using their own frequencies as:

$$Ci_{se_{k=k}} = \begin{bmatrix} C_{dc}\langle v_{dc}\rangle_0(s + jk\omega) + \langle \frac{\frac{3}{2}v_{sed}.i_{sed} + \frac{3}{2}v_{seq}.i_{seq} - i_{sed}^2.R_{se}}{v_{dc}} \rangle_0 & 0 \\ 0 & 1 \end{bmatrix}$$

$$cci_{se_{k=k}} = \begin{bmatrix} C_{dc}\langle v_{dc}\rangle_0(s - jk\omega) + \langle \frac{\frac{3}{2}v_{sed}.i_{sed} + \frac{3}{2}v_{seq}.i_{seq} - i_{sed}^2.R_{se}}{v_{dc}} \rangle_0 & 0 \\ 0 & 0 \end{bmatrix}$$

$$cli_{se_{k=k}} = \begin{bmatrix} C_{dc}\langle v_{dc}\rangle_k s + \langle \frac{\frac{3}{2}v_{sed}.i_{sed} + \frac{3}{2}v_{seq}.i_{seq} - i_{sed}^2.R_{se}}{v_{dc}} \rangle_0 & 0 \\ 0 & 0 \end{bmatrix}$$

$$Ei_{se_{k=k}} = \begin{bmatrix} \langle \frac{3}{2}v_{sed} - 2i_{sed}.R_f \rangle_0 & \frac{3}{2}\langle v_{seq}\rangle_0 \\ 0 & \langle \frac{v_{seq}}{i_{seq}^2} \rangle_0 \end{bmatrix} \quad dci_{se_{k=k}} = \begin{bmatrix} \frac{3}{2}\langle i_{sed}\rangle_k & \frac{3}{2}\langle i_{seq}\rangle_k \\ 0 & \langle \frac{1}{i_{seq}} \rangle_k \end{bmatrix}$$

$$eci_{se_{k=k}} = \begin{bmatrix} \langle \frac{3}{2}v_{sed} - 2i_{sed}.R_f \rangle_k & \langle \frac{3}{2}v_{seq} \rangle_k \\ 0 & 0 \end{bmatrix} \quad Di_{se_{k=k}} = \begin{bmatrix} \langle \frac{3}{2}i_{sed} \rangle_0 & \langle \frac{3}{2}i_{seq} \rangle_0 \\ 0 & \langle \frac{1}{i_{seq}} \rangle_0 \end{bmatrix}$$

5.7 Stability assessment of SSSC with impedance control mode

In this section, the effect of harmonics and unbalanced operation on the SSSC with impedance control model is presented as an example. The test system including the SSSC is presented in Figure 5.12 and the SSSC parameters are shown in Table 5.3. The SSSC analysis is carried out by the impedance analysis to presents the differences between different operating conditions.

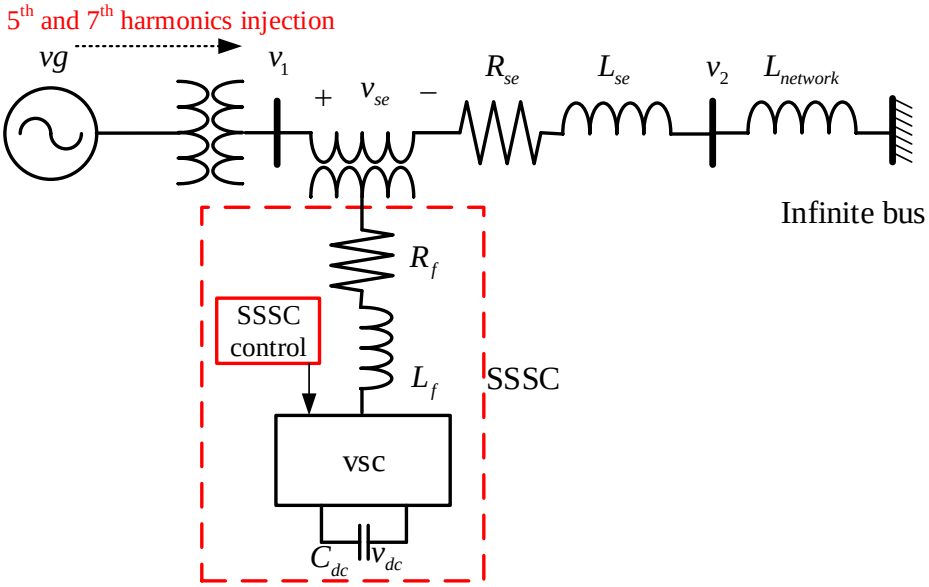

Figure 5.12. SSSC compensates load in presence of harmonics.

Table 5.3. SSSC control modes parameters.

Parameter	Value
R_f, L_f	5 Ω, 5 mH
R_{se}, L_{se}	25 Ω, 161.4 mH
C_{dc}	800 µF
v_{dc}	50 kV
K_{pvd}, K_{ivd}	0.01 V/A, 0.01 V/A.s
K_{pvq}, K_{ivq}	-0.22 V/A, 2 V/A.s
v_{seq}	1000V

5.7.1 Balanced operation of SSSC with no harmonic

This modelling of SSSC is carried out by the synchronous dq impedance model of the SSSC with power control where the harmonics are ignored in the model. The SSSC impedance at the fundamental frequency is shown by the dotted line in Figure 5.13. It is seen that the SSSC impedance with no harmonics matches the SSSC impedance without harmonics coupling.

5.7.2 Unbalanced operation of the SSSC

The proposed generalised SSSC model is employed to assess its capability to identify the unbalanced operation of the SSSC. Three levels of voltage magnitude will be examined in this section as the magnitude of phase-b as [1 0.85 0.65] pu. It is clear that the dq-dynamic phasor model of SSSC is efficiently identified the unbalanced operation without any transformation to the model. The identification is based on the existence of $(k = 0)$ at the fundamental and $(k = -2)$ to represent the unbalanced operation. Figure 5.13 shows the plot of four impedances as the synchronous dq impedance of SSSC (dotted line), the negative sequence impedance for the balanced system (solid line), the negative sequence impedance at 0.85 pu voltage (dash-dot line) and the negative sequence impedance at the 0.65 pu (dotted line). As shown in Figure 5.13, the negative sequence impedance (dotted line) for the balanced case is slightly greater than the positive sequence impedance (dashed line) which is referred to the existence of controller gains in the coupling matrix. The increase of the unbalance increases the magnitude of the coupling matrix which consequently increases the SSSC impedance especially at low frequencies. This is referred to the parameters of the SSSC controller which will become zero at high frequencies and the only effect remains is the measured negative sequence components $(k = -2)$. The identification of the unbalanced operation becomes more obvious as much as the coupling between the system components increases and the control system becomes more complex.

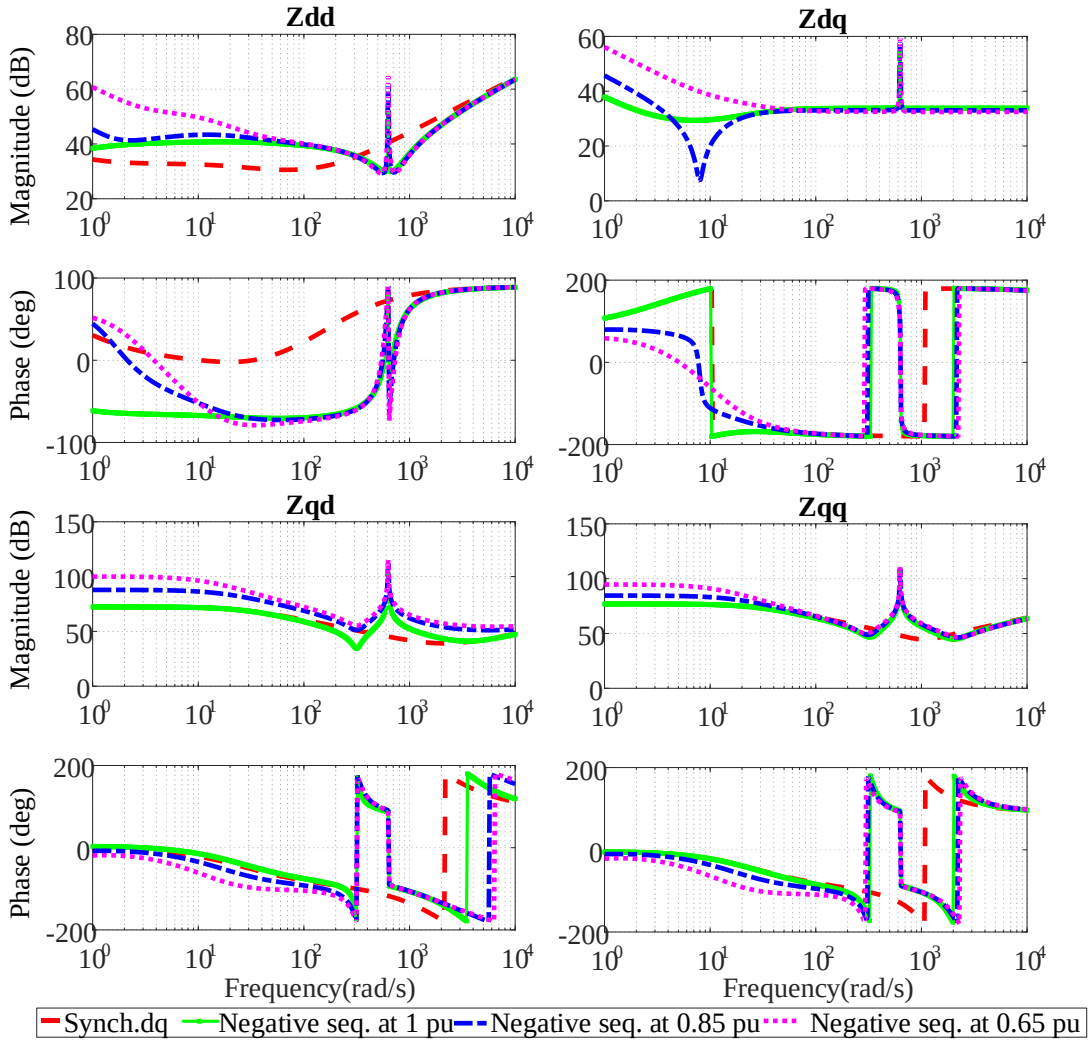

Figure 5.13. SSSC impedance with impedance control model under unbalanced operation.

As stated previously, the sharp changes in SSSC impedances are caused due to the complex part at the studied harmonics in dq-dynamic phasor domain.

5.7.3 SSSC operation under the existence of harmonics

In this section, the effect of harmonics on the SSSC impedance with the impedance control model is presented. The source injects the 5^{th} and 7^{th} harmonics to the system in order to assess the response of the SSSC control modes due to the existence of the harmonics. The SSSC has a frequency coupling in both control inputs, where the coupling in d-axis is referred to the active power while the q-axis coupling is referred to the reactive power. As shown in Figure 5.14, the existence of harmonics has almost no effect on the impedance of the SSSC for all frequencies. This is referred to

the simplified controller that has been used which causes a slight frequency coupling between the fundamental frequency and the other harmonics, where the control systems are one of the main causes of coupling in VSC-FACTS devices as will be presented in the following section.

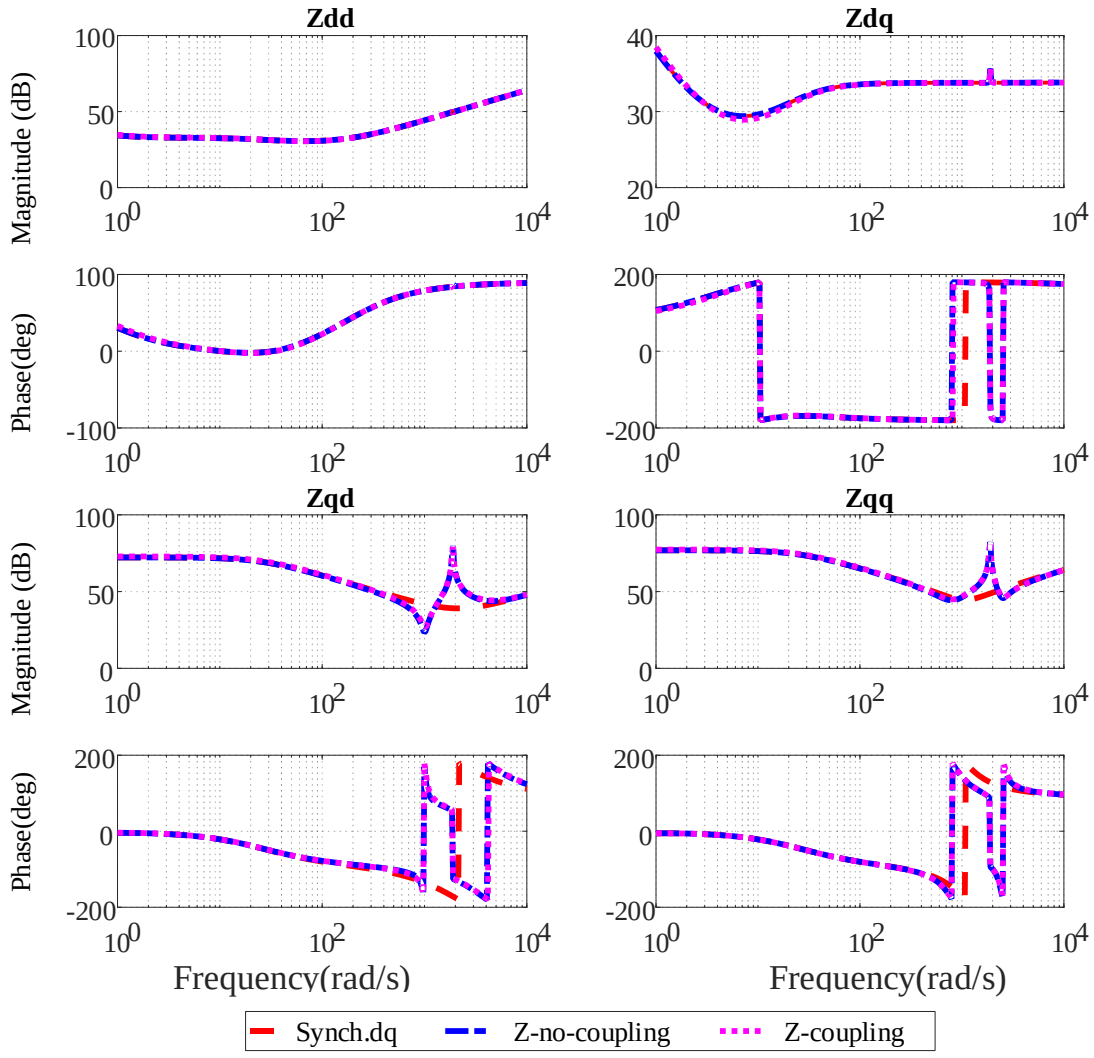

Figure 5.14. Harmonics effect on SSSC controlled with impedance control mode.

As a conclusion, the frequency coupling can be ignored in case of this control mode is employed in harmonic polluted environment.

5.8 The concept of frequency coupling in VSC-FACTS devices

In VSC-FACTS devices and other power system components, the coupling between the fundamental frequency and other harmonics might affect the operation and the

stability of the device. The main observations regarding the frequency coupling in VSC-FACTS devices in dq-dynamic phasor modelling are:

- The control systems such as the existence of integrators and differentiators as well as phase-locked loop (PLL) especially in the weak grids, which cause coupling between the fundamental frequency and other frequencies and between the harmonics to each other.
- The existence of the harmonics in the dc link of the VSC-FACTS device which causes due to the power variations.

The frequency coupling in VSC-FACTS devices is illustrated in Figure 5.15 using dq-dynamic phasor model. It shows the system inputs are analysed based on their frequency to an infinite number of harmonics. This result in the operation of the VSC-FACTS device is seen as an infinite number of devices operate at these harmonics which might affect each other at certain cases. The sum of the response of all these systems is added at the output of the device to present the total response of the device. The coupling between the fundamental frequency and the harmonics is shown in Figure 5.15 by a bold solid line. It is assumed in this thesis that each frequency affects its conjugate (bold dashed line in Figure 5.15) and the fundamental frequency without considering any interaction between different harmonics. The improved design of these devices eliminates or declines the strength of the link between the frequencies which help to improve the immunity of the VSC-FACTS devices against harmonic effects. From the impedance perspective, the frequency coupling describes the effects of the harmonics on the device impedance, both the magnitude and the phase. For instance, the STATCOM impedance presented in (5.25) can be written as:

$$Z_{DP} = \begin{bmatrix} Z_f + p & \varepsilon_{k=\overline{k_1}} & \varepsilon_{k=k_1} & \cdots & \varepsilon_{k=\overline{k_n}} & \varepsilon_{k=k_n} \\ \mu_{k_1,0} & Z_{k=k_1} + p & 0 & & 0 & 0 \\ \mu_{\overline{k_1},0} & 0 & Z_{k=\overline{k_1}} + p & & 0 & 0 \\ \vdots & & & \ddots & & \\ \mu_{k_n,0} & 0 & 0 & & Z_{k=k_n} + p & 0 \\ \mu_{\overline{k_n},0} & 0 & 0 & & 0 & Z_{k=\overline{k_n}} + p \end{bmatrix} \tag{5.46}$$

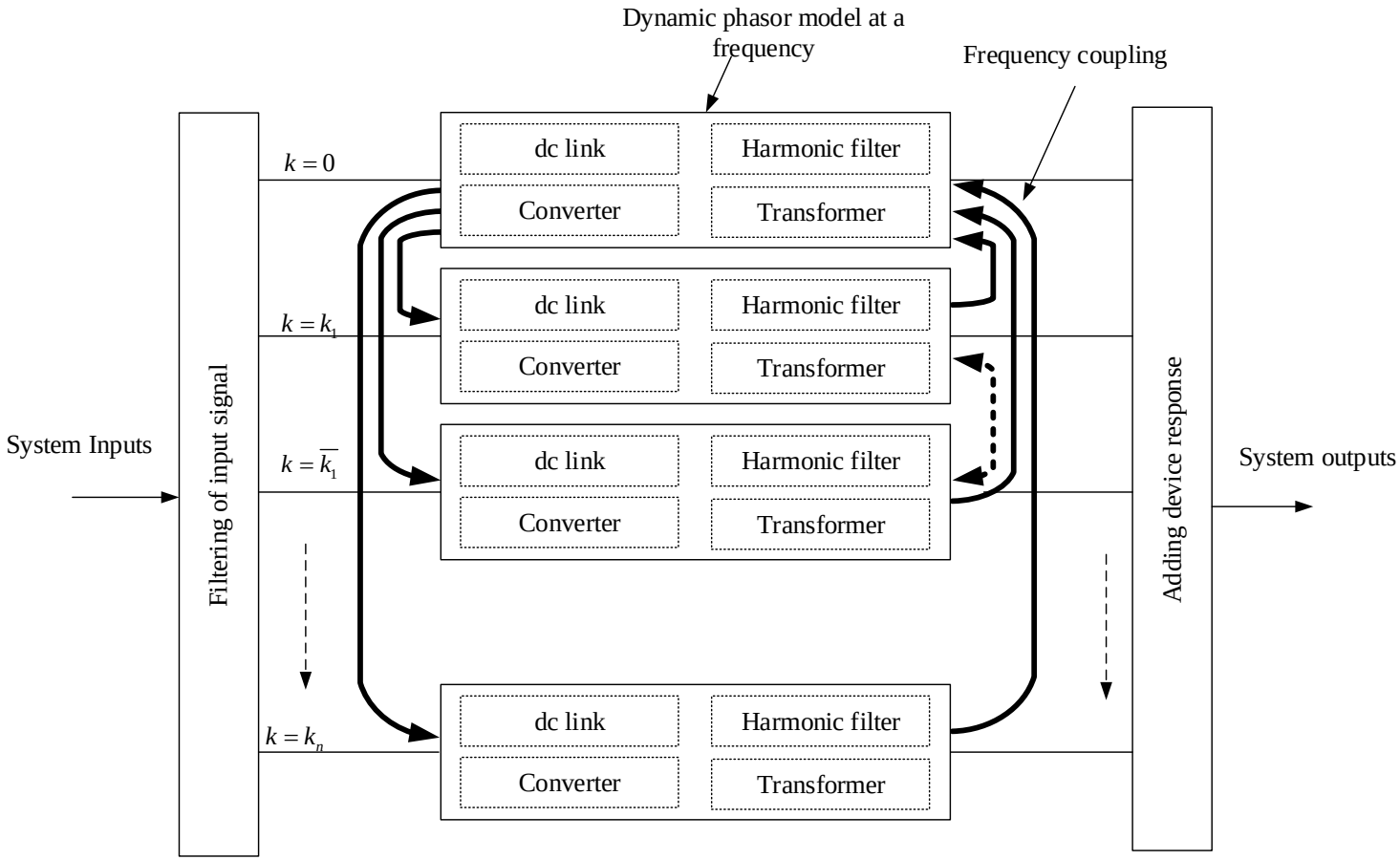

Figure 5.15. Frequency coupling in VSC-FACTS devices.

Equation (5.46) is generalised and written in a compact form as:

$$Z_{DP} = \begin{cases} z_f|_{k=0} + p + \sum_{k=-\infty}^{\infty}(\varepsilon_k) & k = 0 \\ z_f|_{k=0} + p + \mu_{k,0} & k \neq 0 \end{cases} \quad (5.47)$$

where,

ε_k is the coupling matrices between fundamental frequency and harmonics.
$\mu_{k,0}$ is the coupling between the harmonics and the fundamental frequency.

The coupling might appear also in the diagonal impedance (p), as the dc link voltage is affected by the presence of the positive and negative sequence components of the voltages and currents. In the case of the 5th and 7th harmonic existence, positive and negative components are generated at ($\pm 6\omega$) which causes a frequency coupling. In case of the system is considered as fully decoupled, where the system is assumed as multi-grids operated at different frequencies, the coupling matrices are:

$$\varepsilon_k = \mu_{k,0} = zeros\ (2,2) \quad (5.48)$$

According to the dynamic phasor transformation in equation (5.48), the measured impedance in abc coordinates at a specific harmonic is equal to the impedance of its generated harmonics in dq-dynamic phasor multiplied by the transformation factor ($e^{\pm jk\omega t}$).

5.9 Comparison between the proposed dq-dynamic phasor modelling analysis and conventional modelling techniques for small signal stability

Several modelling techniques have been employed in the literature for stability assessment in the existence of harmonics and their effects on the operation of system devices. These models are summarised in Table 5.4 by comparing their main features in comparison with the proposed modelling. The comparison shows superior advantages of the proposed modelling for stability analysis. However, the complexity of the derivation is the main disadvantage. The selection between these modelling techniques is carried out based on the purpose of the study and the operating conditions of the studied system. Although the harmonic state space (HSS) technique

is based on a similar concept, there are some differences between it and the proposed model as:

- The proposed modelling is very efficient in identifying unbalanced operation of the systems in the frequency domain.
- The frequency range of HSS in stability assessment is $(-\frac{\omega}{2}, +\frac{\omega}{2})$ where it is based on periodic quantities. In the meantime, unlimited range is required to assess the stability using the proposed model because the proposed method is based on linear time invariant parameters.
- The positioning of the eigenvalues in the proposed modelling technique is located in the opposite of that one resultant using the HSS. This is referred to the assumptions made in the analysis of both modelling techniques.
- Each state variable expands by {6×h} in the HSS method while the proposed model expands by {4×h}, where (h) is the number of harmonics. So, the proposed modelling has 2/3 the size of HSS.

Table 5.4. Comparison between the proposed model and other techniques for small signal stability.

Characteristic	Identify harmonics effect	Complexity of derivation	Matrices size of each state variable	Identify unbalanced operation	Type of parameters	Stability assessment range
Synchronous dq [3] [18]	Multiple coordinates required	Simple	Small	Using (2^{nd}) order harmonic	Linear time-invariant	$(-\infty, +\infty)$
Unified modelling using αβ [30]	Multiple coordinates required	Simple	Small	Limited for $\omega_s > 2\omega$	Linear time-variant	$(-\infty, +\infty)$
Single phase dynamic phasor [65], [105], [106]	Not applicable	Simple	Small	Not applicable	Linear time-invariant	$(-\infty, +\infty)$
Harmonics linearization method-LTI [36][37]	Yes	Moderate	Moderate	Using positive negative transformation	Linear time-invariant	$(-\infty, +\infty)$
Harmonic state space (HSS) [1][47]	Yes	Difficult	Large	Using positive negative transformation	Linear time-variant	$(-\frac{\omega}{2}, +\frac{\omega}{2})$
Proposed dq-dynamic phasor	Yes	Difficult	Moderate $(2/3)$ of HSS	Using positive-negative components	Linear time-invariant	$(-\infty, +\infty)$

5.10 Summary

A generalised dq-dynamic phasor of the state space model and impedance modelling for small signal stability analysis has been proposed. Two types of VSC-FACTS devices were employed to demonstrate the proposed modelling. The developed criteria combined the criteria of synchronous dq modelling and HSS criteria. The nature of the developed criteria is based on LTI systems while this system included the effect of harmonics on stability. The unbalanced operation of the derived systems appeared as a displacement of the eigenvalues in state space analysis and as an unmatched plot of positive and negative impedances in impedance analysis. The frequency coupling matrix presented a good sign of the unbalanced conditions of the devices where its parameters are equal to zero for balanced systems. Also, ignoring the frequency coupling presented repeated eigenvalues and the same impedance at all frequencies. In the meantime, considering the coupling affects the stability margin of the system and can lead to instability. In addition, the inclusion of harmonics in the SSSC with impedance control caused no influence on the SSSC impedance due the simplicity of the controller and the small effect of harmonics appeared in comparison with the fundamental frequency quantities. Nevertheless, with respect to the complexity of the analysis, the proposed modelling has a better performance than conventional modelling. The proposed generalised modelling manages successfully to reproduce their typical response at the fundamental frequency as well as at significant low-order harmonics using both eigenvalues and impedance analysis. It successfully includes the harmonics and identifies unbalanced conditions as well as presenting the effects of harmonic coupling on the fundamental frequency. The proposed modelling was more convenient be compared to the synchronous dq models and to be simpler to extend the current criteria on synchronous dq to the proposed form. The validity of the developed mathematical models was confirmed using time-domain simulations performed in MATLAB/Simulink environment.

CHAPTER 6

SMALL SIGNAL STABILITY MONITORING, IMPROVEMENT AND CONTROL

In this chapter, an impedance measurement unit (IMU) is proposed to monitor the small signal stability by measuring the system impedance. It has a fast response which can be utilised by the network operators or a stability based control system as a tool for fast assessment. Also, the effect of changing the STATCOM parameters on the impedance norms is investigated. In addition, the effect of implementing control parameters (virtual impedance) on infinite norm of STATCOM impedance is presented. These control parameters might be utilised by the control system to adjust the device impedance. Lastly, the effectiveness of SSSC control modes is investigated on damping the system oscillations. The stability assessment is carried out using the impedance concept for a series compensated system connected to a synchronous machine.

6.1 Introduction

Power systems experience many events affecting their operating conditions or that might lead to instability. From an impedance based stability perspective, the definition of the instability is that when the load-source impedance ratio is greater than a specific limit. So, by maintaining the impedance ratio below this limit, the stability will be insured. A fast measurement of the impedance at the interfacing point improves the response time to retain the system stability. Making the decision about the required actions, to maintain the stability, can also be improved by utilising the mathematical based criteria such as impedance norms. Even though the impedance norms are not sensitive to the phase-related-instability, it can be utilised to monitor the stability by network operators or a control system. As well as, having a direct relationship between the control parameters of the network or the device will aid the control system to maintain stability.

6.2 Monitoring the stability of power system

Stability monitoring can be carried out by designing an impedance measurement unit (IMU) and using its measurements to control device/load impedance norm. The IMU should provide the required information of the system to change its impedance under different operating conditions. The fast response of this measurement unit should be guaranteed to ensure effective stability monitoring. In the following sections, the design of the proposed IMU is presented.

6.2.1 Proposed impedance measurement unit (IMU)

In this section, an impedance measurement unit (IMU) for stability assessment applications is proposed. The basic principle of IMU is to inject a perturbation signal into the system and then calculate the response using current and voltage measurements at the point of interest. Impedance identification is carried out using several frequencies to ensure fast response and give a good estimation. The selection of the injected frequencies should avoid any coupling between these frequencies in dq coordinates. A multi-tone signal is chosen to perturb the measured device. This is more effective in comparison with the chirp signal, especially if several frequencies are considered [97]. The resultant impedance is less noisy measurements. Also, the injected frequencies should be distributed within the range of interest and be multiples of the sampling time to reduce the Fast Fourier Transform (FFT) error. Two measurements approach is chosen to measure the impedance using series injection voltage. The voltage is injected by the injection circuit for a range of the frequencies in the first half with positive frequency $(+\omega_i)$ and negative frequency $(-\omega_i)$ for the other half of the measurement time $(t_{measure})$. The time (t_a) is the period required for each injected signal. It is specified based on the time required to finish one duty cycle of the smallest injected frequency or the response time of the measured system, and it is defined as:

$$t_a = \frac{t_{measure}}{2} \tag{6.1}$$

The selection of the IMU parameters and injection technique is based on the following factors:

- The sampling time is chosen based on the frequency range where the maximum range of measured impedance is equal to:

$$\text{Maximum frequency range} = \frac{1}{2(\text{Sampling time})} \tag{6.2}$$

- The measurement time ($t_{measure}$) is selected based on the expected time constant of the measured system and the duty cycle of smallest injected frequency. Increasing of the measurement time ensures more accurate measurements.
- The number of injected frequencies is selected based on the number of impedances that can present the impedance trend over the frequency range.
- The distribution of the injected frequencies should avoid frequency coupling between injected frequency components.
- The injection technique 'series voltage or shunt current' of the injected circuit is chosen based on the topology of measured system. For instance, current injection is more suitable for VSC based devices that use the voltage as an input to phase locked loop (PLL), while the voltage injection is easier to implement and suits the devices using current as an input to PLL. This is referred to the effect of harmonics on the PLL and phase shift of injected signal on the measured impedance of these devices.

6.2.1.1 Proposed structure of IMU

The impedance measurement unit (IMU) structure is illustrated in Figure 6.1. The measurement stages can be defined as:

- Signal filtering and discretization block: it filters the measurement based on the injected frequencies, it transforms the voltages and the currents from abc to synchronous dq coordinates. Also, it discretises the measured signals of voltages and currents according to the sampling time.
- Time-based selector block: it splits the measured signals to two parts and delays the first parts of the measurements according to the injected time measurement ($t_{measure}$) to differentiate between the first and the second measurement.

- Frequency-based magnitude and phase extraction: it finds the magnitude and phase of measured voltages and currents at each injected frequency using FFT transform and designed frequency selection blocks.
- Impedance measurement block: it calculates the impedances at each frequency using the extracted voltages and currents.

6.2.1.2 Performance validation of the proposed IMU

The parameters of the IMU are listed in Table 6.1 where the selection of these parameters is carried out based on the previous discussion in section 6.2.1. The proposed IMU measurements are compared with a mathematical model of SSSC controlled with voltage control mode as an example of VSC-FACTS devices. The series injection topology is used to inject the perturbation signal to avoid the effect of oscillations on the SSSC performance where the PLL input of SSSC is the quadrature voltage. Generally, the IMU is managed to extract the small signal impedance of the SSSC precisely over the range of interested frequency as shown in Figure 6.2. The SSSC impedance is extracted within 1s which is quick enough to respond to the network requirements. The error appearing in the impedances at high frequencies is to a low noise ratio (SNR) which can be improved by a selecting different combination of injected frequencies [74]. In addition, the accuracy of the proposed IMU increases by increasing the measurement time and the number of injected frequencies. The measured impedance is sufficient to predict the stability of the system and take any corrective actions to maintain the stability of the system.

Table 6.1. Proposed IMU parameters

Parameter	Value
Sampling time	10 μs
Measurement time ($t_{measure}$)	1 s
Number of injected frequencies	10
Frequency vector	[10 60 150 200 250 400 500 700 800 900]

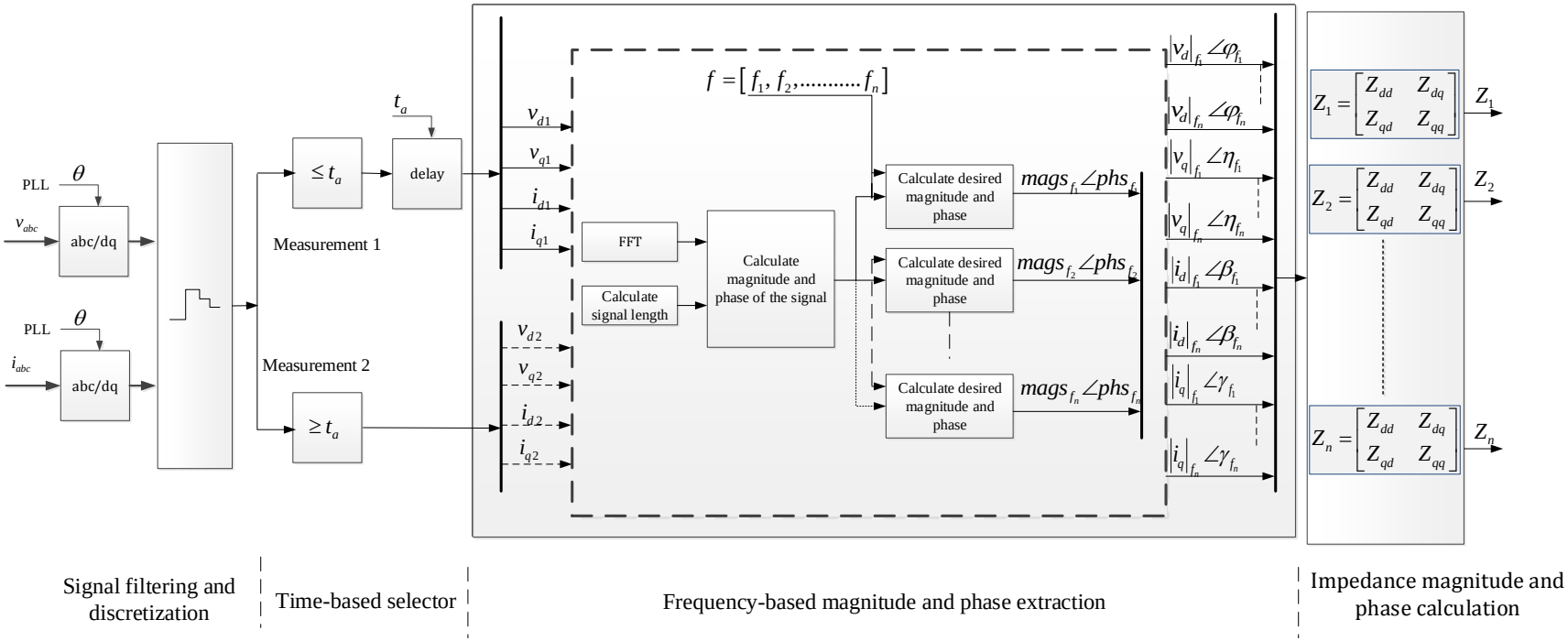

Figure 6.1. Structure of proposed IMU.

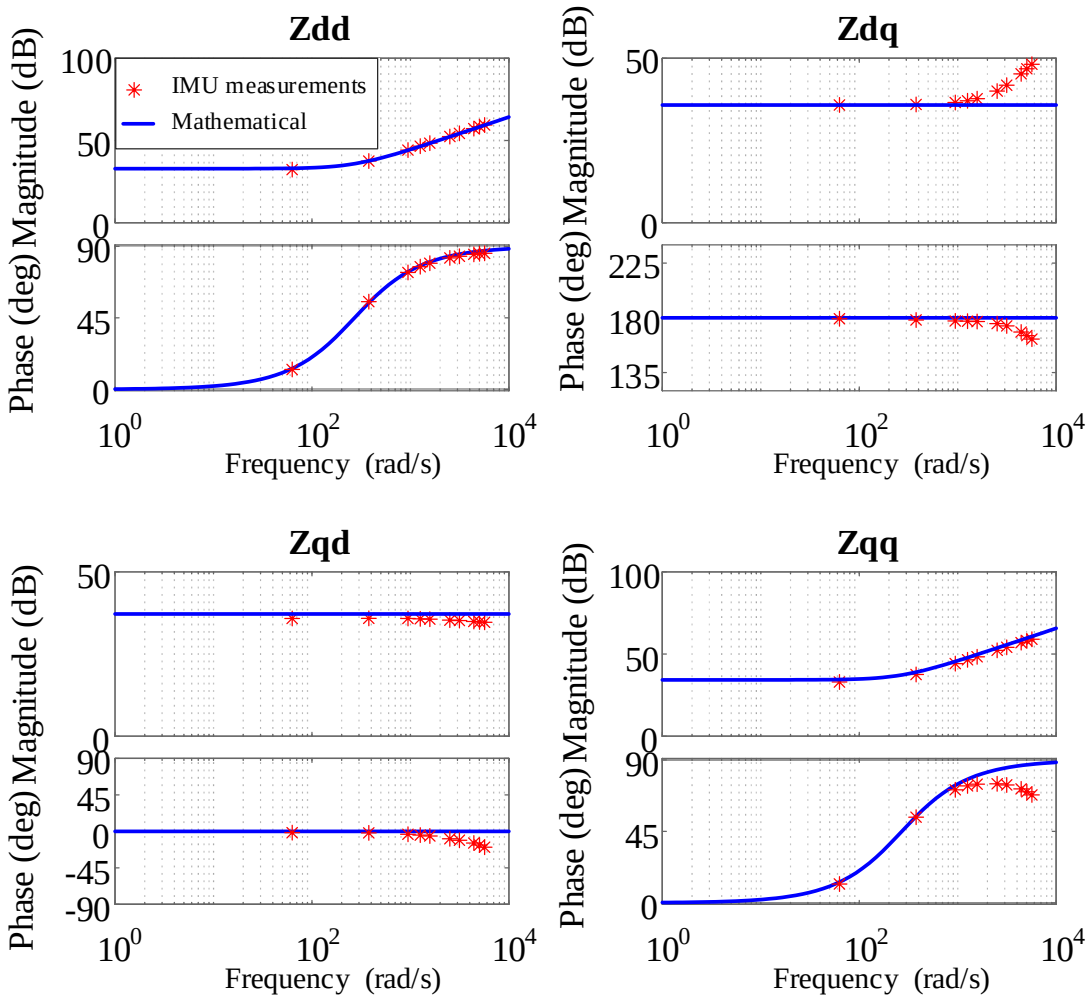

Figure 6.2. Comparison between SSSC mathematical model and proposed IMU.

The increase of the frequency range of measured impedance the sampling time should be decreased which might cause a further delay on the operation of the proposed IMU.

6.2.2 Comparison between the proposed IMU and conventional IMUs

Many publications have proposed impedance measurement units in the literature. The focus of these methods was about the injected methods [69], the measurement algorithm [70][71] or a design of the IMU [74][72], [107]. However, the main limitation of the previous research was the long time required to measure the impedance as well as the filtering requirements of the impedances as the objective was the accuracy of the measured impedance rather than its fast assessment.

Table 6.2 presents the main components and features of the IMUs found in the literature in comparison with the proposed IMU. The IMUs used different injection methods and different types of signals. The noisy impedance measurement were filtered using cross-correlation techniques with a notch filter or discrete Fourier transform (DFT). The units that are based on wide-band signals (the proposed IMU and in [74][72]) provide a faster measurement time compared to the methods based on sinusoidal signal. As stated, fast measurement processing is crucial for maintaining the stability whether by the network operators or by control systems.

Table 6.2. Comparison between different IMUs performances

	IMU_1 [74]	IMU_2 [72]	IMU_3 [107]	Proposed IMU
Injection method	Series injection	Series-shunt injection	Series-shunt injection	Series injection
Signal type	Chirp signal	Multi-tone injection	Sinusoidal signal	Multi-tone injection
Processing time	Depends on the number of inputs	Depends on the number of inputs	Not specified Considerably slow	Less than 1 s
Impedance extraction procedure	Cross-correlation techniques	Single phase based models	Cross-correlation techniques	Direct measurement
Filtering requirements	Discrete Fourier transform (DFT)	Large inductance	Notch filter	Not required
Number of repeated injections	One & ten injections for each segment	Two at each frequency	Two at each frequency	Two measurements

6.3 Controlling the STATCOM impedance

From the small signal impedance perspective, improving ac system stability at the interfacing point is a function of the impedances of the two connected systems. The dq impedance of an ac system has four parts which together define system stability based on the impedance matrix. For instance, the use of stability criteria in control system requires having a mathematical relationship between the chosen criterion and a control variable. The generalized Nyquist criterion (GNC) can ensure the stability at the interface; however, it is hard to convert it into a mathematical form. This

feature is found in the stability norms-based criteria which can facilitate the use of stability norms by the network operators by direct control as shown in Figure 6.3. Such relationship presents the actual effect of system parameters on the stability and how to maintain it. Such tuning can be carried out by changing system parameters or by utilising virtual impedance which might be more effective for controlling the impedance.

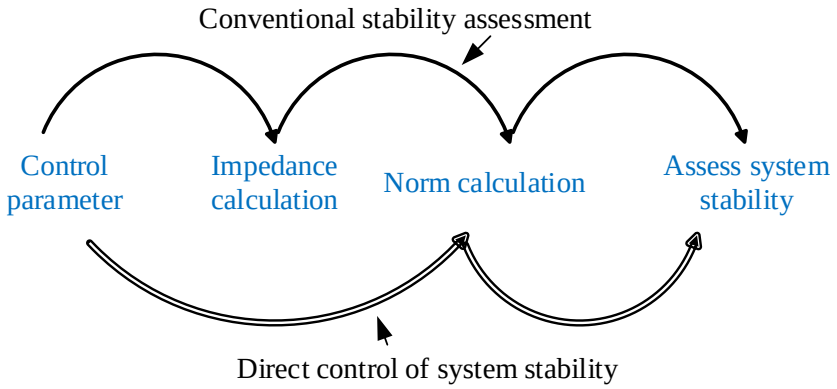

Figure 6.3. Concept of stability based impedance control.

There are some challenges when building a control system based on small signal impedance:

- Noise introduced by the injection circuit used to measure the impedance could lead to poor power quality of the system. The existence of noise reduces the visibility of continuous stability measurement. Solving this challenge might be done by measuring the impedance at specific conditions such where the system parameters fail to maintain stability.
- Even though the stability norms are the only mathematical stability criteria found in the literature that can be used in a control system, the dependency on magnitude only to find the norm presents some shortages of the stability norms to measure the stability of all systems. This is referred to the use of magnitude information only in the calculation and ignoring the phase of the impedance. Developing other criteria based on magnitude and phase are essential to tackle this problem.

6.3.1 Effect on stability norms of changing STATCOM control parameters

As presented in the STATCOM equations in Chapter 4, the STATCOM control parameters have a varying effect on the STATCOM's total impedance. However, this relationship is not obvious for stability norms of impedance matrices. Finding the relationship between these control system and stability can improve the time response to stabilize the system and take corrective actions by system operators. In this section, the same test system presented in Chapter 3 is used to present the effect of the STATCOM control system on the infinite norm. The test system and STATCOM parameters are shown in Table 6.3.

Table 6.3. System and STATCOM Parameters

Parameter	Value	Parameter	Value
v_d, v_q	410 V, 0 V	K_{pvd}	10 V/A
R_f, L_f	0.5 Ω, 5 mH	K_{ivd}	0.001 V/A.s
C_{dc}	400 μF	K_{piq}	800 V/A
v_{dc}	1000 V	K_{iiq}	8000 V/A.s
K_{pid}	800 V/A	K_{pvq}	0.01 V/A
K_{iid}	8000 V/A.s	K_{ivq}	2 V/A.s

Figure 6.4 shows how the STATCOM controller voltage and current gains affect the infinite norm of the impedance matrix. The STATCOM impedance is calculated at different frequencies (10, 200, 800, 1500 and 2500 rad/s) to cover a wide range of the STATCOM operation. The effect of STATCOM gains is appeared for some of gains, and insignificant for other gains. This response refers to the fact that changing gains could affect the phase shift rather than the magnitude of the impedance. For the gains of voltage controller, the integral gains (K_{ivd}, K_{ivq}) have less impact on the infinite norm compared with the proportional gains (K_{pvd}, K_{pvq}) due to the range of change of these gains. The increase of the quadrature proportional voltage gain (K_{pvd}) tends to decrease the infinite norm as well as the direct proportional voltage gain as seen in Figure 6.4a. The current controller gains have similar effect of the voltage gains. The increase of the proportional current gain (K_{piq}) tends to reduce the infinite norm except for small period while the increase proportional current gain

(K_{pid}) has positive and negative effect on the infinite norms as shown in Figure 6.4b. In the meantime, the integral current controller gains (K_{iid}, K_{iiq}) have an insignificant effect on the impedance norm. The effect of the STATCOM controllers' gains might not change the impedance norm, but the affect the phase shift of the STATCOM impedance. Such a change can be assessed only by the generalised Nyquist criterion to assess the stability. The chosen values of control gain influence significantly their ability to adjust the infinite norm and might be restricted by the steady-state or transient requirement of the connected network. Another restriction could be the device setting point where the infinite norm cannot be reduced. This conclusion leads to the need to identify another control variable that can control the stability norms over a wide range which can be represented by a simple mathematical relationship. The possibility of using a control variable to control directly the stability norm of the STATCOM impedance matrix that might be added to the control system is discussed in the following section.

6.3.2 Virtual impedance implementation for STATCOM impedance Control

This section presents the application of virtual impedance to control the STATCOM's behaviour and to reshape its impedances. The basic idea of virtual impedance is to add the effect and behaviour of physical series or parallel impedance (passive impedance) to the control system (active impedance). The benefit of using virtual impedance along with other active techniques is that the active techniques regulate the STATCOM impedance magnitude and phase margins within a specific range without affecting the output voltage and currents. The aim of this section is to examine a simple virtual impedance implementation in a control system. The focus of this section is the implementation of virtual pure and complex impedances while the other techniques such as the virtual synchronous machine [108] are beyond the scope of this thesis. The aims of using virtual impedance here can be summarised as:

- Find a suitable control variable that has a direct relation with stability norms.
- Find a control variable that can adjust the infinite norm of the STATCOM impedance matrix.

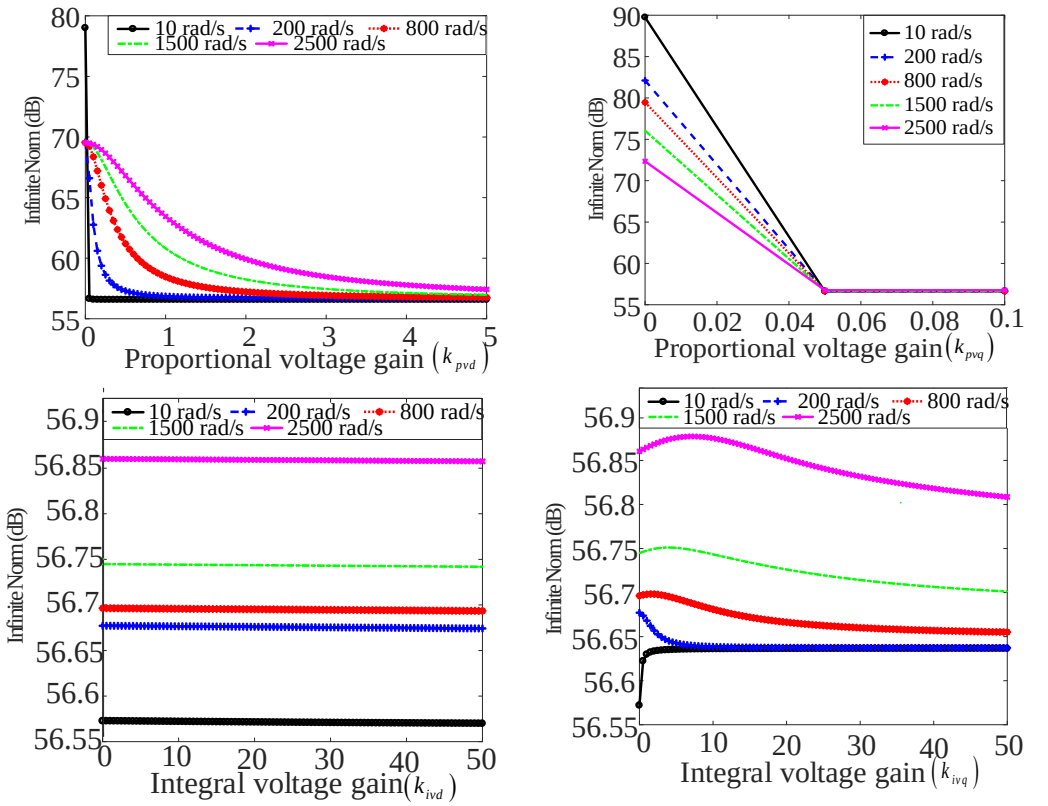

(a)

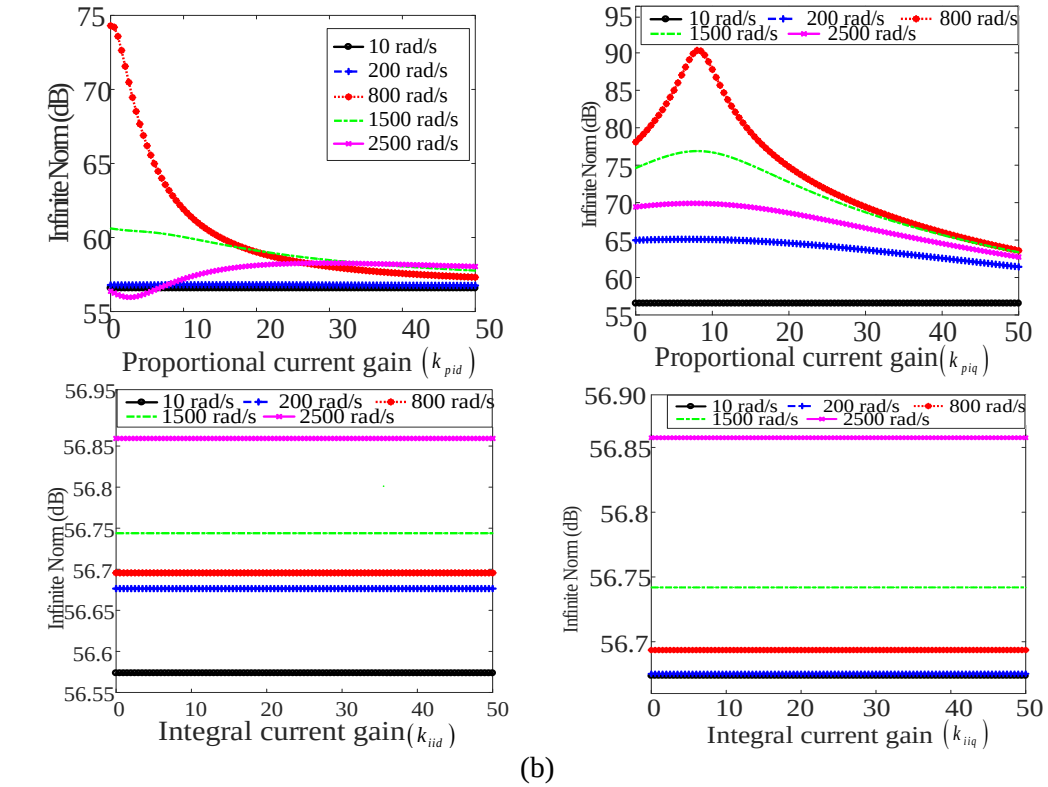

(b)

Figure 6.4. Relation between control parameters and stability criteria:

(a) Voltage control loop and (b) Current control loop.

6.3.2.1 Series virtual impedance (SVI)

The basic implementation of series impedance is to connect the virtual impedance between the STATCOM output current and the input voltage. However, the actual implementation is achieved by connecting the STATCOM output current to the reference voltage, as shown in Figure 6.5. For simplicity, the effect of the PLL is ignored. The effect virtual impedance is proposed to be as a diagonal matrix as shown in (6.3) which is chosen due to the large effect of STATACOM diagonal impedances on the norm of STATCOM impedance. Also, the effect of the implemented virtual impedance should be defined to be effective within the frequency range of interest otherwise equal to zero, as presented in equation (6.3). Limiting of the functionality of the virtual impedance can be achieved using low-pass and high-pass filters, or a second-order band-pass filter. The proposed SVI has the form:

$$Z_{seVir} = \begin{cases} \begin{bmatrix} \frac{Z_{Vir}}{G_{se}} & 0 \\ 0 & \frac{Z_{Vir}}{G_{se}} \end{bmatrix} & f \in [f_1, f_2] \\ 0 & f \notin [f_1, f_2] \end{cases} \tag{6.3}$$

where, f_1 and f_2 are the effective boundaries of the virtual impedance frequency range of interest.

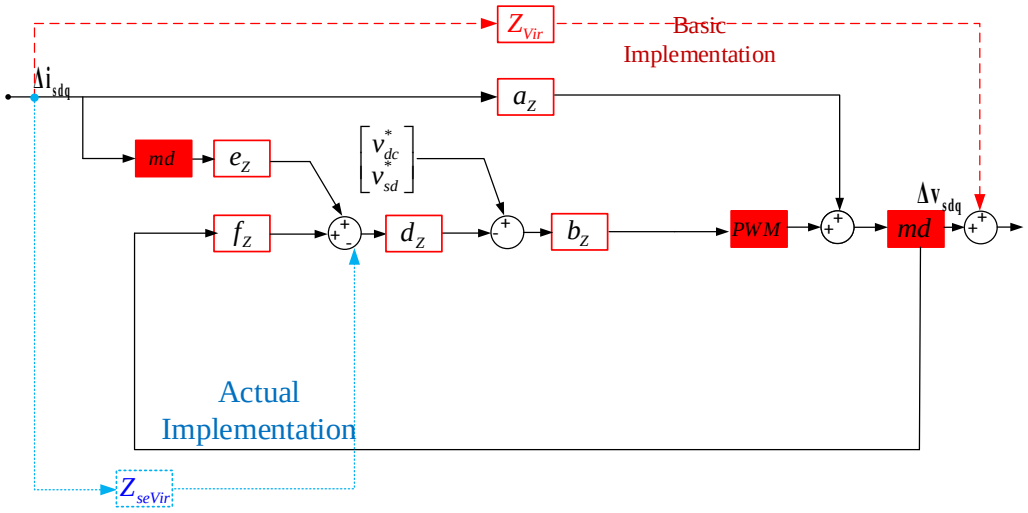

Figure 6.5. Implementation of series virtual impedance in STATCOM model.

The definition of the matrices in Figure 6.5 is found in Chapter 4. The transfer function (G_{se}) of the SVI denominator of the diagonal terms in equation (6.3) is derived with the help of Figure 6.5 gives:

$$G_{se} = d_Z . b_Z = -\begin{bmatrix} \frac{sC_{dc}v_{dc}^2 - \alpha_{dc}}{v_{dc}}\left(K_{pid} + \frac{K_{iid}}{s}\right) & 0 \\ 0 & \left(K_{piq} + \frac{K_{iiq}}{s}\right) \end{bmatrix} \tag{6.4}$$

Three types of virtual impedances (Z_{Vir}) are tested here to identify their relation to the STATCOM infinite norm. There are the purely resistance virtual impedance (SRI), the resistive-inductive virtual impedance (RLI) and the resistive-capacitive virtual impedance (RCI), which can be presented as:

$$Z_{Vir} = \begin{Bmatrix} R_v \\ R_v + SL_v \\ R_v + \frac{1}{SC_v} \end{Bmatrix} \tag{6.5}$$

In this study, the power frequency range is defined between 10 rad/s and 2500 rad/s, therefore the results are plotted at these frequencies. The impedance norms at other intermediate frequencies can be found by interpolating any bounded frequencies. The magnitudes of both inductance (L_v) and capacitance (C_v) are equal to the resistance magnitude (R_v) when plotting the relationships between the infinite norm and virtual impedances presented in Figure 6.6. Figure 6.6 parts (a) and (b) presents the effects of changing series-resistive virtual impedance and the series-capacitive virtual impedance on the STATCOM impedance infinite norm over a range of frequencies. Both impedances have insignificant effect on the STATCOM infinite norm. Alternatively, the increase of series resistive-inductive increases the infinite norms as shown in Figure 6.6(c), which worsen the stability of the system.

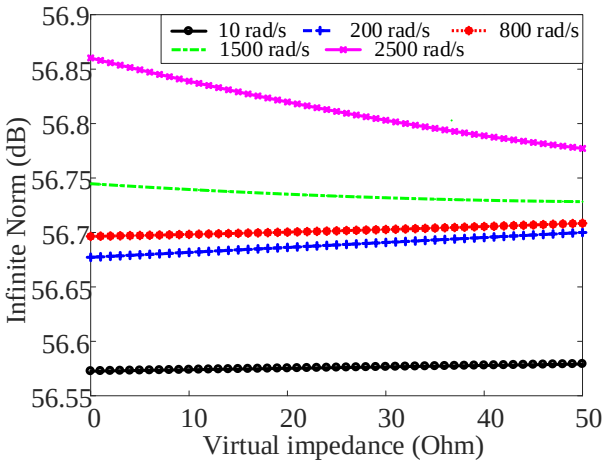

(a)

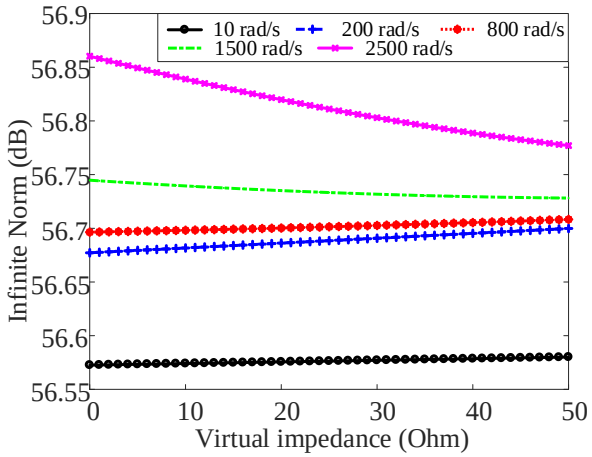

(b)

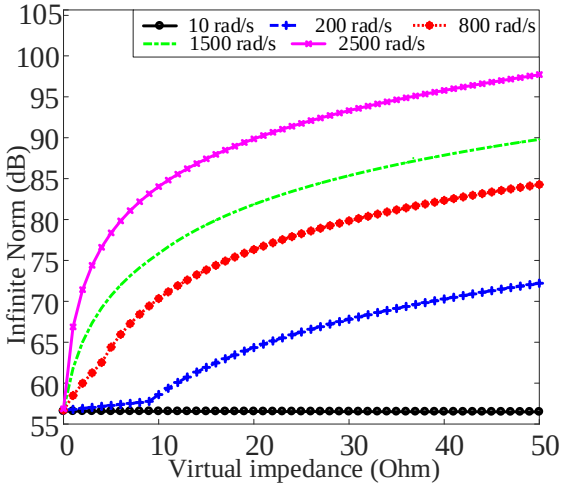

(c)

Figure 6.6. Effect of virtual impedance on stability norm at different perturbation frequencies:

(a)Series resistive, (b) Series resistive-capacitive and (c) Series resistive-inductive.

6.3.2.2 Shunt virtual impedance (SHVI)

Shunt virtual impedance is connected between the input voltage and the current reference to reduce the amount of current flow of the STATCOM and, consequently, reduce the total impedance of the STATCOM as shown by the dotted line in Figure 6.7. SHVI is proposed to react similarly to impedances in (6.3). The shunt virtual impedance is connected between the STATCOM output voltage and the input of STATCOM controller as shown in Figure 6.7. The same frequency boundaries as in (6.3) are applied to the shunt virtual impedance, as shown in Figure 6.7:

$$Z_{shVir} = \begin{cases} \begin{bmatrix} \frac{Z_{Vir}}{G_{se}} & 0 \\ 0 & \frac{Z_{Vir}}{G_{se}} \end{bmatrix} & f \in [f_1, f_2] \\ 0 & f \notin [f_1, f_2] \end{cases} \tag{6.6}$$

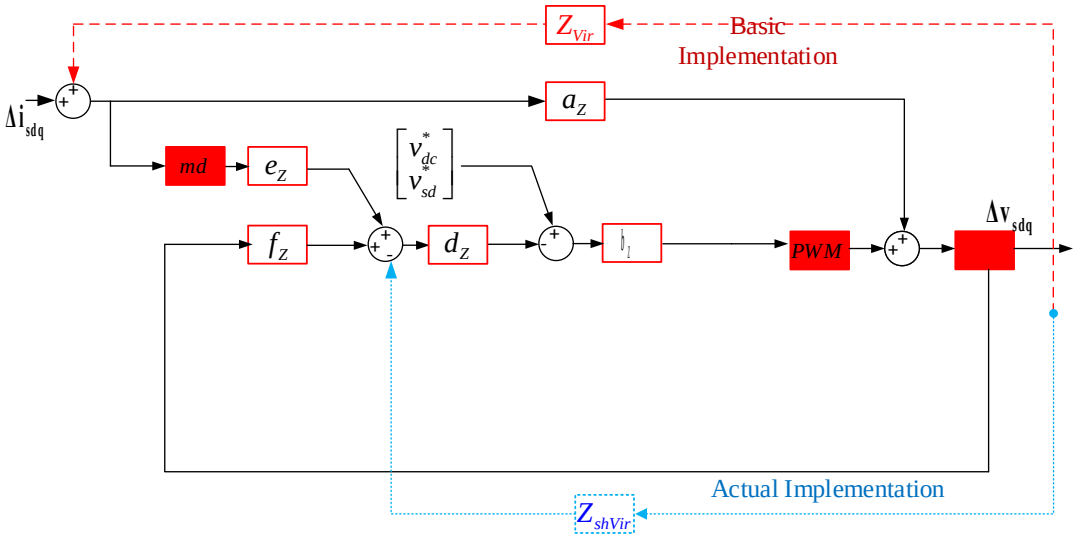

Figure 6.7. Implementation of shunt virtual impedance in STATCOM model.

Figure 6.8 presents the effects of shunt virtual impedances (SHVI) at different frequencies. Shunt resistive and shunt resistive-capacitive impedances have negative effect at all frequencies, as shown in Figure 6.8 parts (a) and (b). Both of the impedances are suitable for decreasing the infinite norm using the resistive and more sharply the resistive-capacitive, consequently, increase the stability margin according

to the stability criteria presented in chapter 4. Nevertheless, the shunt resistive and shunt resistive-capacitive impedances decrease the STATCOM norm; the inductive impedance has almost no effect on the infinite norm except at low frequencies as shown in Figure 6.8(c). In general, reducing the current using shunt connections is sufficient to reduce the STATCOM impedance; this is because of the nature of the STATCOM controller.

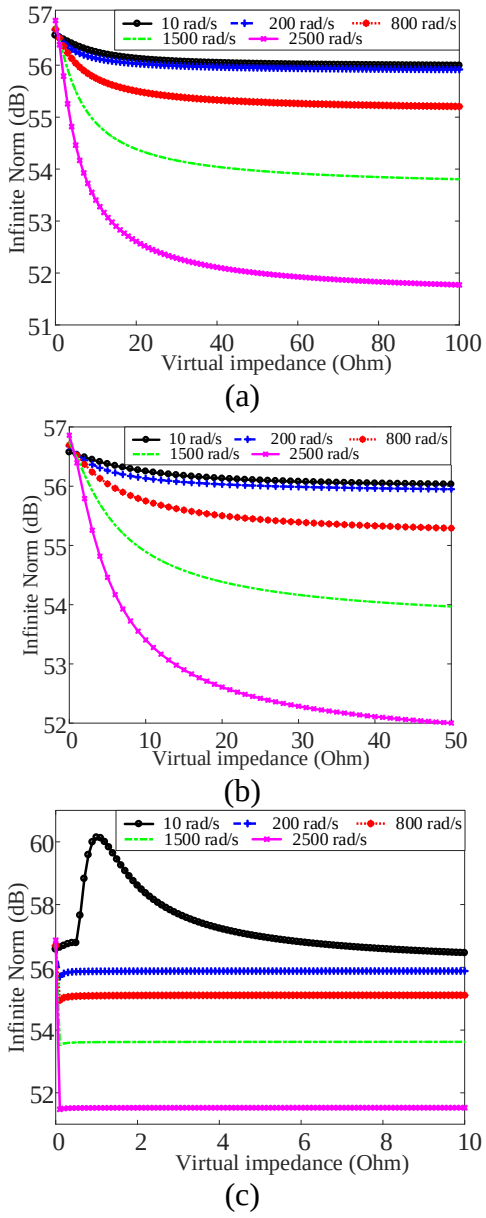

Figure 6.8. Shunt virtual impedance:

(a)Shunt resistive, (b) Shunt resistive-capacitive and (c) Shunt resistive-inductive.

To conclude, series virtual impedance has an adverse effect on the infinite norm of the STATCOM impedance matrix; whereas shunt connected virtual impedance demonstrates better performance. Changing the amount of resistive and resistive-capacitive virtual impedances can both increase and decrease the STATCOM infinite norms. The range over which these impedances may be varied should be limited to ensure the required response. The Nyquist plot has been done for four values of shunt resistive-capacitive virtual impedance (Z_{Vir} =[20, 30, 40, 50]) as shown in Figure 6.9. The effect of decreasing the infinite norm can be seen on the generalised Nyquist plot as a shrinking in the plot and moving it to the right-hand side (more stable system).

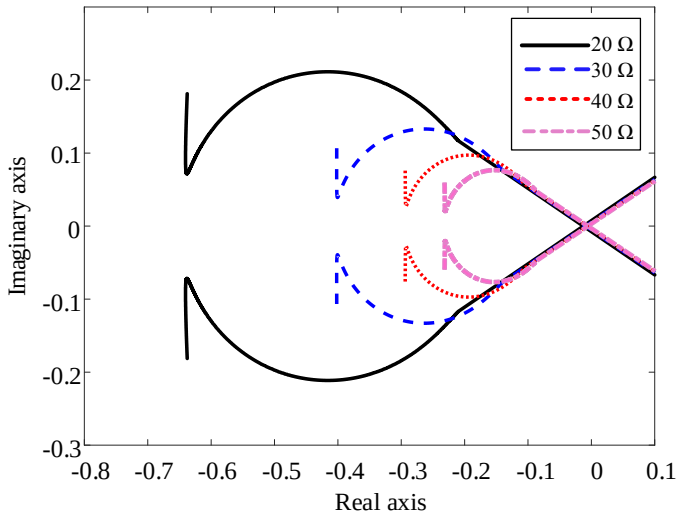

Figure 6.9. Nyquist plot of series resistive-capacitive impedance.

6.4 Improving the oscillatory response of series-compensated power network using SSSC

Power system oscillations such as sub-synchronous resonance (SSR) are caused by the undesirable interaction between the power network and the mechanical parts of generators. These oscillations cause a low-frequency variation in the systems [6]. Damping those oscillations is one of the main functions of the VSC-FACTS devices, especially the series connected devices such as static synchronous series compensator (SSSC). In this section, the stability of series compensated systems is

investigated and the effectiveness of different operating modes of SSSC on damping system oscillations is studied.

6.4.1 Dynamic performance of series compensated system

Figure 6.10 shows the series compensated system which contains a synchronous machine driven by a turbine system, and a transmission line connected to an infinite bus. The impedance based stability is utilised to assess the stability of the system at the generator terminals, where the system-side represents the transformer, transmission line and network admittance as well as the SSSC impedance. The parameters used for studying the sub-synchronous resonance (SSR) are listed in Table 6.4 for the series compensated network while the synchronous machine parameters can be found in Chapter 4. The selection of the test system parameters is chosen to ensure the existence of SSR frequency in the test system.

Table 6.4. Network parameters.

Base Power	500 MVA
Secondary side base voltage	500 kV
Primary side base voltage	22 kV
R_f, L_f	0.012, 0.180 pu
R_L, L_L	0.0202, 0.5157 pu
L_{sys}	1.148 pu

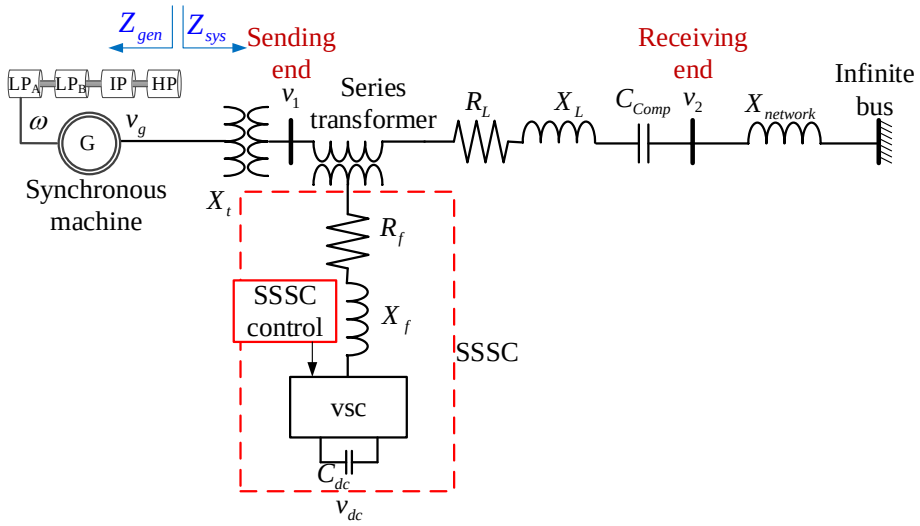

Figure 6.10. Series compensation system.

According to the parameters in Table 6.4, the natural frequency (f_n) at (20%) compensation which represents the oscillatory mode of the test system for example is equal to [91]:

$$f_n = f_0\sqrt{\frac{X_c}{X_L}} = 27 \text{ Hz}$$

So, the slip frequency which represents the difference between the fundamental frequency and the oscillatory mode frequency is:

Slip frequency = 60 – 27 = 33 Hz

The network impedance at different compensation levels is shown in Figure 6.11. The network compensation levels are studies at 20%, 40% and 80%. The network impedance has the same magnitude and phase at frequencies higher than 550 rad/s where the capacitive part of the network becomes small in comparison with the inductive part. The spikes in the impedance magnitude represent the oscillatory modes at different compensation levels of the power network. The 20% compensation level leads to an interaction between the synchronous machine and the compensated system.

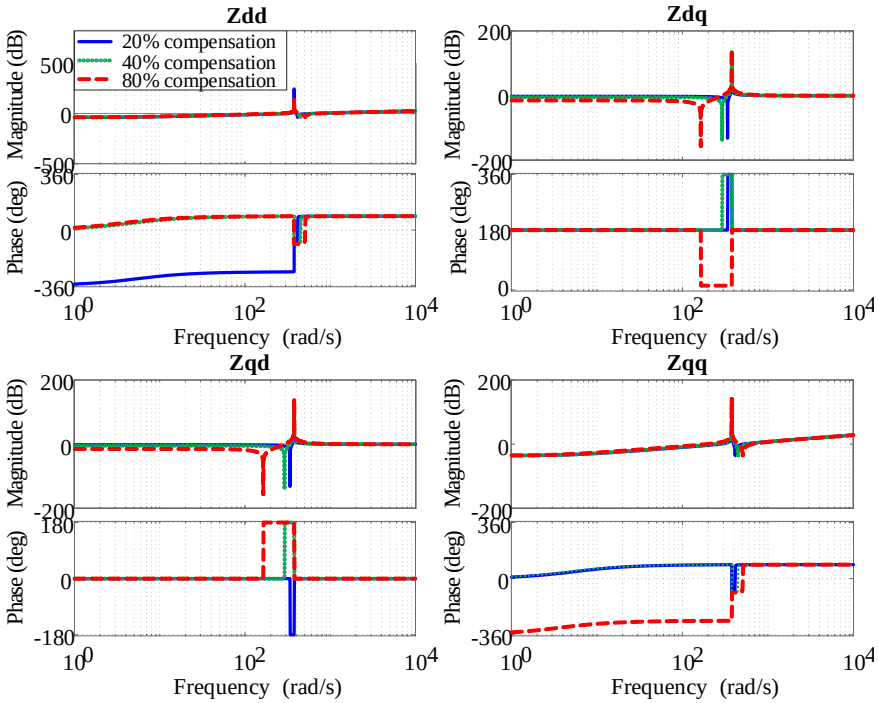

Figure 6.11. Network impedance at different compensation levels.

The synchronous machine output voltages, output currents and speed deviations of turbine masses are presented in Figure 6.12. It shows an increase of the oscillations in the currents and voltages due to the disturbances caused by the speed deviation which took about 30 s to settle down.

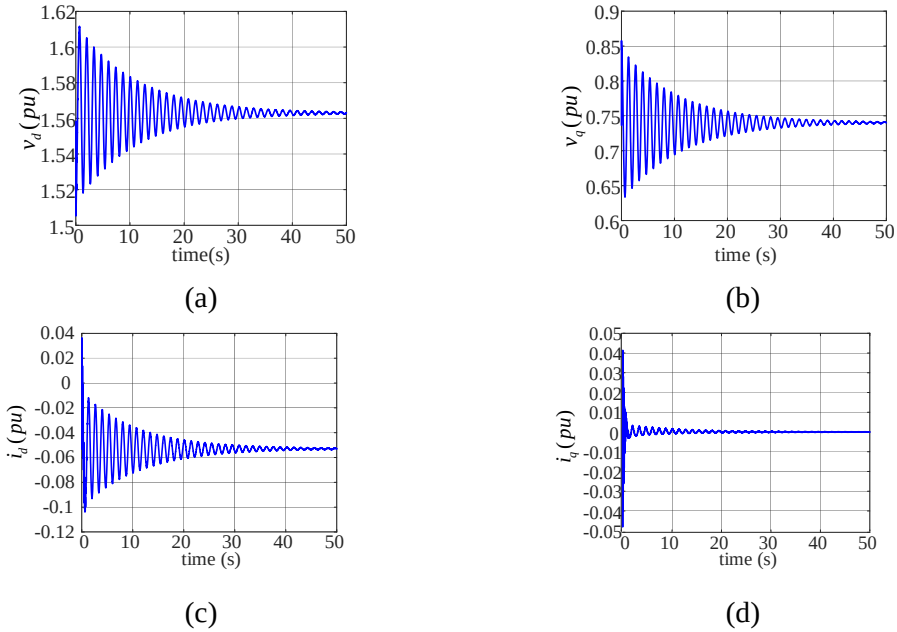

Figure 6.12. Synchronous machine measurements for series compensated system (20%): (a) Direct stator voltage (v_d), (b) Quadrature stator voltage (v_q), (c) Direct stator current (i_d), and (d) Quadrature stator current (i_q).

6.4.2 Effectiveness of SSSC on damping oscillations

The key function of the SSSC in steady-state application is to control the power flow in a transmission line by changing the line impedance. Alternatively, in dynamic control, it is to damp system oscillations [109]. The small signal impedance is utilised here to assess the effectiveness of different SSSC control modes on damping the oscillations. A series compensated network presented in Figure 6.10 is used to assess the effectiveness on damping the oscillations. The impedance at the interfacing point is calculated for the system side (Z_{sys}) and the generator side (Z_{gen}) as:

$$Z_{net} = (Z_t + Z_{SSSC} + Z_L + Z_{comp} + Z_{sys}) \tag{6.7}$$

$$Z_{SSSC} = \begin{bmatrix} Z_{dd} & Z_{dq} \\ Z_{qd} & Z_{qq} \end{bmatrix} \qquad Z_L = \begin{bmatrix} R_L + sL_L & -\omega L_L \\ \omega L_L & R_L + sL_L \end{bmatrix}$$

$$Z_{sys} = \begin{bmatrix} sL_{sys} & -\omega L_{sys} \\ \omega L_{sys} & sL_{sys} \end{bmatrix} \qquad Z_{comp} = \begin{bmatrix} sC_{comp} & -\omega C_{comp} \\ \omega C_{comp} & sC_{comp} \end{bmatrix}^{-1}$$

where,

Z_{net} is the network impedance.

Z_t is the transformer series impedance.

Z_{SSSC} is the SSSC impedance.

Z_L is the transmission line impedance.

Z_{comp} is the compensation impedance.

Z_{sys} is the rest of system impedance.

The transformer here is modelled using approximate circuit and equal to:

$$Z_t = \begin{bmatrix} R_t + sL_t & -\omega L_t \\ \omega L_t & R_t + sL_t \end{bmatrix}$$

In the meantime, the synchronous generator side impedance (Z_{gen}) which was derived in Chapter 4 is:

$$Z_{gen} = Z_{synch} \tag{6.8}$$

The performance of the SSSC is tested for voltage control mode on damping the SSR frequency of series compensated system at 20% compensation level. Using the generalised Nyquist plot, the system was unstable where the plot intersects at the left side of point (0, -1). However, the use of the SSSC improves the stability of the system and eliminates the oscillations as shown in Figure 6.13.

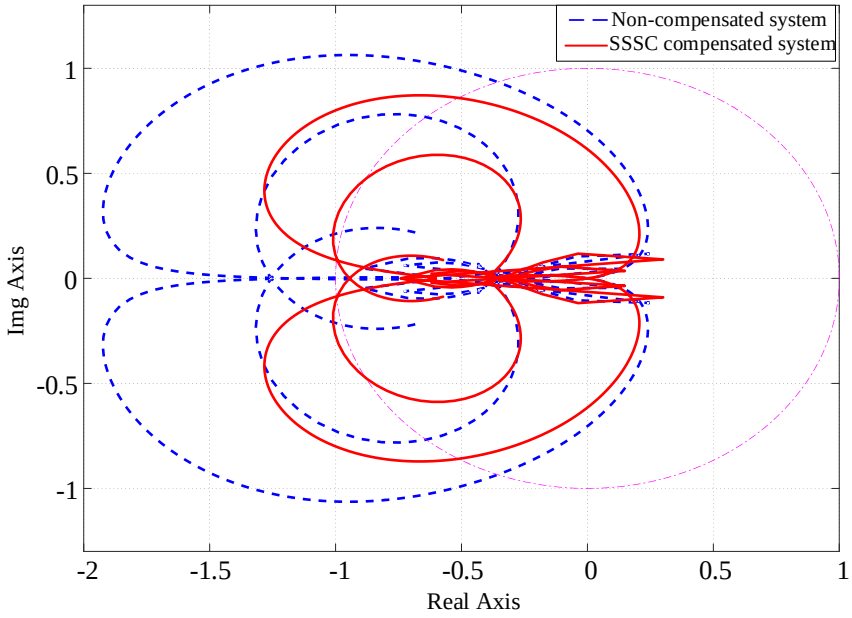

Figure 6.13. Generalised Nyquist plot of compensated and non-compensated system.

6.4.3 Comparison between SSSC control modes on damping oscillations

This section investigates the effectiveness of different control modes of SSSC on damping system oscillations. The SSSC improvement on damping the oscillation of a series compensated system is presented in Figure 6.14. It is clearly seen that all the control modes of the SSSC improve the performance of the system. However, the comparison between these modes is difficult in time domain. Therefore, the Nyquist plots of these control modes are shown in Figure 6.15 under the same operating conditions. The SSSC parameters are shown in Table 5.3, where the same settings for the three control modes are maintained for the comparison.

Table 6.5. SSSC control modes parameters.

Parameter	Value	Parameter	Value
R_f, L_f	0.5 Ω, 5 mH	K_{pvd}, K_{ivd}	-0.1 V/A, -0.05 V/A.s
R_{se}, L_{se}	15.60 Ω, 70 mH	K_{pvq}, K_{ivq}	-0.08 V/A, 0.05 V/A.s
C_{dc}	800 µF	v_{seq}	170 V
v_{dc}	1000 V		

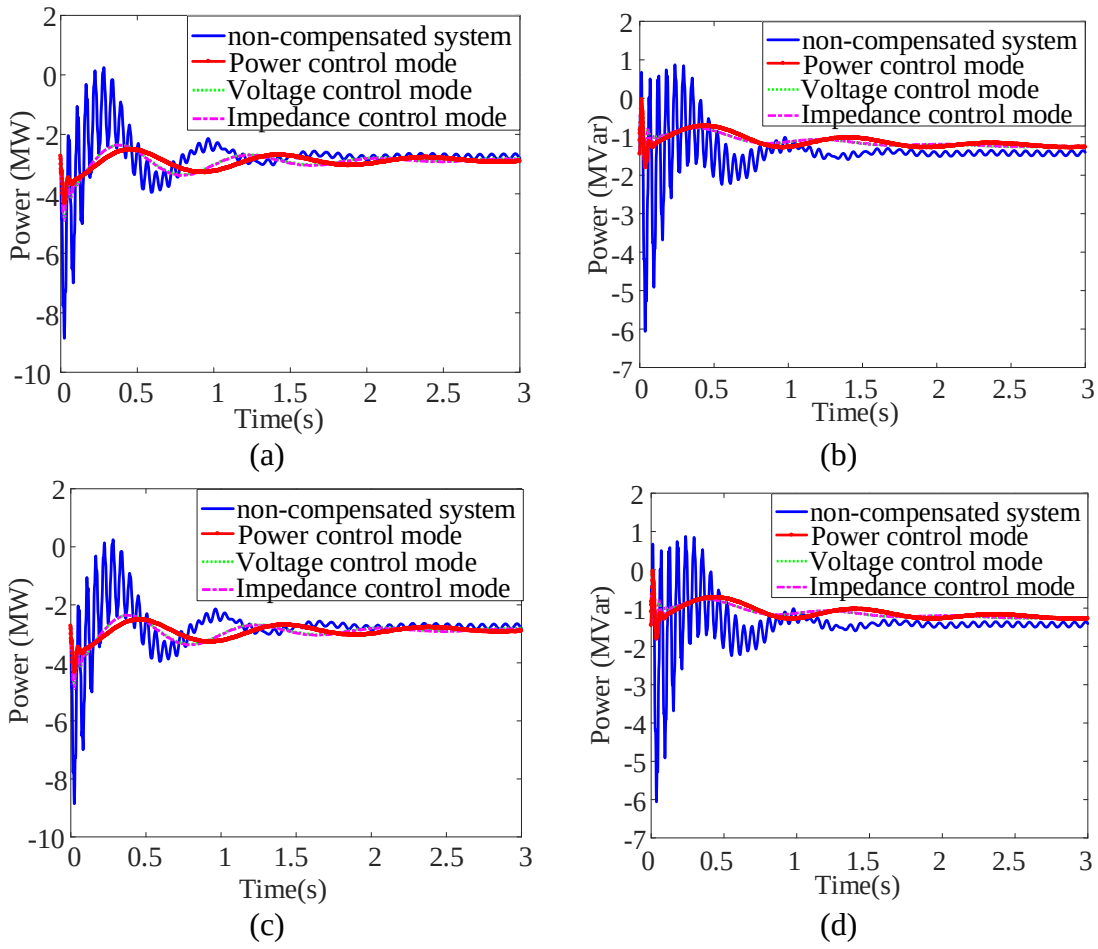

Figure 6.14. Time-domain plots of active and reactive powers of the system:

(a) Active power-sending end, (b) Reactive power-sending end, (c) Active power-receiving end and (d) Reactive power- receiving end.

It is concluded from Figure 6.15 that the impedance control mode introduces more stable system in comparison with the voltage and power control modes. Alternatively, the power control mode shows less effective characteristics on stabilising the system compared to the other methods.

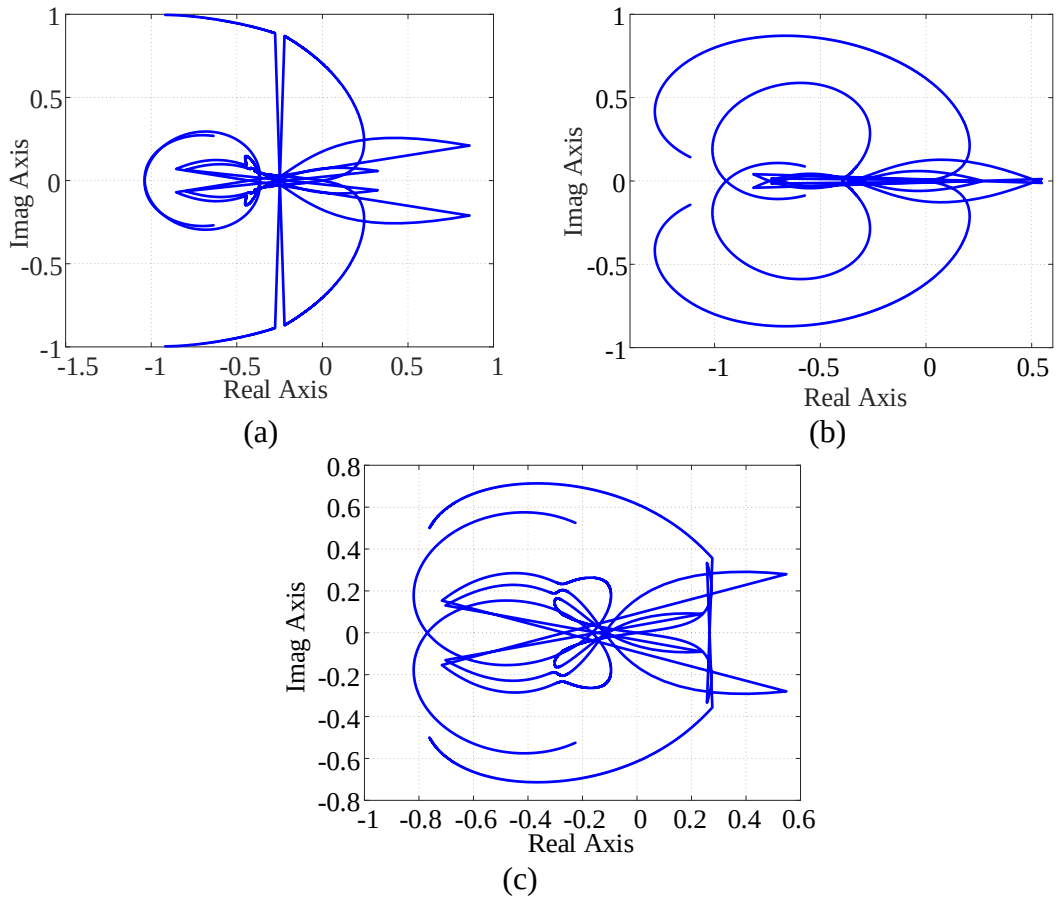

Figure 6.15. Nyquist plot of SSSC control modes:

(a) Power control mode, (b) Voltage control mode and (c) Impedance control mode.

6.5 Summary

In this chapter, monitoring, controlling and improving the stability were presented. In the monitoring section, a fast impedance measurement unit (IMU) was proposed to facilitate an effective stability monitoring by the network operators. Changing the VSC-FACTS device parameters as well as the virtual impedance on the stability was examined. Lastly, the performance of the VSC-FACTS device on improving the stability of series compensated system was investigated. The following can be summarised from this chapter:

- Using a small number of frequencies to estimate the system impedance ensures fast performance of the impedance measurement unit (IMU).
- The measurement time of the proposed IMU is based on the response of the network and the accuracy required.

- Several challenges face the development of a control system based on impedance such as the suitable stability criteria and power quality level of the networks.
- Controlling the impedance using device's parameters could be limited by the operating constraints of the device and its capability to effectively control the stability.
- Generally, the series virtual impedance has an adverse effect on the infinite norm of the STATCOM impedance matrix; whereas shunt connected virtual impedance demonstrates better performance.
- Even though the time domain plot of active and reactive powers of the compensated system looks similar for the three control modes of SSSC, the impedance control mode shows more effective performance in comparison with other control modes as indicated by the generalised Nyquist plot.

CHAPTER 7

CONCLUSIONS AND FUTURE WORK

7.1 General conclusions

The increase in the number of installed VSC-FACTS in power system has increased the efforts needed to model these systems, especially when modelling transient response or the contribution of harmonics on the systems. Studying system's stability depends on deriving their mathematical models which are distinguished in accuracy and complexity. Conventional modelling techniques such as synchronous dq modelling and $\alpha\beta$ modelling are usually employed to identify the causes of the harmonics, while, the harmonic linearization method and harmonic state space are used to present the effect of these harmonics on the systems. In this thesis, the use of dq-dynamic phasor in stability assessment was proposed. The dq-dynamic phasor has the capability to include harmonics and suits the linearization required for small signal stability studies. The basics of modelling in dq-dynamic phasor and how to model some of power components were presented in Chapter 3. It was shown that modelling using dq-dynamic phasor at the fundamental frequency was equal to the synchronous dq modelling. Also, the chapter presented the capability of dq-dynamic phasor on modelling balanced and unbalanced responses of the systems. A derivation of some VSC-FACTS devices in synchronous dq coordinates was presented in Chapter 4. The state space and impedance models of STATCOM controlled with voltage control model and reactive power control model were presented. Similarly, the SSSC models were derived for three control modes, power control mode, voltage control mode and impedance control mode. The SSSC with power control mode appeared different impedance in comparison with the other control modes. Also, the effects of different sections of synchronous machine and its driving system on the impedance were presented. The inclusion of the mechanical section was seen at low frequency while it disappeared at high frequencies. A state space and impedance

models where proposed based on dq-dynamic phasor for the STATCOM and the SSSC in Chapter 5. The models were sufficient to include the harmonics for stability analysis and identify the unbalanced operation based on frequency coupling. The proposed models were linearized around a steady state point where the dq-dynamic phasor parameters are linear time invariant which reduces the linearization errors in comparison with other modelling techniques. Using the proposed modelling, the unbalanced operation was appeared as a displacement of the eigenvalues in state space analysis and as an unmatched plot of positive and negative impedances in impedance analysis. The effect of harmonic coupling on the VSC-FACTS operation was obvious for the STATCOM and was limited for the SSSC depending on the complexity of their control systems. An impedance measurement unit (IMU) was proposed in Chapter 6 for fast monitoring applications. The IMU was developed based on the FFT analysis using a multi-tone signal. The validity of the proposed IMU was carried out by comparing the results with time domain measurements. The accuracy of this measurement unit depends on the measurement time and the time delay of the measured system. It discussed the effect of different control parameters and virtual impedance on the system stability. Also, the chapter presented the efficiency of SSSC control modes on damping system oscillations and the effect of different parts of synchronous machine on stability. MATLAB-SIMULINK simulations results demonstrated the validity of the proposed models in synchronous dq and dq-dynamic phasor modelling as well as the effectiveness of the impedance measurement unit.

7.2 Author's contributions

This thesis focused on the modelling of VSC-FACTS devices for small signal stability studies including the effects of harmonics and unbalance. The thesis contributions can be summarised as follows:

- STATCOM and SSSC dq-dynamic phasor state space and impedance models for small signal stability analysis have been proposed which can include harmonics and can also be linearized around steady state point.

- An identification method of unbalanced operation of VSC-FACTS devices depending on the frequency coupling in the negative sequence harmonic has been proposed.
- A new impedance measurement unit (IMU) based on a multi-tone signal has been proposed. It could be used to monitor the short circuit ratio (SCR) in weak grids.
- The direct relationship between the control parameters of the STATCOM and the stability criterion has been revealed for fast stability control. Also, the effect of including different types of virtual impedance on stability criteria has been investigated.
- The effectiveness of SSSC control modes on damping system oscillations using small signal impedance for series compensated system has been investigated and evaluated.
- The effect of electrical and mechanical parts of the synchronous machine on the impedance the machine has been presented. It shows the importance of including the turbine dynamic at frequencies below the fundamental frequency.

7.3 Recommendations for future work

The work presented in this thesis is mainly focused on the development of mathematical models for investigating the small signal stability of VSC-FACTS devices. In order to further evaluate the effectiveness and performance of the presented work, some possible areas of interest for future work are:

- Validate the derived dq-dynamic phasor model of VSC-FACTS devices using experimental tests when the harmonics co-exist. The number of harmonics that should be included can be identified by the frequency scanning of most effective harmonics in the analysis.
- Compare the effectiveness of the proposed method with other modelling techniques such as multi-coordinate synchronous dq, harmonic linearization method and harmonic state space method.
- Use the proposed method to design harmonic filters, robust control systems and analyse the unbalanced operation of power system devices.

- Use the proposed model on damping system oscillations' design which can be used to present the improvements in reducing the harmonics effect and their participation on the system performance.
- Build control system-based impedance for controlling the stability which can be used to have an auto-tuning devices: such a control system can be built if the mathematical relationship between the device's impedance and the stability is clear. As well as the mentioned challenges presented in this thesis have been resolved.

7.4 Publications

- K. Abojlala, D. Holliday and L. Xu, "Transient analysis of an interline dynamic voltage restorer using dynamic phasor representation," *2016 IEEE 17th Workshop on Control and Modeling for Power Electronics (COMPEL)*, Trondheim, 2016, pp. 1-7.
- K. Abojlala, D. Holliday and L. Xu, "Stability norms control using the virtual impedance concept for power frequency applications," *2017 International Symposium on Power Electronics (Ee)*, Novi Sad, 2017, pp. 1-6.
- K. Abojlala, G. P. Asad, K. Ahmed, D. Holliday and L. Xu " Generalised dq-dynamic phasor modelling of STATCOM connected to a grid for stability analysis", 2018, (submitted to IET Power Electronics).

BIBLIOGRAPHY

[1] M. Hwang and A. Wood, "A new modelling framework for power supply networks with converter based loads and generators-the Harmonic State-Space," *IEEE Int. Conf. Power Syst. Technol.*, pp. 1–6, 2012.

[2] I. Power and E. Society, *IEEE Guide for Application of Power Electronics for Power Quality Improvement on Distribution Systems Rated 1 kV Through 38 kV*, no. April. 2012.

[3] M. Amin and M. Molinas, "Small-Signal Stability Assessment of Power Electronics Based Power Systems: A Discussion of Impedance-and Eigenvalue-Based Methods," *IEEE Trans. Ind. Appl.*, vol. 53, no. 5, pp. 5014–5030, 2017.

[4] L. Wang and D. N. Truong, "Dynamic stability improvement of four parallel-operated PMSG-based offshore wind turbine generators fed to a power system using a STATCOM," *IEEE Trans. Power Deliv.*, vol. 28, no. 1, pp. 111–119, 2013.

[5] N. Kumar, T. R. Chelliah, and S. P. Srivastava, "Voltage sag effects on energy-optimal controlled induction motor with time-varying loads," *PEDES 2012 - IEEE Int. Conf. Power Electron. Drives Energy Syst.*, 2012.

[6] N. Prabhu, M. Janaki, and R. Thirumalaivasan, "Damping of subsynchronous resonance by subsynchronous current injector with STATCOM," *IEEE Reg. 10 Annu. Int. Conf. Proceedings/TENCON*, pp. 1–6, 2009.

[7] X. Wang, F. Blaabjerg, and W. Wu, "Modeling and analysis of harmonic stability in an AC power-electronics- based power system," *IEEE Trans. Power Electron.*, vol. 29, no. 12, pp. 6421–6432, 2014.

[8] Y. Shujun, B. Mingran, H. Minxiao, H. Junxian, and W. Lei, "Modeling for VSC-HVDC Electromechanical Transient Based on Dynamic Phasor Method," *2nd IET Renew. Power Gener. Conf. (RPG 2013)*, p. 2.58-2.58,

2013.

[9] A. E. Leon and J. A. Solsona, “Sub-synchronous interaction damping control for DFIG wind turbines,” *IEEE Trans. Power Syst.*, vol. 30, no. 1, pp. 419–428, 2015.

[10] A. Moharana and R. K. Varma, “Subsynchronous resonance in single-cage self-excited-induction-generator-based wind farm connected to series-compensated lines,” *IET Gener. Transm. Distrib.*, vol. 5, no. 12, pp. 1221–1232, 2011.

[11] V. Jalili-Marandi, V. Dinavahi, K. Strunz, J. A. Martinez, and A. Ramirez, “Interfacing techniques for transient stability and electromagnetic transient programs: IEEE task force on interfacing techniques for simulation tools,” *IEEE Trans. Power Deliv.*, vol. 24, no. 4, pp. 2385–2395, 2009.

[12] T. Demiray and G. Andersson, “Simulation of power system dynamics using dynamic phasor models,” *Xth Symp. Spec. Electr. Oper. Expans. Plan.*, p. 9, 2006.

[13] T. Demiray and G. Andersson, “Comparison of the efficiency of dynamic phasor models derived from abc and dq0 reference frame in power system dynamic simulations,” *7th IEE Conf. Adv. Power Syst. Control. Oper. Manag. Hong Kong*, p. 8, 2006.

[14] D. A. Copp, F. Wilches-Bernal, I. Gravagne, and D. A. Schoenwald, “Time-domain analysis of power system stability with damping control and asymmetric feedback delays,” in *2017 North American Power Symposium (NAPS)*, 2017, pp. 1–6.

[15] D. Povh, P. Thepparat, and D. Westermann, “Further development of HVDC control,” in *2011 IEEE Trondheim PowerTech*, 2011, pp. 1–8.

[16] P. Mattavelli, “Ssr analysis with dynamic phasor model of thyristor-controlled series capacitor,” *IEEE Trans. Power Syst.*, vol. 14, no. 1, pp. 200–208, 1999.

[17] R. H. Park, “Two-Reaction Theory of Synchronous Machine - Generalized Method of Analysis,” *AIEE Transactions*, vol. 48. pp. 716–727, 1929.

[18] S. Skogestad, I. Postelthwaite, I. Postlethwaite, I. P. Sigurd Skogestad, and I. Postelthwaite, *Multivariable feedback control: analysis and design*, vol. 8, no. 14. John Wiley, 2005.

[19] E. Ebrahimzadeh, F. Blaabjerg, X. Wang, and C. L. Bak, "Modeling and identification of harmonic instability problems in wind farms," *ECCE 2016 - IEEE Energy Convers. Congr. Expo. Proc.*, pp. 1–6, 2016.

[20] M. Amin, A. Rygg, and M. Molinas, "Impedance-based and eigenvalue based stability assessment compared in VSC-HVDC system," in *ECCE 2016 - IEEE Energy Conversion Congress and Exposition, Proceedings*, 2016, pp. 1–8.

[21] H. Liu, X. Xie, Y. Li, H. Liu, and Y. Hu, "A small-signal impedance method for analyzing the SSR of series-compensated DFIG-based wind farms," *IEEE Power Energy Soc. Gen. Meet.*, vol. 2015–Septe, 2015.

[22] Y. Liao, S. Member, Z. Liu, S. Member, G. Zhang, and C. Xiang, "Vehicle-Grid System Stability Analysis Considering Impedance Specification Based on Norm Criterion," pp. 118–123, 2016.

[23] C. Li, R. Burgos, Y. Tang, and D. Boroyevich, "Impedance-based stability analysis of multiple STATCOMs in proximity," in *2016 IEEE 17th Workshop on Control and Modeling for Power Electronics, COMPEL 2016*, 2016, pp. 1–6.

[24] B. Wen, D. Boroyevich, P. Mattavelli, R. Burgos, and Z. Shen, "Modeling the output impedance negative incremental resistance behavior of grid-tied inverters," in *Conference Proceedings - IEEE Applied Power Electronics Conference and Exposition - APEC*, 2014, pp. 1799–1806.

[25] F. Feng, F. Wu, and H. B. Gooi, "Small Signal Impedance Model and Stability Analysis of Bidirectional Two-Stage DC-DC-AC System," *2017 IEEE 3rd Int. Futur. Energy Electron. Conf. ECCE Asia (IFEEC 2017 - ECCE Asia)*, pp. 1817–1821, Jun. 2017.

[26] B. Wen, D. Dong, D. Boroyevich, R. Burgos, P. Mattavelli, and Z. Shen, "Impedance-based analysis of grid-synchronization stability for three-phase

paralleled converters," *IEEE Trans. Power Electron.*, vol. 31, no. 1, pp. 26–38, Jan. 2016.

[27] H. Yang and H. Nian, "Stability analysis of grid-connected converter based on interconnected system impedance modeling under unbalanced grid conditions," *2014 17th Int. Conf. Electr. Mach. Syst. ICEMS 2014*, pp. 2631–2636, 2015.

[28] Y. Huang, X. Yuan, J. Hu, and P. Zhou, "Modeling of VSC Connected to Weak Grid for Stability Analysis of DC-Link Voltage Control," *IEEE J. Emerg. Sel. Top. Power Electron.*, vol. 3, no. 4, pp. 1193–1204, 2015.

[29] W. C. Duesterhoeft, M. W. Schulz, and E. Clarke, "Determination of Instantaneous Currents and Voltages by Means of Alpha, Beta, and Zero Components," *Trans. Am. Inst. Electr. Eng.*, vol. 70, no. 2, pp. 1248–1255, Jul. 1951.

[30] X. Wang, L. Harnefors, and F. Blaabjerg, "Unified Impedance Model of Grid-Connected Voltage-Source Converters," *IEEE Trans. Power Electron.*, vol. 33, no. 2, pp. 1775–1787, 2018.

[31] M. Cespedes and J. Sun, "Impedance modeling and analysis of grid-connected voltage-source converters," *IEEE Trans. Power Electron.*, vol. 29, no. 3, pp. 1254–1261, Mar. 2014.

[32] M. K. Bakhshizadeh, X. Wang, F. Blaabjerg, J. Hjerrild, L. Kocewiak, C. L. Bak, and B. Hesselbak, "Couplings in Phase Domain Impedance Modeling of Grid-Connected Converters," *IEEE Trans. Power Electron.*, vol. 31, no. 10, pp. 6792–6796, 2016.

[33] A. Rygg, M. Molinas, C. Zhang, and X. Cai, "A Modified Sequence-Domain Impedance Definition and Its Equivalence to the dq-Domain Impedance Definition for the Stability Analysis of AC Power Electronic Systems," *IEEE J. Emerg. Sel. Top. Power Electron.*, vol. 4, no. 4, pp. 1383–1396, 2016.

[34] X. Wang and F. Blaabjerg, "Harmonic Stability in Power Electronic Based Power Systems: Concept, Modeling, and Analysis," *IEEE Trans. Smart Grid,*

vol. 3053, no. c, pp. 1–12, 2018.

[35] J. Lyu, X. Cai, and M. Molinas, “Impedance modeling of modular multilevel converters,” *IECON 2015 - 41st Annu. Conf. IEEE Ind. Electron. Soc.*, pp. 180–185, Nov. 2015.

[36] H. Liu and J. Sun, “Modeling and analysis of DC-link harmonic instability in LCC HVDC systems,” *2013 IEEE 14th Work. Control Model. Power Electron. COMPEL 2013*, no. Lcc, 2013.

[37] T. Li, A. M. Gole, and C. Zhao, “Harmonic Instability in MMC-HVDC Converters Resulting from Internal Dynamics,” *IEEE Trans. Power Deliv.*, vol. 31, no. 4, pp. 1738–1747, 2016.

[38] Y. Wang, X. Chen, Y. Zhang, J. Chen, and C. Gong, “Impedance modeling of three-phase grid-connected inverters and analysis of interaction stability in grid-connected system,” in *2016 IEEE 8th International Power Electronics and Motion Control Conference, IPEMC-ECCE Asia 2016*, 2016, pp. 3606–3612.

[39] Y. Cen, M. Huang, and X. Zha, “Modeling method of sequence admittance for three-phase voltage source converter under unbalanced grid condition,” *J. Mod. Power Syst. Clean Energy*, vol. 6, no. 3, pp. 595–606, 2018.

[40] S. Filizadeh and A. M. Gole, “Harmonic Performance Analysis of an OPWM-Controlled STATCOM in Network Applications,” *IEEE Trans. Power Deliv.*, vol. 20, no. 2, pp. 1001–1008, Apr. 2005.

[41] R. Z. Scapini, L. V. Bellinaso, and L. Michels, “Stability analysis of half-bridge rectifier employing LTP approach,” *IECON Proc. (Industrial Electron. Conf.*, pp. 780–785, 2012.

[42] N. M. Wereley and S. R. Hall, “Frequency response of linear time periodic systems,” *Proc. 29th IEEE Conf. Decis. Control*, vol. 6, pp. 3650–3655, 1990.

[43] İ. Uyanık, M. M. Ankaralı, N. J. Cowan, Ö. Morgül, and U. Saranlı, “Identification of a Hybrid Spring Mass Damper via Harmonic Transfer Functions as a Step Towards Data-Driven Models for Legged Locomotion,”

Jan. 2015.

[44] J. B. Kwon, X. Wang, F. Blaabjerg, and C. L. Bak, “Precise model analysis for 3-phase high power converter using the Harmonic State Space modeling,” *2015 9th Int. Conf. Power Electron. ECCE Asia (ICPE-ECCE Asia)*, pp. 2628–2635, 2015.

[45] V. Salis, A. Costabeber, S. M. Cox, and P. Zanchetta, “Stability assessment of power-converter-based AC systems by LTP theory: Eigenvalue analysis and harmonic impedance estimation,” *IEEE J. Emerg. Sel. Top. Power Electron.*, vol. 5, no. 4, pp. 1513–1525, 2017.

[46] W. Xu, J. E. Drakos, Y. Mansour, A. Chang, and B. C. Hydro, “A three-phase converter model for harmonic analysis of HVDC systems,” *IEEE Trans. Power Deliv.*, vol. 9, no. 3, pp. 1724–1731, 1994.

[47] J. Kwon, X. Wang, F. Blaabjerg, C. L. Bak, V. S. Sularea, and C. Busca, “Harmonic Interaction Analysis in a Grid-Connected Converter Using Harmonic State-Space (HSS) Modeling,” *IEEE Trans. Power Electron.*, vol. 32, no. 9, pp. 6823–6835, 2017.

[48] W. Yao, J. Wen, and S. Cheng, “Modeling and simulation of VSC-HVDC with dynamic phasors,” *Istanbul Univ. - J. Electr. Electron. Eng.*, vol. 8, no. 2, pp. 715–724, 2008.

[49] K. W. C. M.A. Hannan, “Transient analysis of FACTS and custom power devices using phasor dynamics,” *J. Appl. Sci.*, pp. 1074–1081, 2006.

[50] W. Gang, L. Zhikeng, L. Haifeng, L. Xiaolin, and F. Chuang, “Modeling of the HVDC convertor using dynamic phasor under asymmetric faults in the AC system,” *1st Int. Conf. Sustain. Power Gener. Supply, SUPERGEN ’09*, no. 2, pp. 1–5, 2009.

[51] H. Sun, X. Yang, X. Wang, and J. Sun, “Improved dynamic phasor model of HVDC system for subsynchronous oscillation study,” in *DRPT 2011 - 2011 4th International Conference on Electric Utility Deregulation and Restructuring and Power Technologies*, 2011, no. 50807036, pp. 485–489.

[52] H. Zhu, Z. Cai, H. Liu, Q. Qi, and Y. Ni, “Hybrid-model transient stability simulation using dynamic phasors based HVDC system model,” *Electr. Power Syst. Res.*, vol. 76, no. 6–7, pp. 582–591, 2006.

[53] Q. Qi, C. Yu, C. K. Wai, and Y. Ni, “Modeling and simulation of a STATCOM system based on 3-level NPC inverter using dynamic phasors,” *IEEE Power Eng. Soc. Gen. Meet. 2004.*, vol. 2, pp. 1559–1564, 2004.

[54] M. A. Hannan, A. Mohamed, and A. Hussain, “Modeling and power quality analysis of STATCOM using phasor dynamics,” *2008 IEEE Int. Conf. Sustain. Energy Technol. ICSET 2008*, pp. 1013–1018, 2008.

[55] H. Zhu, Z. Cai, H. Liu, Y. Ni, and S. Member, “Multi-infeed HVDC / AC power system modeling and analysis with dynamic phasor application,”,2005 IEEE/PES Transmission & Distribution Conference & Exposition: Asia and Pacific, pp. 1–6, 2005.

[56] M. a Hannan, A. Mohamed, S. Member, a Hussain, and M. Ieee, “Dynamic Phasor Modeling and EMT Simulation of USSC,” *October*, vol. I, pp. 1–7, 2009.

[57] H. Liu, H. Zhu, Y. Li, and Y. Ni, “Including UPFC Dynamic Phasor Model into Transient Stability Program,” *IEEE Power Engineering Society General Meeting, 2005*, San Francisco, CA, 2005, pp. 302-307 Vol. 1.

[58] M. A. A. Hannan, A. Mohamed, A. Hussain, and M. AI-Dabbagh, “Power quality analysis of STATCOM using dynamic phasor modeling,” *Electr. Power Syst. Res.*, vol. 79, no. 6, pp. 993–999, 2009.

[59] A. M. Stanković, P. Mattavelli, V. Caliskan, G. C. C. Verghese, a. M. Stankovic, P. Mattavelli, V. Caliskan, and G. C. C. Verghese, “Modeling and analysis of FACTS devices with dynamic phasors,” *2000 IEEE Power Eng. Soc. Conf. Proc.*, vol. 2, pp. 1440–1446, 2000.

[60] P. C. Stefanov and A. M. Stankovic, “Modeling of UPFC operation under unbalanced conditions with dynamic phasors,” *IEEE Trans. Power Syst.*, vol. 17, no. 2, pp. 395–403, 2002.

[61] C. Liu, A. Bose, and P. Tian, “Modeling and analysis of HVDC converter by three-phase dynamic phasor,” *IEEE Trans. Power Deliv.*, vol. 29, no. 1, pp. 3–12, 2014.

[62] S. R. Sanders, J. M. Noworolski, X. Z. Liu, and G. C. Verghese, “Generalized Averaging Method for Power Conversion Circuits,” *IEEE Trans. Power Electron.*, vol. 6, no. 2, pp. 333–340, 1991.

[63] M. Parimi, M. Monika, M. Rane, S. Wagh, and A. Stankovic, “Dynamic phasor-based small-signal stability analysis and control of solid state transformer,” *2016 IEEE 6th Int. Conf. Power Syst. ICPS 2016*, 2016.

[64] M. C. Chudasama and A. M. Kulkarni, “Dynamic phasor analysis of SSR mitigation schemes based on passive phase imbalance,” *IEEE Trans. Power Syst.*, vol. 26, no. 3, pp. 1668–1676, 2011.

[65] L. Piyasinghe, Z. Miao, J. Khazaei, L. Fan, J. Khazaei, L. Fan, “Impedance model-based SSR analysis for TCSC compensated type-3 wind energy delivery systems,” *IEEE Trans. Sustain. Energy*, vol. 6, no. 1, pp. 179–187, Jul. 2015.

[66] S. Chandrasekar and R. Gokaraju, “Dynamic Phasor Modeling of Type 3 DFIG Wind Generators (Including SSCI Phenomenon) for Short-Circuit Calculations,” *IEEE Trans. Power Deliv.*, vol. 30, no. 2, pp. 887–897, 2015.

[67] Y. Familiant, K. Corzine, J. Huang, and M. Belkhayat, “AC Impedance Measurement Techniques,” *IEEE Int. Conf. Electr. Mach. Drives, 2005.*, pp. 1850–1857, 2005.

[68] Z. Shuai, Y. Peng, J. M. Guerrero, Y. Li, and J. Z. Shen, “Transient Response Analysis of Inverter-based Microgrids under Unbalanced Conditions using Dynamic Phasor Model,” *IEEE Trans. Ind. Electron.*, vol. 0046, no. c, pp. 1–11, 2018.

[69] Y. Familiant and K. Corzine, “AC impedance measurement techniques,” *Electr. Mach. Drives, 2005 IEEE Int. Conf.*, pp. 1850–1857, 2005.

[70] J. Huang, K. A. Corzine, and M. Belkhayat, “Small-signal impedance

measurement of power-electronics-based AC power systems using line-to-line current injection," *IEEE Trans. Power Electron.*, vol. 24, no. 2, pp. 445–455, Feb. 2009.

[71] J. Huang and K. A. Corzine, "AC impedance measurement by line-to-line injected current," *Conf. Rec. - IAS Annu. Meet. (IEEE Ind. Appl. Soc.*, vol. 1, no. c, pp. 300–306, 2006.

[72] Z. Shen, I. Cvetkovic, M. Jaksic, C. Dimarino, D. Boroyevich, R. Burgos, F. Chen, and W. Hall, "Design of a modular and scalable small-signal dq impedance measurement unit for grid applications utilizing 10 kV SiC MOSFETs," *2015 17th Eur. Conf. Power Electron. Appl. EPE-ECCE Eur. 2015*, 2015.

[73] M. John, P. A. Mendoza-Araya, and G. Venkataramanan, "Small signal impedance measurement in droop controlled AC microgrids," *2014 IEEE Energy Convers. Congr. Expo. ECCE 2014*, pp. 702–709, 2014.

[74] Z. Shen, M. Jaksic, P. Mattavelli, D. Boroyevich, J. Verhulst, and M. Belkhayat, "Three-phase AC system impedance measurement unit (IMU) using chirp signal injection," *Conf. Proc. - IEEE Appl. Power Electron. Conf. Expo. - APEC*, pp. 2666–2673, 2013.

[75] M. Cespedes and J. Sun, "Online grid impedance identification for adaptive control of grid-connected inverters," *2012 IEEE Energy Convers. Congr. Expo. ECCE 2012*, pp. 914–921, 2012.

[76] U. D. Annakkage, N. K. C. C. Nair, Y. Liang, a. M. Gole, V. Dinavahi, B. Gustavsen, T. Noda, H. Ghasemi, A. Monti, M. Matar, R. Iravani, and J. a. Martinez, "Dynamic system equivalents: A survey of available techniques," *IEEE Trans. Power Deliv.*, vol. 27, no. 1, pp. 411–420, 2012.

[77] E. Zhijun, K. W. Chan, and D. Z. Fang, "Dynamic Phasor Modelling of TCR based FACTS Devices for High Speed Power System Fast Transients Simulation," no. May, pp. 42–48, 2007.

[78] A. M. Stanković and T. Aydin, "Analysis of asymmetrical faults in power

systems using dynamic phasors," *IEEE Trans. Power Syst.*, vol. 15, no. 3, pp. 1062–1068, 2000.

[79] B. Zhou and P. Zhang, "Analysis of modeling and simulation of Buck-boost converter considering dynamic phasor method," *Proc. 2011 Int. Conf. Electron. Mech. Eng. Inf. Technol. EMEIT 2011*, vol. 8, no. 5, pp. 4081–4084, 2011.

[80] T. Yang, "Development of Dynamic Phasors for the Modelling of Aircraft Electrical Power Systems,",Ph.D. thesis, University of Notingham, May, p. 232, 2013.

[81] K. Abojlala, D. Holliday, and L. Xu, "Transient analysis of an interline dynamic voltage restorer using dynamic phasor representation," in *2016 IEEE 17th Workshop on Control and Modeling for Power Electronics, COMPEL 2016*, 2016, pp. 1–7.

[82] X. Guo, Z. Lu, B. Wang, X. Sun, L. Wang, J. M. Guerrero, "Dynamic phasors-based modeling and stability analysis of droop-controlled inverters for microgrid applications," *IEEE Trans. Smart Grid*, vol. 5, no. 6, pp. 2980–2987, 2014.

[83] P. C. Krause, O. Wasynczuk, and S. D. Sudhoff, Analysis of Electric Machinery and Drive Systems, *Wiley inter-science,*. 2002.

[84] L. L. Grigsby, *Power system stability and control*, vol. 9, no. 2. 2017.

[85] L. Gyugyi, A. A. Edris, and M. Eremia, "Static Synchronous Series Compensator (SSSC)," in *Advanced Solutions in Power Systems: HVDC, FACTS, and AI Techniques*, Hoboken, NJ, USA: John Wiley & Sons, Inc., 2016, pp. 527–557.

[86] A. Alidemaj, V. Komoni, G. Kabashi, and I. Krasniqi, "Control Active and Reactive Power Flow with UPFC connected in Transmission Line," *8th Mediterr. Conf. Power Gener. Transm. Distrib. Energy Convers. (MEDPOWER 2012)*, pp. 31–31, 2012.

[87] B. Wen, D. Boroyevich, R. Burgos, P. Mattavelli, and Z. Shen, "Analysis of

D-Q Small-Signal Impedance of Grid-Tied Inverters," *IEEE Trans. Power Electron.*, vol. 31, no. 1, pp. 675–687, Jan. 2016.

[88] C. Schauder and H. Mehta, "Vector analysis and control of advanced static VAR compensators," *IEE Proc. C Gener. Transm. Distrib.*, vol. 140, no. 4, p. 299, 1993.

[89] X. Lombard and P. G. Therond, "Control of unified power flow controller: Comparison of methods on the basis of a detailed numerical model," *IEEE Trans. Power Syst.*, vol. 12, no. 2, pp. 824–830, 1997.

[90] T. M. Haileselassie, "Control of multi-terminal VSC-HVDC systems," Norwegian University of Science and Technology,Trondheim, Norway, 2008.

[91] P. Kundur, "Power System Stability and Control." p. 1197, 1994.

[92] M. B. and M. L. Williams, "Impedance Extraction Techniques for DC and AC Systems," in *Proceedings of the Naval Symposium on Electric Machines*, 2000.

[93] Z. Yao, "Stability analysis of power systems by the generalised Nyquist criterion," in *International Conference on Control '94*, 1994, vol. 1994, no. 389, pp. 739–744.

[94] Z. Liu, J. Liu, W. Bao, Y. Zhao, and F. Liu, "A Novel Stability Criterion of AC Power System with Constant Power Load," *2012 Twenty-Seventh Annu. IEEE Appl. Power Electron. Conf. Expo.*, no. 2009, pp. 1946–1950, Feb. 2012.

[95] M. Belkhayat, "Stability criteria for ac power systems with regulated loads," 1997.

[96] Y. Familiant, K. Corzine, J. Huang, and M. Belkhayat, "AC Impedance Measurement Techniques," in *IEEE International Conference on Electric Machines and Drives, 2005.*, 2005, pp. 1850–1857.

[97] M. Jaksic, Z. Shen, I. Cvetkovic, D. Boroyevich, R. Burgos, P. Street, W. Hall, and P. Mattavelli, "Wide-bandwidth Identification of small-signal dq impedances of ac power systems via single-phase series voltage injection,"

2015 17th Eur. Conf. Power Electron. Appl. EPE-ECCE Eur. 2015, no. 1, 2015.

[98] P. C. Krause, O. Wasynczuk, and S. D. Sudhoff, *Analysis of Electric Machinery and Drive Systems*. 2002.

[99] P. Kundur, "POWERFLOW AND STABILITY SIMULATIONS," vol. 11, no. 4, pp. 1944–1950, 1996.

[100] J. R. C. Orillaza and A. R. Wood, "Harmonic state-space model of a controlled TCR," *IEEE Trans. Power Deliv.*, vol. 28, no. 1, pp. 197–205, 2013.

[101] E. Möllerstedt, "Dynamic Analysis of Harmonics in Electrical Systems," , *Ph.D thesis, Lund University Publications* p. 148, 2000.

[102] N. M. Wereley, "Analysis and Control of Linear Periodically Time Varying Systems," no. January 1990, 1991.

[103] K. Corzine, J. Huang, S. Member, K. A. Corzine, and M. Belkhayat, "Small-Signal Impedance Measurement of Power- Electronics-Based AC Power Systems Using Line- to-Line Current Injection," 2009.

[104] M. K. Das, A. M. Kulkarni, and P. B. Darji, "Comparison of DQ and Dynamic Phasor based frequency scanning analysis of grid-connected Power Electronic Systems," *19th Power Syst. Comput. Conf. PSCC 2016*, no. 1, 2016.

[105] S. Lissandron, L. D. Santa, P. Mattavelli, and B. Wen, "Validation of Impedance-Based Small-Signal Stability Analysis for Single-Phase Grid-Feeding Inverters with PLL," 2015.

[106] G. N. Love and a. R. Wood, "Harmonic State Space model of power electronics," *2008 13th Int. Conf. Harmon. Qual. Power*, vol. 1, pp. 2–7, 2008.

[107] Z. Shen, M. Jaksic, P. Mattavelli, and V. Tech, "Design and Implementation of Three-phase AC Impedance Measurement Unit (IMU) with Series and Shunt Injection," no. 1, pp. 2674–2681, 2013.

[108] C. Li, R. Burgos, I. Cvetkovic, L. Mili, V. Tech, and P. Rodriguez,

"Evaluation and Control Design of Virtual- Synchronous-Machine-Based STATCOM for Grids with High Penetration of Renewable Energy," pp. 5652–5658, 2014.

[109] M. S. Castro, H. M. Ayres, V. F. Costa, and L. C. P. Silva, "Impacts of the SSSC control modes on small-signal and transient stability of a power system," vol. 77, pp. 1–9, 2007.

[110] J. Huang, K. A. Corzine, and M. Belkhayat, "Online synchronous machine parameter extraction from small-signal injection techniques," *IEEE Trans. Energy Convers.*, vol. 24, no. 1, pp. 43–51, 2009.

APPENDIX-A DYNAMIC PHASOR FORMS EXPANSION

1. Two variable expansion

$$\langle xy\rangle_0 = \langle x\rangle_{\bar{k}}\langle y\rangle_k + \langle x\rangle_0\langle y\rangle_0 + \langle x\rangle_k\langle y\rangle_{\bar{k}} \tag{A.1}$$

$$\langle xy\rangle_k = \langle x\rangle_k\langle y\rangle_0 + \langle x\rangle_0\langle y\rangle_k \tag{A.2}$$

$$\langle xy\rangle_{\bar{k}} = \langle x\rangle_{\bar{k}}\langle y\rangle_0 + \langle x\rangle_0\langle y\rangle_{\bar{k}} \tag{A.3}$$

2. Three variable expansion

$$\langle xyz\rangle_0 = \sum_i^{k=0}\langle x\rangle_{k-i}\langle y\rangle_i\langle z\rangle_0 + \sum_i^{k=\bar{k}}\langle x\rangle_{k-i}\langle y\rangle_i\langle z\rangle_k + \sum_i^{k=k}\langle x\rangle_{k-i}\langle y\rangle_i\langle z\rangle_{\bar{k}} \tag{A.4}$$

$$\langle xyz\rangle_k = \sum_i^{k=0}\langle x\rangle_{k-i}\langle y\rangle_i\langle z\rangle_k + \sum_i^{k=k}\langle x\rangle_{k-i}\langle y\rangle_i\langle z\rangle_0 \tag{A.5}$$

$$\langle xyz\rangle_{\bar{k}} = \sum_i^{k=0}\langle x\rangle_{k-i}\langle y\rangle_i\langle z\rangle_{\bar{k}} + \sum_i^{k=\bar{k}}\langle x\rangle_{k-i}\langle y\rangle_i\langle z\rangle_0 \tag{A.6}$$

3. Four variable expansion

$$\begin{aligned}&\langle xyzm\rangle_k = \\ &\left(\sum_i^{k=0}\langle x\rangle_{k-i}\langle y\rangle_i\langle z\rangle_k + \sum_i^{k=k}\langle x\rangle_{k-i}\langle y\rangle_i\langle z\rangle_0\right)\langle m\rangle_0 + \left(\left(\sum_i^{k=0}\langle x\rangle_{k-i}\langle y\rangle_i\right)\langle z\rangle_0 + \right. \\ &\left.\left(\sum_i^{k=\bar{k}}\langle x\rangle_{k-i}\langle y\rangle_i\right)\langle z\rangle_k + \left(\sum_i^{k=k}\langle x\rangle_{k-i}\langle y\rangle_i\right)\langle z\rangle_{\bar{k}}\right)\langle m\rangle_k\end{aligned} \tag{A.7}$$

$$\begin{aligned}&\langle xyzm\rangle_{\bar{k}} = \\ &\left(\sum_i^{k=0}\langle x\rangle_{k-i}\langle y\rangle_i\langle z\rangle_k + \sum_i^{k=\bar{k}}\langle x\rangle_{k-i}\langle y\rangle_i\langle z\rangle_0\right)\langle m\rangle_0 + \left(\left(\sum_i^{k=0}\langle x\rangle_{k-i}\langle y\rangle_i\right)\langle z\rangle_0 + \right. \\ &\left.\left(\sum_i^{k=\bar{k}}\langle x\rangle_{k-i}\langle y\rangle_i\right)\langle z\rangle_k + \left(\sum_i^{k=k}\langle x\rangle_{k-i}\langle y\rangle_i\right)\langle z\rangle_{\bar{k}}\right)\langle m\rangle_{\bar{k}}\end{aligned} \tag{A.8}$$

$$\begin{aligned}&\langle xyzm\rangle_0 = \\ &+\left(\sum_i^{k=0}\langle x\rangle_{k-i}\langle y\rangle_i\langle z\rangle_0 + \sum_i^{k=\bar{k}}\langle x\rangle_{k-i}\langle y\rangle_i\langle z\rangle_k + \sum_i^{k=k}\langle x\rangle_{k-i}\langle y\rangle_i\langle z\rangle_{\bar{k}}\right)\langle m\rangle_0 + \\ &\left(\sum_i^{k=0}\langle x\rangle_{k-i}\langle y\rangle_i\langle z\rangle_{\bar{k}} + \sum_i^{k=\bar{k}}\langle x\rangle_{k-i}\langle y\rangle_i\langle z\rangle_0\right)\langle m\rangle_k + \left(\sum_i^{k=0}\langle x\rangle_{k-i}\langle y\rangle_i\langle z\rangle_k + \right. \\ &\left.\sum_i^{k=k}\langle x\rangle_{k-i}\langle y\rangle_i\langle z\rangle_0\right)\langle m\rangle_{\bar{k}}\end{aligned} \tag{A.9}$$

APPENDIX-B STATCOM PERFORMANCE IN SYNCHRONOUS DQ

1. State space analysis of STATCOM

This section presents the state derivation of the STATCOM controlled with the reactive power and the direct voltage. The linearized state space equations of the STATCOM are given by:

$$\Delta i'_{sd} = \frac{1}{L_f}\Delta v_{sd} - \frac{R_f}{L_f}\Delta i_{sd} - \frac{1}{L_f}(\Delta u_{sd}) + \omega\Delta i_{sq} \tag{B.10}$$

$$\Delta i'_{sq} = \frac{1}{L_f}\Delta v_{sq} - \frac{R_f}{L_f}\Delta i_{sq} - \frac{1}{L_f}(\Delta u_{sq}) - \omega\Delta i_{sd} \tag{B.11}$$

$$\Delta x'_1 = K_{iid}(\Delta i^*_{sd} - \Delta i_{sd}) \tag{B.12}$$

$$\Delta x'_2 = K_{iiq}(\Delta i^*_{sq} - \Delta i_{sq}) \tag{B.13}$$

The internal signal of the STATCOM is given as:

$$\Delta u_{sd} = -K_{pid}(\Delta i^*_{sd} - \Delta i_{sd}) - \Delta x_1 \tag{B.14}$$

$$\Delta u_{sq} = -K_{piq}(\Delta i^*_{sq} - \Delta i_{sq}) - \Delta x_2 \tag{B.15}$$

$$\Delta x'_3 = K_{ivd}(v^*_{dc} - \Delta v_{dc}) \tag{B.16}$$

$$\Delta x'_4 = K_{ivq}(Q^* - \Delta Q) \tag{B.17}$$

The reference currents of the STATCOM controlled with reactive power are given for as:

$$\Delta i^*_{sd} = K_{pvd}(v^*_{dc} - \Delta v_{dc}) + \Delta x_3 \tag{B.18}$$

$$\Delta i^*_{sq} = K_{pvq}(Q^* - \Delta Q) + \Delta x_4 \tag{B.19}$$

where, the reactive power is:

$$Q = \frac{3}{2}(v_{sq}i_{sd} - v_{sd}i_{sq})$$

$$\Delta Q = \frac{3}{2}i_{sd}\Delta v_{sq} + \frac{3}{2}v_{sq}\Delta i_{sd} - \frac{3}{2}i_{sq}\Delta v_{sd} - \frac{3}{2}v_{sd}\Delta i_{sq}$$

In the meantime, the reference currents of the STATCOM controlled with direct voltage are given for as:

$$\Delta i^*_{sd} = K_{pvd}(v^*_{dc} - \Delta v_{dc}) + \Delta x_3 \tag{B.20}$$

$$\Delta i_{sq}^{*} = K_{pvq}(v_{sd}^{*} - \Delta v_{sd}) + \Delta x_4 \tag{B.21}$$

While, the dc link voltage is:

$$\Delta v'_{dc} = \frac{3}{2}\frac{i_{sd}}{C_{dc}v_{dc}}\Delta v_{sd} + \frac{\frac{3}{2}v_{sd}-2i_{sd}.R_f}{C_{dc}v_{dc}}\Delta i_{sd} + \frac{\alpha_{dc}}{C_{dc}v_{dc}^2}\Delta v_{dc} + \frac{3}{2}\frac{i_{sq}}{C_{dc}v_{dc}}\Delta v_{sq} + \frac{3}{2}\frac{v_{sq}}{C_{dc}v_{dc}}\Delta i_{sq} \tag{B.22}$$

$$\alpha_{dc} = i_{sd}^2.R_f - \frac{3}{2}v_{sd}.i_{sd} - \frac{3}{2}v_{sq}.i_{sq}$$

The state space vectors of the STATCOM controlled with reactive power control are:

$$\mathbf{\Delta i_{sdq}} = [\Delta i_{sd} \quad \Delta i_{sq}]$$

$$\mathbf{\Delta X} = [\Delta x_1 \quad \Delta x_2 \quad \Delta \mathrm{x}_3 \quad \Delta x_4 \quad \Delta i_{sdq} \quad \Delta v_{dc}]^T$$

$$\mathbf{\Delta U} = [\Delta v_{sd} \quad \Delta v_{sq} \quad \Delta v_{dc}^{*} \quad \Delta Q^{*}]^T$$

$$\mathbf{\Delta X'} = Asq\mathbf{\Delta X} + Bsq\mathbf{\Delta U} \tag{B.23}$$

$$\mathbf{\Delta i_{sdq}} = C\mathbf{\Delta X} \tag{B.24}$$

$$Asq = \begin{bmatrix} 0 & 0 & K_{iid} & 0 & -K_{iid} & 0 & -K_{iid}K_{pvd} \\ 0 & 0 & 0 & K_{iiq} & -\frac{3}{2}K_{iiq}K_{pvq}v_{sq} & \frac{3}{2}K_{iiq}K_{pvq}v_{sd} - K_{iiq} & 0 \\ 0 & 0 & 0 & 0 & 0 & 0 & -K_{ivd} \\ 0 & 0 & 0 & 0 & -\frac{3}{2}K_{ivq}v_{sq} & \frac{3}{2}K_{ivq}v_{sd} & 0 \\ \frac{1}{L_f} & 0 & \frac{K_{pid}}{L_f} & 0 & \frac{-R_f-K_{pid}}{L_f} & \omega & \frac{-K_{pid}K_{pvd}}{L_f} \\ 0 & \frac{1}{L_f} & 0 & \frac{K_{piq}}{L_f} & -\frac{3}{2}\frac{K_{piq}K_{pvq}v_{sq}}{L_f} - \omega & \frac{-R_f-K_{piq}+\frac{3}{2}K_{piq}K_{pvq}v_{sd}}{L_f} & 0 \\ 0 & 0 & 0 & 0 & \frac{\frac{3}{2}v_{sd}-2i_{sd}.R_f}{C_{dc}v_{dc}} & \frac{3}{2}\frac{v_{sq}}{C_{dc}v_{dc}} & \frac{\alpha_{dc}}{C_{dc}v_{dc}^2} \end{bmatrix}$$

$$Bsq = \begin{bmatrix} 0 & 0 & K_{iid}K_{pvd} & 0 \\ \frac{3}{2}K_{iiq}K_{pvq}i_{sq} & \frac{-3}{2}K_{iiq}K_{pvq}i_{sd} & 0 & K_{iiq}K_{pvq} \\ 0 & 0 & K_{ivd} & 0 \\ \frac{3}{2}K_{ivq}i_{sq} & \frac{-3}{2}K_{ivq}i_{sd} & 0 & Ki_{vq} \\ \frac{1}{L_f} & 0 & \frac{K_{pid}K_{pvd}}{L_f} & 0 \\ \frac{3}{2}\frac{K_{piq}K_{pvq}i_{sq}}{L_f} & \frac{1-\frac{3}{2}K_{piq}K_{pvq}i_{sd}}{L_f} & 0 & \frac{K_{piq}}{L_f} \\ \frac{3}{2}\frac{i_{sd}}{C_{dc}v_{dc}} & \frac{3}{2}\frac{i_{sq}}{C_{dc}v_{dc}} & 0 & 0 \end{bmatrix}$$

While, the state space vectors of STATCOM model controlled with direct voltage is:

$$\mathbf{\Delta i_{sdq}} = [\Delta i_{sd} \quad \Delta i_{sq}]$$

$$\mathbf{\Delta X} = [\Delta x_1 \quad \Delta x_2 \quad \Delta x_3 \quad \Delta x_4 \quad \Delta i_{sdq} \quad \Delta v_{dc}]^T$$

$$\mathbf{\Delta U} = [\Delta v_{sd} \quad \Delta v_{sq} \quad \Delta v_{dc}^* \quad \Delta v_{sd}^*]^T$$

$$\mathbf{\Delta X'} = Asv\mathbf{\Delta X} + Bsv\mathbf{\Delta U} \tag{B.25}$$

$$\mathbf{\Delta i_{sdq}} = C\mathbf{\Delta X} \tag{B.26}$$

$$Asv = \begin{bmatrix} 0 & 0 & K_{iid} & 0 & -K_{iid} & 0 & -K_{iid}K_{pvd} \\ 0 & 0 & 0 & K_{iiq} & 0 & -K_{iiq} & 0 \\ 0 & 0 & 0 & 0 & 0 & 0 & -K_{ivd} \\ 0 & 0 & 0 & 0 & 0 & 0 & 0 \\ \frac{1}{L_f} & 0 & \frac{K_{pid}}{L_f} & 0 & \frac{K_{pid}-R_f}{L_f} & \omega & \frac{K_{pid}K_{pvd}}{L_f} \\ 0 & \frac{1}{L_f} & 0 & \frac{K_{piq}}{L_f} & -\omega & \frac{K_{piq}-R_f}{L_f} & 0 \\ 0 & 0 & 0 & 0 & \frac{\frac{3}{2}v_{sd}-2i_{sd}.R_f}{C_{dc}v_{dc}} & \frac{3}{2}\frac{v_{sq}}{C_{dc}v_{dc}} & \frac{i_{sd}^2.R_f-\frac{3}{2}v_{sd}.i_{sd}-\frac{3}{2}v_{sq}.i_{sq}}{C_{dc}v_{dc}^2} \end{bmatrix}$$

$$Bsv = \begin{bmatrix} 0 & 0 & 0 & K_{iid}K_{pvd} \\ -K_{iiq}K_{pvq} & 0 & K_{iiq}K_{pvq} & 0 \\ 0 & 0 & 0 & K_{ivd} \\ -K_{ivq} & 0 & K_{ivq} & 0 \\ \frac{1}{L_f} & 0 & 0 & \frac{K_{pid}K_{pvd}}{L_f} \\ -\frac{K_{piq}K_{pvq}}{L_f} & \frac{1}{L_f} & \frac{K_{piq}K_{pvq}}{L_f} & 0 \\ \frac{3}{2}\frac{i_{sd}}{C_{dc}v_{dc}} & \frac{3}{2}\frac{i_{sq}}{C_{dc}v_{dc}} & 0 & 0 \end{bmatrix}$$

2. STATCOM impedance in synchronous dq frame

$$\Delta v_{sd} = \left(L_f + R_f\right)\Delta i_{sd} - \omega L_f \Delta i_{sq} + \Delta u_{sd} \tag{B.27}$$

$$\Delta v_{sq} = \left(R_f + L_f \mathrm{s}\right)\Delta i_{sq} + \omega L_f \Delta i_{sd} + \Delta u_{sq} \tag{B.28}$$

$$\Delta u_{sd} = -\left(K_{pid} + \frac{K_{iid}}{s}\right)\left(\Delta i_{sd}^* - \Delta i_{sd}\right) \tag{B.29}$$

$$\Delta u_{sq} = -\left(K_{piq} + \frac{K_{iiq}}{s}\right)\left(\Delta i_{sq}^* - \Delta i_{sq}\right) \tag{B.30}$$

Substituting (B.27) to (B.30) to have:

$$\Delta v_{sd} = \left(L_f + R_f + \left(K_{pid} + \frac{K_{iid}}{s}\right)\right)\Delta i_{sd} - \omega L_f \Delta i_{sq} - \left(K_{pid} + \frac{K_{iid}}{s}\right)\Delta i^*_{sd} \quad \text{(B.31)}$$

$$\Delta v_{sq} = \left(R_f + L_f \mathrm{s} + \left(K_{piq} + \frac{K_{iiq}}{s}\right)\right)\Delta i_{sq} + \omega L_f \Delta i_{sd} - \left(K_{piq} + \frac{K_{iiq}}{s}\right)\Delta i^*_{sq} \quad \text{(B.32)}$$

$$\begin{bmatrix}\Delta v_{sd} \\ \Delta v_{sq}\end{bmatrix} = a_Z \begin{bmatrix}\Delta i_{sd} \\ \Delta i_{sq}\end{bmatrix} - b_Z \begin{bmatrix}\Delta i^*_{sd} \\ \Delta i^*_{sq}\end{bmatrix} \quad \text{(B.33)}$$

where,

$$a_Z = \begin{bmatrix} L_f + R_f + \left(K_{pid} + \frac{K_{iid}}{s}\right) & -\omega L_f \\ \omega L_f & R_f + L_f \mathrm{s} + \left(K_{piq} + \frac{K_{iiq}}{s}\right) \end{bmatrix}$$

$$b_Z = -\begin{bmatrix} \left(K_{pid} + \frac{K_{iid}}{s}\right) & 0 \\ 0 & \left(K_{piq} + \frac{K_{iiq}}{s}\right) \end{bmatrix}$$

The reference currents of the STATCOM controlled with reactive power are:

$$\Delta i^*_{sd} = \left(K_{pvd} + \frac{K_{ivd}}{s}\right) v^*_{dc} - \left(K_{pvd} + \frac{K_{ivd}}{s}\right) \Delta v_{dc} \quad \text{(B.34)}$$

$$\Delta i^*_{sq} = \left(K_{pvq} + \frac{K_{ivq}}{s}\right) Q^* - \left(K_{pvq} + \frac{K_{ivq}}{s}\right) \Delta Q \quad \text{(B.35)}$$

By reforming equations (B.34) and (B.35) as:

$$\begin{bmatrix}\Delta i^*_{sd} \\ \Delta i^*_{sq}\end{bmatrix} = c_Z \begin{bmatrix}v^*_{dc} \\ \mathrm{Q}^*\end{bmatrix} - c_Z \begin{bmatrix}v_{dc} \\ \mathrm{Q}\end{bmatrix} \quad \text{(B.36)}$$

where,

$$c_Z = \begin{bmatrix} \left(K_{pvd} + \frac{K_{ivd}}{s}\right) & 0 \\ 0 & \left(K_{pvq} + \frac{K_{ivq}}{s}\right) \end{bmatrix}$$

While, the reference currents of the STATCOM controlled with direct voltage control are:

$$\Delta i^*_{sd} = \left(K_{pvd} + \frac{K_{ivd}}{s}\right)(v^*_{dc} - \Delta v_{dc}) \quad \text{(B.37)}$$

$$\Delta i^*_{sq} = \left(K_{pvq} + \frac{K_{ivq}}{s}\right)(v^*_{sd} - \Delta v_{sd}) \quad \text{(B.38)}$$

These equations can be reformed as:

$$\begin{bmatrix}\Delta i^*_{sd} \\ \Delta i^*_{sq}\end{bmatrix} = c_Z \begin{bmatrix}v^*_{dc} \\ v^*_{sd}\end{bmatrix} - c_Z \begin{bmatrix}v_{dc} \\ v_{sd}\end{bmatrix}$$

By substituting the relations between the device and the network measurements in the dc link voltage to have:

$$\left\{\frac{C_{dc}v_{dc}.s-i_{sd}^2.R_f+\frac{3}{2}v_{sd}.i_{sd}+\frac{3}{2}v_{sq}.i_{sq}}{v_{dc}}\right\}\Delta v_{dc}=\left(\frac{3}{2}v_{sd}-2i_{sd}.R_f\right)\Delta i_{sd}+\frac{3}{2}v_{sq}\Delta i_{sq}+\frac{3}{2}i_{sd}\Delta v_{sd}+\frac{3}{2}i_{sq}\Delta v_{sq} \quad \text{(B.39)}$$

Also the reactive power equation, which is given as:

$$\Delta Q=i_{sd}\Delta v_{sq}+v_{sq}\Delta i_{sd}-i_{sq}\Delta v_{sd}-v_{sd}\Delta i_{sq}$$

So, for the STATCOM controlled with reactive power control is given as:

$$d_z\begin{bmatrix}\Delta v_{dc}\\ \Delta Q\end{bmatrix}=f_z\begin{bmatrix}\Delta v_{sd}\\ \Delta v_{sq}\end{bmatrix}+e_z\begin{bmatrix}\Delta i_{sd}\\ \Delta i_{sq}\end{bmatrix} \quad \text{(B.40)}$$

where,

$$d_z=\begin{bmatrix}\frac{sC_{dc}v_{dc}^2-\alpha_{dc}}{v_{dc}} & 0\\ 0 & 1\end{bmatrix} \qquad e_z=\begin{bmatrix}\left(\frac{3}{2}v_{sd}-2i_{sd}.R_f\right) & \frac{3}{2}v_{sq}\\ \frac{3}{2}v_{sq} & -\frac{3}{2}v_{sd}\end{bmatrix}$$

$$f_z=\begin{bmatrix}\frac{3}{2}i_{sd} & \frac{3}{2}i_{sq}\\ -\frac{3}{2}i_{sq} & \frac{3}{2}i_{sd}\end{bmatrix}$$

In the meantime, the STATCOM controlled with direct voltage control is:

$$d_z\begin{bmatrix}\Delta v_{dc}\\ \Delta Q\end{bmatrix}=fv_z\begin{bmatrix}\Delta v_{sd}\\ \Delta v_{sq}\end{bmatrix}+ev_z\begin{bmatrix}\Delta i_{sd}\\ \Delta i_{sq}\end{bmatrix} \quad \text{(B.41)}$$

where,

$$d_z=\begin{bmatrix}\frac{sC_{dc}v_{dc}^2-\alpha_{dc}}{v_{dc}} & 0\\ 0 & 1\end{bmatrix} \quad ev_z=\begin{bmatrix}\left(\frac{3}{2}v_{sd}-2i_{sd}.R_f\right) & \frac{3}{2}v_{sq}\\ 0 & 0\end{bmatrix} \quad fv_z=\begin{bmatrix}\frac{3}{2}i_{sd} & \frac{3}{2}i_{sq}\\ 1 & 0\end{bmatrix}$$

So, the impedance of the STATCOM controlled with reactive power is:

$$\begin{bmatrix}\Delta v_{sd}\\ \Delta v_{sq}\end{bmatrix}=Z_{STATCOMQ}\begin{bmatrix}\Delta i_{sd}\\ \Delta i_{sq}\end{bmatrix}+C_x\begin{bmatrix}v_{dc}^*\\ v_{sd}^*\end{bmatrix} \quad \text{(B.42)}$$

where,

$$Z_{STATCOMQ}=\frac{a_Z+b_Zc_Zd_z^{-1}e_z}{I-b_Zc_Zd_z^{-1}f_z}$$

$$C_x = -\frac{b_Z c_Z}{(I - b_Z c_Z d_z^{-1} f_z)}$$

While, the impedance of the STATCOM controlled with direct voltage control is:

$$\begin{bmatrix}\Delta v_{sd}\\ \Delta v_{sq}\end{bmatrix} = Z_{STATCOMV}\begin{bmatrix}\Delta i_{sd}\\ \Delta i_{sq}\end{bmatrix} + C_x\begin{bmatrix}v_{dc}^*\\ v_{sd}^*\end{bmatrix} \quad \text{(B.43)}$$

Where: The STATCOM impedance $(Z_{STATCOMV})$ is given as:

$$Z_{STATCOMV} = \frac{a_Z + b_Z c_Z d_z^{-1} e v_z}{I - b_Z c_Z d_z^{-1} f v_z}$$

$$C_x = -\frac{b_Z c_Z}{(I - b_Z c_Z d_z^{-1} f v_z)}$$

APPENDIX-C SYNCHRONOUS GENERATOR

1. dq impedance of synchronous generator

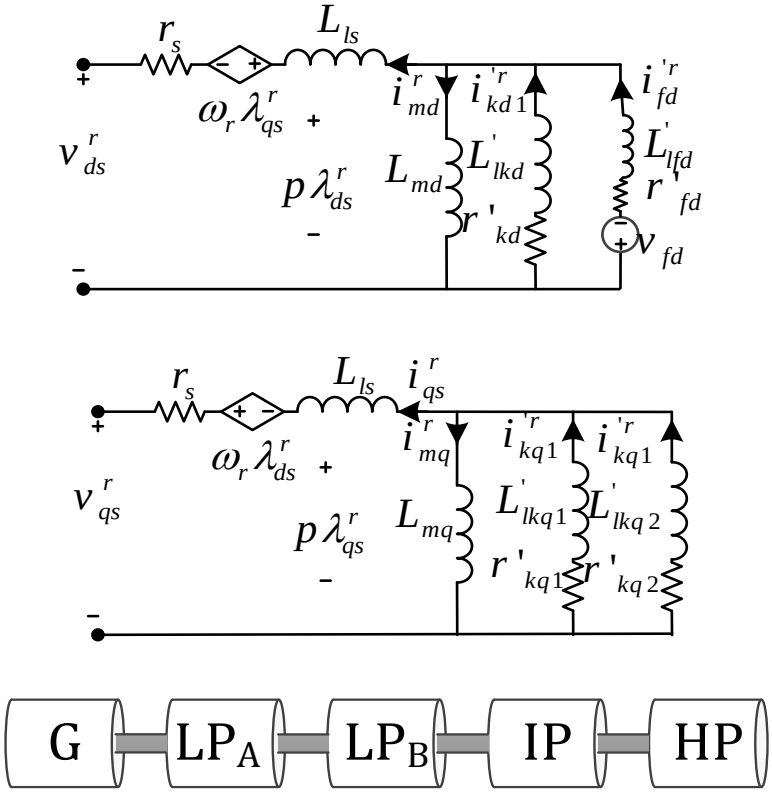

Figure (1) synchronous generator equivalent circuit

The equations of the synchronous machine can be expressed as[83] [110] as:

$$v^r_{ds} = -r_s i^r_{ds} - \omega_r \lambda^r_{qs} + \frac{d}{dt}\lambda^r_{ds} \quad \text{(C.44)}$$

$$v^r_{qs} = -r_s i^r_{qs} + \omega_r \lambda^r_{ds} + \frac{d}{dt}\lambda^r_{qs} \quad \text{(C.45)}$$

$$v^{`r}_{kd1} = -r^{`r}_{kd1} i^{`r}_{kd1} + \frac{d}{dt}\lambda^{`r}_{kd1} \quad \text{(C.46)}$$

$$v^{`r}_{kq1} = -r^{`r}_{kq1} i^{`r}_{kq1} + \frac{d}{dt}\lambda^{`r}_{kq1} \quad \text{(C.47)}$$

$$v^{`}_{fd} = -r^{`r}_{fd} i^{`}_{fd} + \frac{d}{dt}\lambda^{`}_{fd} \quad \text{(C.48)}$$

$$v^{`r}_{kq2} = -r^{`r}_{kq1} i^{`r}_{kq2} + \frac{d}{dt}\lambda^{`r}_{kq2} \quad \text{(C.49)}$$

The flux linkages may be written as:

$$\lambda_{ds}^{r} = -L_{ls} i_{ds}^{r} + L_{md} i_{md}^{r} \tag{C.50}$$

$$\lambda_{kd1}^{`r} = L_{lkd1}^{`} i_{kd1}^{`r} + L_{md} i_{md}^{r} \tag{C.51}$$

$$\lambda_{fd}^{`} = L_{lfd}^{`} i_{fd}^{`} + L_{md} i_{md}^{r} \tag{C.52}$$

$$\lambda_{qs}^{r} = -L_{ls} i_{ds}^{r} + L_{mq} i_{mq}^{r} \tag{C.53}$$

$$\lambda_{kq1}^{`r} = L_{lkq1}^{`} i_{kq1}^{`r} + L_{mq} i_{mq}^{r} \tag{C.54}$$

$$\lambda_{kq2}^{`r} = L_{lkq2}^{`} i_{kq2}^{`r} + L_{mq} i_{mq}^{r} \tag{C.55}$$

where (ω_r) is the speed of the rotor reference frame, *x* represents the number of damper windings on the *q*-axis, which can be 1, 2, or 3, and *y* represents the number of dumper on the *d*-axis, which can be 1 or 2. The rotor variables are referred to the stator windings for convenience.

By linearizing above equations from (C.45) to (C.55) to have:

$$\begin{bmatrix} \mathbf{\Delta v_{dqs}^{r}} \\ \mathbf{\Delta v_{lfkd}^{`r}} \\ \mathbf{\Delta v_{kq12}^{`r}} \end{bmatrix} = \begin{bmatrix} -r_s & 0 & 0 & 0 & 0 & 0 \\ 0 & -r_s & 0 & 0 & 0 & 0 \\ 0 & 0 & -r_{kd1}^{`r} & 0 & 0 & 0 \\ 0 & 0 & 0 & -r_{fd}^{`r} & 0 & 0 \\ 0 & 0 & 0 & 0 & -r_{kq1}^{`r} & 0 \\ 0 & 0 & 0 & 0 & 0 & -r_{kq2}^{`r} \end{bmatrix} \begin{bmatrix} \mathbf{\Delta i_{dqs}^{r}} \\ \mathbf{\Delta i_{lfkd}^{`r}} \\ \mathbf{\Delta i_{kq12}^{`r}} \end{bmatrix} + \frac{d}{dt} \begin{bmatrix} \boldsymbol{\Delta \lambda_{dqs}^{r}} \\ \boldsymbol{\Delta \lambda_{fkd}^{`r}} \\ \boldsymbol{\Delta \lambda_{kq12}^{`r}} \end{bmatrix} +$$

$$\begin{bmatrix} 0 & -\omega_r & 0 & 0 & 0 & 0 \\ 0 & 0 & 0 & 0 & 0 & 0 \\ 0 & 0 & 0 & 0 & 0 & 0 \\ \omega_r & 0 & 0 & 0 & 0 & 0 \\ 0 & 0 & 0 & 0 & 0 & 0 \\ 0 & 0 & 0 & 0 & 0 & 0 \end{bmatrix} \begin{bmatrix} \boldsymbol{\Delta \lambda_{dqs}^{r}} \\ \boldsymbol{\Delta \lambda_{fkd}^{`r}} \\ \boldsymbol{\Delta \lambda_{kq12}^{`r}} \end{bmatrix} + \begin{bmatrix} -\lambda_{qs}^{r} & 0 \\ \lambda_{ds}^{r} & 0 \\ 0 & 0 \\ 0 & 0 \\ 0 & 0 \\ 0 & 0 \end{bmatrix} \boldsymbol{\Delta \omega \delta} \tag{C.56}$$

And for mutual flux equations:

$$\begin{bmatrix} \mathbf{\Delta \lambda_{dqs}^{r}} \\ \mathbf{\Delta \lambda_{fkd}^{`r}} \\ \mathbf{\Delta \lambda_{kq12}^{`r}} \end{bmatrix} = \begin{bmatrix} -L_{ls} & 0 & 0 & 0 & 0 & 0 \\ 0 & -L_{ls} & 0 & 0 & 0 & 0 \\ 0 & 0 & L_{lkd1}^{`} & 0 & 0 & 0 \\ 0 & 0 & 0 & L_{lfd}^{`} & 0 & 0 \\ 0 & 0 & 0 & 0 & L_{lkq1}^{`} & 0 \\ 0 & 0 & 0 & 0 & 0 & L_{lkq2}^{`} \end{bmatrix} \begin{bmatrix} \mathbf{\Delta i_{dqs}^{r}} \\ \mathbf{\Delta i_{lfkd}^{`r}} \\ \mathbf{\Delta i_{kq12}^{`r}} \end{bmatrix} + \begin{bmatrix} L_{md} & 0 \\ 0 & L_{mq} \\ L_{md} & 0 \\ L_{md} & 0 \\ 0 & L_{mq} \\ 0 & L_{mq} \end{bmatrix} \mathbf{\Delta i_{mdq}^{r}}$$

(C.57)

Substituting mutual inductance equation in voltage equations to have:

$$\begin{bmatrix} \mathbf{\Delta v^r_{dqs}} \\ \mathbf{\Delta v^{`r}_{lfkd}} \\ \mathbf{\Delta v^{`r}_{kq12}} \end{bmatrix} =$$

$$\begin{bmatrix} -r_s - SL_{ls} & \omega_r L_{ls} & 0 & 0 & 0 & 0 \\ -\omega_r L_{ls} & -r_s - SL_{ls} & 0 & 0 & 0 & 0 \\ 0 & 0 & -r^{`r}_{kd1} + SL^{`}_{lkd1} & 0 & 0 & 0 \\ 0 & 0 & 0 & -r^{`r}_{fd} + SL^{`}_{lfd} & 0 & 0 \\ 0 & 0 & 0 & 0 & -r^{`r}_{kq1} + SL^{`}_{lkq1} & 0 \\ 0 & 0 & 0 & 0 & 0 & -r^{`r}_{kq2} + SL^{`}_{lkq2} \end{bmatrix} \begin{bmatrix} \mathbf{\Delta i^r_{dqs}} \\ \mathbf{\Delta i^{`r}_{lfkd}} \\ \mathbf{\Delta i^{`r}_{kq12}} \end{bmatrix} +$$

$$\begin{bmatrix} SL_{md} & -\omega_r L_{mq} \\ \omega_r L_{md} & SL_{mq} \\ SL_{md} & 0 \\ SL_{md} & 0 \\ 0 & SL_{mq} \\ 0 & SL_{mq} \end{bmatrix} \mathbf{\Delta i^r_{mdq}} + \begin{bmatrix} L_{ls} i^r_{qs} - L_{mq} i^r_{mq} & 0 \\ L_{md} i^r_{md} - L_{ls} i^r_{ds} & 0 \\ 0 & 0 \\ 0 & 0 \\ 0 & 0 \\ 0 & 0 \end{bmatrix} \mathbf{\Delta \omega \delta} \qquad \text{(C.58)}$$

$$\mathbf{\Delta \omega \delta} = [\Delta\omega_r \quad \Delta\delta_r]$$

According to figure (1) current directions and using KCL:

$$\Delta i^{`}_{fd} = \Delta i^r_{ds} + \Delta i^r_{md} - \Delta i^{`r}_{kd1} \qquad \text{(C.59)}$$

$$\Delta i^{`r}_{kq2} = \Delta i^r_{qs} + \Delta i^r_{mq} - \Delta i^{`r}_{kq1} \qquad \text{(C.60)}$$

From figure (1) :

$$\Delta v^r_{md} = SL_{md} \Delta i^r_{md} \qquad \text{(C.61)}$$

$$\Delta v^r_{mq} = SL_{mq} \Delta i^r_{mq} \qquad \text{(C.62)}$$

$$\Delta i^{`r}_{kd1} = \frac{1}{\left(r^{`r}_{kd1} + SL^{`}_{lkd1}\right)} \Delta v^{`r}_{kd1} \qquad \text{(C.63)}$$

$$\Delta i^{`r}_{kq1} = \frac{1}{\left(r^{`r}_{kq1} + SL^{`}_{lkq1}\right)} \Delta v^{`r}_{kq1} \qquad \text{(C.64)}$$

$$\Delta v^r_{md} = -\Delta v^{`r}_{kd1} = \Delta v^{`}_{fd} - \left(r^{`r}_{fd} + SL^{`}_{lfd}\right) \Delta i^{`}_{fd} \qquad \text{(C.65)}$$

Due to the assumption that the field voltage is constant during the operation ($\Delta v^{`}_{fd} = 0$) so:

$$\Delta v^r_{md} = -\Delta v^{`r}_{kd1} = -\left(r^{`r}_{fd} + SL^{`}_{lfd}\right) \Delta i^{`}_{fd} \qquad \text{(C.66)}$$

$$\Delta i^{`r}_{kd1} = -\frac{SL_{md}}{\left(r^{`r}_{kd1} + SL^{`}_{lkd1}\right)} \Delta i^r_{md} \qquad \text{(C.67)}$$

$$\Delta i_{fd}^{`} = -\frac{SL_{md}}{r_{fd}^{`r} + SL_{lfd}^{`}} \Delta i_{md}^{r} \tag{C.68}$$

$$\Delta v_{mq}^{r} = -\Delta v_{kq1}^{`r} = -\Delta v_{kq2}^{`r} \tag{C.69}$$

$$\Delta i_{kq1}^{`r} = -\frac{SL_{mq}}{\left(r_{kq1}^{`r} + SL_{lkq1}^{`}\right)} \Delta i_{mq}^{r} \tag{C.70}$$

$$\Delta i_{kq2}^{`r} = -\frac{SL_{mq}}{\left(r_{kq2}^{`r} + SL_{lkq2}^{`}\right)} \Delta i_{mq}^{r} \tag{C.71}$$

From(C.59) , (C.67), (C.70), (C.71) to have :

$$\Delta i_{md}^{r} = A_{msd} \Delta i_{ds}^{r} \tag{C.72}$$

$$A_{msd} = \frac{1}{SL_{md}\left(-\frac{1}{r_{fd}^{`r} + SL_{lfd}^{`}} - \frac{1}{\left(r_{kd1}^{`r} + SL_{lkd1}^{`}\right)} - \frac{1}{SL_{md}}\right)}$$

$$\Delta i_{kd1}^{`r} = -\frac{SL_{md} A_{msd}}{\left(r_{kd1}^{`r} + SL_{lkd1}^{`}\right)} \Delta i_{ds}^{r} \tag{C.73}$$

$$\Delta i_{fd}^{`} = -\frac{SL_{md} A_{msd}}{\left(r_{fd}^{`r} + SL_{lfd}^{`}\right)} \Delta i_{ds}^{r} \tag{C.74}$$

And from (C.60) and (C.70) to have:

$$\Delta i_{mq}^{r} = A_{msq} \Delta i_{qs}^{r} \tag{C.75}$$

$$A_{msq} = \frac{1}{SL_{mq}\left(-\frac{1}{\left(r_{kq2}^{`r} + SL_{lkq2}^{`}\right)} - \frac{1}{\left(r_{kq1}^{`r} + SL_{lkq1}^{`}\right)} - \frac{1}{SL_{mq}}\right)}$$

$$\Delta i_{kq1}^{`r} = -\frac{SL_{mq} A_{msq}}{\left(r_{kq1}^{`r} + SL_{lkq1}^{`}\right)} \Delta i_{qs}^{r} \tag{C.76}$$

$$\Delta i_{kq2}^{`r} = -\frac{SL_{mq} A_{msq}}{\left(r_{kq2}^{`r} + SL_{lkq2}^{`}\right)} \Delta i_{qs}^{r} \tag{C.77}$$

Substituting equations from (C.66) to(C.77) in(4.49) to have:

$$\mathbf{\Delta v_{dqs}^{r}} = \begin{bmatrix} (-r_s - SL_{ls}) + SL_{md} A_{msd} & \omega_r L_{ls} - \omega_r L_{mq} A_{msq} \\ -\omega_r L_{ls} + \omega_r L_{md} A_{msd} & (-r_s - SL_{ls}) + SL_{mq} A_{msq} \end{bmatrix} \mathbf{\Delta i_{dqs}^{r}} +$$

$$\begin{bmatrix} (L_{ls}i_{qs}^{r} - L_{mq}i_{mq}^{r}) & 0 \\ (L_{md}i_{md}^{r} - L_{ls}i_{ds}^{r}) & 0 \end{bmatrix} \boldsymbol{\Delta\omega\delta} \tag{C.78}$$

$$\mathbf{\Delta v_{dqs}^{r}} = \begin{bmatrix} Z_{dd} & Z_{dq} \\ Z_{qd} & Z_{qq} \end{bmatrix} \mathbf{\Delta i_{dqs}^{r}} + \begin{bmatrix} (L_{ls}i_{qs}^{r} - L_{mq}i_{mq}^{r}) & 0 \\ (L_{md}i_{md}^{r} - L_{ls}i_{ds}^{r}) & 0 \end{bmatrix} \boldsymbol{\Delta\omega\delta} \tag{C.79}$$

$$\mathbf{\Delta v_{dqs}^{r}} = ZZ.\mathbf{\Delta i_{dqs}^{r}} + A\lambda.\boldsymbol{\Delta\omega\delta} \tag{C.80}$$

1.1. Including the effect of the electrical torque:

The electric torque equation can be linearized on the form:

$$\Delta T_e = \left(\frac{3}{2}\right)\left(\frac{P}{2}\right)\{\Delta\lambda_{ds}^{r}.i_{qs}^{r} + \lambda_{ds}^{r}.\Delta i_{qs}^{r} - \Delta\lambda_{qs}^{r}i_{ds}^{r} - \lambda_{qs}^{r}\Delta i_{ds}^{r}\} \tag{C.81}$$

Substituting the mutual inductance and the currents in (C.81) to have:

$$\begin{aligned}\Delta T_e = \left(\tfrac{3}{2}\right)\left(\tfrac{P}{2}\right)\{&(-L_{ls}i_{qs}^{r} - L_{mq}i_{mq}^{r} + L_{md}i_{qs}^{r}A_{msd} + L_{ls}i_{qs}^{r})\Delta i_{ds}^{r} + (-L_{ls}i_{ds}^{r} + \\ &L_{md}i_{md}^{r} + L_{ls}i_{ds}^{r} - L_{mq}i_{ds}^{r}A_{msq})\Delta i_{qs}^{r}\}\end{aligned}$$

$$\begin{aligned}\Delta T_e = \left(\tfrac{3}{2}\right)\left(\tfrac{P}{2}\right)\{&-L_{ls}i_{qs}^{r}\Delta i_{ds}^{r} + L_{md}i_{qs}^{r}\Delta i_{fd}^{`} + L_{md}i_{qs}^{r}\Delta i_{kd1}^{`r} - L_{md}i_{qs}^{r}\Delta i_{ds}^{r} - \\ &L_{ls}i_{ds}^{r}\Delta i_{qs}^{r} + L_{md}i_{fd}^{`}\Delta i_{qs}^{r} + L_{md}i_{kd1}^{`r}\Delta i_{qs}^{r} - L_{md}i_{ds}^{r}\Delta i_{qs}^{r} + L_{ls}i_{ds}^{r}\Delta i_{ds}^{r} - \\ &L_{mq}i_{ds}^{r}\Delta i_{kq2}^{`r} - L_{mq}i_{ds}^{r}\Delta i_{kq1}^{`r} + L_{mq}i_{ds}^{r}\Delta i_{qs}^{r} + L_{ls}i_{ds}^{r}\Delta i_{ds}^{r} - L_{mq}i_{kq2}^{`r}\Delta i_{ds}^{r} - \\ &L_{mq}i_{kq1}^{`r}\Delta i_{ds}^{r} + L_{mq}i_{qs}^{r}\Delta i_{ds}^{r}\}\end{aligned} \tag{C.82}$$

$$\Delta T_e = \left(\frac{3}{2}\right)\left(\frac{P}{2}\right)\{\, T_d\Delta i_{ds}^{r} + T_q\Delta i_{qs}^{r}\} \tag{C.83}$$

$$\begin{bmatrix} \Delta T_e \\ \Delta T_m \end{bmatrix} = \left(\frac{3}{2}\right)\left(\frac{P}{2}\right)\begin{bmatrix} T_d & T_q \\ 0 & 0 \end{bmatrix}\mathbf{\Delta i_{dqs}^{r}} \tag{C.84}$$

$$\begin{bmatrix} \Delta T_e \\ \Delta T_m \end{bmatrix} = GT_{dq}\mathbf{\Delta i_{dqs}^{r}} \tag{C.85}$$

$$\frac{d}{dt}\Delta\omega_r = \frac{1}{2H}(\Delta T_m - \Delta T_e - K_D.\Delta\omega_r) \tag{C.86}$$

$$\Delta\omega_r = -\frac{\Delta T_e}{(2HS + K_D)} \qquad\qquad \frac{\mathrm{d}\Delta\delta_r}{dt} = \Delta\omega_r$$

$$\boldsymbol{\Delta\omega\delta} = AH\begin{bmatrix} \Delta T_e \\ \Delta T_m \end{bmatrix} \tag{C.87}$$

$$AH = \begin{bmatrix} \dfrac{-1}{2HS + K_D} & 0 \\ 0 & 0 \end{bmatrix}$$

$$\mathbf{\Delta\omega\delta} = AH.GT_{dq}\mathbf{\Delta i^r_{dqs}} \tag{C.88}$$

Substituting (4.56) in (4.52) to have:

$$\mathbf{\Delta v^r_{dqs}} = ZZ + A\lambda\,.AH.GT_{dq}\mathbf{\Delta i^r_{dqs}} \tag{C.89}$$

$$\mathbf{\Delta v^r_{dqs}} = Z_{synch}\mathbf{\Delta i^r_{dqs}} \tag{C.90}$$

The impedance Z_{synch} represents the impedance of the synchronous machine including the effect of the mechanical part.

1.2. Eigenvalue analysis

$$\frac{d}{dt}\begin{bmatrix} \mathbf{\Delta i^r_{dqs}} \\ \mathbf{\Delta i`^r_{kq12}} \\ \mathbf{\Delta i`^r_{fkd}} \\ \mathbf{\Delta i^r_{mdq}} \\ \mathbf{\Delta\omega\delta} \end{bmatrix} = -D_{syn}^{-1}A_{Syn}\begin{bmatrix} \mathbf{\Delta i^r_{dqs}} \\ \mathbf{\Delta i`^r_{kq12}} \\ \mathbf{\Delta i`^r_{fkd}} \\ \mathbf{\Delta i^r_{mdq}} \\ \mathbf{\Delta\omega\delta} \end{bmatrix} + D_{syn}^{-1}\begin{bmatrix} \mathbf{\Delta v^r_{dqs}} \\ \mathbf{\Delta v`^r_{fkd}} \\ \mathbf{\Delta v`^r_{kq12}} \\ \Delta T_m \\ 0 \end{bmatrix}$$

$$AA = \begin{bmatrix} -L_{ls} - L_{md} & L_{md} & L_{md} & 0 & 0 & 0 & 0 & 0 \\ 0 & 0 & 0 & -L_{ls} - L_{mq} & L_{mq} & L_{mq} & 0 & 0 \\ -L_{md} & \grave{L}_{lkd1} + L_{md} & L_{md} & 0 & 0 & 0 & 0 & 0 \\ -L_{md} & L_{md} & \grave{L}_{lfd} + L_{md} & 0 & 0 & 0 & 0 & 0 \\ 0 & 0 & 0 & -L_{mq} & \grave{L}_{lkq1} + L_{mq} & L_{mq} & 0 & 0 \\ 0 & 0 & 0 & -L_{mq} & L_{mq} & \grave{L}_{lkq2} + L_{mq} & 0 & 0 \\ 0 & 0 & 0 & 0 & 0 & 0 & 2H_1 & 0 \\ 0 & 0 & 0 & 0 & 0 & 0 & 0 & 1 \end{bmatrix}$$

$$EE = \begin{bmatrix} r_s & 0 & 0 & -\omega_r L_{ls} - \omega_r L_{mq} & \omega_r L_{mq} & \omega_r L_{mq} & -L_{ls}i^r_{ds} + L_{mq}\left(-i^{\grave{}r}_{kq2} - i^{\grave{}r}_{kq1} + i^r_{qs}\right) & 0 \\ 0 & r^{\grave{}r}_{kd1} & 0 & 0 & 0 & 0 & 0 & 0 \\ 0 & 0 & r^{\grave{}r}_{fd} & 0 & 0 & 0 & 0 & 0 \\ \omega_r L_{ls} + \omega_r L_{md} & -\omega_r L_{md} & -\omega_r L_{md} & r_s & 0 & 0 & L_{ls}i^r_{ds} - L_{md}\left(i^{\grave{}}_{fd} + i^{\grave{}r}_{kd1} - i^r_{ds}\right) & 0 \\ 0 & 0 & 0 & 0 & r^{\grave{}r}_{kq1} & 0 & 0 & 0 \\ 0 & 0 & 0 & 0 & 0 & r^{\grave{}r}_{kq2} & 0 & 0 \\ \beta 1_T & -\left(\frac{3}{2}\right)\left(\frac{P}{2}\right)L_{md}i^r_{qs} - \left(\frac{3}{2}\right)\left(\frac{P}{2}\right)L_{md}i^r_{qs} & \beta 2_T & \left(\frac{3}{2}\right)\left(\frac{P}{2}\right)L_{mq}i^r_{ds}\left(\frac{3}{2}\right)\left(\frac{P}{2}\right)L_{mq}i^r_{ds} & & -D_1 & 0 \\ 0 & 0 & 0 & 0 & 0 & 0 & 1 & 0 \end{bmatrix}$$

1.3. Derivation of electrical damping of the synchronous machine

Solving (4.50) for the currents Δi^r_{ds} and Δi^r_{qs}:

$$\mathbf{\Delta i^{r}_{dqs}} =$$

$$\left(\frac{1}{Z_{dd}Z_{qq}-Z_{dq}Z_{qd}}\right)\begin{bmatrix} Z_{qq} & -Z_{dq} \\ -Z_{qd} & Z_{dd} \end{bmatrix}\mathbf{\Delta v^{r}_{dqs}} +$$

$$\begin{bmatrix} -Z_{qq}\left(L_{ls}i^{r}_{qs}-L_{mq}i^{r}_{mq}\right)+Z_{dq}\left(L_{ls}i^{r}_{qs}-L_{mq}i^{r}_{mq}\right) & 0 \\ Z_{qd}\left(L_{ls}i^{r}_{qs}-L_{mq}i^{r}_{mq}\right)-Z_{dd}\left(L_{ls}i^{r}_{qs}-L_{mq}i^{r}_{mq}\right) & 0 \end{bmatrix}\mathbf{\Delta\omega\delta}$$

$$\begin{bmatrix} \Delta T_e \\ \Delta T_m \end{bmatrix} =$$

$$\left(\frac{GT_{dq}}{Z_{dd}Z_{qq}-Z_{dq}Z_{qd}}\right)\begin{bmatrix} Z_{qq} & -Z_{dq} \\ -Z_{qd} & Z_{dd} \end{bmatrix}\mathbf{\Delta v^{r}_{dqs}} +$$

$$GT_{dq}\begin{bmatrix} -Z_{qq}\left(L_{ls}i^{r}_{qs}-L_{mq}i^{r}_{mq}\right)+Z_{dq}\left(L_{ls}i^{r}_{qs}-L_{mq}i^{r}_{mq}\right) & 0 \\ Z_{qd}\left(L_{ls}i^{r}_{qs}-L_{mq}i^{r}_{mq}\right)-Z_{dd}\left(L_{ls}i^{r}_{qs}-L_{mq}i^{r}_{mq}\right) & 0 \end{bmatrix}\mathbf{\Delta\omega\delta} \quad \text{(C.91)}$$

1.4. Including the mechanical part of the synchronous machine

The mechanical part is described in including [91] and included into the model as:

Generator: $2H_1 s\Delta\omega_1 = K_{12}(\Delta\delta_2 - \Delta\delta_1) - T_e - D_1(\Delta\omega_1)$

$$\Delta\delta_1 = \frac{\Delta\omega_1}{s}\omega_0 \quad \text{(C.92)}$$

LP_A $2H_2 s\Delta\omega_2 = \Delta T_{LP_A} + k_{23}(\Delta\delta_3 - \Delta\delta_2) - k_{12}(\Delta\delta_2 - \Delta\delta_1) - D_2(\Delta\omega_2)$

$$\Delta\delta_2 = \frac{\Delta\omega_2}{s}\omega_0 \quad \text{(C.93)}$$

LP_B $2H_3 s\Delta\omega_3 = \Delta T_{LP_B} + k_{34}\,(\Delta\delta_4 - \Delta\delta_3) - k_{23}(\Delta\delta_3 - \Delta\delta_2) - D_3(\Delta\omega_3)$ (C.94)

$$\Delta\delta_3 = \frac{\Delta\omega_3}{s}\omega_0$$

IP $2H_4 s\Delta\omega_4 = \Delta T_{IP} + k_{45}\,(\Delta\delta_5 - \Delta\delta_4) - k_{34}(\Delta\delta_4 - \Delta\delta_3) - D_4(\Delta\omega_4)$

$$\Delta\delta_4 = \frac{\Delta\omega_4}{s}\omega_0 \quad \text{(C.95)}$$

HP $2H_5 s\Delta\omega_5 = \Delta T_{HP} - k_{45}(\Delta\delta_5 - \Delta\delta_4) - D_5(\Delta\omega_5)$

$$\Delta\delta_5 = \frac{\Delta\omega_5}{s}\omega_0 \quad \text{(C.96)}$$

By replacing $(\Delta\delta)$ by $\left(\frac{\Delta\omega}{s}\omega_0\right)$ and substitute the equations to have:

$$\Delta\omega_1 =$$

$$\frac{K_{12}\omega_0}{s\mathrm{A}_4A_5}\,\Delta T_{LP_A} + \frac{K_{12}k_{23}\omega_0^2}{s^2A_3\mathrm{A}_4A_5}\Delta T_{LP_B} + \frac{K_{12}k_{23}k_{34}\omega_0^3}{s^3A_2A_3\mathrm{A}_4A_5}\Delta T_{IP} + \frac{K_{12}k_{23}k_{34}k_{45}\omega_0^4}{s^4A_1A_2A_3\mathrm{A}_4A_5}\Delta T_{HP} - \frac{1}{A_5}T_e$$

$$A_5 = 2H_1\mathrm{s} - \frac{(k_{12}\omega_0)^2}{s^2\mathrm{A}_4} + K_{12}\frac{\omega_0}{s} + D_1 \tag{C.97}$$

$$\Delta\omega_2 = \frac{1}{\mathrm{A}_4}\,\Delta T_{LP_A} + \frac{k_{23}\omega_0}{sA_3\mathrm{A}_4}\Delta T_{LP_B} + \frac{k_{23}k_{34}\omega_0^2}{s^2A_2A_3\mathrm{A}_4}\Delta T_{IP} + \frac{k_{23}k_{34}k_{45}\omega_0^3}{s^3A_1A_2A_3\mathrm{A}_4}\Delta T_{HP} + \frac{k_{12}\omega_0}{s\mathrm{A}_4}\Delta\omega_1$$

$$\mathrm{A}_4 = 2H_2s - \frac{(k_{23}\omega_0)^2}{s^2A_3} + k_{23}\frac{\omega_0}{s} + k_{12}\frac{\omega_0}{s} + D_2 \tag{C.98}$$

$$\Delta\omega_3 = \frac{1}{A_3}\Delta T_{LP_B} + \frac{k_{34}\omega_0}{sA_2A_3}\Delta T_{IP} + \frac{k_{34}k_{45}\omega_0^2}{s^2A_1A_2A_3}\Delta T_{HP} + \frac{k_{23}\omega_0}{sA_3}\Delta\omega_2 \tag{C.99}$$

$$A_3 = 2H_3s - \frac{(k_{34}\omega_0)^2}{s^2A_2} + k_{34}\frac{\omega_0}{s} + k_{23}\frac{\omega_0}{s} + D_3$$

$$\Delta\omega_4 = \frac{1}{A_2}\Delta T_{IP} + \frac{k_{45}\omega_0}{sA_1A_2}\Delta T_{HP} + k_{34}\frac{\omega_0}{sA_2}\Delta\omega_3 \tag{C.100}$$

$$A_2 = 2H_4s - \frac{(k_{45}\omega_0)^2}{s^2A_1} + k_{45}\frac{\omega_0}{s} + k_{34}\frac{\omega_0}{s} + D_4$$

$$\Delta\omega_5 = \frac{1}{A_1}\Delta T_{HP} + k_{45}\frac{\omega_0}{sA_1}\Delta\omega_4 \tag{C.101}$$

$$A_1 = 2H_5s + k_{45}\frac{\omega_0}{s} + D_5$$

The relation between the electrical torque including the mechanical part can be found by modifying the equation (C.87) to be on the form:

$$\boldsymbol{\Delta\omega\delta} = AH_M\begin{bmatrix}\Delta T_e\\ \Delta T_m\end{bmatrix} + AH_{M2}\boldsymbol{T_{tu}} \tag{C.102}$$

Where:

$$AH_M = \begin{bmatrix}-\frac{1}{A_5} & 0\\ 0 & 0\end{bmatrix}$$

$$AH_{M2} = \begin{bmatrix}\frac{K_{12}\omega_0}{sA_4A_5} & \frac{K_{12}k_{23}\omega_0^2}{s^2A_3A_4A_5} & \frac{K_{12}k_{23}k_{34}\omega_0^3}{s^3A_2A_3\mathrm{A}_4A_5} & \frac{K_{12}k_{23}k_{45}\omega_0^4}{s^4A_1A_2A_3\mathrm{A}_4A_5}\\ 0 & 0 & 0 & 0\end{bmatrix}$$

$$\boldsymbol{T_{tu}} = [T_{LP_A} \quad T_{LP_B} \quad T_{IP} \quad T_{HP}]^T$$

Substituting equation (4.65) and equation (C.85)into equation (4.52) will have:

$$\mathbf{T_{tu}} = ZZ + A\lambda\,.AH_M.GT_{dq}\mathbf{\Delta i^r_{dqs}} + A\lambda\,.AH_{M2}\mathbf{T_{tu}} \tag{C.103}$$

$$\mathbf{T_{tu}} = Z_{synch\_M}\mathbf{\Delta} \boldsymbol{i}^{\boldsymbol{r}}_{\boldsymbol{dqs}} \tag{C.104}$$

2. Eigenvalue analysis of synchronous machine including the mechanical part

$$\frac{d}{dt} D_{syn} \begin{bmatrix} \mathbf{\Delta i^r_{dqs}} \\ \mathbf{\Delta i`^r_{kq12}} \\ \mathbf{\Delta i`^r_{fkd}} \\ \mathbf{\Delta \delta} \\ \mathbf{\Delta \omega} \end{bmatrix} = AA \begin{bmatrix} \mathbf{\Delta i^r_{dqs}} \\ \mathbf{\Delta i`^r_{kq12}} \\ \mathbf{\Delta i`^r_{fkd}} \\ \mathbf{\Delta \delta} \\ \mathbf{\Delta \omega} \end{bmatrix} + BB \begin{bmatrix} \boldsymbol{T_{tu}} \\ \mathbf{\Delta} \boldsymbol{v}^{`r}_{kq12} \\ \mathbf{\Delta} \boldsymbol{v}^{`r}_{fkd} \\ \mathbf{T_{tu}} \end{bmatrix} \tag{C.105}$$

$$AA = \begin{bmatrix} AA_{11} & AA_{12} & AA_{13} \\ AA_{21} & AA_{22} & AA_{23} \\ AA_{31} & AA_{32} & AA_{33} \end{bmatrix}$$

$$A_{11} = \begin{bmatrix} r_s & 0 & 0 & -\omega_r L_{ls} - \omega_r L_{mq} & \omega_r L_{mq} & \omega_r L_{mq} \\ 0 & r^{`r}_{kd1} & 0 & 0 & 0 & 0 \\ 0 & 0 & r^{`r}_{fd} & 0 & 0 & 0 \\ \omega_r L_{ls} + \omega_r L_{md} & -\omega_r L_{md} & -\omega_r L_{md} & r_s & 0 & 0 \\ 0 & 0 & 0 & 0 & r^{`r}_{kq1} & 0 \\ 0 & 0 & 0 & 0 & 0 & r^{`r}_{kq2} \end{bmatrix}$$

$$AA_{21} = zeros\ [5 \times 6]$$

$$AA_{31} = \begin{bmatrix} \frac{\omega_1}{2H_1}\left(-L_{md} i^r_{qs0} + L_{mq} i^r_{qs0}\right) & \frac{\omega_1}{2H_1}\left(L_{mq} i^r_{ds0} - L_{md}(i^r_{ds0} - i^{`r}_{fd0})\right) & \frac{\omega_1}{2H_1}\left(L_{mq} i^r_{ds0}\right) & \frac{\omega_1}{2H_1}\left(L_{mq} i^r_{ds0}\right) & \frac{-\omega_1}{2H_1}\left(L_{md} i^r_{qs0}\right) & \frac{-\omega_1}{2H_1}\left(L_{md} i^r_{qs0}\right) \\ zeros\ [4 \times 6] \end{bmatrix}$$

$$AA_{32} = \begin{bmatrix} -\frac{k_{12}}{2H_1} & \frac{k_{12}}{2H_1} & 0 & 0 & 0 \\ \frac{k_{12}}{2H_2} & -\frac{k_{23}}{2H_2} - \frac{k_{12}}{2H_2} & \frac{k_{23}}{2H_2} & 0 & 0 \\ 0 & \frac{k_{23}}{2H_3} & -\frac{k_{34}}{2H_3} - \frac{k_{23}}{2H_3} & \frac{k_{34}}{2H_3} & 0 \\ 0 & 0 & \frac{k_{34}}{2H_4} & -\frac{k_{45}}{2H_4} - \frac{k_{34}}{2H_4} & \frac{k_{45}}{2H_4} \\ 0 & 0 & 0 & \frac{k_{45}}{2H_5} & -\frac{k_{45}}{2H_5} \end{bmatrix}$$

$$AA_{12} = Zeros[6 \times 5] \qquad AA_{22} = Zeros[5 \times 5]$$

$$AA_{13} = \begin{bmatrix} -L_{ls} i^r_{ds} + L_{mq}\left(-i^{`r}_{kq2} - i^{`r}_{kq1} + i^r_{qs}\right) & 0 & 0 & 0 & 0 \\ L_{ls} i^r_{ds} - L_{md}\left(i^{`}_{fd} + i^{`r}_{kd1} - i^r_{ds}\right) & 0 & 0 & 0 & 0 \\ 0 & 0 & 0 & 0 & 0 \\ 0 & 0 & 0 & 0 & 0 \\ 0 & 0 & 0 & 0 & 0 \\ 0 & 0 & 0 & 0 & 0 \end{bmatrix}$$

$$AA_{23} = \begin{bmatrix} \omega_0 & 0 & 0 & 0 & 0 \\ 0 & \omega_0 & 0 & 0 & 0 \\ 0 & 0 & \omega_0 & 0 & 0 \\ 0 & 0 & 0 & \omega_0 & 0 \\ 0 & 0 & 0 & 0 & \omega_0 \end{bmatrix} \quad AA_{33} = \begin{bmatrix} -\frac{D_1}{2H_1} & 0 & 0 & 0 & 0 \\ 0 & -\frac{D_2}{2H_2} & 0 & 0 & 0 \\ 0 & 0 & -\frac{D_3}{2H_3} & 0 & 0 \\ 0 & 0 & 0 & -\frac{D_4}{2H_4} & 0 \\ 0 & 0 & 0 & 0 & -\frac{D_5}{2H_5} \end{bmatrix}$$

$$D_{syn} =$$

$$\begin{bmatrix} -L_{ls} - L_{md} & L_{md} & L_{md} & 0 & 0 & 0 & \\ -L_{md} & L_{lkd1}^{`} + L_{md} & L_{md} & 0 & 0 & 0 & \\ -L_{md} & L_{md} & L_{lfd}^{`} + L_{md} & 0 & 0 & 0 & zeros(6 \times 10) \\ 0 & 0 & 0 & -L_{ls} - L_{mq} & L_{mq} & L_{mq} & \\ 0 & 0 & 0 & -L_{mq} & L_{lkq1}^{`} + L_{mq} & L_{mq} & \\ 0 & 0 & 0 & -L_{mq} & L_{mq} & L_{lkq2}^{`} + L_{mq} & \\ & & & zeros(10 \times 6) & & & I(10 \times 6) \end{bmatrix}$$

$$BB = \begin{bmatrix} I(6 \times 6) & & & zeros(6 \times 3) \\ & zeros(6 \times 9) & & \\ & \frac{1}{2H_2} & 0 & 0 & 0 \\ & 0 & \frac{1}{2H_3} & 0 & 0 \\ zeros(4 \times 5) & 0 & 0 & \frac{1}{2H_4} & 0 \\ & 0 & 0 & 0 & \frac{1}{2H_5} \end{bmatrix}$$

The state space equation of the synchronous machine

$$\boldsymbol{\Delta X'} = A\boldsymbol{\Delta X} + B\boldsymbol{\Delta u} \quad , \quad \boldsymbol{\Delta Y} = C\boldsymbol{\Delta X}$$

$$A = inv(D_{syn}) * AA \qquad B = inv(D_{syn}) * BB$$

$$X = \left[\mathbf{\Delta i^r_{dqs}} \quad \mathbf{\Delta i`^r_{kq12}} \quad \mathbf{\Delta i`^r_{fkd}} \quad \mathbf{\Delta\delta} \quad \mathbf{\Delta\omega}\right]^T$$

$$u = \left[\mathbf{\Delta v^r_{dqs}} \quad \mathbf{\Delta v`^r_{kq12}} \quad \mathbf{\Delta v`^r_{fkd}} \quad \Delta T_m \quad \mathbf{T}\right]^T$$

$$C = \begin{bmatrix} 0 & 1 & 0 & 0 & 0 & 0 & 0 & 0 \\ 1 & 0 & 0 & 0 & 0 & 0 & 0 & 0 \end{bmatrix}$$

APPENDIX-D DQ-DYNAMIC PHASOR MODELLING OF STATCOM

1. State-space analysis of STATCOM

$$\Delta x_1' = K_{iid}\Delta x_3 - K_{iid}\Delta i_{sd} - K_{iid}K_{pvd}\Delta v_{dc} + K_{iid}K_{pvd}v_{dc}^* \tag{D.106}$$

$$\Delta x_2' = K_{iiq}\Delta x_4 - \frac{3}{2}K_{iiq}K_{pvq}v_{sq}\Delta i_{sd} + \left(\frac{3}{2}K_{iiq}K_{pvq}v_{sd} - K_{iiq}\right)\Delta i_{sq} + \frac{3}{2}K_{iiq}K_{pvq}i_{sq}\Delta v_{sd} - \frac{3}{2}K_{iiq}K_{pvq}\Delta i_{sd}\Delta v_{sq} + K_{iiq}K_{pvq}Q^* \tag{D.107}$$

$$\Delta x_3' = K_{ivd}v_{dc}^* - K_{ivd}\Delta v_{dc} \tag{D.108}$$

$$\Delta x_4' = -\frac{3}{2}K_{ivq}v_{sq}\Delta i_{sd} + \frac{3}{2}K_{ivq}v_{sd}\Delta i_{sq} + \frac{3}{2}K_{ivq}i_{sq}\Delta v_{sd} - \frac{3}{2}K_{ivq}i_{sd}\Delta v_{sq} + K_{ivq}Q^* \tag{D.109}$$

$$\Delta i_d' = -\frac{1}{L_f}\Delta x_1 - \frac{K_{pid}}{L_f}\Delta x_3 + \left(-\frac{R_f}{L_f} + \frac{K_{pid}}{L_f}\right)\Delta i_{sd} + \omega\Delta i_{sq} + \frac{K_{pid}K_{pvd}}{L_f}\Delta v_{dc} + \frac{1}{L_f}\Delta v_{sd} - \frac{K_{pid}K_{pvd}}{L_f}v_{dc}^* \tag{D.110}$$

$$\Delta i_q' = \frac{1}{L_f}\Delta x_2 + \frac{K_{piq}}{L_f}\Delta x_4 + \left(-\frac{3}{2}\frac{K_{piq}K_{pvq}v_{sq}}{L_f} - \omega\right)\Delta i_{sd} + \left(-\frac{R_f}{L_f} + \frac{3}{2}\frac{K_{piq}K_{pvq}v_{sd}}{L_f} - \frac{K_{piq}}{L_f}\right)\Delta i_{sq} + \frac{3}{2}\frac{K_{piq}K_{pvq}i_{sq}}{L_f}\Delta v_{sd} + \left(\frac{1}{L_f} - \frac{3}{2}\frac{K_{piq}K_{pvq}i_{sd}}{L_f}\right)\Delta v_{sq} + \frac{K_{piq}K_{pvq}}{L_f}Q^* \tag{D.111}$$

$$\Delta v_{dc}' = \frac{3}{2}\frac{i_{sd}}{C_{dc}v_{dc}}v_{sd} + \frac{vs_d - 2i_{sd}.R_f}{C_{dc}v_{dc}}\Delta i_{sd} + \left\{\frac{i_{sd}^2.R_f - \frac{3}{2}vs_d.i_{sd} - \frac{3}{2}vs_q.is_q}{C_{dc}v_{dc}^2}\right\}\Delta v_{dc} + \frac{3}{2}\frac{is_q}{C_{dc}v_{dc}}\Delta v_{sq} + \frac{3}{2}\frac{vs_q}{C_{dc}v_{dc}}\Delta i_{sq} \tag{D.112}$$

The transformation of the equations (D.106) to (D.112) to dynamic phasor is given by:

$$\langle\Delta x_1'\rangle_0 = K_{iid}\langle\Delta x_3\rangle_0 - K_{iid}\langle\Delta is_d\rangle_0 - K_{iid}K_{pvd}\langle\Delta v_{dc}\rangle_0 + K_{iid}K_{pvd}\langle v_{dc}^*\rangle_0 \tag{D.113}$$

$$\langle\Delta x_2'\rangle_0 = K_{iiq}\langle\Delta x_4\rangle_0 - \frac{3}{2}K_{iiq}K_{pvq}\langle v_{sq}\rangle_0\langle\Delta i_{sd}\rangle_0 + \left(\frac{3}{2}K_{iiq}K_{pvq}\langle v_{sd}\rangle_0 - K_{iiq}\right)\langle\Delta i_{sq}\rangle_0 + \frac{3}{2}K_{iiq}K_{pvq}\langle is_q\rangle_0\langle\Delta v_{sd}\rangle_0 - \frac{3}{2}K_{iiq}K_{pvq}\langle i_{sd}\rangle_0\langle\Delta v_{sq}\rangle_0 + K_{iiq}K_{pvq}\langle Q^*\rangle_0 - \frac{3}{2}K_{iiq}K_{pvq}\langle v_{sq}\rangle_{\bar{k}}\langle\Delta i_{sd}\rangle_k + \frac{3}{2}K_{iiq}K_{pvq}\langle vs_d\rangle_{\bar{k}}\langle\Delta i_{sq}\rangle_k + \frac{3}{2}K_{iiq}K_{pvq}\langle i_{sq}\rangle_{\bar{k}}\langle\Delta v_{sd}\rangle_k - \frac{3}{2}K_{iiq}K_{pvq}\langle i_{sd}\rangle_{\bar{k}}\langle\Delta v_{sq}\rangle_k - \frac{3}{2}K_{iiq}K_{pvq}\langle v_{sq}\rangle_k\langle\Delta i_{sd}\rangle_{\bar{k}} + \frac{3}{2}K_{iiq}K_{pvq}\langle v_{sd}\rangle_k\langle\Delta is_q\rangle_{\bar{k}} + \frac{3}{2}K_{iiq}K_{pvq}\langle is_q\rangle_k\langle\Delta v_{sd}\rangle_{\bar{k}} - \frac{3}{2}K_{iiq}K_{pvq}\langle i_{sd}\rangle_k\langle\Delta v_{sq}\rangle_{\bar{k}} \tag{D.114}$$

$$\langle\Delta x_3'\rangle_0 = K_{ivd}\langle v_{dc}^*\rangle_0 - K_{ivd}\langle\Delta v_{dc}\rangle_0 \tag{D.115}$$

$$\langle\Delta x_4'\rangle_0 = -\frac{3}{2}Ki_{vq}\langle v_{sq}\rangle_0\langle\Delta i_{sd}\rangle_0 + \frac{3}{2}Ki_{vq}\langle v_{sd}\rangle_0\langle\Delta i_{sq}\rangle_0 + \frac{3}{2}Ki_{vq}\langle i_{sq}\rangle_0\langle\Delta v_{sd}\rangle_0 - \tag{D.116}$$

$$\frac{3}{2}Ki_{vq}\langle i_{sd}\rangle_0\langle\Delta v_{sq}\rangle_0 + Ki_{vq}\langle Q^*\rangle_0 - \frac{3}{2}Ki_{vq}\langle vs_q\rangle_{\bar{k}}\langle\Delta i_{sd}\rangle_k +$$
$$\frac{3}{2}Ki_{vq}\langle v_{sd}\rangle_{\bar{k}}\langle\Delta i_{sq}\rangle_k + \frac{3}{2}Ki_{vq}\langle i_{sq}\rangle_{\bar{k}}\langle\Delta v_{sd}\rangle_k - \frac{3}{2}Ki_{vq}\langle i_{sd}\rangle_{\bar{k}}\langle\Delta v_{sq}\rangle_k -$$
$$\frac{3}{2}Ki_{vq}\langle vs_q\rangle_k\langle\Delta i_{sd}\rangle_{\bar{k}} + \frac{3}{2}Ki_{vq}\langle vs_d\rangle_k\langle\Delta i_{sq}\rangle_{\bar{k}} + \frac{3}{2}Ki_{vq}\langle i_{sq}\rangle_k\langle\Delta v_{sd}\rangle_{\bar{k}} -$$
$$\frac{3}{2}Ki_{vq}\langle i_{sd}\rangle_k\langle\Delta v_{sq}\rangle_{\bar{k}}$$

$$\langle\Delta i'_{sd}\rangle_0 = -\frac{1}{L_f}\langle\Delta x_1\rangle_0 - \frac{K_{pid}}{L_f}\langle\Delta x_3\rangle_0 + \left(-\frac{R_f}{L_f} + \frac{K_{pid}}{L_f}\right)\langle\Delta i_{sd}\rangle_0 + \omega\langle\Delta i_{sq}\rangle_0 -$$
$$\frac{K_{pid}K_{pvd}}{L_f}\langle\Delta v_{dc}\rangle_0 + \frac{1}{L_f}\langle\Delta v_{sd}\rangle_0 + \frac{K_{pid}K_{pvd}}{L_f}\langle v^*_{dc}\rangle_0 \quad \text{(D.117)}$$

$$\langle\Delta is'_q\rangle_0 = \frac{1}{L_f}\langle\Delta x_2\rangle_0 + \frac{K_{piq}}{L_f}\langle\Delta x_4\rangle_0 + \left(-\omega - \frac{3}{2}\frac{K_{piq}K_{pvq}}{L_f}\langle vs_q\rangle_0\right)\langle\Delta i_{sd}\rangle_0 +$$
$$\left(\frac{3}{2}\frac{K_{piq}K_{pvq}}{L_f}\langle v_{sd}\rangle_0 - \frac{R_f}{L_f} - \frac{K_{piq}}{L_f}\right)\langle\Delta i_{sq}\rangle_0 + \frac{3}{2}\frac{K_{piq}K_{pvq}}{L_f}\langle is_q\rangle_0\langle\Delta v_{sd}\rangle_0 + \left(\frac{1}{L_f} -$$
$$\frac{3}{2}\frac{K_{piq}K_{pvq}}{L_f}\langle i_{sd}\rangle_0\right)\langle\Delta v_{sq}\rangle_0 + \frac{K_{piq}K_{pvq}}{L_f}\langle Q^*\rangle_0 - \frac{3}{2}\frac{K_{piq}K_{pvq}}{L_f}\langle vs_q\rangle_{\bar{k}}\langle\Delta i_{sd}\rangle_k +$$
$$\frac{3}{2}\frac{K_{piq}K_{pvq}}{L_f}\langle vs_d\rangle_{\bar{k}}\langle\Delta i_{sq}\rangle_k + \frac{3}{2}\frac{K_{piq}K_{pvq}}{L_f}\langle i_{sq}\rangle_{k^*}\langle\Delta v_{sd}\rangle_k - \frac{3}{2}\frac{K_{piq}K_{pvq}}{L_f}\langle is_d\rangle_{\bar{k}}\langle\Delta v_{sq}\rangle_k -$$
$$\frac{3}{2}\frac{K_{piq}K_{pvq}}{L_f}\langle vs_q\rangle_k\langle\Delta i_{sd}\rangle_{\bar{k}} + \frac{3}{2}\frac{K_{piq}K_{pvq}}{L_f}\langle vs_d\rangle_k\langle\Delta i_{sq}\rangle_{\bar{k}} + \frac{3}{2}\frac{K_{piq}K_{pvq}}{L_f}\langle i_{sq}\rangle_k\langle\Delta v_{sd}\rangle_{\bar{k}} -$$
$$\frac{3}{2}\frac{K_{piq}K_{pvq}}{L_f}\langle i_{sd}\rangle_k\langle\Delta v_{sq}\rangle_{\bar{k}} \quad \text{(D.118)}$$

For $k = k$

$$\langle\Delta x'_1\rangle_k = K_{iid}\langle\Delta x_3\rangle_k - K_{iid}\langle\Delta i_{sd}\rangle_k - K_{iid}K_{pvd}\langle\Delta v_{dc}\rangle_k + K_{iid}K_{pvd}\langle v^*_{dc}\rangle_k -$$
$$jk\omega\langle\Delta x_1\rangle_k \quad \text{(D.119)}$$

$$\langle\Delta x'_2\rangle_k =$$
$$-\frac{3}{2}K_{iiq}K_{pvq}\langle v_{sq}\rangle_k\langle\Delta i_{sd}\rangle_0 + \frac{3}{2}K_{iiq}K_{pvq}\langle v_{sd}\rangle_k\langle\Delta i_{sq}\rangle_0 +$$
$$\frac{3}{2}K_{iiq}K_{pvq}\langle i_{sq}\rangle_k\langle\Delta v_{sd}\rangle_0 - \frac{3}{2}K_{iiq}K_{pvq}\langle i_{sd}\rangle_k + K_{iiq}\langle\Delta x_4\rangle_k -$$
$$\frac{3}{2}K_{iiq}K_{pvq}\langle v_{sq}\rangle_0\langle\Delta i_{sd}\rangle_k + \frac{3}{2}K_{iiq}K_{pvq}\langle v_{sd}\rangle_0\langle\Delta is_q\rangle_k - K_{iiq}\langle\Delta i_{sq}\rangle_k +$$
$$\frac{3}{2}K_{iiq}K_{pvq}\langle i_{sq}\rangle_0\langle\Delta v_{sd}\rangle_k - \frac{3}{2}K_{iiq}K_{pvq}\langle i_{sd}\rangle_0\langle\Delta v_{sq}\rangle_k + K_{iiq}K_{pvq}\langle Q^*\rangle_k -$$
$$jk\omega\langle\Delta x_2\rangle_k \quad \text{(D.120)}$$

$$\langle\Delta x'_3\rangle_k = K_{ivd}\langle v^*_{dc}\rangle_k - K_{ivd}\langle\Delta v_{dc}\rangle_k - jk\omega\langle\Delta x_3\rangle_k \quad \text{(D.121)}$$

$$\langle\Delta x'_4\rangle_k = -\frac{3}{2}K_{ivq}\langle v_{sq}\rangle_k\langle\Delta i_{sd}\rangle_0 + \frac{3}{2}K_{ivq}\langle v_{sd}\rangle_k\langle\Delta i_{sq}\rangle_0 + \frac{3}{2}K_{ivq}\langle i_{sq}\rangle_k\langle\Delta v_{sd}\rangle_0 -$$
$$\frac{3}{2}K_{ivq}\langle i_{sd}\rangle_k\langle\Delta vs_q\rangle_0 - \frac{3}{2}K_{ivq}\langle v_{sq}\rangle_0\langle\Delta i_{sd}\rangle_k + \frac{3}{2}K_{ivq}\langle vs_d\rangle_0\langle\Delta i_{\mathrm{sq}}\rangle_k + \quad \text{(D.122)}$$

$$\frac{3}{2}K_{ivq}\langle i_{sq}\rangle_0\langle\Delta v_{sd}\rangle_k - \frac{3}{2}K_{ivq}\langle i_{sd}\rangle_0\langle\Delta vs_q\rangle_k + K_{ivq}\langle Q^*\rangle_k - jk\omega\langle\Delta x_4\rangle_k$$

$$\begin{aligned}\langle\Delta i'_{sd}\rangle_k \;&= -\frac{1}{L_f}\langle\Delta x_1\rangle_k - \frac{K_{pid}}{L_f}\langle\Delta x_3\rangle_k + \left(-\frac{R_f}{L_f} + \frac{K_{pid}}{L_f}\right)\langle\Delta i_{sd}\rangle_k + \omega\langle\Delta i_{sq}\rangle_k + \\ &\frac{K_{pid}K_{pvd}}{L_f}\langle\Delta v_{dc}\rangle_k + + \frac{1}{L_f}\langle\Delta v_{sd}\rangle_k - \frac{K_{pid}K_{pvd}}{L_f}\langle v^*_{dc}\rangle_k - jk\omega\langle\Delta i_{sd}\rangle_k\end{aligned} \tag{D.123}$$

$$\begin{aligned}&\langle\Delta is'_q\rangle_k = \\ &-\frac{3}{2}\frac{K_{piq}K_{pvq}}{L_f}\langle v_{sq}\rangle_k\langle\Delta i_{sd}\rangle_0 + \frac{3}{2}\frac{K_{piq}K_{pvq}}{L_f}\langle v_{sd}\rangle_k\langle\Delta i_{sq}\rangle_0 + \frac{3}{2}\frac{K_{piq}K_{pvq}}{L_f}\langle is_q\rangle_k\langle\Delta v_{sd}\rangle_0 - \\ &\frac{3}{2}\frac{K_{piq}K_{pvq}}{L_f}\langle i_{sd}\rangle_k\langle\Delta v_{sq}\rangle_0 + \frac{1}{L_f}\langle\Delta x_2\rangle_k + \frac{Kp_{iq}}{L_f}\langle\Delta x_4\rangle_k + \\ &\left(-\omega - \frac{3}{2}\frac{K_{piq}K_{pvq}}{L_f}\langle v_{sq}\rangle_0\right)\langle\Delta i_{sd}\rangle_k + \\ &\left(\frac{3}{2}\frac{K_{piq}K_{pvq}}{L_f}\langle v_{sd}\rangle_0 - \frac{R_f}{L_f} - \frac{Kp_{iq}}{L_f} - jk\omega\right)\langle\Delta i_{sq}\rangle_k + \frac{3}{2}\frac{K_{piq}K_{pvq}}{L_f}\langle i_{\mathrm{sq}}\rangle_0\langle\Delta v_{sd}\rangle_k + \\ &\left(\frac{1}{L_f} - \frac{3}{2}\frac{K_{piq}K_{pvq}}{L_f}\langle i_{sd}\rangle_0\right)\langle\Delta v_{sq}\rangle_k + \frac{Kp_{iq}Kp_{vq}}{L_f}\langle Q^*\rangle_k\end{aligned} \tag{D.124}$$

For $k = \bar{k}$ (D.125)

$$\langle\Delta x'_1\rangle_{\bar{k}} = Ki_{id}\langle\Delta x_3\rangle_{\bar{k}} - Ki_{id}\langle\Delta i_{sd}\rangle_{\bar{k}} - Ki_{id}Kp_{vd}\langle\Delta v_{dc}\rangle_{\bar{k}} + Ki_{id}Kp_{vd}\langle v^*_{dc}\rangle_{\bar{k}} + jk\omega\langle\Delta x_1\rangle_{\bar{k}} \tag{D.126}$$

$$\begin{aligned}\langle\Delta x'_2\rangle_{\bar{k}} &= -\frac{3}{2}Ki_{iq}Kp_{vq}\langle vs_q\rangle_{\bar{k}}\langle\Delta i_{sd}\rangle_0 + \frac{3}{2}Ki_{iq}Kp_{vq}\langle v_{sd}\rangle_{\bar{k}}\langle\Delta i_{sq}\rangle_0 + \\ &\frac{3}{2}Ki_{iq}Kp_{vq}\langle i_{sq}\rangle_{\bar{k}}\langle\Delta v_{sd}\rangle_0 - \frac{3}{2}Ki_{iq}Kp_{vq}\langle i_{sd}\rangle_{\bar{k}}\langle\Delta v_{sq}\rangle_0 + Ki_{iq}\langle\Delta x_4\rangle_{\bar{k}} - \\ &\frac{3}{2}Ki_{iq}Kp_{vq}\langle v_{sq}\rangle_0\langle\Delta i_{sd}\rangle_{\bar{k}} + \frac{3}{2}Ki_{iq}Kp_{vq}\langle v_{sd}\rangle_0\langle\Delta i_{sq}\rangle_{\bar{k}} - Ki_{iq}\langle\Delta i_{sq}\rangle_{\bar{k}} + \\ &\frac{3}{2}Ki_{iq}Kp_{vq}\langle i_{sq}\rangle_0\langle\Delta v_{sd}\rangle_{\bar{k}} - \frac{3}{2}Ki_{iq}Kp_{vq}\langle i_{sd}\rangle_0\langle\Delta v_{sq}\rangle_{\bar{k}} + Ki_{iq}Kp_{vq}\langle Q^*\rangle_{\bar{k}} + \\ &jk\omega\langle\Delta x_2\rangle_{\bar{k}}\end{aligned} \tag{D.127}$$

$$\langle\Delta x'_3\rangle_{\bar{k}} = K_{ivd}\langle v^*_{dc}\rangle_{\bar{k}} - K_{ivd}\langle\Delta v_{dc}\rangle_{\bar{k}} + jk\omega\langle\Delta x_3\rangle_{\bar{k}} \tag{D.128}$$

$$\begin{aligned}\langle\Delta x'_4\rangle_{\bar{k}} &= -\frac{3}{2}K_{ivq}\langle v_{sq}\rangle_{\bar{k}}\langle\Delta i_{sd}\rangle_0 + \frac{3}{2}K_{ivq}\langle v_{sd}\rangle_{\bar{k}}\langle\Delta i_{sq}\rangle_0 + \frac{3}{2}K_{ivq}\langle i_{sq}\rangle_{\bar{k}}\langle\Delta v_{sd}\rangle_0 - \\ &\frac{3}{2}K_{ivq}\langle i_{sd}\rangle_{\bar{k}}\langle\Delta v_{sq}\rangle_0 - \frac{3}{2}K_{ivq}\langle v_{sq}\rangle_0\langle\Delta i_{sd}\rangle_{\bar{k}} + \frac{3}{2}K_{ivq}\langle v_{sd}\rangle_0\langle\Delta i_{sq}\rangle_{\bar{k}} + \\ &\frac{3}{2}K_{ivq}\langle i_{sq}\rangle_0\langle\Delta v_{sd}\rangle_{\bar{k}} - \frac{3}{2}K_{ivq}\langle i_{sq}\rangle_0\langle\Delta v_{sq}\rangle_{\bar{k}} + K_{ivq}\langle Q^*\rangle_{\bar{k}} + jk\omega\langle\Delta x_4\rangle_{\bar{k}}\end{aligned} \tag{D.129}$$

$$\begin{aligned}\langle\Delta i'_{sd}\rangle_{\bar{k}} \;&= -\frac{1}{L_f}\langle\Delta x_1\rangle_{\bar{k}} - \frac{K_{pid}}{L_f}\langle\Delta x_3\rangle_{\bar{k}} + \left(-\frac{R_f}{L_f} + \frac{K_{pid}}{L_f}\right)\langle\Delta i_{sd}\rangle_{\bar{k}} + \omega\langle\Delta i_{sq}\rangle_{\bar{k}} + \\ &\frac{K_{pid}K_{pvd}}{L_f}\langle\Delta v_{dc}\rangle_{\bar{k}} + \frac{1}{L_f}\langle\Delta v_{sd}\rangle_{\bar{k}} - \frac{K_{pid}K_{pvd}}{L_f}\langle v^*_{dc}\rangle_{\bar{k}} + jk\omega\langle\Delta i_{sd}\rangle_{\bar{k}}\end{aligned} \tag{D.130}$$

$$\langle \Delta is'_q \rangle_{\bar{k}} =$$
$$-\frac{3}{2}\frac{K_{piq}K_{pvq}}{L_f}\langle v_{sq}\rangle_{\bar{k}}\langle \Delta i_{sd}\rangle_0 + \frac{3}{2}\frac{K_{piq}K_{pvq}}{L_f}\langle v_{sd}\rangle_{\bar{k}}\langle \Delta i_{sq}\rangle_0 + \frac{3}{2}\frac{K_{piq}K_{pvq}}{L_f}\langle i_{sq}\rangle_k\langle \Delta v_{sd}\rangle_0 -$$
$$\frac{3}{2}\frac{K_{piq}K_{pvq}}{L_f}\langle i_{sd}\rangle_k\langle \Delta v_{sq}\rangle_0 + \frac{1}{L_f}\langle \Delta x_2\rangle_{\bar{k}} + \frac{K_{piq}}{L_f}\langle \Delta x_4\rangle_{\bar{k}} +$$
$$\left(-\omega - \frac{3}{2}\frac{K_{piq}K_{pvq}}{L_f}\langle v_{sq}\rangle_0\right)\langle \Delta i_{sd}\rangle_{\bar{k}} + \tag{D.131}$$
$$\left(\frac{3}{2}\frac{K_{piq}K_{pvq}}{L_f}\langle v_{sd}\rangle_0 - \frac{R_f}{L_f} - \frac{Kp_{iq}}{L_f} + jk\omega\right)\langle \Delta i_{sq}\rangle_{\bar{k}} + \frac{3}{2}\frac{K_{piq}K_{pvq}}{L_f}\langle i_{sq}\rangle_0\langle \Delta v_{sd}\rangle_{\bar{k}} +$$
$$\left(\frac{1}{L_f} - \frac{3}{2}\frac{K_{piq}K_{pvq}}{L_f}\langle i_{sd}\rangle_0\right)\langle \Delta v_{sq}\rangle_{\bar{k}} + \frac{K_{piq}K_{pvq}}{L_f}\langle Q^*\rangle_{\bar{k}}$$

The dc voltage at the fundamental frequency is derived as:

$$\langle \Delta v'_{dc}\rangle_0 =$$
$$\langle \frac{3}{2}\frac{i_{sd}}{C_{dc}v_{dc}}\Delta v_{sd}\rangle_0 + \langle \frac{\frac{3}{2}v_{sd}-2i_{sd}.R_f}{C_{dc}v_{dc}}\Delta i_{sd}\rangle_0 + \langle \left\{\frac{i_{sd}^2.R_f-\frac{3}{2}v_{sd}i_{sd}-\frac{3}{2}v_{sq}.i_{sq}}{C_{dc}v_{dc}^2}\right\}\Delta v_{dc}\rangle_0 +$$
$$\langle \frac{3}{2}\frac{i_{sq}}{C_{dc}v_{dc}}\Delta v_{sq}\rangle_0 + \langle \frac{3}{2}\frac{v_{sq}}{C_{dc}v_{dc}}\Delta i_{sq}\rangle_0$$

$$\langle \Delta v'_{dc}\rangle_0 =$$
$$\langle \frac{\frac{3}{2}v_{sd}-2i_{sd}.R_f}{C_{dc}v_{dc}}\rangle_0 \langle \Delta i_{sd}\rangle_0 + \langle \frac{3}{2}\frac{vs_q}{C_{dc}v_{dc}}\rangle_0 \langle \Delta i_{sq}\rangle_0 + \langle \frac{i_{sd}^2.R_f-\frac{3}{2}v_{sd}i_{sd}-\frac{3}{2}v_{sq}.i_{sq}}{C_{dc}v_{dc}^2}\rangle_0 \langle \Delta v_{dc}\rangle_0 +$$
$$\langle \frac{3}{2}\frac{i_{sd}}{C_{dc}v_{dc}}\rangle_0 \langle \Delta v_{sd}\rangle_0 + \langle \frac{3}{2}\frac{i_{sq}}{C_{dc}v_{dc}}\rangle_0 \langle v_{sq}\rangle_0 + \langle \frac{\frac{3}{2}v_{sd}-2i_{sd}.R_f}{C_{dc}v_{dc}}\rangle_{\bar{k}} \langle \Delta i_{sd}\rangle_k +$$
$$\langle \frac{3}{2}\frac{v_{sq}}{C_{dc}v_{dc}}\rangle_{\bar{k}} \langle \Delta i_{sq}\rangle_k + \langle \frac{i_{sd}^2.R_f-\frac{3}{2}v_{sd}i_{sd}-\frac{3}{2}v_{sq}.i_{sq}}{C_{dc}v_{dc}^2}\rangle_{\bar{k}} \langle \Delta v_{dc}\rangle_k + \langle \frac{3}{2}\frac{i_{sd}}{C_{dc}v_{dc}}\rangle_{\bar{k}} \langle \Delta v_{sd}\rangle_k + \tag{D.132}$$
$$\langle \frac{3}{2}\frac{i_{sq}}{C_{dc}v_{dc}}\rangle_{\bar{k}} \langle \Delta v_{sq}\rangle_k + \langle \frac{\frac{3}{2}v_{sd}-2i_{sd}.R_f}{C_{dc}v_{dc}}\rangle_k \langle \Delta i_{sd}\rangle_{\bar{k}} + \langle \frac{3}{2}\frac{v_{sq}}{C_{dc}v_{dc}}\rangle_k \langle \Delta i_{sq}\rangle_{\bar{k}} +$$
$$\langle \frac{i_{sd}^2.R_f-\frac{3}{2}v_{sd}i_{sd}-\frac{3}{2}v_{sq}.i_{sq}}{C_{dc}v_{dc}^2}\rangle_k \langle \Delta v_{dc}\rangle_{\bar{k}} + \langle \frac{3}{2}\frac{i_{sd}}{C_{dc}v_{dc}}\rangle_k \langle \Delta v_{sd}\rangle_{\bar{k}} + \langle \frac{3}{2}\frac{i_{sq}}{C_{dc}v_{dc}}\rangle_k \langle \Delta v_{sq}\rangle_{\bar{k}}$$

$$\langle \Delta v'_{dc}\rangle_k =$$
$$\langle \frac{\frac{3}{2}v_{sd}-2i_{sd}.R_f}{C_{dc}v_{dc}}\rangle_k \langle \Delta i_{sd}\rangle_0 + \langle \frac{3}{2}\frac{v_{sq}}{C_{dc}v_{dc}}\rangle_k \langle \Delta i_{sq}\rangle_0 + \langle \frac{i_{sd}^2.R_f-\frac{3}{2}v_{sd}i_{sd}-\frac{3}{2}v_{sq}.i_{sq}}{C_{dc}v_{dc}^2}\rangle_k \langle \Delta v_{dc}\rangle_0 +$$
$$\langle \frac{3}{2}\frac{i_{sd}}{C_{dc}v_{dc}}\rangle_k \langle \Delta v_{sd}\rangle_0 + \langle \frac{3}{2}\frac{i_{sq}}{C_{dc}v_{dc}}\rangle_k \langle \Delta v_{sq}\rangle_0 + \langle \frac{\frac{3}{2}v_{sd}-2i_{sd}.R_f}{C_{dc}v_{dc}}\rangle_0 \langle \Delta i_{sd}\rangle_k + \tag{D.133}$$
$$\langle \frac{3}{2}\frac{v_{sq}}{C_{dc}v_{dc}}\rangle_0 \langle \Delta i_{sq}\rangle_k + \left\{\langle \frac{i_{sd}^2.R_f-\frac{3}{2}v_{sd}i_{sd}-\frac{3}{2}v_{sq}.i_{sq}}{C_{dc}v_{dc}^2}\rangle_0 - jk\omega\right\}\langle \Delta v_{dc}\rangle_k +$$
$$\langle \frac{3}{2}\frac{i_{sd}}{C_{dc}v_{dc}}\rangle_0 \langle \Delta v_{sd}\rangle_k + \langle \frac{3}{2}\frac{i_{sq}}{C_{dc}v_{dc}}\rangle_0 \langle \Delta v_{sq}\rangle_k$$

$$\langle \Delta v'_{dc} \rangle_{\bar{k}} =$$

$$+ \langle \frac{\frac{3}{2}v_{sd} - 2i_{sd}.R_f}{C_{dc}v_{dc}} \rangle_{\bar{k}} \langle \Delta i_{sd} \rangle_0 + \langle \frac{3}{2}\frac{v_{sq}}{C_{dc}v_{dc}} \rangle_{\bar{k}} \langle \Delta i_{sq} \rangle_0 + \langle \frac{i_{sd}^2.R_f - \frac{3}{2}v_{sd}i_{sd} - \frac{3}{2}v_{sq}.i_{sq}}{C_{dc}v_{dc}^2} \rangle_{\bar{k}} \langle \Delta v_{dc} \rangle_0 +$$

$$\langle \frac{3}{2}\frac{i_{sd}}{C_{dc}v_{dc}} \rangle_{\bar{k}} \langle \Delta v_{sd} \rangle_0 + \langle \frac{3}{2}\frac{i_{sq}}{C_{dc}v_{dc}} \rangle_{\bar{k}} \langle \Delta v_{sq} \rangle_0 + \langle \frac{\frac{3}{2}v_{sd} - 2i_{sd}.R_f}{C_{dc}v_{dc}} \rangle_0 \langle \Delta i_{sd} \rangle_{\bar{k}} + \quad \text{(D.134)}$$

$$\langle \frac{3}{2}\frac{v_{sq}}{C_{dc}v_{dc}} \rangle_0 \langle \Delta i_{sq} \rangle_{\bar{k}} + \left\{ \langle \frac{i_{sd}^2.R_f - \frac{3}{2}v_{sd}i_{sd} - \frac{3}{2}v_{sq}.i_{sq}}{C_{dc}v_{dc}^2} \rangle_0 + jk\omega \right\} \langle \Delta v_{dc} \rangle_{\bar{k}} +$$

$$\langle \frac{3}{2}\frac{i_{sd}}{C_{dc}v_{dc}} \rangle_0 \langle \Delta v_{sd} \rangle_{\bar{k}} + \langle \frac{3}{2}\frac{i_{sq}}{C_{dc}v_{dc}} \rangle_0 \langle \Delta v_{sq} \rangle_{\bar{k}}$$

The arrangement of equations (D.113) to (D.134) as a generalised matrices

$$\begin{bmatrix} \langle \Delta X' \rangle_0 \\ \langle \Delta X' \rangle_k \\ \langle \Delta X' \rangle_{\bar{k}} \\ \vdots \\ \langle \Delta X' \rangle_{k_n} \\ \langle \Delta X' \rangle_{\overline{k_n}} \end{bmatrix} = A_{DP} \begin{bmatrix} \langle \Delta X \rangle_0 \\ \langle \Delta X \rangle_k \\ \langle \Delta X \rangle_{\bar{k}} \\ \vdots \\ \langle \Delta X \rangle_{k_n} \\ \langle \Delta X \rangle_{\overline{k_n}} \end{bmatrix} + B_{DP} \begin{bmatrix} \langle u \rangle_0 \\ \langle u \rangle_k \\ \langle u \rangle_{\bar{k}} \\ \vdots \\ \langle u \rangle_{k_n} \\ \langle u \rangle_{\overline{k_n}} \end{bmatrix} \quad \text{(D.135)}$$

$$A_{DP} = \begin{bmatrix} A_{0,0} & A_{0,k_1} & A_{0\overline{k_1}} & \dots & A_{0,k_2} & A_{0,\overline{k_2}} \\ A_{k_1,0} & A_{k_1,k_1} & 0 & 0 & 0 & 0 \\ A_{\overline{k_1},0} & 0 & A_{\overline{k_1}\overline{k_1}} & & \cdots & \vdots \\ \vdots & & & \ddots & & \\ A_{kn,0} & A_{kn,k_1} & & \cdots & A_{kn,kn} & 0 \\ A_{\overline{kn},0} & A_{\overline{kn},k1} & & \cdots & 0 & A_{\overline{kn},\overline{kn}} \end{bmatrix},$$

$$B_{DP} = \begin{bmatrix} B_0 \\ B_{k_1} \\ B_{\overline{k_1}} \\ \vdots \\ B_{kn} \\ B_{\overline{kn}} \end{bmatrix} \qquad A_{DP} = \begin{bmatrix} a_{k=0} & ac_{k=\overline{k_1}} & ac_{k=k_1} & \cdots & ac_{k=\overline{k_n}} & ac_{k=k_n} \\ ac_{k=k_1} & a_{k=k_1} & & & 0 & 0 \\ ac_{k=\overline{k_1}} & & a_{k=\overline{k_1}} & & 0 & 0 \\ \vdots & & & \ddots & & \vdots \\ & 0 & 0 & & a_{k=kn} & \\ ac_{k=\overline{k_n}} & 0 & 0 & \cdots & & a_{\overline{k_n}} \end{bmatrix}$$

$a_{k,k}$

$$= \begin{bmatrix} -jk\omega & 0 & K_{iid} & 0 & -K_{iid} & 0 & -K_{iid}K_{pvd} \\ 0 & -jk\omega & 0 & K_{iiq} & -\frac{3}{2}K_{iiq}K_{pvq}\langle v_{sq} \rangle_0 & \frac{3}{2}K_{iiq}K_{pvq}\langle v_{sd} \rangle_0 - Ki_{iq} & 0 \\ 0 & 0 & -jk\omega & 0 & 0 & 0 & -K_{ivd} \\ 0 & 0 & 0 & -jk\omega & -\frac{3}{2}K_{ivq}\langle v_{sq} \rangle_0 & \frac{3}{2}K_{ivq}\langle v_{sd} \rangle_0 & 0 \\ \frac{1}{L_f} & 0 & \frac{K_{pid}}{L_f} & 0 & \left(-\frac{R_f}{L_f} - \frac{K_{pid}}{L_f} - jk\omega \right) & \omega & -\frac{K_{pid}K_{pvd}}{L_f} \\ 0 & \frac{1}{L_f} & 0 & \frac{Kp_{iq}}{L_f} & -\omega - \frac{3}{2}\frac{K_{piq}K_{pvq}}{L_f}\langle v_{sq} \rangle_0 & \frac{3}{2}\frac{K_{piq}K_{pvq}}{L_f}\langle v_{sd} \rangle_0 - \frac{R_f}{L_f} - \frac{K_{piq}}{L_f} - jk\omega & 0 \\ 0 & 0 & 0 & 0 & \alpha_1 & \alpha 2 & \alpha 3 - jk\omega \end{bmatrix}$$

$$\alpha_1 = \frac{3}{2}\langle\frac{v_{sd}}{C_{dc}v_{dc}}\rangle_0 - \langle\frac{2R_f i_{sd}}{C_{dc}v_{dc}}\rangle_0$$

$$\alpha 2 = \frac{3}{2}\langle\frac{v_{sq}}{C_{dc}v_{dc}}\rangle_0$$

$$\alpha 3 = \langle\frac{i_{sd}^2.R_f}{C_{dc}v_{dc}^2}\rangle_0 - \frac{3}{2}\langle\frac{v_{sd}i_{sd}}{C_{dc}v_{dc}^2}\rangle_0 - \frac{3}{2}\langle\frac{v_{sq}i_{sq}}{C_{dc}v_{dc}^2}\rangle_0$$

$$ac_{0,k} = \begin{bmatrix} 0 & 0 & 0 & 0 & 0 & 0 & 0 \\ 0 & 0 & 0 & 0 & -\frac{3}{2}K_{iiq}K_{pvq}\langle v_{sq}\rangle_{\bar{k}} & \frac{3}{2}K_{iiq}K_{pvq}\langle v_{sd}\rangle_{\bar{k}} & 0 \\ 0 & 0 & 0 & 0 & 0 & 0 & 0 \\ 0 & 0 & 0 & 0 & -\frac{3}{2}K_{ivq}\langle v_{sq}\rangle_{\bar{k}} & \frac{3}{2}K_{ivq}\langle v_{sd}\rangle_{\bar{k}} & 0 \\ 0 & 0 & 0 & 0 & 0 & 0 & 0 \\ 0 & 0 & 0 & 0 & -\frac{3}{2}\frac{K_{piq}K_{pvq}}{L_f}\langle v_{sq}\rangle_{\bar{k}} & \frac{3}{2}\frac{K_{piq}K_{pvq}}{L_f}\langle v_{sd}\rangle_0 - \frac{R_f}{L_f} - \frac{K_{piq}}{L_f} & 0 \\ 0 & 0 & 0 & 0 & \alpha 4 & \alpha 5 & \alpha 6 \end{bmatrix}$$

$$\alpha 4 = \frac{3}{2}\langle\frac{v_{sd}}{C_{dc}v_{dc}}\rangle_{\bar{k}} - \langle\frac{2R_f i_{sd}}{C_{dc}v_{dc}}\rangle_{\bar{k}} \qquad \alpha 5 = \frac{3}{2}\langle\frac{v_{sq}}{C_{dc}v_{dc}}\rangle_{\bar{k}} \qquad \alpha 6 = \langle\frac{i_{sd}^2.R_f}{C_{dc}v_{dc}^2}\rangle_{\bar{k}} - \frac{3}{2}\langle\frac{v_{sd}i_{sd}}{C_{dc}v_{dc}^2}\rangle_{\bar{k}} - \frac{3}{2}\langle\frac{v_{sq}i_{sq}}{C_{dc}v_{dc}^2}\rangle_{\bar{k}}$$

$$B_{DP} = \begin{bmatrix} b_{k=0} & bc_{k=\overline{k_1}} & bc_{k=k_1} & \cdots & bc_{k=\overline{k_n}} & bc_{k=k_n} \\ bc_{k=k_1} & b_{k=k_1} & & & 0 & 0 \\ bc_{k=\overline{k_1}} & & b_{k=\overline{k_1}} & & 0 & 0 \\ \vdots & & & \ddots & & \vdots \\ bc_{k=k_n} & 0 & 0 & & b_{k=kn} & \\ bc_{k=\overline{k_n}} & 0 & 0 & \cdots & & b_{k=\overline{k_n}} \end{bmatrix}$$

$$B_{k,k} = \begin{bmatrix} 0 & 0 & K_{iid}K_{pvd} & 0 \\ \frac{3}{2}K_{iiq}K_{pvq}\langle i_{sq}\rangle_0 & -\frac{3}{2}K_{iiq}K_{pvq}\langle i_{sd}\rangle_0 & 0 & K_{iiq}K_{pvq} \\ 0 & 0 & Ki_{vd} & 0 \\ \frac{3}{2}K_{ivq}\langle i_{sq}\rangle_0 & -\frac{3}{2}K_{ivq}\langle i_{sd}\rangle_0 & 0 & Ki_{vq} \\ \frac{1}{L_f} & 0 & \frac{Kp_{id}Kp_{vd}}{L_f} & 0 \\ \frac{3}{2}\frac{K_{piq}K_{pvq}}{L_f}\langle i_{sq}\rangle_0 & \frac{1}{L_f} - \frac{3}{2}\frac{K_{piq}K_{pvq}}{L_f}\langle i_{sd}\rangle_0 & 0 & \frac{K_{piq}K_{pvq}}{L_f} \\ \frac{3}{2}\langle\frac{i_{sd}}{C_{dc}v_{dc}}\rangle_0 & \frac{3}{2}\langle\frac{i_{sq}}{C_{dc}v_{dc}}\rangle_0 & 0 & 0 \end{bmatrix}$$

$$bc_{k=k} = \begin{bmatrix} Zeros(6\times 4) & & & \\ \frac{3}{2}\langle\frac{i_{sd}}{C_{dc}v_{dc}}\rangle_k & \frac{3}{2}\langle\frac{i_{sq}}{C_{dc}v_{dc}}\rangle_k & 0 & 0 \end{bmatrix}$$

2. The impedance analysis of STATCOM

Using the synchronous dq model, the transformation to dq-dynamic phasor results:

$$\begin{bmatrix}\langle \Delta v_{sd}\rangle_0\\ \langle \Delta v_{Sq}\rangle_0\\ \langle \Delta v_{sd}\rangle_k\\ \langle \Delta v_{sq}\rangle_k\\ \langle \Delta v_{sd}\rangle_{\bar{k}}\\ \langle \Delta v_{sq}\rangle_{\bar{k}}\end{bmatrix} = A_z \begin{bmatrix}\langle \Delta i_{sd}\rangle_0\\ \langle \Delta i_{sq}\rangle_0\\ \langle \Delta i_{sd}\rangle_k\\ \langle \Delta i_{sq}\rangle_k\\ \langle \Delta i_{sd}\rangle_{\bar{k}}\\ \langle \Delta i_{sq}\rangle_{\bar{k}}\end{bmatrix} + B_z \begin{bmatrix}\langle \Delta i^*_{sd}\rangle_0\\ \langle \Delta i^*_{sq}\rangle_0\\ \langle \Delta i^*_{sd}\rangle_k\\ \langle \Delta i^*_{sq}\rangle_k\\ \langle \Delta i^*_{sd}\rangle_{\bar{k}}\\ \langle \Delta i^*_{sq}\rangle_{\bar{k}}\end{bmatrix} \tag{D.136}$$

$$A_z = \begin{bmatrix} hd_{k=0} & hl_{k=\overline{k_1}} & hl_{k=k_1} & & hl_{k=k_n}\\ hl_{k=k_1} & hd_{k=k_1} & 0 & & 0\\ hl_{k=\overline{k_1}} & 0 & hd_{k=\overline{k_1}} & & 0\\ & 0 & 0 & \ddots & 0\\ hl_{k=\overline{k_n}} & 0 & 0 & & hd_{k=\overline{k_n}}\end{bmatrix}$$

$$hl_{k=k_1} = \begin{bmatrix} -\langle \frac{K_{iid}}{s+jk\omega}\rangle_k & 0\\ 0 & -\langle \frac{K_{iiq}}{s+jk\omega}\rangle_k\end{bmatrix}$$

$$hd_k = \begin{bmatrix} L_f(s+jk\omega) + R_f - \langle K_{pid} + \frac{K_{iid}}{s}\rangle_0 & -\omega L_f\\ \omega L_f & L_f(s+jk\omega) + R_f - \langle K_{piq} + \frac{K_{iiq}}{s}\rangle_0\end{bmatrix}$$

$$hl_{k=\overline{k_1}} = \begin{bmatrix} -\langle \frac{K_{iid}}{s-jk\omega}\rangle_{k^*} & 0\\ 0 & -\langle \frac{K_{iiq}}{s-jk\omega}\rangle_{k^*}\end{bmatrix}$$

$$B_z = \begin{bmatrix} Bd_{k=0} & Bl_{k=\overline{k_1}} & Bl_{k=k_1} & & Bl_{k=k_n}\\ Bl_{k=k_1} & bd_{k=k_1} & 0 & & 0\\ Bl_{k=\overline{k_1}} & 0 & Bd_{k=\overline{k_1}} & & 0\\ & 0 & 0 & \ddots & 0\\ Bl_{k=\overline{k_n}} & 0 & 0 & & Bd_{k=\overline{k_n}}\end{bmatrix}$$

$$Bd_k = \begin{bmatrix} \langle K_{pid} + \frac{K_{iid}}{s}\rangle_0 & 0\\ 0 & \langle K_{piq} + \frac{K_{iiq}}{s}\rangle_0\end{bmatrix} \quad Bl_{k=\overline{k_1}} = \begin{bmatrix} \langle \frac{K_{iid}}{s-jk\omega}\rangle_{\bar{k}} & 0\\ 0 & \langle \frac{K_{iiq}}{s-jk\omega}\rangle_{\bar{k}}\end{bmatrix}$$

$$Bl_{k=k_1} = \begin{bmatrix} \langle \frac{K_{iid}}{s+jk\omega}\rangle_k & 0\\ 0 & \langle \frac{K_{iiq}}{s+jk\omega}\rangle_k\end{bmatrix}$$

The generalised form of the STATCOM reference currents is:

$$\begin{bmatrix}\langle\Delta i_{sd}^{*}\rangle_0\\ \langle\Delta i_{sq}^{*}\rangle_0\\ \langle\Delta i_{sd}^{*}\rangle_k\\ \langle\Delta i_{sq}^{*}\rangle_k\\ \langle\Delta i_{sd}^{*}\rangle_{\bar{k}}\\ \langle\Delta i_{sq}^{*}\rangle_{\bar{k}}\end{bmatrix} = C_z\begin{bmatrix}\langle v_{dc}^{*}\rangle_0\\ \langle v_{sd}^{*}\rangle_0\\ \langle v_{dc}^{*}\rangle_k\\ \langle v_{sd}^{*}\rangle_k\\ \langle v_{dc}^{*}\rangle_{\bar{k}}\\ \langle v_{sd}^{*}\rangle_{\bar{k}}\end{bmatrix} - C_z\begin{bmatrix}\langle v_{dc}\rangle_0\\ \langle\Delta Q\rangle_0\\ \langle v_{dc}\rangle_k\\ \langle\Delta Q\rangle_k\\ \langle v_{dc}\rangle_{\bar{k}}\\ \langle\Delta Q\rangle_{\bar{k}}\end{bmatrix} \tag{D.137}$$

$$C_z = \begin{bmatrix} Cd_{k=0} & Cl_{k=\overline{k_1}} & Cl_{k=k_1} & & Cl_{k=k_n}\\ Cl_{k=k_1} & Cd_{k=k_1} & 0 & & 0\\ Cl_{k=\overline{k_1}} & 0 & Cd_{k=\overline{k_1}} & & 0\\ & 0 & 0 & \ddots & 0\\ Cl_{k=\overline{k_n}} & 0 & 0 & & Cd_{k=\overline{k_n}}\end{bmatrix}$$

$$Cd_k = \begin{bmatrix} K_{pvd} + \langle\frac{K_{ivd}}{s}\rangle_0 & 0\\ 0 & K_{pvq} + \langle\frac{K_{ivq}}{s}\rangle_0\end{bmatrix} \quad Cl_{k=\overline{k_1}} = \begin{bmatrix}\langle\frac{K_{ivd}}{s-jk\omega}\rangle_{\bar{k}} & 0\\ 0 & \langle\frac{K_{ivq}}{s-jk\omega}\rangle_{\bar{k}}\end{bmatrix}$$

$$Cl_{k=k_1} = \begin{bmatrix}\langle\frac{K_{ivd}}{s+jk\omega}\rangle_k & 0\\ 0 & \langle\frac{K_{ivq}}{s+jk\omega}\rangle_k\end{bmatrix}$$

While, the inputs of the STATCOM controller are generalised as:

$$D_z\begin{bmatrix}\langle v_{dc}\rangle_0\\ \langle\Delta Q\rangle_0\\ \langle v_{dc}\rangle_k\\ \langle\Delta Q\rangle_k\\ \langle v_{dc}\rangle_{\bar{k}}\\ \langle\Delta Q\rangle_{\bar{k}}\end{bmatrix} = E_z\begin{bmatrix}\langle\Delta v_{sd}\rangle_0\\ \langle\Delta v_{sq}\rangle_0\\ \langle\Delta v_{sd}\rangle_k\\ \langle\Delta v_{sq}\rangle_k\\ \langle\Delta v_{sd}\rangle_{\bar{k}}\\ \langle\Delta v_{sq}\rangle_{\bar{k}}\end{bmatrix} + F_z\begin{bmatrix}\langle\Delta i_{sd}\rangle_0\\ \langle\Delta i_{sq}\rangle_0\\ \langle\Delta i_{sd}\rangle_k\\ \langle\Delta i_{sq}\rangle_k\\ \langle\Delta i_{sd}\rangle_{\bar{k}}\\ \langle\Delta i_{sq}\rangle_{\bar{k}}\end{bmatrix} \tag{D.138}$$

$$D_z = \begin{bmatrix} Dd_{k=0} & Dl_{k=\overline{k_1}} & Dl_{k=k_1} & & Dl_{k=k_n}\\ Dl_{k=k_1} & Dd_{k=k_1} & 0 & & 0\\ Dl_{k=\overline{k_1}} & 0 & Dd_{k=\overline{k_1}} & & 0\\ & 0 & 0 & \ddots & 0\\ Dl_{k=\overline{k_n}} & 0 & 0 & & Dd_{k=\overline{k_n}}\end{bmatrix}$$

$$Dd_k = \begin{bmatrix}\alpha l_k & 0\\ 0 & 1\end{bmatrix} \quad Dl_{k=\overline{k_1}} = \begin{bmatrix}\alpha m_{k=\bar{k}} & 0\\ 0 & 0\end{bmatrix} \quad Dl_{k=k_1} = \begin{bmatrix}\alpha m_{k=k} & 0\\ 0 & 0\end{bmatrix}$$

$$\alpha l = C_{dc}s\langle v_{dc}\rangle_0 + \alpha_1$$

$$\alpha m_{k=k} = C_{dc}(s + jk\omega\,)\langle v_{dc}\rangle_k + \alpha_2$$

$$\alpha_1 = -\langle \frac{1}{v_{dc}} i_{sd}^2 R_f \rangle_0 + \frac{3}{2} \langle \frac{1}{v_{dc}} v_{sd} i_{sd} \rangle_0 + \langle \frac{3}{2} \frac{1}{v_{dc}} v_{sq} i_{sq} \rangle_0$$

$$\alpha_2 = -\langle \frac{1}{v_{dc}} i_{sd}^2 R_f \rangle_k + \frac{3}{2} \langle \frac{1}{v_{dc}} v_{sd} i_{sd} \rangle_k + \langle \frac{3}{2} \frac{1}{v_{dc}} v_{sq} i_{sq} \rangle_k$$

$$E_z = \begin{bmatrix} Ed_{k=0} & El_{k=\overline{k_1}} & El_{k=k_1} & & El_{k=k_n} \\ El_{k=k_1} & Ed_{k=k_1} & 0 & & 0 \\ El_{k=\overline{k_1}} & 0 & Ed_{k=\overline{k_1}} & & 0 \\ & 0 & 0 & \ddots & 0 \\ El_{k=\overline{k_n}} & 0 & 0 & & Ed_{k=\overline{k_n}} \end{bmatrix}$$

$$Ed_k = \frac{3}{2} \begin{bmatrix} \langle i_{sd} \rangle_0 & \langle i_{sq} \rangle_0 \\ -\langle i_{sq} \rangle_0 & \langle i_{sd} \rangle_0 \end{bmatrix} \quad El_{k=\overline{k_1}} = \frac{3}{2} \begin{bmatrix} \langle i_{sd} \rangle_{\bar{k}} & \langle i_{sq} \rangle_{\bar{k}} \\ -\langle i_{sq} \rangle_{\bar{k}} & \langle i_{sd} \rangle_{\bar{k}} \end{bmatrix}$$

$$El_{k=k_1} = \frac{3}{2} \begin{bmatrix} \langle i_{sd} \rangle_k & \langle i_{sq} \rangle_k \\ -\langle i_{sq} \rangle_{\bar{k}} & \langle i_{sd} \rangle_{\bar{k}} \end{bmatrix}$$

$$F_z = \begin{bmatrix} Fd_{k=0} & Fl_{k=\overline{k_1}} & Fl_{k=k_1} & & Fl_{k=k_n} \\ Fl_{k=k_1} & Fd_{k=k_1} & 0 & & 0 \\ Fl_{k=\overline{k_1}} & 0 & Fd_{k=\overline{k_1}} & & 0 \\ & 0 & 0 & \ddots & 0 \\ Fl_{k=\overline{k_n}} & 0 & 0 & & Fd_{k=\overline{k_n}} \end{bmatrix}$$

$$Fd_k = \begin{bmatrix} \left(\langle \frac{3}{2} v_{sd} \rangle_0 - \langle 2R_f i_{sd} \rangle_0 \right) & \langle \frac{3}{2} v_{sq} \rangle_0 \\ \frac{3}{2} \langle v_{sq} \rangle_0 & -\frac{3}{2} \langle v_{sd} \rangle_0 \end{bmatrix}$$

$$Fl_{k=\overline{k_1}} = \begin{bmatrix} \langle \frac{3}{2} v_{sd} \rangle_{\bar{k}} - \langle 2R_f i_{sd} \rangle_{\bar{k}} & \langle \frac{3}{2} v_{sq} \rangle_{\bar{k}} \\ \langle \frac{3}{2} v_{sq} \rangle_{\bar{k}} & -\frac{3}{2} \langle v_{sd} \rangle_{\bar{k}} \end{bmatrix}$$

$$Fl_{k=k_1} = \begin{bmatrix} \langle \frac{3}{2} v_{sd} \rangle_k - \langle 2R_f i_{sd} \rangle_k & \langle \frac{3}{2} v_{sq} \rangle_k \\ \frac{3}{2} \langle v_{sq} \rangle_k & -\frac{3}{2} \langle v_{sd} \rangle_k \end{bmatrix}$$

APPENDIX-E DQ-DYNAMIC PHASOR MODELLING OF SSSC

1. Power control mode

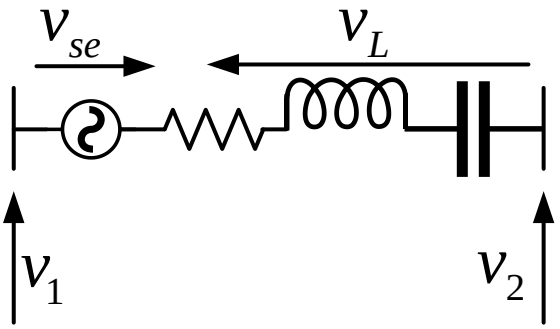

For SSSC controlled by power control mode is:

$$\frac{d}{dt}\Delta i_{sed} = \frac{1}{L_{se}}\Delta v_{sed} - \frac{R_{se}}{L_{se}}\Delta i_{sed} + \omega\Delta i_{seq} - \frac{1}{L_{se}}\Delta m_{sed} \quad \text{(E.139)}$$

$$\frac{d}{dt}\Delta i_{seq} = \frac{1}{L_{se}}\Delta v_{seq} - \omega\Delta i_{sed} - \frac{R_{se}}{L_{se}}\Delta i_{seq} - \frac{1}{L_{se}}\Delta m_{seq} \quad \text{(E.140)}$$

$$\frac{d}{dt}\Delta x_1 = K_{ivd}P_2^* - K_{ivd}\Delta P_2 \quad \text{(E.141)}$$

$$\frac{d}{dt}\Delta x_2 = K_{ivq}Q_2^* - K_{ivq}\Delta Q_2 \quad \text{(E.142)}$$

$$\Delta m_{sed} = K_{pvd}P_{line}^* - K_{pvd}\Delta P_{line} + \Delta x_1 \quad \text{(E.143)}$$

$$\Delta m_{seq} = K_{pvq}Q_{line}^* - K_{pvq}\Delta Q_{line} + \Delta x_2 \quad \text{(E.144)}$$

$$\Delta P_1 = \frac{3}{2}\left(i_{sed}\Delta v_{1d} + i_{seq}\Delta v_{1q} + v_{1d}\,\Delta i_{sed} + v_{1q}\,\Delta i_{seq}\right) \quad \text{(E.145)}$$

$$\Delta Q_1 = \frac{3}{2}\left(i_{seq}\Delta v_{1d} - i_{sed}\Delta v_{1q} - v1_q\,\Delta i_{sed} + v_{1d}\,\Delta i_{seq}\right) \quad \text{(E.146)}$$

$$\Delta P_2 = \frac{3}{2}\left(i_{sed}\Delta v_{2d} + i_{seq}\Delta v_{2q} + v_{2d}\,\Delta i_{sed} + v_{2q}\,\Delta i_{seq}\right) \quad \text{(E.147)}$$

$$\Delta Q_2 = \frac{3}{2}\left(i_{seq}\Delta v_{2d} - i_{sed}\Delta v_{2q} - v_{2q}\,\Delta i_{sed} + v_{2d}\,\Delta i_{seq}\right) \quad \text{(E.148)}$$

$$\Delta P_{line} = \Delta P_1 - \Delta P_2 \quad \text{(E.149)}$$

$$\Delta Q_{line} = \Delta Q_1 - \Delta Q_2 \quad \text{(E.150)}$$

The transformation of the SSSC equations from (E.139) to (E.150) to dynamic phasor is:

$$\langle\frac{d}{dt}\Delta i_{sed}\rangle_k = \frac{1}{L_{se}}\langle\Delta v_{sed}\rangle_k - \langle\frac{R_{se}}{L_{se}}\Delta i_{sed}\rangle_k + \langle\omega\Delta i_{seq}\rangle_k - \langle\frac{1}{L_{se}}\Delta m_{seq}\rangle_k \quad \text{(E.151)}$$

$$\langle\frac{d}{dt}\Delta i_{seq}\rangle_k = \langle\frac{1}{L_{se}}\Delta v_{seq}\rangle_k - \langle\omega\Delta i_{sed}\rangle_k - \langle\frac{R_{se}}{L_{se}}\Delta i_{seq}\rangle_k - \langle\frac{1}{L_{se}}\Delta m_{seq}\rangle_k \quad \text{(E.152)}$$

$$\langle\frac{d}{dt}\Delta x_1\rangle_k = \langle K_{ivd}P_{line}^*\rangle_k - \langle K_{ivd}\Delta P_{line}\rangle_k - jk\omega\Delta x_1 \quad \text{(E.153)}$$

$$\langle\frac{d}{dt}\Delta x_2\rangle_k = \langle K_{ivq}Q_{line}^*\rangle_k - \langle K_{ivq}\Delta Q_{line}\rangle_k - jk\omega\Delta x_2 \quad \text{(E.154)}$$

$$\langle\Delta m_{sed}\rangle_k = \langle K_{pvd}P_{line}^*\rangle_k - \langle K_{pvd}\Delta P_{line}\rangle_k + \langle\Delta x_1\rangle_k \quad \text{(E.155)}$$

$$\langle \Delta m_{seq} \rangle_k = \langle K_{pvq} Q^*_{line} \rangle_k - \langle K_{pvq} \Delta Q_{line} \rangle_k + \langle \Delta x_2 \rangle_k \quad \text{(E.156)}$$

$$\langle \Delta P_1 \rangle_k = \langle \tfrac{3}{2} \left(i_{sed} \Delta v_{1d} + i_{seq} \Delta v_{1q} + v_{1d}\, \Delta i_{sed} + v_{1q}\, \Delta i_{seq} \right) \rangle_k \quad \text{(E.157)}$$

$$\langle \Delta Q_1 \rangle_k = \langle \tfrac{3}{2} \left(i_{seq} \Delta v_{1d} - i_{sed} \Delta v_{1q} - v_{1q}\, \Delta i_{sed} + v_{1d}\, \Delta i_{seq} \right) \rangle_k \quad \text{(E.158)}$$

$$\langle \Delta P_2 \rangle_k = \langle \tfrac{3}{2} \left(i_{sed} \Delta v_{2d} + i_{seq} \Delta v_{2q} + v_{2d}\, \Delta i_{sed} + v_{2q}\, \Delta i_{seq} \right) \rangle_k \quad \text{(E.159)}$$

$$\langle \Delta Q_2 \rangle_k = \langle \tfrac{3}{2} \left(i_{seq} \Delta v_{2d} - i_{sed} \Delta v_{2q} - v_{2q}\, \Delta i_{sed} + v_{2d}\, \Delta i_{seq} \right) \rangle_k \quad \text{(E.160)}$$

$$\langle \Delta P_{line} \rangle_k = \langle \Delta P_1 \rangle_k - \langle \Delta P_2 \rangle_k \quad \text{(E.161)}$$

$$\langle \Delta Q_{line} \rangle_k = \langle \Delta Q_1 \rangle_k - \langle \Delta Q_2 \rangle_k \quad \text{(E.162)}$$

The expansion of the equations (E.151) to (E.162) will result a generalised form of state-space equation of the SSSC as:

$$AP_{DP} = \begin{bmatrix} ap_{k=0} & acp_{k=\bar{k}} & acp_{k=k} & \dots & acp_{k=kn} \\ acp_{k=k} & ap_{k=k} & & & \\ acp_{k=\bar{k}} & & ap_{k=\bar{k}} & & \vdots \\ \vdots & & & \ddots & \\ acp_{k=\overline{kn}} & & & \dots & ap_{k=\overline{kn}} \end{bmatrix}$$

$$ap_{k=k} =$$

$$\begin{bmatrix} -jk\omega & 0 & -\frac{3}{2}K_{ivd}(\langle v_{1d} \rangle_0 - \langle v_{2d} \rangle_0) & -\frac{3}{2}K_{ivd}\left(\langle v_{1q} \rangle_0 - \langle v_{2q} \rangle_0\right) \\ 0 & -jk\omega & -\frac{3}{2}K_{ivq}\left(-\langle v_{1q} \rangle_0 + \langle v_{2q} \rangle_0\right) & -\frac{3}{2}K_{ivq}(\langle v_{1d} \rangle_0 - \langle v_{2d} \rangle_0) \\ -\frac{1}{L_{se}} & 0 & \frac{3}{2}\frac{K_{pvd}}{L_{se}}(\langle v_{1d} \rangle_0 - \langle v_{2d} \rangle_0) - \frac{R_{se}}{L_{se}} - jk\omega & \frac{3}{2}\frac{K_{pvd}}{L_{se}}\left(\langle v_{1q} \rangle_0 - \langle v_{2q} \rangle_0\right) + \omega \\ 0 & -\frac{1}{L_{se}} & \frac{3}{2}\frac{K_{pvq}}{L_{se}}\left(-\langle v_{1q} \rangle_0 + \langle v_{2q} \rangle_0\right) - \omega & \frac{3}{2}\frac{K_{pvq}}{L_{se}}(\langle v_{1d} \rangle_0 - \langle v_{2d} \rangle_0) - \frac{R_{se}}{L_{se}} - jk\omega \end{bmatrix}$$

$$acp_{k=k} = \frac{3}{2}\begin{bmatrix} 0 & 0 & -K_{ivd}(\langle v_{1d} \rangle_k - \langle v_{2d} \rangle_k) & -K_{ivd}\left(\langle v_{1q} \rangle_k - \langle v_{2q} \rangle_k\right) \\ 0 & 0 & -K_{ivq}\left(-\langle v_{1q} \rangle_k + \langle v_{2q} \rangle_k\right) & -K_{ivq}(\langle v_{1d} \rangle_k - \langle v_{2d} \rangle_k) \\ 0 & 0 & \frac{K_{pvd}}{L_{se}}(\langle v_{1d} \rangle_k - \langle v_{2d} \rangle_k) & \frac{K_{pvd}}{L_{se}}\left(\langle v_{1q} \rangle_k - \langle v_{2q} \rangle_k\right) \\ 0 & 0 & \frac{K_{pvq}}{L_{se}}\left(-\langle v_{1q} \rangle_k + \langle v_{2q} \rangle_k\right) & \frac{K_{pvq}}{L_{se}}(\langle v_{1d} \rangle_k - \langle v_{2d} \rangle_k) \end{bmatrix}$$

$$BP_{DP} = \begin{bmatrix} bp_{k=0} & bcp_{k=\bar{k}} & bcp_{k=k} & \dots & bcp_{k=kn} \\ bcp_{k=k} & bp_{k=k} & & & \\ bcp_{k=\bar{k}} & & bp_{k=\bar{k}} & & \vdots \\ \vdots & & & \ddots & \\ bcp_{k=\overline{kn}} & & & \dots & bp_{k=\overline{kn}} \end{bmatrix}$$

$$bp_{k=k} =$$

$$\begin{bmatrix} 0 & 0 & -\frac{3}{2}K_{ivd}\langle i_{sed} \rangle_0 & -\frac{3}{2}K_{ivd}\langle i_{seq} \rangle_0 & \frac{3}{2}K_{ivd}\langle i_{sed} \rangle_0 & \frac{3}{2}K_{ivd}\langle i_{seq} \rangle_0 & K_{ivd} & 0 \\ 0 & 0 & -\frac{3}{2}K_{ivq}\langle i_{seq} \rangle_0 & \frac{3}{2}K_{ivq}\langle i_{sed} \rangle_0 & \frac{3}{2}K_{ivq}\langle i_{seq} \rangle_0 & -\frac{3}{2}K_{ivq}\langle i_{sed} \rangle_0 & 0 & K_{ivq} \\ \frac{1}{L_{se}} & 0 & \frac{3}{2}\frac{K_{pvd}}{L_{se}}\langle i_{sed} \rangle_0 & \frac{3}{2}\frac{K_{pvd}}{L_{se}}\langle i_{seq} \rangle_0 & -\frac{3}{2}\frac{K_{pvd}}{L_{se}}\langle i_{sed} \rangle_0 & -\frac{3}{2}\frac{K_{pvd}}{L_{se}}\langle i_{seq} \rangle_0 & -\frac{K_{pvd}}{L_{se}} & 0 \\ 0 & \frac{1}{L_{se}} & \frac{3}{2}\frac{K_{pvq}}{L_{se}}\langle i_{seq} \rangle_0 & -\frac{3}{2}\frac{K_{pvq}}{L_{se}}\langle i_{sed} \rangle_0 & -\frac{3}{2}\frac{K_{pvq}}{L_{se}}\langle i_{seq} \rangle_0 & \frac{3}{2}\frac{K_{pvq}}{L_{se}}\langle i_{sed} \rangle_0 & 0 & -\frac{K_{pvq}}{L_{se}} \end{bmatrix}$$

$$bcp_{k=k} = \frac{3}{2}\begin{bmatrix} 0 & 0 & -K_{ivd}\langle i_{sed}\rangle_k & -K_{ivd}\langle i_{seq}\rangle_k & K_{ivd}\langle i_{sed}\rangle_k & K_{ivd}\langle i_{seq}\rangle_k & 0 & 0 \\ 0 & 0 & -K_{ivq}\langle i_{seq}\rangle_k & K_{ivq}\langle i_{sed}\rangle_k & K_{ivq}\langle i_{seq}\rangle_k & -K_{ivq}\langle i_{sed}\rangle_k & 0 & 0 \\ 0 & 0 & \frac{K_{pvd}}{L_{se}}\langle i_{sed}\rangle_k & \frac{K_{pvd}}{L_{se}}\langle i_{seq}\rangle_k & -\frac{K_{pvd}}{L_{se}}\langle i_{sed}\rangle_k & -\frac{K_{pvd}}{L_{se}}\langle i_{seq}\rangle_k & 0 & 0 \\ 0 & 0 & \frac{K_{pvq}}{L_{se}}\langle i_{seq}\rangle_k & -\frac{K_{pvq}}{L_{se}}\langle i_{sed}\rangle_k & -\frac{K_{pvq}}{L_{se}}\langle i_{seq}\rangle_k & \frac{K_{pvq}}{L_{se}}\langle i_{sed}\rangle_k & 0 & 0 \end{bmatrix}$$

2. Voltage control mode

The SSSC is controlled in voltage control mode as:

$$\Delta x_1' = Ki_{vd}(v_{dc}^* - \Delta v_{dc}) \tag{E.163}$$

$$\Delta x_2' = Ki_{vq}\left(v_{seq}^* - \Delta v_{seq}\right) \tag{E.164}$$

$$\frac{d}{dt}\Delta i_{sed} = -\frac{1}{L_{se}}\Delta x_1 - \frac{R_{se}}{L_{se}}\Delta i_{sed} + \omega\Delta i_{seq} + \frac{K_{pvd}}{L_{se}}\Delta v_{dc} + \frac{1}{L_{se}}\Delta v_{sed} - \frac{K_{pvd}}{L_{se}}v_{dc}^* \tag{E.165}$$

$$\frac{d}{dt}\Delta i_{seq} = -\frac{1}{L_{se}}\Delta x_2 - \omega\Delta i_{sed} - \frac{R_{se}}{L_{se}}\Delta i_{seq} + \left(\frac{1}{L_{se}} + \frac{K_{pvq}}{L_{se}}\right)\Delta v_{seq} - \frac{K_{pvq}}{L_{se}}v_{seq}^* \tag{E.166}$$

$$\frac{d(\Delta v_{dc})}{dt} = \frac{3}{2}\left\{\frac{\Delta v_{sed}.i_{sed}}{C_{dc}v_{dc}} + \frac{v_{sed}\Delta i_{sed}}{C_{dc}v_{dc}} - \frac{v_{sed}.i_{sed}}{C_{dc}v_{dc}^2}\Delta v_{dc}\right\} + \frac{3}{2}\left\{\frac{\Delta v_{seq}.i_{seq}}{C_{dc}v_{dc}} + \frac{v_{seq}.\Delta i_{seq}}{C_{dc}v_{dc}} - \frac{v_{seq}.i_{seq}}{C_{dc}v_{dc}^2}\Delta v_{dc}\right\} - \frac{2i_{sed}\Delta ise_d.R_{se}}{C_{dc}v_{dc}} + \frac{i_{sed}^2.R_{se}}{C_{dc}v_{dc}^2}\Delta v_{dc} \tag{E.167}$$

The transformation to dq-dynamic phasor is:

$$\langle\Delta x_1'\rangle_k = K_{ivd}\langle v_{dc}^*\rangle_k - K_{ivd}\langle\Delta v_{dc}\rangle_k \tag{E.168}$$

$$\langle\Delta x_2'\rangle_k = K_{ivq}\langle v_{seq}^*\rangle_k - K_{ivq}\langle\Delta v_{seq}\rangle_k \tag{E.169}$$

$$\left\langle\frac{d}{dt}\Delta i_{sed}\right\rangle_k = -\frac{1}{L_{se}}\langle\Delta x_1\rangle_k - \frac{R_{se}}{L_{se}}\langle\Delta i_{sed}\rangle_k + \langle\omega\Delta i_{seq}\rangle_k + \frac{K_{pvd}}{L_{se}}\langle\Delta v_{dc}\rangle_k + \frac{1}{L_{se}}\langle\Delta v_{sed}\rangle_k - \frac{K_{pvd}}{L_{se}}\langle v_{dc}^*\rangle_k \tag{E.170}$$

$$\left\langle\frac{d}{dt}\Delta i_{seq}\right\rangle_k = -\frac{1}{L_{se}}\langle\Delta x_2\rangle_k - \langle\omega\Delta i_{sed}\rangle_k - \frac{R_{se}}{L_{se}}\langle\Delta i_{seq}\rangle_k + \left(\frac{1}{L_{se}} + \frac{K_{pvq}}{L_{se}}\right)\langle\Delta v_{seq}\rangle_k - \frac{K_{pvq}}{L_{se}}\langle v_{seq}^*\rangle_k \tag{E.171}$$

$$\left\langle\frac{d(\Delta v_{dc})}{dt}\right\rangle_k = \frac{3}{2}\left\langle\frac{\Delta v_{sed}i_{sed}}{C_{dc}v_{dc}}\right\rangle_k + \frac{3}{2}\left\langle\frac{v_{sed}.\Delta i_{sed}}{C_{dc}v_{dc}}\right\rangle_k - \frac{3}{2}\left\langle\frac{v_{sed}i_{sed}}{C_{dc}v_{dc}^2}\Delta v_{dc}\right\rangle_k + \frac{3}{2}\left\langle\frac{\Delta v_{seq}.i_{seq}}{C_{dc}v_{dc}}\right\rangle_k + \frac{3}{2}\left\langle\frac{v_{seq}.\Delta i_{seq}}{C_{dc}v_{dc}}\right\rangle_k - \frac{3}{2}\left\langle\frac{v_{seq}.i_{seq}}{C_{dc}v_{dc}^2}\Delta v_{dc}\right\rangle_k - \left\langle\frac{2i_{sed}\Delta i_{sed}.R_{se}}{C_{dc}v_{dc}}\right\rangle_k + \left\langle\frac{i_{sed}^2.R_{se}}{C_{dc}v_{dc}^2}\Delta v_{dc}\right\rangle_k \tag{E.172}$$

$$\langle\Delta v_{dc}'\rangle_0 = \left\langle\frac{\frac{3}{2}v_{sed} - 2i_{sed}.R_f}{C_{dc}v_{dc}}\right\rangle_0\langle\Delta i_{sed}\rangle_0 + \left\langle\frac{3}{2}\frac{v_{seq}}{C_{dc}v_{dc}}\right\rangle_0\langle\Delta i_{seq}\rangle_0 + \left\langle\frac{i_{sed}^2.R_f - \frac{3}{2}v_{sed}i_{sed} - \frac{3}{2}v_{seq}.i_{seq}}{C_{dc}v_{dc}^2}\right\rangle_0\langle\Delta v_{dc}\rangle_0 + \left\langle\frac{3}{2}\frac{i_{sed}}{C_{dc}v_{dc}}\right\rangle_0\langle\Delta v_{sed}\rangle_0 + \tag{E.173}$$

$$\langle\frac{3}{2}\frac{i_{seq}}{C_{dc}v_{dc}}\rangle_0\langle\Delta v_{seq}\rangle_0+\langle\frac{\frac{3}{2}v_{sed}-2i_{sed}.R_f}{C_{dc}v_{dc}}\rangle_{\bar{k}}\langle\Delta i_{sed}\rangle_k+\langle\frac{3}{2}\frac{v_{seq}}{C_{dc}v_{dc}}\rangle_{\bar{k}}\langle\Delta i_{seq}\rangle_k+$$

$$\langle\frac{i_{sed}^2.R_f-\frac{3}{2}v_{sed}i_{sed}-\frac{3}{2}v_{seq}.i_{seq}}{C_{dc}v_{dc}^2}\rangle_{\bar{k}}\langle\Delta v_{dc}\rangle_k+\langle\frac{3}{2}\frac{i_{sed}}{C_{dc}v_{dc}}\rangle_{\bar{k}}\langle\Delta v_{sed}\rangle_k+$$

$$\langle\frac{3}{2}\frac{i_{seq}}{C_{dc}v_{dc}}\rangle_{\bar{k}}\langle\Delta v_{seq}\rangle_k+\langle\frac{\frac{3}{2}v_{sed}-2i_{sed}.R_f}{C_{dc}v_{dc}}\rangle_k\langle\Delta i_{sed}\rangle_{\bar{k}}+\langle\frac{3}{2}\frac{v_{seq}}{C_{dc}v_{dc}}\rangle_k\langle\Delta i_{seq}\rangle_{\bar{k}}+$$

$$\langle\frac{i_{sed}^2.R_f-\frac{3}{2}v_{sed}i_{sed}-\frac{3}{2}v_{seq}.i_{seq}}{C_{dc}v_{dc}^2}\rangle_k\langle\Delta v_{dc}\rangle_{\bar{k}}+\langle\frac{3}{2}\frac{i_{sed}}{C_{dc}v_{dc}}\rangle_k\langle\Delta v_{sed}\rangle_{\bar{k}}+\langle\frac{3}{2}\frac{i_{seq}}{C_{dc}v_{dc}}\rangle_k\langle\Delta v_{seq}\rangle_{\bar{k}}$$

$$\langle\Delta v'_{dc}\rangle_k=$$

$$\langle\frac{\frac{3}{2}v_{sed}-2i_{sed}.R_f}{C_{dc}v_{dc}}\rangle_k\langle\Delta i_{sed}\rangle_0+\langle\frac{3}{2}\frac{v_{seq}}{C_{dc}v_{dc}}\rangle_k\langle\Delta i_{seq}\rangle_0+$$

$$\langle\frac{i_{sed}^2.R_f-\frac{3}{2}v_{sed}i_{sed}-\frac{3}{2}v_{seq}.i_{seq}}{C_{dc}v_{dc}^2}\rangle_k\langle\Delta v_{dc}\rangle_0+\langle\frac{3}{2}\frac{i_{sed}}{C_{dc}v_{dc}}\rangle_k\langle\Delta v_{sed}\rangle_0+$$

$$\langle\frac{3}{2}\frac{i_{seq}}{C_{dc}v_{dc}}\rangle_k\langle\Delta v_{seq}\rangle_0+\langle\frac{\frac{3}{2}v_{sed}-2i_{sed}.R_f}{C_{dc}v_{dc}}\rangle_0\langle\Delta i_{sed}\rangle_k+\langle\frac{3}{2}\frac{v_{seq}}{C_{dc}v_{dc}}\rangle_0\langle\Delta i_{seq}\rangle_k+ \quad \text{(E.174)}$$

$$\left\{\langle\frac{i_{sed}^2.R_f-\frac{3}{2}v_{sed}i_{sed}-\frac{3}{2}v_{seq}.i_{seq}}{C_{dc}v_{dc}^2}\rangle_0-jk\omega\right\}\langle\Delta v_{dc}\rangle_k+\langle\frac{3}{2}\frac{i_{sed}}{C_{dc}v_{dc}}\rangle_0\langle\Delta v_{sed}\rangle_k+$$

$$\langle\frac{3}{2}\frac{i_{seq}}{C_{dc}v_{dc}}\rangle_0\langle\Delta v_{seq}\rangle_k$$

$$\langle\Delta v'_{dc}\rangle_{\bar{k}}=$$

$$\langle\frac{\frac{3}{2}v_{sed}-2i_{sed}.R_f}{C_{dc}v_{dc}}\rangle_{\bar{k}}\langle\Delta i_{sed}\rangle_0+\langle\frac{3}{2}\frac{v_{seq}}{C_{dc}v_{dc}}\rangle_{\bar{k}}\langle\Delta i_{seq}\rangle_0+$$

$$\langle\frac{i_{sed}^2.R_f-\frac{3}{2}v_{sed}i_{sed}-\frac{3}{2}v_{seq}.i_{seq}}{C_{dc}v_{dc}^2}\rangle_{\bar{k}}\langle\Delta v_{dc}\rangle_0+\langle\frac{3}{2}\frac{i_{sed}}{C_{dc}v_{dc}}\rangle_{\bar{k}}\langle\Delta v_{sed}\rangle_0+$$

$$\langle\frac{3}{2}\frac{i_{seq}}{C_{dc}v_{dc}}\rangle_{\bar{k}}\langle\Delta v_{seq}\rangle_0+\langle\frac{\frac{3}{2}v_{sed}-2i_{sed}.R_f}{C_{dc}v_{dc}}\rangle_0\langle\Delta i_{sed}\rangle_{\bar{k}}+\langle\frac{3}{2}\frac{v_{seq}}{C_{dc}v_{dc}}\rangle_0\langle\Delta i_{seq}\rangle_{\bar{k}}+ \quad \text{(E.175)}$$

$$\left\{\langle\frac{i_{sed}^2.R_f-\frac{3}{2}v_{sed}i_{sed}-\frac{3}{2}v_{seq}.i_{seq}}{C_{dc}v_{dc}^2}\rangle_0+jk\omega\right\}\langle\Delta v_{dc}\rangle_{\bar{k}}+\langle\frac{3}{2}\frac{i_{sed}}{C_{dc}v_{dc}}\rangle_0\langle\Delta v_{sed}\rangle_{\bar{k}}+$$

$$\langle\frac{3}{2}\frac{i_{seq}}{C_{dc}v_{dc}}\rangle_0\langle\Delta v_{seq}\rangle_{\bar{k}}$$

So, the generalised form of voltage control mode is given as:

$$AV_{DP}=\begin{bmatrix} av_{k=0} & acv_{k=\bar{k}} & acv_{k=k} & \dots & acv_{k=kn} \\ acv_{k=k} & av_{k=k} & & & \\ acv_{k=\bar{k}} & & av_{k=\bar{k}} & & \vdots \\ \vdots & & & \ddots & \\ acv_{k=\overline{kn}} & & & \dots & av_{k=\overline{kn}} \end{bmatrix}$$

$$av_{k=k} =$$

$$\begin{bmatrix} -jk\omega & 0 & 0 & 0 & -K_{ivd} \\ 0 & -jk\omega & 0 & 0 & 0 \\ -\frac{1}{L_{se}} & 0 & -\frac{R_{se}}{L_{se}} - jk\omega & \omega & \frac{K_{pvd}}{L_{se}} \\ 0 & -\frac{1}{L_{se}} & -\omega & -\frac{R_{se}}{L_{se}} - jk\omega & 0 \\ 0 & 0 & \left\langle \frac{\frac{3}{2}v_{sed} - 2i_{sed}.R_f}{C_{dc}v_{dc}} \right\rangle_0 & \left\langle \frac{3}{2}\frac{v_{seq}}{C_{dc}v_{dc}} \right\rangle_0 & \left\langle \frac{i_{sed}^2.R_f - \frac{3}{2}v_{sed}i_{sed} - \frac{3}{2}v_{seq}.i_{seq}}{C_{dc}v_{dc}^2} \right\rangle_0 - jk\omega \end{bmatrix}$$

$$acv_{k=k} = \begin{bmatrix} 0 & 0 & 0 & 0 & 0 \\ 0 & 0 & 0 & 0 & 0 \\ 0 & 0 & 0 & 0 & 0 \\ 0 & 0 & 0 & 0 & 0 \\ 0 & 0 & \left\langle \frac{\frac{3}{2}v_{sed} - 2i_{sed}.R_f}{C_{dc}v_{dc}} \right\rangle_k & \left\langle \frac{3}{2}\frac{v_{seq}}{C_{dc}v_{dc}} \right\rangle_k & \left\langle \frac{i_{sed}^2.R_f - \frac{3}{2}v_{sed}i_{sed} - \frac{3}{2}v_{seq}.i_{seq}}{C_{dc}v_{dc}^2} \right\rangle_k \end{bmatrix}$$

$$BV_{DP} = \begin{bmatrix} bv_{k=0} & bcv_{k=\bar{k}} & bcv_{k=k} & \dots & bcv_{k=kn} \\ bcv_{k=k} & bv_{k=k} & & & \\ bcv_{k=\bar{k}} & & bv_{k=\bar{k}} & & \vdots \\ \vdots & & & \ddots & \\ bcv_{k=\overline{kn}} & & & \dots & bv_{k=\overline{kn}} \end{bmatrix}$$

$$bv_{k=k} = \begin{bmatrix} 0 & 0 & K_{ivd} & 0 \\ 0 & -K_{ivq} & 0 & K_{ivq} \\ \frac{1}{L_{se}} & 0 & -\frac{K_{pvd}}{L_{se}} & 0 \\ 0 & \left(\frac{1}{L_{se}} + \frac{K_{pvq}}{L_{se}}\right) & 0 & -\frac{K_{pvq}}{L_{se}} \\ \left\langle \frac{3}{2}\frac{i_{sed}}{C_{dc}v_{dc}} \right\rangle_0 & \left\langle \frac{3}{2}\frac{i_{seq}}{C_{dc}v_{dc}} \right\rangle_0 & 0 & 0 \end{bmatrix}$$

$$bcv_{k=k} = \begin{bmatrix} 0 & 0 & 0 & 0 \\ 0 & 0 & 0 & 0 \\ 0 & 0 & 0 & 0 \\ 0 & 0 & 0 & 0 \\ \left\langle \frac{3}{2}\frac{i_{sed}}{C_{dc}v_{dc}} \right\rangle_k & \left\langle \frac{3}{2}\frac{i_{seq}}{C_{dc}v_{dc}} \right\rangle_k & 0 & 0 \end{bmatrix}$$

3. Impedance control mode

$$\Delta x_{seq} = \frac{1}{i_{seq}}\Delta v_{seq} - \frac{v_{seq}}{i_{seq}^2}\,\Delta i_{seq} \tag{E.176}$$

$$\Delta x_2' = K_{ivq}\left(x_{seq}^* - \Delta x_{seq}\right) \tag{E.177}$$

$$\Delta m_{seq} = K_{pvq}\left(x_{seq}^* - \Delta x_{seq}\right) + \Delta x_2 \tag{E.178}$$

$$\Delta x_2' = K_{ivq}x_{seq}^* - \frac{K_{ivq}}{ise_q}\Delta v_{seq} + \frac{K_{ivq}v_{seq}}{ise_q^2}\,\Delta i_{seq} \tag{E.179}$$

$$\Delta i_{seq}' = -\frac{1}{L_{se}}\Delta x_2 - \omega\Delta i_{sed} - \frac{R_{se}}{L_{se}}\Delta i_{seq} - \frac{K_{pvq}v_{seq}}{L_{se}i_{seq}^2}\,\Delta i_{seq} + \frac{1}{L_{se}}\,\Delta v_{seq} + \frac{K_{pvq}}{L_{se}i_{seq}}\Delta v_{seq} - \frac{K_{pvq}}{L_{se}}x_{seq}^* \tag{E.180}$$

The transformation to dynamic phasor result:

For $k = 0$

$$\langle \Delta x_2' \rangle_0 = K_{ivq} \langle x_{seq}^* \rangle_0 - \langle \frac{K_{ivq}}{i_{seq}} \Delta v_{seq} \rangle_0 + \langle \frac{K_{ivq} v_{seq}}{i_{seq}^2} \Delta i_{seq} \rangle_0 \tag{E.181}$$

$$\langle \Delta i_{seq}' \rangle_0 = -\frac{1}{L_{se}} \langle \Delta x_2 \rangle_0 - \omega \langle \Delta i_{sed} \rangle_0 - \frac{R_{se}}{L_{se}} \langle \Delta i_{seq} \rangle_0 - \langle \frac{K_{pvq} v_{seq}}{L_{se} i_{seq}^2} \Delta i_{seq} \rangle_0 + \frac{1}{L_{se}} \langle \Delta v_{seq} \rangle_0 + \langle \frac{K_{pvq}}{L_{se} i_{seq}} \Delta v_{seq} \rangle_0 - \frac{K_{pvq}}{L_{se}} \langle x_{seq}^* \rangle_0 \tag{E.182}$$

$$\langle \Delta x_2' \rangle_0 = \langle \frac{K_{ivq} v_{seq}}{i_{seq}^2} \rangle_0 \langle \Delta i_{seq} \rangle_0 - \langle \frac{K_{ivq}}{i_{seq}} \rangle_0 \langle \Delta v_{seq} \rangle_0 + K_{ivq} \langle x_{seq}^* \rangle_0 + \langle \frac{K_{ivq} v_{seq}}{i_{seq}^2} \rangle_{\bar{k}} \langle \Delta i_{seq} \rangle_k - \langle \frac{K_{ivq}}{i_{seq}} \rangle_{\bar{k}} \langle \Delta v_{seq} \rangle_k + \langle \frac{K_{ivq} v_{seq}}{i_{seq}^2} \rangle_k \langle \Delta i_{seq} \rangle_{\bar{k}} - \langle \frac{K_{ivq}}{i_{seq}} \rangle_k \langle \Delta v_{seq} \rangle_{\bar{k}} \tag{E.183}$$

$$\langle \Delta i_{seq}' \rangle_0 = -\frac{1}{L_{se}} \langle \Delta x_2 \rangle_0 - \omega \langle \Delta i_{sed} \rangle_0 + \left\{ -\frac{R_{se}}{L_{se}} - \langle \frac{K_{pvq} v_{seq}}{L_{se} i s e_q^2} \rangle_0 \right\} \langle \Delta i_{seq} \rangle_0 + \left\{ \frac{1}{L_{se}} + \langle \frac{K_{pvq}}{L_{se} i_{seq}} \rangle_0 \right\} \langle \Delta v_{seq} \rangle_0 - \frac{K_{pvq}}{L_{se}} \langle x_{seq}^* \rangle_0 - \langle \frac{K_{pvq} v_{seq}}{L_{se} i_{seq}^2} \rangle_{\bar{k}} \langle \Delta i_{seq} \rangle_k + \langle \frac{K_{pvq}}{L_{se} i_{seq}} \rangle_{\bar{k}} \langle \Delta v_{seq} \rangle_k - \langle \frac{K_{pvq} v_{seq}}{L_{se} i_{seq}^2} \rangle_k \langle \Delta i_{seq} \rangle_{\bar{k}} + \langle \frac{K_{pvq}}{L_{se} i_{seq}} \rangle_k \langle \Delta v_{seq} \rangle_{\bar{k}} \tag{E.184}$$

For $k = k$

$$\langle \Delta x_2' \rangle_k = \langle K_{ivq} x_{seq}^* \rangle_k - \langle \frac{K_{ivq}}{i_{seq}} \Delta v_{seq} \rangle_k + \langle \frac{K_{ivq} v_{seq}}{i_{seq}^2} \Delta i_{seq} \rangle_k \tag{E.185}$$

$$\langle \Delta i_{seq}' \rangle_k = -\frac{1}{L_{se}} \langle \Delta x_2 \rangle_k - \omega \langle \Delta i_{sed} \rangle_k - \frac{R_{se}}{L_{se}} \langle \Delta i_{seq} \rangle_k - \langle \frac{K_{pvq} v_{seq}}{L_{se} i_{seq}^2} \Delta i_{seq} \rangle_k + \frac{1}{L_{se}} \langle \Delta v_{seq} \rangle_k + \langle \frac{K_{pvq}}{L_{se} i_{seq}} \Delta v_{seq} \rangle_k - \frac{K_{pvq}}{L_{se}} \langle x_{seq}^* \rangle_k \tag{E.186}$$

$$\langle \Delta x_2' \rangle_k = \langle \frac{K_{ivq} v_{seq}}{i_{seq}^2} \rangle_k \langle \Delta i_{seq} \rangle_0 - \langle \frac{K_{ivq}}{i_{seq}} \rangle_k \langle \Delta v_{seq} \rangle_0 - jk\omega \langle \Delta x_2 \rangle_k + \langle \frac{K_{ivq} v_{seq}}{i_{seq}^2} \rangle_0 \langle \Delta i_{seq} \rangle_k - \langle \frac{K_{ivq}}{i_{seq}} \rangle_0 \langle \Delta v_{seq} \rangle_k + K_{ivq} \langle x_{seq}^* \rangle_k \tag{E.187}$$

$$\langle \Delta i_{seq}' \rangle_k = -\langle \frac{K_{pvq} v_{seq}}{L_{se} i_{seq}^2} \rangle_k \langle \Delta i_{seq} \rangle_0 + \langle \frac{K_{pvq}}{L_{se} i_{seq}} \rangle_k \langle \Delta v_{seq} \rangle_0 - \frac{1}{L_{se}} \langle \Delta x_2 \rangle_k - \omega \langle \Delta i_{sed} \rangle_k + \left\{ -\frac{R_{se}}{L_{se}} - \langle \frac{K_{pvq} v_{seq}}{L_{se} i_{seq}^2} \rangle_0 - jk\omega \right\} \langle \Delta i_{seq} \rangle_k + \left\{ \frac{1}{L_{se}} + \langle \frac{K_{pvq}}{L_{se} i_{seq}} \rangle_0 \right\} \langle \Delta v_{seq} \rangle_k - \frac{K_{pvq}}{L_{se}} \langle x_{seq}^* \rangle_k \tag{E.188}$$

For $k = \bar{k}$

$$\langle \Delta x_2' \rangle_{\bar{k}} = \langle \frac{K_{ivq} v_{seq}}{i_{seq}^2} \rangle_{\bar{k}} \langle \Delta i_{seq} \rangle_0 - \langle \frac{K_{ivq}}{i_{seq}} \rangle_{\bar{k}} \langle \Delta v_{seq} \rangle_0 + \langle \frac{K_{ivq} v_{seq}}{i_{seq}^2} \rangle_0 \langle \Delta i_{seq} \rangle_{\bar{k}} - \langle \frac{K_{ivq}}{i_{seq}} \rangle_0 \langle \Delta v_{seq} \rangle_{\bar{k}} + K_{ivq} \langle x_{seq}^* \rangle_{\bar{k}} + jk\omega \langle \Delta x_2 \rangle_{\bar{k}} \tag{E.189}$$

$$\langle \Delta i_{seq}' \rangle_{\bar{k}} = -\langle \frac{K_{pvq} v_{seq}}{L_{se} i_{seq}^2} \rangle_{\bar{k}} \langle \Delta i_{seq} \rangle_0 + \langle \frac{K_{pvq}}{L_{se} i_{seq}} \rangle_{\bar{k}} \langle \Delta v_{seq} \rangle_0 - \frac{1}{L_{se}} \langle \Delta x_2 \rangle_{\bar{k}} - \tag{E.190}$$

$$\omega\langle\Delta i_{sed}\rangle_{\bar{k}} + \left\{-\frac{R_{se}}{L_{se}} - \langle\frac{K_{pvq}v_{seq}}{L_{se}i_{seq}^2}\rangle_0 + jk\omega\right\}\langle\Delta i_{seq}\rangle_{\bar{k}} + \left\{\frac{1}{L_{se}} + \langle\frac{K_{pvq}}{L_{se}i_{seq}}\rangle_0\right\}\langle\Delta v_{seq}\rangle_{\bar{k}} -$$

$$\frac{K_{pvq}}{L_{se}}\langle x_{seq}^*\rangle_{\bar{k}}$$

So, the generalised form of impedance control mode is:

$$AI_{DP} = \begin{bmatrix} ai_{k=0} & aci_{k=\bar{k}} & aci_{k=k} & \dots & aci_{k=kn} \\ aci_{k=k} & ai_{k=k} & & & \\ aci_{k=\bar{k}} & & ai_{k=\bar{k}} & & \vdots \\ \vdots & & & \ddots & \\ aci_{k=\overline{kn}} & & & \dots & ai_{k=\overline{kn}} \end{bmatrix}$$

$$ai_{k=k} =$$

$$\begin{bmatrix} -jk\omega & 0 & 0 & 0 & -K_{ivd} \\ 0 & -jk\omega & 0 & \langle\frac{K_{ivq}v_{seq}}{i_{seq}^2}\rangle_0 & 0 \\ -\frac{1}{L_{se}} & 0 & \frac{-R_{se}}{L_{se}} - jk\omega & \omega & \frac{K_{pvd}}{L_{se}} \\ 0 & -\frac{1}{L_{se}} & -\omega & \frac{-R_{se}}{L_{se}} - \langle\frac{K_{pvq}v_{seq}}{L_{se}i_{seq}^2}\rangle_0 - jk\omega & 0 \\ 0 & 0 & \langle\frac{\frac{3}{2}v_{sed} - 2i_{sed}.R_f}{C_{dc}v_{dc}}\rangle_0 & \langle\frac{3}{2}\frac{v_{seq}}{C_{dc}v_{dc}}\rangle_0 & \langle\frac{i_{sed}^2.R_f - \frac{3}{2}v_{sed}i_{sed} - \frac{3}{2}v_{seq}.i_{seq}}{C_{dc}v_{dc}^2}\rangle_0 - jk\omega \end{bmatrix}$$

$$aci_{k=k} = \begin{bmatrix} 0 & 0 & 0 & 0 & 0 \\ 0 & 0 & 0 & \langle\frac{K_{ivq}v_{seq}}{i_{seq}^2}\rangle_k & 0 \\ 0 & 0 & 0 & 0 & 0 \\ 0 & 0 & 0 & -\langle\frac{K_{pvq}v_{seq}}{L_{se}i_{seq}^2}\rangle_k & 0 \\ 0 & 0 & \langle\frac{\frac{3}{2}v_{sed} - 2i_{sed}.R_f}{C_{dc}v_{dc}}\rangle_k & \langle\frac{3}{2}\frac{v_{seq}}{C_{dc}v_{dc}}\rangle_k & \langle\frac{i_{sed}^2.R_f - \frac{3}{2}v_{sed}i_{sed} - \frac{3}{2}v_{seq}.i_{seq}}{C_{dc}v_{dc}^2}\rangle_k \end{bmatrix}$$

$$BI_{DP} = \begin{bmatrix} bi_{k=0} & bci_{k=\bar{k}} & bci_{k=k} & \dots & bci_{k=kn} \\ bci_{k=k} & bi_{k=k} & & & \\ bci_{k=\bar{k}} & & bi_{k=\bar{k}} & & \vdots \\ \vdots & & & \ddots & \\ bci_{k=\overline{kn}} & & & \dots & bi_{k=\overline{kn}} \end{bmatrix}$$

$$bi_{k=k} = \begin{bmatrix} 0 & 0 & K_{ivd} & 0 \\ 0 & -\langle\frac{K_{ivq}}{i_{seq}}\rangle_0 & 0 & K_{ivq} \\ \frac{1}{L_{se}} & 0 & -\frac{K_{pvd}}{L_{se}} & 0 \\ 0 & \left\{\frac{1}{L_{se}} + \langle\frac{K_{pvq}}{L_{se}i_{seq}}\rangle_0\right\} & 0 & -\frac{Kp_{vq}}{L_{se}} \\ \langle\frac{3}{2}\frac{i_{sed}}{C_{dc}v_{dc}}\rangle_0 & \langle\frac{3}{2}\frac{i_{seq}}{C_{dc}v_{dc}}\rangle_0 & 0 & 0 \end{bmatrix}$$

$$bci_{k=k} = \begin{bmatrix} 0 & 0 & 0 & 0 \\ 0 & -\langle\frac{K_{ivq}}{i_{seq}}\rangle_k & 0 & 0 \\ 0 & 0 & 0 & 0 \\ 0 & \langle\frac{K_{pvq}}{L_{se}i_{seq}}\rangle_k & 0 & 0 \\ \langle\frac{3}{2}\frac{i_{sed}}{C_{dc}v_{dc}}\rangle_k & \langle\frac{3}{2}\frac{i_{seq}}{C_{dc}v_{dc}}\rangle_k & 0 & 0 \end{bmatrix}$$

4. Impedance of SSSC power control mode

$$\Delta v_{sed} = (sL_{se} + R_{se})\Delta i_{sed} - \omega L_{se}\Delta i_{seq} + \Delta m_{sed} \quad \text{(E.191)}$$

$$\Delta v_{seq} = sL_{se}\Delta i_{seq} + R_{se}\Delta i_{seq} + \omega L_{se}\Delta i_{sed} + \Delta m_{seq} \quad \text{(E.192)}$$

$$\Delta m_{sed} = \left(K_{pvd} + \frac{K_{ivd}}{s}\right)(P^*_{line} - \Delta P_{line}) \quad \text{(E.193)}$$

$$\Delta m_{seq} = \left(K_{pvq} + \frac{K_{ivq}}{s}\right)(Q^*_{line} - \Delta Q_{line}) \quad \text{(E.194)}$$

$$\Delta P_{line} = \Delta P_1 - \Delta P_2 \quad \text{(E.195)}$$

$$\Delta Q_{line} = \Delta Q_1 - \Delta Q_2 \quad \text{(E.196)}$$

Using KVL (E.197)

$$-v_1 - v_{se} + v_L + v_2 = 0 \quad \text{(E.198)}$$

$$v_L - v_{se} = v_1 - v_2 \quad \text{(E.199)}$$

$$\Delta v_{Ld} - \Delta v_{sed} = \Delta v_{1d} - \Delta v_{2d} \quad \text{(E.200)}$$

$$\Delta v_{Lq} - \Delta v_{seq} = \Delta v_{1q} - \Delta v_{2q} \quad \text{(E.201)}$$

The transformation to dynamic phasor will be:

For $k = 0$

$$\langle\Delta v_{sed}\rangle_0 = (sL_{se} + R_{se})\langle\Delta i_{sed}\rangle_0 - \omega L_{se}\langle\Delta i_{seq}\rangle_0 + \langle\Delta m_{sed}\rangle_0 \quad \text{(E.202)}$$

$$\langle\Delta v_{seq}\rangle_0 = (sL_{se} + R_{se})\langle\Delta i_{seq}\rangle_0 + \omega L_{se}\langle\Delta i_{sed}\rangle_0 + \langle\Delta m_{seq}\rangle_0 \quad \text{(E.203)}$$

$$\langle\Delta m_{sed}\rangle_0 = \left(K_{pvd} + \langle\frac{K_{ivd}}{s}\rangle_0\right)\langle P^*_{line}\rangle_0 + \langle\frac{K_{ivd}}{s-jk\omega}\rangle_{\bar{k}}\langle P^*_{line}\rangle_k + \langle\frac{K_{ivd}}{s+jk\omega}\rangle_k\langle P^*_{line}\rangle_{\bar{k}} - \left(K_{pvd} - \langle\frac{K_{ivd}}{s}\rangle_0\right)\langle\Delta P_{line}\rangle_0 - \langle\frac{K_{ivd}}{s-jk\omega}\rangle_{\bar{k}}\langle\Delta P_{line}\rangle_k - \langle\frac{K_{ivd}}{s+jk\omega}\rangle_k\langle\Delta P_{line}\rangle_{\bar{k}} \quad \text{(E.204)}$$

$$\langle\Delta m_{seq}\rangle_0 = -\left(K_{pvq} + \langle\frac{K_{ivq}}{s}\rangle_0\right)\langle\Delta Q_{line}\rangle_0 - \langle\frac{K_{ivq}}{s-jk\omega}\rangle_{\bar{k}}\langle\Delta Q_{line}\rangle_k - \langle\frac{K_{ivq}}{s+jk\omega}\rangle_k\langle\Delta Q_{line}\rangle_{\bar{k}} + \left(K_{pvq} + \langle\frac{K_{ivq}}{s}\rangle_0\right)\langle Q^*_{line}\rangle_0 + \langle\frac{K_{ivq}}{s-jk\omega}\rangle_{\bar{k}}\langle Q^*_{line}\rangle_k + \langle\frac{K_{ivq}}{s+jk\omega}\rangle_k\langle Q^*_{line}\rangle_{\bar{k}} \quad \text{(E.205)}$$

$$\langle\Delta P_{line}\rangle_0 = \langle\Delta P_1\rangle_0 - \langle\Delta P_2\rangle_0 \quad \text{(E.206)}$$

$$\langle\Delta Q_{line}\rangle_0 = \langle\Delta Q_1\rangle_0 - \langle\Delta Q_2\rangle_0 \quad \text{(E.207)}$$

For $k = k$

$$\langle\Delta v_{sed}\rangle_k = (sL_{se} + R_{se} + jk\omega)\langle\Delta i_{sed}\rangle_k - \omega L_{se}\langle\Delta i_{seq}\rangle_k + \langle\Delta m_{sed}\rangle_k \quad \text{(E.208)}$$

$$\langle \Delta v_{seq} \rangle_k = (sL_{se} + R_{se} + jk\omega)\langle \Delta i_{seq} \rangle_k + \omega L_{se} \langle \Delta i_{sed} \rangle_k + \langle \Delta m_{seq} \rangle_k \quad \text{(E.209)}$$

$$\langle \Delta m_{sed} \rangle_k = - \langle \frac{K_{ivd}}{s+jk\omega} \rangle_k \langle \Delta P_{line} \rangle_0 - \left(K_{pvd} + \langle \frac{K_{ivd}}{s} \rangle_0 \right) \langle \Delta P_{line} \rangle_k + \langle \frac{K_{ivd}}{s+jk\omega} \rangle_k \langle P^*_{line} \rangle_0 + \left(K_{pvd} + \langle \frac{K_{ivd}}{s} \rangle_0 \right) \langle P^*_{line} \rangle_k \quad \text{(E.210)}$$

$$\langle \Delta m_{seq} \rangle_k = \left(K_{pvq} + \langle \frac{K_{ivq}}{s+jk\omega} \rangle_0 \right) \langle Q^*_{line} \rangle_k + \langle \frac{K_{ivq}}{s+jk\omega} \rangle_k \langle Q^*_{line} \rangle_0 - K_{pvq} \langle \Delta Q_{line} \rangle_k - \langle \frac{K_{ivq}}{s+jk\omega} \rangle_k \langle \Delta Q_{line} \rangle_0 - \langle \frac{K_{ivq}}{s+jk\omega} \rangle_0 \langle \Delta Q_{line} \rangle_k \quad \text{(E.211)}$$

$$\langle \Delta P_{line} \rangle_k = \langle \Delta P_1 \rangle_k - \langle \Delta P_2 \rangle_k \quad \text{(E.212)}$$

$$\langle \Delta Q_{line} \rangle_k = \langle \Delta Q_1 \rangle_k - \langle \Delta Q_2 \rangle_k \quad \text{(E.213)}$$

For $k = \bar{k}$

$$\langle \Delta v_{sed} \rangle_{\bar{k}} = (sL_{se} + R_{se} - jk\omega)\langle \Delta i_{sed} \rangle_{\bar{k}} - \omega L_{se} \langle \Delta i_{seq} \rangle_{\bar{k}} + \langle \Delta m_{sed} \rangle_{\bar{k}} \quad \text{(E.214)}$$

$$\langle \Delta v_{seq} \rangle_{\bar{k}} = (sL_{se} + R_{se} - jk\omega)\langle \Delta i_{seq} \rangle_{\bar{k}} + \omega L_{se} \langle \Delta i_{sed} \rangle_{\bar{k}} + \langle \Delta m_{seq} \rangle_{\bar{k}} \quad \text{(E.215)}$$

$$\langle \Delta m_{sed} \rangle_{\bar{k}} = - \langle \frac{K_{ivd}}{s-jk\omega} \rangle_{\bar{k}} \langle \Delta P_{line} \rangle_0 - \left(K_{pvd} + \langle \frac{K_{ivd}}{s} \rangle_0 \right) \langle \Delta P_{line} \rangle_{\bar{k}} + \langle \frac{K_{ivd}}{s-jk\omega} \rangle_{\bar{k}} \langle P^*_{line} \rangle_0 + \left(K_{pvd} + \langle \frac{K_{ivd}}{s} \rangle_0 \right) \langle P^*_{line} \rangle_{\bar{k}} \quad \text{(E.216)}$$

$$\langle \Delta m_{seq} \rangle_{\bar{k}} = \left(K_{pvq} + \langle \frac{K_{ivq}}{s-jk\omega} \rangle_0 \right) \langle Q^*_{line} \rangle_{\bar{k}} + \langle \frac{K_{ivq}}{s-jk\omega} \rangle_{\bar{k}} \langle Q^*_{line} \rangle_0 - K_{pvq} \langle \Delta Q_{line} \rangle_{\bar{k}} - \langle \frac{K_{ivq}}{s-jk\omega} \rangle_{\bar{k}} \langle \Delta Q_{line} \rangle_0 - \langle \frac{K_{ivq}}{s-jk\omega} \rangle_0 \langle \Delta Q_{line} \rangle_{\bar{k}} \quad \text{(E.217)}$$

$$\langle \Delta P_{line} \rangle_{\bar{k}} = \langle \Delta P_1 \rangle_{\bar{k}} - \langle \Delta P_2 \rangle_{\bar{k}} \quad \text{(E.218)}$$

$$\langle \Delta Q_{line} \rangle_{\bar{k}} = \langle \Delta Q_1 \rangle_{\bar{k}} - \langle \Delta Q_2 \rangle_{\bar{k}} \quad \text{(E.219)}$$

Equations from (E.202) to (E.219) equations can be generalised as:

$$\langle \mathbf{\Delta v_{sedq}} \rangle_{\mathbf{k}} = AP_{seDP} \langle \mathbf{\Delta i_{sedq}} \rangle_{\mathbf{k}} + \langle \mathbf{\Delta m_{sedq}} \rangle_{\mathbf{k}}$$

$$AP_{seDP} = \begin{bmatrix} ap_{se_{k=0}} & 0 & 0 & 0 & 0 \\ 0 & ap_{se_{k=k}} & 0 & 0 & 0 \\ 0 & 0 & ap_{se_{k=\bar{k}}} & 0 & 0 \\ 0 & 0 & 0 & \ddots & 0 \\ 0 & 0 & 0 & 0 & ap_{se_{k=\bar{k}\bar{n}}} \end{bmatrix}$$

$$ap_{se_{k=k}} = \begin{bmatrix} (s + jk\omega)L_{se} + R_{se} & -\omega L_{se} \\ \omega L_{se} & (s + jk\omega)L_{se} + R_{se} \end{bmatrix}$$

$$\langle \mathbf{\Delta m_{sedq}} \rangle_{\mathbf{k}} = BP_{se} \langle \mathbf{\Delta PQ^*_{line}} \rangle_{\mathbf{k}} - BP_{se} \langle \mathbf{\Delta PQ_{line}} \rangle_{\mathbf{k}}$$

$$BP_{se} = \begin{bmatrix} Bp_{se_{k=0}} & bcp_{se_{k=\bar{k}}} & bcv_{se_{k=k}} & 0 & bcv_{se_{k=kn}} \\ bcp_{se_{k=k}} & Bp_{se_{k=k}} & 0 & 0 & 0 \\ bcp_{se_{k=\bar{k}}} & 0 & Bv_{se_{k=\bar{k}}} & 0 & 0 \\ 0 & 0 & 0 & \ddots & 0 \\ bcp_{se_{k=\overline{kn}}} & 0 & 0 & 0 & Bv_{se_{k=\overline{kn}}} \end{bmatrix}$$

$$Bp_{se_{k=k}} = \begin{bmatrix} \left(K_{pvd} + \langle\frac{K_{ivd}}{s}\rangle_0\right) & 0 \\ 0 & \left(K_{pvq} + \langle\frac{K_{ivq}}{s}\rangle_0\right) \end{bmatrix}$$

$$bcp_{se_{k=k}} = \begin{bmatrix} \langle\frac{K_{ivd}}{s+jk\omega}\rangle_k & 0 \\ 0 & \langle\frac{K_{ivq}}{s+jk\omega}\rangle_k \end{bmatrix}$$

$$\langle\mathbf{\Delta PQ_{line}}\rangle_\mathbf{k} = -CP_{se}\langle\mathbf{\Delta v_{sedq}}\rangle_\mathbf{k} + CP_{se}\langle\mathbf{\Delta v_{Ldq}}\rangle_\mathbf{k} + DP_{se}\langle\mathbf{\Delta i_{sedq}}\rangle_\mathbf{k} - FP_{se}\langle\mathbf{\Delta i_{sedq}}\rangle_\mathbf{k}$$

$$CP_{se} = \begin{bmatrix} Cp_{se_{k=0}} & ccp_{se_{k=\bar{k}}} & ccp_{se_{k=k}} & 0 & ccp_{se_{k=kn}} \\ ccp_{se_{k=k}} & Cp_{se_{k=k}} & 0 & 0 & 0 \\ ccp_{se_{k=\bar{k}}} & 0 & Cp_{se_{k=\bar{k}}} & 0 & 0 \\ 0 & 0 & 0 & \ddots & 0 \\ ccp_{se_{k=\overline{kn}}} & 0 & 0 & 0 & Cp_{se_{k=\overline{kn}}} \end{bmatrix}$$

$$Cp_{se_{k=k}} = \frac{3}{2}\begin{bmatrix} \langle i_{sed}\rangle_0 & \langle i_{seq}\rangle_0 \\ \langle i_{seq}\rangle_0 & -\langle i_{sed}\rangle_0 \end{bmatrix} \qquad ccp_{se_{k=k}} = \frac{3}{2}\begin{bmatrix} \langle i_{sed}\rangle_k & \langle i_{seq}\rangle_k \\ \langle i_{seq}\rangle_k & -\langle i_{sed}\rangle_k \end{bmatrix}$$

$$DP_{se} = \begin{bmatrix} Dp_{se_{k=0}} & dcp_{se_{k=\bar{k}}} & dcp_{se_{k=k}} & 0 & dcp_{se_{k=kn}} \\ dcp_{se_{k=k}} & Dp_{se_{k=k}} & 0 & 0 & 0 \\ dcp_{se_{k=\bar{k}}} & 0 & Dp_{se_{k=\bar{k}}} & 0 & 0 \\ 0 & 0 & 0 & \ddots & 0 \\ dcp_{se_{k=\overline{kn}}} & 0 & 0 & 0 & Dp_{se_{k=\overline{kn}}} \end{bmatrix}$$

$$Dp_{se_{k=k}} = \frac{3}{2}\begin{bmatrix} \langle v_{sed}\rangle_0 & \langle v_{seq}\rangle_0 \\ -\langle v_{seq}\rangle_0 & \langle v_{sed}\rangle_0 \end{bmatrix} \qquad dcp_{se_{k=k}} = \frac{3}{2}\begin{bmatrix} \langle v_{sed}\rangle_k & \langle v_{seq}\rangle_k \\ -\langle v_{seq}\rangle_k & \langle v_{sed}\rangle_k \end{bmatrix}$$

$$FP_{se} = \begin{bmatrix} Fp_{se_{k=0}} & fcp_{se_{k=\bar{k}}} & fcp_{se_{k=k}} & 0 & fcp_{se_{k=kn}} \\ fcp_{se_{k=k}} & Fp_{se_{k=k}} & 0 & 0 & 0 \\ fcp_{se_{k=\bar{k}}} & 0 & Fp_{se_{k=\bar{k}}} & 0 & 0 \\ 0 & 0 & 0 & \ddots & 0 \\ fcp_{se_{k=\overline{kn}}} & 0 & 0 & 0 & Fp_{se_{k=\overline{kn}}} \end{bmatrix}$$

$$Fp_{se_{k=k}} = \frac{3}{2}\begin{bmatrix} \langle v_{Ld}\rangle_0 & \langle v_{Lq}\rangle_0 \\ -\langle v_{Lq}\rangle_0 & \langle v_{Ld}\rangle_0 \end{bmatrix} \qquad fcp_{k=k} = \frac{3}{2}\begin{bmatrix} \langle v_{Ld}\rangle_k & \langle v_{Lq}\rangle_k \\ -\langle v_{Lq}\rangle_k & \langle v_{Ld}\rangle_k \end{bmatrix}$$

$$\langle\mathbf{\Delta v_{sedq}}\rangle_\mathbf{k} = (I - BP_{se}CP_{se})^{-1}(AP_{seDP} + BP_{se}FP_{se} - BP_{se}DP_{se})\langle\mathbf{\Delta i_{sedq}}\rangle_\mathbf{k} + (I - BP_{se}CP_{se})^{-1}BP_{se}\langle\mathbf{\Delta PQ^*_{line}}\rangle_\mathbf{k} - (I - BP_{se}CP_{se})^{-1}BP_{se}CP_{se}\langle\mathbf{\Delta v_{Ldq}}\rangle_\mathbf{k}$$

$$ZP_{SSSC} = (I - BP_{se}CP_{se})^{-1}(AP_{seDP} + BP_{se}FP_{se} - BP_{se}DP_{se})$$

5. Impedance of SSSC voltage control mode

The SSSC is controlled in voltage control mode as:

$$\langle \Delta v_{sed} \rangle_0 = (L_{se}s + R_{se})\langle \Delta i_{sed} \rangle_0 - \omega L_{se}\langle \Delta i_{seq} \rangle_0 + \langle \Delta m_{sed} \rangle_0 \quad \text{(E.220)}$$

$$\langle \Delta v_{seq} \rangle_0 = (L_{se}s + R_{se})\langle \Delta i_{seq} \rangle_0 + \omega L_{se}\langle \Delta i_{sed} \rangle_0 + \langle \Delta m_{seq} \rangle_0 \quad \text{(E.221)}$$

$$\langle \Delta v_{sed} \rangle_k = (L_{se}(s + jk\omega) + R_{se})\langle \Delta i_{sed} \rangle_k - \omega L_{se}\langle \Delta i_{seq} \rangle_k + \langle \Delta m_{sed} \rangle_k \quad \text{(E.222)}$$

$$\langle \Delta v_{seq} \rangle_k = (L_{se}(s + jk\omega) + R_{se})\langle \Delta i_{seq} \rangle_k + \omega L_{se}\langle \Delta i_{sed} \rangle_k + \langle \Delta m_{seq} \rangle_k \quad \text{(E.223)}$$

$$\langle \Delta v_{sed} \rangle_{\bar{k}} = (L_{se}(s - jk\omega) + R_{se})\langle \Delta i_{sed} \rangle_{\bar{k}} - \omega L_{se}\langle \Delta i_{seq} \rangle_{\bar{k}} + \langle \Delta m_{sed} \rangle_{\bar{k}} \quad \text{(E.224)}$$

$$\langle \Delta v_{seq} \rangle_{\bar{k}} = (L_{se}(s - jk\omega) + R_{se})\langle \Delta i_{seq} \rangle_{\bar{k}} + \langle \omega L_{se}\Delta i_{sed} \rangle_{\bar{k}} + \langle \Delta m_{seq} \rangle_{\bar{k}} \quad \text{(E.225)}$$

$$\Delta m_{sed} = K_{pvd}v^*_{dc} + \frac{Ki_{vd}}{s}v^*_{dc} - K_{pvd}\Delta v_{dc} - \frac{K_{ivd}}{s}\Delta v_{dc} \quad \text{(E.226)}$$

$$\Delta m_{seq} = K_{pvq}v^*_{seq} + \frac{K_{ivq}}{s}v^*_{seq} - K_{pvq}\Delta v_{seq} - \frac{K_{ivq}}{s}\Delta v_{seq} \quad \text{(E.227)}$$

$$\begin{aligned}\langle \Delta m_{sed} \rangle_0 = &-\left(K_{pvd} + \langle \tfrac{K_{ivd}}{s} \rangle_0\right)\langle \Delta v_{dc} \rangle_0 + \left(K_{pvd} + \langle \tfrac{K_{ivd}}{s} \rangle_0\right)\langle v^*_{dc} \rangle_0 + \\ &\langle \tfrac{K_{ivd}}{s-jk\omega} \rangle_{\bar{k}} \langle v^*_{dc} \rangle_k - \langle \tfrac{K_{ivd}}{s-jk\omega} \rangle_{\bar{k}} \langle \Delta v_{dc} \rangle_k + \langle \tfrac{K_{ivd}}{s+jk\omega} \rangle_k \langle v^*_{dc} \rangle_{\bar{k}} - \langle \tfrac{K_{ivd}}{s+jk\omega} \rangle_k \langle \Delta v_{dc} \rangle_{\bar{k}}\end{aligned} \quad \text{(E.228)}$$

$$\begin{aligned}\langle \Delta m_{seq} \rangle_0 = &-\left(K_{pvq} + \langle \tfrac{K_{ivq}}{s} \rangle_0\right)\langle \Delta v_{seq} \rangle_0 + \left(K_{pvq} + \langle \tfrac{K_{ivq}}{s} \rangle_0\right)\langle v^*_{seq} \rangle_0 - \\ &\langle \tfrac{K_{ivq}}{s-jk\omega} \rangle_{\bar{k}} \langle \Delta v_{seq} \rangle_k + \langle \tfrac{K_{ivq}}{s-jk\omega} \rangle_{\bar{k}} \langle v^*_{seq} \rangle_k - \langle \tfrac{K_{ivq}}{s+jk\omega} \rangle_k \langle \Delta v_{seq} \rangle_{\bar{k}} + \langle \tfrac{K_{ivq}}{s+jk\omega} \rangle_k \langle v^*_{seq} \rangle_{\bar{k}}\end{aligned} \quad \text{(E.229)}$$

$$\begin{aligned}\langle \Delta m_{sed} \rangle_k = &-\langle \tfrac{K_{ivd}}{s+jk\omega} \rangle_k \langle \Delta v_{dc} \rangle_0 + \langle \tfrac{K_{ivd}}{s+jk\omega} \rangle_k \langle v^*_{dc} \rangle_0 + \left(K_{pvd} + \langle \tfrac{K_{ivd}}{s} \rangle_0\right)\langle v^*_{dc} \rangle_k - \\ &\left(K_{pvd} + \langle \tfrac{K_{ivd}}{s} \rangle_0\right)\langle \Delta v_{dc} \rangle_k\end{aligned} \quad \text{(E.230)}$$

$$\begin{aligned}\langle \Delta m_{seq} \rangle_k = &\\ &-\langle \tfrac{K_{ivq}}{s+jk\omega} \rangle_k \langle \Delta v_{seq} \rangle_0 + \langle \tfrac{K_{ivq}}{s+jk\omega} \rangle_k \langle v^*_{seq} \rangle_0 + \left(K_{pvq} + \langle \tfrac{K_{ivq}}{s} \rangle_0\right)\langle v^*_{seq} \rangle_k - \\ &\left(K_{pvq} + \langle \tfrac{K_{ivq}}{s} \rangle_0\right)\langle \Delta v_{seq} \rangle_k\end{aligned} \quad \text{(E.231)}$$

$$\begin{aligned}\langle \Delta m_{sed} \rangle_{\bar{k}} = &-\langle \tfrac{K_{ivd}}{s-jk\omega} \rangle_{\bar{k}} \langle \Delta v_{dc} \rangle_0 + \langle \tfrac{K_{ivd}}{s-jk\omega} \rangle_{\bar{k}} \langle v^*_{dc} \rangle_0 + \left(K_{pvd} + \langle \tfrac{K_{ivd}}{s} \rangle_0\right)\langle v^*_{dc} \rangle_{\bar{k}} - \\ &\left(K_{pvd} + \langle \tfrac{K_{ivd}}{s} \rangle_0\right)\langle \Delta v_{dc} \rangle_{\bar{k}}\end{aligned} \quad \text{(E.232)}$$

$$\begin{aligned}\langle \Delta m_{seq} \rangle_{\bar{k}} = &\\ &-\langle \tfrac{K_{ivq}}{s-jk\omega} \rangle_{\bar{k}} \langle \Delta v_{seq} \rangle_0 + \langle \tfrac{K_{ivq}}{s-jk\omega} \rangle_{\bar{k}} \langle v^*_{seq} \rangle_0 + \left(K_{pvq} + \langle \tfrac{K_{ivq}}{s} \rangle_0\right)\langle v^*_{seq} \rangle_{\bar{k}} - \\ &\left(K_{pvq} + \langle \tfrac{K_{ivq}}{s} \rangle_0\right)\langle \Delta v_{seq} \rangle_{\bar{k}}\end{aligned} \quad \text{(E.233)}$$

$$\langle \mathbf{\Delta v_{sedq}} \rangle_{\mathbf{k}} = AI_{se}\langle \mathbf{\Delta i_{sedq}} \rangle_{\mathbf{k}} + \langle \mathbf{\Delta m_{sedq}} \rangle_{\mathbf{k}}$$

$$AV_{se} = \begin{bmatrix} Av_{se_{k=0}} & 0 & 0 & \cdots & 0 \\ 0 & Av_{se_{k=k}} & 0 & 0 & 0 \\ 0 & 0 & Av_{se_{k=\bar{k}}} & & 0 \\ \vdots & & 0 & \ddots & \vdots \\ 0 & 0 & \ldots & 0 & Av_{se_{k=\overline{kn}}} \end{bmatrix}$$

$$Av_{se_{k=k}} = \begin{bmatrix} L_{se}(s + jk\omega) + R_{se} & -\omega L_{se} \\ \omega L_{se} & L_{se}(s + jk\omega) + R_{se} \end{bmatrix}$$

$$\langle \mathbf{\Delta m_{sedq}} \rangle_{\mathbf{k}} = BV_{se} \langle \mathbf{\Delta V V^{*}} \rangle_{\mathbf{k}} - BV_{se} \langle \mathbf{\Delta V V} \rangle_{\mathbf{k}}$$

$$BV_{se} = \begin{bmatrix} Bv_{se_{k=0}} & bcv_{se_{k=\bar{k}}} & bcv_{se_{k=k}} & \cdots & bcv_{se_{k=kn}} \\ bcv_{se_{k=k}} & Bv_{se_{k=k}} & 0 & 0 & 0 \\ bcv_{se_{k=\bar{k}}} & 0 & Bv_{se_{k=\bar{k}}} & & 0 \\ \vdots & & 0 & \ddots & \vdots \\ bcv_{se_{k=\overline{kn}}} & 0 & \dots & 0 & Bv_{se_{k=\overline{kn}}} \end{bmatrix}$$

$$Bv_{se_{k=k}} = \begin{bmatrix} \left(K_{pvd} + \langle \frac{K_{ivd}}{s} \rangle_0\right) & 0 \\ 0 & \left(K_{pvq} + \langle \frac{K_{ivq}}{s} \rangle_0\right) \end{bmatrix} bcv_{se_{k=k}} = \begin{bmatrix} \langle \frac{K_{ivd}}{s+jk\omega} \rangle_k & 0 \\ 0 & \langle \frac{K_{ivq}}{s+jk\omega} \rangle_k \end{bmatrix}$$

$$CV_{se} \langle \mathbf{\Delta V V} \rangle_{\mathbf{k}} = DV_{se} \langle \mathbf{\Delta v_{sedq}} \rangle_{\mathbf{k}} + EV_{se} \langle \mathbf{\Delta i_{sedq}} \rangle_{\mathbf{k}}$$

$$CV_{se} = \begin{bmatrix} Cv_{se_{k=0}} & ccv_{se_{k=\bar{k}}} & ccv_{se_{k=k}} & \cdots & ccv_{se_{k=kn}} \\ clv_{se_{k=k}} & Cv_{se_{k=k}} & 0 & 0 & 0 \\ clv_{se_{k=\bar{k}}} & 0 & Cv_{se_{k=\bar{k}}} & & 0 \\ \vdots & & 0 & \ddots & \vdots \\ clv_{se_{k=\overline{kn}}} & 0 & \dots & 0 & Cv_{se_{k=\overline{kn}}} \end{bmatrix}$$

$$Cv_{se_{k=k}} = \begin{bmatrix} C_{dc} \langle v_{dc} \rangle_0 (s + jk\omega) + \frac{3}{2} \langle \frac{\frac{3}{2} v_{sed} . i_{sed} + \frac{3}{2} v_{seq} . i_{seq} - i_{sed}^2 . R_{se}}{v_{dc}} \rangle_0 & 0 \\ 0 & 1 \end{bmatrix}$$

$$ccv_{se_{k=k}} = \begin{bmatrix} C_{dc} \langle v_{dc} \rangle_k (s - jk\omega) + \langle \frac{\frac{3}{2} v_{sed} . i_{sed} + \frac{3}{2} v_{seq} . i_{seq} - i_{sed}^2 . R_{se}}{v_{dc}} \rangle_k & 0 \\ 0 & 0 \end{bmatrix}$$

$$clv_{se_{k=k}} = \begin{bmatrix} C_{dc} \langle v_{dc} \rangle_k s + \langle \frac{\frac{3}{2} v_{sed} . i_{sed} + \frac{3}{2} v_{seq} i_{seq} - i_{sed}^2 . R_{se}}{v_{dc}} \rangle_k & 0 \\ 0 & 0 \end{bmatrix}$$

$$DV_{se} = \begin{bmatrix} Dv_{se_{k=0}} & dcv_{se_{k=\bar{k}}} & dcv_{se_{k=k}} & \cdots & dcv_{se_{k=kn}} \\ dcv_{se_{k=k}} & Dv_{se_{k=k}} & 0 & 0 & 0 \\ dcv_{se_{k=\bar{k}}} & 0 & Dv_{se_{k=\bar{k}}} & & 0 \\ \vdots & & 0 & \ddots & \vdots \\ dcv_{se_{k=\overline{kn}}} & 0 & \dots & 0 & Dv_{se_{k=\overline{kn}}} \end{bmatrix}$$

$$Dv_{se_{k=k}} = \begin{bmatrix} \langle \frac{3}{2} i_{sed} \rangle_0 & \langle \frac{3}{2} i_{seq} \rangle_0 \\ 0 & 1 \end{bmatrix} \qquad dcv_{se_{k=k}} = \begin{bmatrix} \langle \frac{3}{2} i_{sed} \rangle_k & \langle \frac{3}{2} i_{seq} \rangle_k \\ 0 & 0 \end{bmatrix}$$

$$EV_{se} = \begin{bmatrix} Ev_{se_{k=0}} & ecv_{se_{k=\bar{k}}} & ecv_{se_{k=k}} & \cdots & ecv_{se_{k=kn}} \\ ecv_{se_{k=k}} & Ev_{se_{k=k}} & 0 & 0 & 0 \\ ecv_{se_{k=\bar{k}}} & 0 & Ev_{se_{k=\bar{k}}} & & 0 \\ \vdots & & 0 & \ddots & \vdots \\ ecv_{se_{k=\overline{kn}}} & 0 & \dots & 0 & Ev_{se_{k=\overline{kn}}} \end{bmatrix}$$

$$Ev_{se_{k=k}} = \begin{bmatrix} \langle \frac{3}{2} v_{sed} - 2 i_{sed} . R_f \rangle_0 & \langle \frac{3}{2} v_{seq} \rangle_0 \\ 0 & 0 \end{bmatrix}$$

$$ecv_{se_{k=k}} = \begin{bmatrix} \langle \frac{3}{2} v_{sed} - 2 i_{sed}.R_f \rangle_k & \langle \frac{3}{2} v_{seq} \rangle_k \\ 0 & 0 \end{bmatrix}$$

$$\langle \mathbf{\Delta v_{sedq}} \rangle_\mathbf{k} = \{\mathbf{I} + BV_{se}(CV_{se})^{-1}DV_{se}\}^{-1}\{AV_{se} - BV_{se}(CV_{se})^{-1}EV_{se}\}\langle \mathbf{\Delta i_{sedq}} \rangle_\mathbf{k} + \{\mathbf{I} + BV_{se}(CV_{se})^{-1}DV_{se}\}^{-1}BV_{se}\langle \mathbf{\Delta V V^*} \rangle_\mathbf{k}$$

So, the SSSC controlled with quadrature voltage impedance is:

$$ZV_{SSSC} = \{\mathbf{I} + BV_{se}(CV_{se})^{-1}DV_{se}\}^{-1}\{AV_{se} - BV_{se}(CV_{se})^{-1}EV_{se}\}$$

6. Impedance of SSSC control mode

$$\Delta x_{seq} = \frac{1}{i_{seq}}\Delta v_{seq} - \frac{v_{seq}}{i_{seq}^2}\,\Delta i_{seq} \tag{E.234}$$

$$\Delta m_{sed} = K_{pvd}v_{dc}^* + \frac{K_{ivd}}{s}v_{dc}^* - K_{pvd}\Delta v_{dc} - \frac{K_{ivd}}{s}\Delta v_{dc} \tag{E.235}$$

$$\Delta m_{seq} = K_{pvq}x_{seq}^* + \frac{K_{ivq}}{s}x_{seq}^* - K_{pvq}\Delta x_{seq} - \frac{K_{ivq}}{s}\Delta x_{seq} \tag{E.236}$$

$$\langle \Delta m_{sed} \rangle_0 = -\left(K_{pvd} + \langle \frac{K_{ivd}}{s} \rangle_0\right)\langle \Delta v_{dc} \rangle_0 + \left(K_{pvd} + \langle \frac{K_{ivd}}{s} \rangle_0\right)\langle v_{dc}^* \rangle_0 + \langle \frac{K_{ivd}}{s-jk\omega} \rangle_{\bar{k}}\langle v_{dc}^* \rangle_k - \langle \frac{K_{ivd}}{s-jk\omega} \rangle_{\bar{k}}\langle \Delta v_{dc} \rangle_k + \langle \frac{K_{ivd}}{s+jk\omega} \rangle_k \langle v_{dc}^* \rangle_{\bar{k}} - \langle \frac{K_{ivd}}{s+jk\omega} \rangle_k \langle \Delta v_{dc} \rangle_{\bar{k}} \tag{E.237}$$

$$\langle \Delta m_{seq} \rangle_0 = -\left(K_{pvq} + \langle \frac{K_{ivq}}{s} \rangle_0\right)\langle \Delta x_{seq} \rangle_0 + \left(K_{pvq} + \langle \frac{K_{ivq}}{s} \rangle_0\right)\langle x_{seq}^* \rangle_0 - \langle \frac{K_{ivq}}{s-jk\omega} \rangle_{\bar{k}}\langle \Delta x_{seq} \rangle_k + \langle \frac{K_{ivq}}{s-jk\omega} \rangle_{\bar{k}}\langle x_{seq}^* \rangle_k - \langle \frac{K_{ivq}}{s+jk\omega} \rangle_k \langle \Delta x_{seq} \rangle_{\bar{k}} + \langle \frac{Ki_{vq}}{s+jk\omega} \rangle_k \langle x_{seq}^* \rangle_{\bar{k}} \tag{E.238}$$

$$\langle \Delta m_{sed} \rangle_k = -\langle \frac{K_{ivd}}{s+jk\omega} \rangle_k \langle \Delta v_{dc} \rangle_0 + \langle \frac{K_{ivd}}{s+jk\omega} \rangle_k \langle v_{dc}^* \rangle_0 + \left(K_{pvd} + \langle \frac{K_{ivd}}{s} \rangle_0\right)\langle v_{dc}^* \rangle_k - \left(K_{pvd} + \langle \frac{K_{ivd}}{s} \rangle_0\right)\langle \Delta v_{dc} \rangle_k \tag{E.239}$$

$$\langle \Delta m_{seq} \rangle_k = -\langle \frac{K_{ivq}}{s+jk\omega} \rangle_k \langle \Delta x_{seq} \rangle_0 + \langle \frac{K_{ivq}}{s+jk\omega} \rangle_k \langle x_{seq}^* \rangle_0 + \left(K_{pvq} + \langle \frac{K_{ivq}}{s} \rangle_0\right)\langle x_{seq}^* \rangle_k - \left(K_{pvq} + \langle \frac{K_{ivq}}{s} \rangle_0\right)\langle \Delta x_{seq} \rangle_k \tag{E.240}$$

$$\langle \Delta m_{sed} \rangle_{\bar{k}} = -\langle \frac{K_{ivd}}{s-jk\omega} \rangle_{\bar{k}} \langle \Delta v_{dc} \rangle_0 + \langle \frac{K_{ivd}}{s-jk\omega} \rangle_{\bar{k}} \langle v_{dc}^* \rangle_0 + \left(K_{pvd} + \langle \frac{K_{ivd}}{s} \rangle_0\right)\langle v_{dc}^* \rangle_{\bar{k}} - \left(K_{pvd} + \langle \frac{K_{ivd}}{s} \rangle_0\right)\langle \Delta v_{dc} \rangle_{\bar{k}} \tag{E.241}$$

$$\langle \Delta m_{seq} \rangle_{\bar{k}} = -\langle \frac{K_{ivq}}{s-jk\omega} \rangle_{\bar{k}} \langle \Delta x_{seq} \rangle_0 + \langle \frac{K_{ivq}}{s-jk\omega} \rangle_{\bar{k}} \langle x_{seq}^* \rangle_0 + \left(K_{pvq} + \langle \frac{K_{ivq}}{s} \rangle_0\right)\langle x_{seq}^* \rangle_{\bar{k}} - \left(K_{pvq} - \langle \frac{K_{ivq}}{s} \rangle_0\right)\langle \Delta x_{seq} \rangle_{\bar{k}} \tag{E.242}$$

$$\langle \Delta x_{seq} \rangle_0 =$$
$$\langle \frac{1}{i_{seq}} \rangle_0 \langle \Delta v_{seq} \rangle_0 - \langle \frac{v_{seq}}{i_{seq}^2} \rangle_0 \langle \Delta i_{seq} \rangle_0 + \langle \frac{1}{i_{seq}} \rangle_{\bar{k}} \langle \Delta v_{seq} \rangle_k - \langle \frac{v_{seq}}{i_{seq}^2} \rangle_{\bar{k}} \langle \Delta i_{seq} \rangle_k + \langle \frac{1}{i_{seq}} \rangle_k \langle \Delta v_{seq} \rangle_{\bar{k}} - \langle \frac{v_{seq}}{i_{seq}^2} \rangle_k \langle \Delta i_{seq} \rangle_{\bar{k}} \quad \text{(E.243)}$$

$$\langle \Delta x_{seq} \rangle_k =$$
$$\langle \frac{1}{i_{seq}} \rangle_k \langle \Delta v_{seq} \rangle_0 - \langle \frac{v_{seq}}{i_{seq}^2} \rangle_k \langle \Delta i_{seq} \rangle_0 + \langle \frac{1}{i_{seq}} \rangle_0 \langle \Delta v_{seq} \rangle_k - \langle \frac{v_{seq}}{i_{seq}^2} \rangle_0 \langle \Delta i_{seq} \rangle_k \quad \text{(E.244)}$$

$$\langle \Delta x_{seq} \rangle_{\bar{k}} =$$
$$\langle \frac{1}{i_{seq}} \rangle_{\bar{k}} \langle \Delta v_{seq} \rangle_0 - \langle \frac{v_{seq}}{i_{seq}^2} \rangle_{\bar{k}} \langle \Delta i_{seq} \rangle_0 + \langle \frac{1}{i_{seq}} \rangle_0 \langle \Delta v_{seq} \rangle_{\bar{k}} - \langle \frac{v_{seq}}{i_{seq}^2} \rangle_0 \langle \Delta i_{seq} \rangle_{\bar{k}} \quad \text{(E.245)}$$

The previous equations can be generalised as:

$$\langle \mathbf{\Delta v_{sedq}} \rangle_\mathbf{k} = AI_{se} \langle \mathbf{\Delta i_{sedq}} \rangle_\mathbf{k} + \langle \mathbf{\Delta m_{sedq}} \rangle_\mathbf{k}$$

$$AI_{se} = \begin{bmatrix} Ai_{se_{k=0}} & 0 & 0 & \cdots & 0 \\ 0 & Ai_{se_{k=k}} & 0 & 0 & 0 \\ 0 & 0 & Ai_{se_{k=\bar{k}}} & & 0 \\ \vdots & & 0 & \ddots & \vdots \\ 0 & 0 & \dots & 0 & Ai_{se_{k=\overline{kn}}} \end{bmatrix}$$

$$Ai_{se_{k=k}} = \begin{bmatrix} L_{se}(s + jk\omega) + R_{se} & -\omega L_{se} \\ \omega L_{se} & L_{se}(s + jk\omega) + R_{se} \end{bmatrix}$$

$$\langle \mathbf{\Delta m_{sedq}} \rangle_\mathbf{k} = BI_{se} \langle \mathbf{\Delta V X^*} \rangle_\mathbf{k} - BI_{se} \langle \mathbf{\Delta V X} \rangle_\mathbf{k}$$

$$BI_{se} = \begin{bmatrix} Bi_{se_{k=0}} & bci_{se_{k=\bar{k}}} & bci_{se_{k=k}} & \cdots & bci_{se_{k=kn}} \\ bci_{se_{k=k}} & Bi_{se_{k=k}} & 0 & 0 & 0 \\ bci_{se_{k=\bar{k}}} & 0 & Bi_{se_{k=\bar{k}}} & & 0 \\ \vdots & & 0 & \ddots & \vdots \\ bci_{se_{k=\overline{kn}}} & 0 & \dots & 0 & Bi_{se_{k=\overline{kn}}} \end{bmatrix}$$

$$Bi_{se_{k=k}} = \begin{bmatrix} \left(K_{pvd} + \langle \frac{K_{ivd}}{s} \rangle_0\right) & 0 \\ 0 & \left(K_{pvq} + \langle \frac{K_{ivq}}{s} \rangle_0\right) \end{bmatrix} \quad bci_{se_{k=k}} = \begin{bmatrix} \langle \frac{K_{ivd}}{s+jk\omega} \rangle_k & 0 \\ 0 & \langle \frac{K_{ivq}}{s+jk\omega} \rangle_k \end{bmatrix}$$

$$CI_{se} = \begin{bmatrix} Ci_{se_{k=0}} & cci_{se_{k=\bar{k}}} & cci_{se_{k=k}} & \cdots & cci_{se_{k=kn}} \\ cli_{se_{k=k}} & Ci_{se_{k=k}} & 0 & 0 & 0 \\ cli_{se_{k=\bar{k}}} & 0 & Ci_{se_{k=\bar{k}}} & & 0 \\ \vdots & & 0 & \ddots & \vdots \\ cli_{se_{k=\overline{kn}}} & 0 & \dots & 0 & Ci_{se_{k=\overline{kn}}} \end{bmatrix}$$

$$Ci_{se_{k=k}} = \begin{bmatrix} C_{dc}\langle v_{dc} \rangle_0 (s + jk\omega) + \langle \frac{\frac{3}{2} v_{sed}.i_{sed} + \frac{3}{2} v_{seq}.i_{seq} - i_{sed}^2.R_{se}}{v_{dc}} \rangle_0 & 0 \\ 0 & 1 \end{bmatrix}$$

$$cci_{se_{k=k}} = \begin{bmatrix} C_{dc}\langle v_{dc}\rangle_k(s - jk\omega) + \langle\frac{\frac{3}{2}v_{sed}.i_{sed}+\frac{3}{2}v_{seq}.i_{seq}-i_{sed}^2.R_{se}}{v_{dc}}\rangle_k & 0 \\ 0 & 0 \end{bmatrix}$$

$$cli_{se_{k=k}} = \begin{bmatrix} C_{dc}\langle v_{dc}\rangle_k s + \langle\frac{\frac{3}{2}v_{sed}.i_{sed}+\frac{3}{2}v_{seq}.i_{seq}-i_{sed}^2.R_{se}}{v_{dc}}\rangle_k & 0 \\ 0 & 0 \end{bmatrix}$$

$$DI_{se} = \begin{bmatrix} Di_{se_{k=0}} & dci_{se_{k=\bar{k}}} & dci_{se_{k=k}} & \cdots & dci_{se_{k=kn}} \\ dci_{se_{k=k}} & Di_{se_{k=k}} & 0 & 0 & 0 \\ dci_{se_{k=\bar{k}}} & 0 & Di_{se_{k=\bar{k}}} & & 0 \\ \vdots & & 0 & \ddots & \vdots \\ dci_{se_{k=\overline{kn}}} & 0 & \dots & 0 & Di_{se_{k=\overline{kn}}} \end{bmatrix}$$

$$Di_{se_{k=k}} = \begin{bmatrix} \langle\frac{3}{2}i_{sed}\rangle_0 & \langle\frac{3}{2}i_{seq}\rangle_0 \\ 0 & \langle\frac{1}{i_{seq}}\rangle_0 \end{bmatrix} \qquad dci_{se_{k=k}} = \begin{bmatrix} \langle\frac{3}{2}i_{sed}\rangle_k & \langle\frac{3}{2}i_{seq}\rangle_k \\ 0 & \langle\frac{1}{i_{seq}}\rangle_k \end{bmatrix}$$

$$EI_{se} = \begin{bmatrix} Ei_{se_{k=0}} & eci_{se_{k=\bar{k}}} & eci_{se_{k=k}} & \cdots & eci_{se_{k=kn}} \\ eci_{se_{k=k}} & Ei_{se_{k=k}} & 0 & 0 & 0 \\ eci_{se_{k=\bar{k}}} & 0 & Ei_{se_{k=\bar{k}}} & & 0 \\ \vdots & & 0 & \ddots & \vdots \\ eci_{se_{k=\overline{kn}}} & 0 & \dots & 0 & Ei_{se_{k=\overline{kn}}} \end{bmatrix}$$

$$Ei_{se_{k=k}} = \begin{bmatrix} \langle\frac{3}{2}v_{sed} - 2i_{sed}.R_f\rangle_0 & \langle\frac{3}{2}v_{seq}\rangle_0 \\ 0 & \langle\frac{v_{seq}}{i_{seq}^2}\rangle_0 \end{bmatrix} eci_{se_{k=k}} = \begin{bmatrix} \langle\frac{3}{2}v_{sed} - 2i_{sed}.R_f\rangle_k & \langle\frac{3}{2}v_{seq}\rangle_k \\ 0 & 0 \end{bmatrix}$$

$$CI_{se}\langle\mathbf{\Delta VX}\rangle_\mathbf{k} = DI_{se}\langle\mathbf{\Delta v_{sedq}}\rangle_\mathbf{k} + EI_{se}\langle\mathbf{\Delta i_{sedq}}\rangle_\mathbf{k}$$

$$\langle\mathbf{\Delta v_{sedq}}\rangle_\mathbf{k} = \{\mathbf{I} + BI_{se}(CI_{se})^{-1}DI_{se}\}^{-1}\{AI_{se} - BI_{se}(CI_{se})^{-1}EI_{se}\}\langle\mathbf{\Delta i_{sedq}}\rangle_\mathbf{k} +$$

$$\{\mathbf{I} + BI_{se}(CI_{se})^{-1}DI_{se}\}^{-1}BI_{se}\langle\mathbf{\Delta VX}^*\rangle_\mathbf{k}$$

Similarly, the impedance SSSC controlled with quadrature impedance

$$ZI_{SSSC} = \{\mathbf{I} + BI_{se}(CI_{se})^{-1}DI_{se}\}^{-1}\{AI_{se} - BI_{se}(CI_{se})^{-1}EI_{se}\}$$